

## ACKNOWLEDGEMENTS

I would like to convey my sincere thanks and appreciation to Dr. N. Serpone for having suggested this project. His continued guidance throughout this project and his scientific integrity and participation have been truly exemplary. He also has my deepest appreciation for his friendship, and financial support (National Research Council of Canada) during the summer of 1977.

I would also wish to extend my many thanks to Drs. B.C. Pant and R.T. Rye for serving on my research committee, and for their constructive criticisms on the first draft of this thesis. Also, I thank Drs. M.Z. Hoffman, T.W. Swaddle, and M. Maestri for their helpful suggestions and comments regarding some aspects of this work.

I am always indebted to my mother and brother for their continued encouragement and guidance in all my endeavors.

## ABSTRACT

### A KINETIC INVESTIGATION OF THE HYDROLYSIS OF TRIS(1,10-PHENANTHROLINE)CHROMIUM(III) AND TRIS(2,2'-BIPYRIDYL)CHROMIUM(III) AND THE PREPARATION OF SOME NEW CHROMIUM(III) POLYPYRIDYL COMPLEXES

Mary A. Jamieson

The kinetics of the thermal hydrolysis of  $[\text{Cr}(\text{NN})_3]^{3+}$  ( $\text{NN}$  = 2,2'-bipyridine and 1,10-phenanthroline) have been investigated in aqueous solutions at constant ionic strength (1.0 M) in the pH range 10.8 - 14 (bipy) and 0 - 14 (phen). The hydrolysis reaction is  $\text{OH}^-$  catalysed. The pH dependence of the rate of hydrolysis was studied at 11° (bipy) and at 31.1° (phen), and exhibits four discrete regions. The stoichiometry of the hydrolysis reaction at  $\text{pH} > 9$  is:  $[\text{Cr}(\text{NN})_3]^{3+} + 20\text{OH}^- \xrightarrow{k_{\text{obs}}} [\text{Cr}(\text{NN})_2(\text{OH})_2]^+ + \text{NN}$ . The pseudo first-order rate constant  $k_{\text{obs}}$  is dependent on hydroxide ion concentration:  $k_{\text{obs}} = [\text{OH}^-]/(\text{B} + \text{A}[\text{OH}^-]) + \text{C}[\text{OH}^-] + \text{E}[\text{OH}^-]^2$  in the pH range 6 - 14. The Eyring activation parameters at 25° were determined via temperature-dependence studies. For the  $[\text{Cr}(\text{bipy})_3]^{3+}$  system, they are: (i) pH 9.8 (see reference 16),  $\Delta H^\ddagger = 22.3 \pm 0.2$  kcal/mol;  $\Delta S^\ddagger = -8.8 \pm 0.6$  eu,  $k_{\text{obs}} = 3.3 \times 10^{-6}$  sec<sup>-1</sup>; (ii) pH 11.82,

$\Delta H^\ddagger = 20.7 \pm 0.2$  kcal/mol,  $\Delta S^\ddagger = -12.6 \pm 0.6$  eu,  $k_{\text{obs}} = 6.9 \times 10^{-6}$  sec $^{-1}$ ; (iii) at 0.50 M OH $^-$ ,  $\Delta H^\ddagger = 18.8 \pm 0.6$  kcal/mol,  $\Delta S^\ddagger = -11 \pm 2$  eu,  $k_{\text{obs}} = 2.9 \times 10^{-4}$  sec $^{-1}$ . For [Cr(phen) $_3$ ] $^{3+}$  at 25 $^\circ$ : (i) pH = 10.10,  $\Delta H^\ddagger = 23.3 \pm 0.7$  kcal/mol,  $\Delta S^\ddagger = -8.4 \pm 2.3$  eu,  $k_{\text{obs}} = 7.9 \times 10^{-7}$  sec $^{-1}$ ; (ii) pH = 12.17,  $\Delta H^\ddagger = 21.6 \pm 1.4$  kcal/mol,  $\Delta S^\ddagger = -10.6 \pm 1.4$  eu,  $k_{\text{obs}} = 4.3 \times 10^{-6}$  sec $^{-1}$ ; (iii) at 0.80 M OH $^-$ ,  $\Delta H^\ddagger = 20.9 \pm 0.4$  kcal/mol,  $\Delta S^\ddagger = -5.4 \pm 1.2$  eu,  $k_{\text{obs}} = 1.9 \times 10^{-4}$  sec $^{-1}$ . The kinetic results are interpreted in terms of an associative (A) mechanism involving the formation of a heptacoordinate intermediate via direct nucleophilic attack of a water molecule (pH 6 - 10.7) and of OH $^-$  (pH 10.8 - 13) at the metal centre. The second-order dependence of  $k_{\text{obs}}$  on [OH $^-$ ] (pH  $\geq$  13) is rationalized in terms of the formation of outer-sphere complexes followed by attack of this complex by another OH $^-$  to form some heptacoordinate intermediate which, also, ultimately and irreversibly, releases NN into solution.

The reactivity of the [Rh(bipy) $_3$ ] $^{3+}$  cation in acidic and basic media has also been studied, and found to be relatively inert in both media at ambient temperature.

Four new substituted polypyridyl chromium(III) complexes have been synthesized for future photochemical studies. These include the perchlorate salts of [Cr(5-Clphen) $_3$ ] $^{3+}$ , [Cr(4,7-Me $_2$ phen) $_3$ ] $^{3+}$ , [Cr(4,7-Ph $_2$ -phen) $_3$ ] $^{3+}$ , and [Cr(4,4'-Ph $_2$ bipy) $_3$ ] $^{3+}$ .

## TABLE OF CONTENTS

	<u>page</u>
I. INTRODUCTION .....	1
II. EXPERIMENTAL SECTION .....	6
A. Preparation of Compounds for Kinetic Measurements .....	6
1. Reagents and Solvents .....	6
2. General Techniques .....	6
3. Elemental Analyses .....	7
4. <u>Tris(1,10-phenanthroline)chromium-</u> <u>(III) Perchlorate</u> .....	7
5. <u>Tris(2,2'-bipyridine)chromium(III)</u> <u>Perchlorate</u> .....	8
6. <u>Diäquobis(1,10-phenanthroline)chromium-</u> <u>(III) Nitrate</u> .....	9
B. Kinetic Measurements .....	10
1. General Techniques .....	10
2. Solvents, Solvent Systems, and Pre- paration of Solutions .....	11
a. Solvents .....	11
b. Preparation of Solutions .....	12
c. Solvent Systems for $[\text{Cr}(\text{phen})_3]^{3+}$ .....	12
d. Solvent Systems for $[\text{Cr}(\text{bipy})_3]^{3+}$ .....	15
3. Calibration Curves .....	15
a. Calibration Curves for $[\text{Cr}-$ $(\text{phen})_3]^{3+}$ .....	16
b. Calibration Curve for $[\text{Cr}-$ $(\text{bipy})_3]^{3+}$ .....	16
4. Determination of the Observed Rate Constant, $k_{\text{obs}}$ .....	21
a. $[\text{Cr}(\text{phen})_3]^{3+}$ System .....	21
b. $[\text{Cr}(\text{bipy})_3]^{3+}$ System .....	21

	<u>Page</u>
5. Isosbestic Points .....	22
a. $[\text{Cr}(\text{phen})_3]^{3+}$ System .....	22
b. $[\text{Cr}(\text{bipy})_3]^{3+}$ System .....	22
#6. Kinetics in Oxygenated and Deoxy- genated Solvents .....	22
a. Oxygenated Solvent System .....	23
b. Deoxygenated Solvent System ...	23
7. Temperature-dependence Studies ....	24
a. $[\text{Cr}(\text{phen})_3]^{3+}$ System .....	24
b. $[\text{Cr}(\text{bipy})_3]^{3+}$ System .....	24
8. Electronic Spectra of the Chromium- (III) Aquated Products .....	25
C. Calculations for Kinetic Studies .....	27
1. Observed Rate Constant, $k_{\text{obs}}$ .....	27
2. Ionic Strength Calculations for Solvent Systems .....	32
3. Activation Parameters .....	33
4. Kinetics in Oxygenated and Deoxy- genated Solvent Systems .....	38
D. Preparation of Rhodium(III) Compound ..	42
1. Reagents and Solvents .....	42
2. <u>Tris(2,2'-bipyridine)rhodium(III)</u> <u>Chloride</u> .....	42
E. Experiments Performed on $[\text{Rh}(\text{bipy})_3]^{3+}$ .	
1. Behaviour of $[\text{Rh}(\text{bipy})_3]^{3+}$ in Acid Solution .....	44
2. Behaviour of $[\text{Rh}(\text{bipy})_3]^{3+}$ in Basic Solution .....	45
F. Preparation of Substituted Phenanthro- line and Bipyridyl Complexes of Chro- mium(III) .....	45
1. Reagents and Solvents .....	45

	<u>Page</u>
2. Elemental Analyses .....	45
3. Techniques .....	46
4. <u>Tris(5-chloro-1,10-phenanthroline)-</u> <u>chromium(III) Perchlorate</u> .....	46
5. <u>Tris(4,7-dimethyl-1,10-phenanthroline)-</u> <u>chromium(III) Perchlorate</u> .....	47
6. <u>Tris(4,7-diphenyl-1,10-phenanthroline)-</u> <u>chromium(III) Perchlorate</u> .....	48
7. <u>Tris(4,4'-diphenyl-2,2'-bipyridyl)-</u> <u>chromium(III) Perchlorate</u> .....	50
III. RESULTS AND DISCUSSION .....	51
A. Octahedral Substitution Mechanisms .....	51
B. Hydrolysis Reactions .....	56
1. Introduction .....	56
2. Acid Hydrolysis .....	57
3. Base Hydrolysis .....	66
C. Kinetics of Base Hydrolysis of [Cr- (bipy) <sub>3</sub> ] <sup>3+</sup> and [Cr(phen) <sub>3</sub> ] <sup>3+</sup> .....	73
1. Introduction .....	73
2. Kinetics .....	76
D. Mechanisms for the Base Hydrolysis of [Cr(bipy) <sub>3</sub> ] <sup>3+</sup> and [Cr(phen) <sub>3</sub> ] <sup>3+</sup> .....	112
1. Dissociative Pathway .....	113
2. Ion-pair Pathway .....	134
3. Gillard's Pathway .....	143
4. Associative Pathway .....	172
5. The Operative Pathway .....	199
E. Activation Parameters .....	212
1. Energy of Activation, E <sub>a</sub> .....	212
2. Entropy and Enthalpy of Activation ..	228
F. Conclusions .....	229
G. Investigation of Rhodium(III) Cations ..	240
1. General Behaviour of Rhodium(III) Cationic Complexes .....	240

	Page
2. Behaviour of $[\text{Rh}(\text{bipy})_3]^{3+}$ .....	245
H. Preparation of Substituted Polypyridyl Chromium(III) Complexes .....	248
IV. APPENDICES	
A. Calibration Curves for 1,10-phenanthroline Monohydrate at Various pH and $[\text{OH}^-]$ .....	259
B. Calibration Curve for 2,2'-bipyridine at pH 10.50 .....	268
C. Data for the Determination of the Ob- served Rate Constant for the $[\text{Cr}(\text{phen})_3]^{3+}$ System at Various pH and $[\text{OH}^-]$ .....	270
D. Data for the Determination of the Observed Rate Constant for the $[\text{Cr}(\text{bipy})_3]^{3+}$ Sys- tem at Various pH and $[\text{OH}^-]$ .....	291
E. Data for the Determination of the Observed Rate Constant at pH 11.82 at 29.5°C, and at 0.50 $[\text{OH}^-]$ at 7.5°C, for the $[\text{Cr}(\text{bipy})_3]^{3+}$ System in Oxygenated and Deoxygenated Solvent Systems .....	300
F. Plots of $\log  (A_f - A_t) $ <u>versus</u> Time for the Reaction Between $[\text{Cr}(\text{bipy})_3]^{3+}$ and Hydroxide Ion in Oxygenated and Deoxygenated Solvent Systems .....	305
G. Data for the Determination of the Observed Rate Constant as a Function of Temperature at Various pH and $[\text{OH}^-]$ for $[\text{Cr}(\text{bipy})_3]^{3+}$ and $[\text{Cr}(\text{phen})_3]^{3+}$ .....	308
H. Absorbance Values and Extinction Coeffi- cients for:	
i) $[\text{Cr}(\text{phen})_2(\text{H}_2\text{O})(\text{OH})]^{2+}$ .....	330
ii) $[\text{Cr}(\text{phen})_2(\text{H}_2\text{O})_2]^{3+}$ .....	333
iii) $[\text{Cr}(\text{phen})_2(\text{OH})_2]^+$ .....	336
I. Determination of the Observed Rate Constants for the $[\text{Cr}(\text{NN})_3]^{3+}$ Systems at Various Temperatures .....	339

	<u>Page</u>
J. Data for the Absorption Spectrum of:	
i) $[\text{Cr}(\text{bipy})_3](\text{ClO}_4)_3 \cdot 1/2 \text{H}_2\text{O}$ in 0.1 M Hydrochloric Acid .....	346
ii) $[\text{Cr}(\text{phen})_3](\text{ClO}_4)_3 \cdot 2\text{H}_2\text{O}$ in 0.1 M Hydrochloric Acid .....	349
K. Data for the Absorption Spectrum of $[\text{Rh}(\text{bipy})_3]\text{Cl}_3 \cdot 4.5 \text{H}_2\text{O}$ in Methanol .....	352
L. Data for the Absorption Spectrum of:	
i) $[\text{Cr}(5\text{-Clphen})_3](\text{ClO}_4)_3 \cdot 2\text{H}_2\text{O}$ in 0.1 M Hydrochloric Acid .....	355
ii) $[\text{Cr}(4,7\text{-Me}_2\text{phen})_3](\text{ClO}_4)_3 \cdot 2\text{H}_2\text{O}$ in Methanol .....	358
iii) $[\text{Cr}(4,7\text{-Ph}_2\text{phen})_3](\text{ClO}_4)_3 \cdot 4\text{H}_2\text{O}$ in Methanol .....	361
iv) $[\text{Cr}(4,4'\text{-Ph}_2\text{bipy})_3](\text{ClO}_4)_3 \cdot 2\text{H}_2\text{O}$ in Methanol .....	364
V. REFERENCES .....	367



LIST OF TABLES

<u>Table</u>	<u>Page</u>
I. Preparation of Solvent Systems for [Cr(bipy) <sub>3</sub> ] <sup>3+</sup> and [Cr(phen) <sub>3</sub> ] <sup>3+</sup> Systems...	13
II. Preparation of Solvent Systems for [Cr(bipy) <sub>3</sub> ] <sup>3+</sup> and [Cr(phen) <sub>3</sub> ] <sup>3+</sup> Systems...	14
III. Data for 1,10-phenanthroline Calibration Curves .....	17
IV. Data for 2,2'-bipyridine Calibration Curve.	20
V. Acid Dissociation Constants for Acetic, o-phosphoric, and Boric Acids .....	34
VI. pH Values for Solvent Systems and Calculated Ionic Strengths .....	35
VII. Activation Energies and Rate Constants for Acid Hydrolysis at 25°C of Some Cobalt(III) and Chromium(III) Complexes .....	64
VIII. Observed Pseudo First-order Rate Constants as a Function of pH or [OH <sup>-</sup> ] for [Cr(bipy) <sub>3</sub> ] <sup>3+</sup> at 11°C, μ = 1.0 M .....	91
IX. Observed Pseudo First-order Rate Constants as a Function of pH or [OH <sup>-</sup> ] for [Cr(phen) <sub>3</sub> ] <sup>3+</sup> at 31.1°C, μ = 1.0 M .....	100
X. Rates for Processes Leading to Racemization at 25°C for Polypyridyl Complexes of Iron- (II) and Nickel(II) .....	124
XI. Observed Rate Constants at Various pH or [OH <sup>-</sup> ] in Oxygenated and Deoxygenated Sol- vents for the Hydrolysis of [Cr(bipy) <sub>3</sub> ] <sup>3+</sup> ..	155
XII. Observed and Calculated Rate Constants for [Cr(bipy) <sub>3</sub> ] <sup>3+</sup> in Region (b) as Determined from Equation (188) .....	190

Table

Page

XIII. Observed and Calculated Rate Constants for  $[\text{Cr}(\text{phen})_3]^{3+}$  in Region (b) as Determined from Equation (188) ..... 191

XIV. Comparison of Observed and Calculated Rate Constants in Region (c) for  $[\text{Cr}(\text{bipy})_3]^{3+}$  System ..... 197

XV. Comparison of Observed and Calculated Rate Constants in Region (c) for  $[\text{Cr}(\text{phen})_3]^{3+}$  System ..... 198

XVI. Calculated and Observed Activation Energies for Several Chromium (III) Aquation Reactions ..... 214

XVII. Arrhenius and Eyring Activation Parameters for the Hydrolysis of  $[\text{Cr}(\text{bipy})_3]^{3+}$  ..... 225

XVIII. Arrhenius and Eyring Activation Parameters for the Hydrolysis of  $[\text{Cr}(\text{phen})_3]^{3+}$  ..... 226

XIX. Rates of Acid Hydrolysis for Some Rhodium-(III) Complexes in 0.1 M Nitric Acid ..... 241

## LIST OF FIGURES

<u>Figure</u>	<u>Page</u>
1. Absorption Spectra of $[\text{Cr}(\text{phen})_2(\text{H}_2\text{O})_2]^{3+}$ , $[\text{Cr}(\text{phen})_2(\text{OH})_2]^+$ , and $[\text{Cr}(\text{phen})_2(\text{H}_2\text{O})(\text{OH})]^{2+}$	28
2. Hydrolysis of $[\text{Cr}(\text{NH}_3)_6]^{3+}$ in 0.1 M Nitric Acid at 40°C	58
3. Hydrolysis of $[\text{Cr}(\text{NH}_3)_6]^{3+}$ in 0.1 M Sodium Hydroxide at 40°C	59
4. Base Hydrolysis of $[\text{Co}(\text{NH}_3)_5\text{Cl}]^{2+}$ via an Ion-pair Pathway	68
5. Base Hydrolysis of Cobalt(III) Complexes via an Electron-transfer Pathway	70
6. Base Hydrolysis of $[\text{Co}(\text{NH}_3)_5]^{2+}$ via an $S_N1cb$ Pathway	72
7. Structure and Numbering System for 2,2'-bipyridine and 1,10-phenanthroline	74
8. Absorption Spectrum of $[\text{Cr}(\text{bipy})_3](\text{ClO}_4)_3 \cdot 1/2\text{H}_2\text{O}$ in 0.1 M Hydrochloric Acid	77
9. Absorption Spectrum of $[\text{Cr}(\text{phen})_3](\text{ClO}_4)_3 \cdot 2\text{H}_2\text{O}$ in 0.1 M Hydrochloric Acid	79
10. Ultraviolet Absorption Spectrum of $[\text{Cr}(\text{bipy})_3]^{3+}$ at pH 11.82 and 29.5°C Depicting the Isosbestic Points	82
11. Plots of $\log \{C_0 - [\text{BIPY}]\}$ versus time in the pH range 6.03 - 10.68: 11.1°C, $C_0 \sim 1 \times 10^{-3}$ M, $\mu = 1.0$ M	85
12. Plots of $\log \{C_0 - [\text{BIPY}]\}$ versus time in the pH range 10.83 - 12.16: 11.1°C, $C_0 \sim 1 \times 10^{-3}$ M, $\mu = 1.0$ M	87

Figure

Page

13. Plots of  $\log \{C_0 - [BIPY]\}$  versus Time in the Range 0.10 - 1.00  $[OH^-]$ : 11.1°C,  $C_0 \sim 1 \times 10^{-3} M^{-1}$ ,  $\mu = 1.0 M$  ..... 89
14. Plot of pH and  $OH^-$  Dependence of the Pseudo First-Order Rate Constant for the Hydrolysis of  $[Cr(bipy)_3]^{3+}$  at 11.1°C,  $\mu = 1.0 M$ .. 92
15. Plots of  $\log \{C_0 - [PHEN]\}$  versus Time in the pH Range 4.66 - 10.50: 31.1°C,  $C_0 \sim 1 \times 10^{-3} M$ ;  $\mu = 1.0 M$  ..... 94
16. Plots of  $\log \{C_0 - [PHEN]\}$  versus Time in the pH Range 11.14 - 12.17: 31.1°C,  $C_0 \sim 1 \times 10^{-3} M$ ,  $\mu = 1.0 M$  ..... 96
17. Plots of  $\log \{C_0 - [PHEN]\}$  versus Time in the Range 0.10 - 1.00  $[OH^-]$ : 31.1°C,  $C_0 \sim 1 \times 10^{-3} M$ ,  $\mu = 1.0 M$  ..... 98
18. Plot of pH and  $OH^-$  Dependence of the Pseudo First-order Rate Constant for the Hydrolysis of  $[Cr(phen)_3]^{3+}$  at 31.1°C,  $\mu = 1.0 M$ .. 101
19. Hydroxide Ion Dependence of  $k_{obs}$  in the Hydrolysis of  $[Cr(bipy)_3]^{3+}$  in the pH Range 10.83 - 12.16 at 11.1°C ..... 105
20. Hydroxide Ion Dependence of  $k_{obs}$  in the Hydrolysis of  $[Cr(bipy)_3]^{3+}$  in the Range 0.10 - 1.00  $[OH^-]$  at 11.1°C ..... 105
21. Hydroxide Ion Dependence of  $k_{obs}$  in the Hydrolysis of  $[Cr(phen)_3]^{3+}$  in the pH Range 6.66 - 10.50 at 31.1°C ..... 107
22. Hydroxide Ion Dependence of  $k_{obs}$  in the Hydrolysis of  $[Cr(phen)_3]^{3+}$  in the pH Range 11.14 - 12.17 at 31.1°C ..... 109

23.	Hydroxide Ion Dependence of $k_{obs}$ in the Hydrolysis of $[\text{Cr}(\text{phen})_3]^{3+}$ in the Range 0.10 - 1.00 $[\text{OH}^-]$ at 31.1°C .....	109
24.	Acid Hydrolysis of $[\text{Fe}(\text{bipy})_3]^{2+}$ via a Dissociative Pathway .....	118
25.	Possible Twist Pathways for the Racemization of $[\text{Fe}(\text{phen})_3]^{2+}$ .....	121
26.	Hydrolysis of $[\text{Fe}(\text{phen})_3]^{2+}$ via Nucleophilic Attack by Water or Hydroxide Ion ...	127
27.	Hydrolysis of $[\text{Cr}(\text{bipy})_3]^{3+}$ via a Dissociative Mechanism .....	130
28.	Hydrolysis of $[\text{Cr}(\text{phen})_3]^{3+}$ via a Dissociative Mechanism .....	131
29.	Hydrolysis of $[\text{Cr}(\text{bipy})_3]^{3+}$ via an Ion-Pair Pathway .....	136
30.	Hydrolysis of $[\text{Cr}(\text{phen})_3]^{3+}$ via an Ion-Pair Pathway .....	137
31.	Hydrolysis of $[\text{Cr}(\text{NN})_3]^{3+}$ in Region (c) via an Ion-pair Pathway .....	141
32.	Equilibria of Polypyridyl Complexes Depicting Their Quaternary Character .....	145
33.	Gillard's Mechanism Applied to $[\text{M}(\text{NN})_3]^{2+}$ Complexes in the Presence of Hydroxide Ion.	147
34.	Reaction Sequence of $[\text{Ru}(\text{bipy})_3]^{3+}$ in Base via Gillard's Mechanism .....	149
35.	Reaction Sequence Between $[\text{Fe}(\text{bipy})_3]^{3+}$ and Hydroxide Ion via Gillard's Mechanism..	152
36.	Reaction of Hydroxide Ion with $[\text{M}(\text{NN})_2]^{2+}$ Complexes via Gillard's Mechanism .....	158
37.	Hydrolysis of $[\text{Cr}(\text{bipy})_3]^{3+}$ via Gillard's Mechanism .....	160

<u>Figure</u>	<u>Page</u>
38. Hydrolysis of $[\text{Cr}(\text{phen})_3]^{3+}$ via Gillard's Mechanism .....	162
39. Hydrolysis of $[\text{Cr}(\text{bipy})_3]^{3+}$ via a General Treatment of Gillard's Mechanism .....	168
40. Hydrolysis of $[\text{Cr}(\text{bipy})_3]^{3+}$ via an Associative Pathway .....	173
41. Hydrolysis of $[\text{Cr}(\text{phen})_3]^{3+}$ via an Associative Pathway .....	175
42. Hydrolysis of $[\text{Cr}(\text{NN})_3]^{3+}$ via an Associative Pathway Which Accounts for the Observed Kinetics .....	181
43. Plot of $(k_{\text{obs}} - k_x)/[\text{OH}^-]$ versus $[\text{OH}^-]$ for the Hydrolysis of $[\text{Cr}(\text{bipy})_3]^{3+}$ in the Range 0.10 - 1.00 $[\text{OH}^-]$ at 11.1°C .....	193
44. Plot of $(k_{\text{obs}} - k_x)/[\text{OH}^-]$ versus $[\text{OH}^-]$ for the Hydrolysis of $[\text{Cr}(\text{phen})_3]^{3+}$ in the Range 0.10 - 1.00 $[\text{OH}^-]$ at 31.1°C .....	195
45. The Thermal Hydrolysis of $[\text{Cr}(\text{NN})_3]^{3+}$ in Acidic and Basic Solution .....	201
46. Arrhenius Plot ( $\log k_{\text{obs}}$ versus $10^3/T$ ) for $[\text{Cr}(\text{bipy})_3]^{3+}$ at pH 11.82 .....	215
47. Arrhenius Plot ( $\log k_{\text{obs}}$ versus $10^3/T$ ) for $[\text{Cr}(\text{bipy})_3]^{3+}$ at 0.50 $[\text{OH}^-]$ .....	217
48. Arrhenius Plot ( $\log k_{\text{obs}}$ versus $10^3/T$ ) for $[\text{Cr}(\text{phen})_3]^{3+}$ at pH 10.10 .....	219
49. Arrhenius Plot ( $\log k_{\text{obs}}$ versus $10^3/T$ ) for $[\text{Cr}(\text{phen})_3]^{3+}$ at pH 12.17 .....	221
50. Arrhenius Plot ( $\log k_{\text{obs}}$ versus $10^3/T$ ) for $[\text{Cr}(\text{phen})_3]^{3+}$ at 0.80 $[\text{OH}^-]$ .....	223
51. Associative Interchange Pathway for the Photochemical Reaction Between $[\text{Cr}(\text{bipy})_3]^{3+}$ and Hydroxide Ion .....	236

Figure

Page

52.	Gillard's Pathway for the Photochemical Reaction Between $[\text{Cr}(\text{bipy})_3]^{3+}$ and Hydroxide Ion .....	237
53.	Proposed Electrochemical Reaction Sequence for $[\text{Rh}(\text{bipy})_3]^{3+}$ in Acetonitrile .....	244
54.	Absorption Spectrum of $[\text{Rh}(\text{bipy})_3]\text{Cl}_3 \cdot 4.5 \text{ H}_2\text{O}$ in Methanol .....	246
55.	Absorption Spectrum of $[(5\text{-Clphen})_3]-(\text{ClO}_4)_3 \cdot 2\text{H}_2\text{O}$ in 0.01 M Hydrochloric Acid ..	251
56.	Absorption Spectrum of $[\text{Cr}(4,7\text{-Me}_2\text{phen})_3]-(\text{ClO}_4)_3 \cdot 2\text{H}_2\text{O}$ in Methanol .....	253
57.	Absorption Spectrum of $[\text{Cr}(4,7\text{-Ph}_2\text{phen})_3]-(\text{ClO}_4)_3 \cdot 4\text{H}_2\text{O}$ in Methanol .....	255
58.	Absorption Spectrum of $[\text{Cr}(4,4'\text{-Ph}_2\text{bipy})_3]-(\text{ClO}_4)_3 \cdot 2\text{H}_2\text{O}$ in Methanol .....	257

## LIST OF APPENDICES

<u>Appendix</u>	<u>Page</u>
A. Calibration Curves (Absorbance <u>versus</u> [PHEN]) for 1,10-phenanthroline mono-hydrate at Various pH and $[\text{OH}^-]$ .....	259
B. Calibration Curve (Absorbance <u>versus</u> [BIPY]) for 2,2'-bipyridine at pH 10.50 .....	268
C. Data for the Determination of the Observed Rate Constant $k_{\text{obs}}$ for the $[\text{Cr}(\text{phen})_3]^{3+}$ System at Various pH and $[\text{OH}^-]$ .....	270
D. Data for the Determination of the Observed Rate Constant $k_{\text{obs}}$ for the $[\text{Cr}(\text{bipy})_3]^{3+}$ System at Various pH and $[\text{OH}^-]$ .....	291
E. Data for the Determination of the Observed Rate Constant $k_{\text{obs}}$ at pH 11.82 at 29.5°C, and 0.50 $[\text{OH}^-]$ at 7.5°C, for the $[\text{Cr}(\text{bipy})_3]^{3+}$ System in Oxygenated and Deoxygenated Solvents .....	300
F. Plots of $\log  (A_f - A_t) $ <u>versus</u> Time for the Reaction Between $[\text{Cr}(\text{bipy})_3]^{3+}$ and $\text{OH}^-$ in Oxygenated and Deoxygenated Solvents .....	305
G. Data for the Determination of the Observed Rate Constant as a Function of Temperature at Various pH and $[\text{OH}^-]$ for the $[\text{Cr}(\text{bipy})_3]^{3+}$ and $[\text{Cr}(\text{phen})_3]^{3+}$ Systems .....	308
H. Spectral Data for:	
i) $[\text{Cr}(\text{phen})_2(\text{H}_2\text{O})(\text{OH})]^{2+}$ .....	330
ii) $[\text{Cr}(\text{phen})_2(\text{H}_2\text{O})_2]^{3+}$ .....	333
iii) $[\text{Cr}(\text{phen})_2(\text{OH})_2]^+$ .....	336



I.	Determination of the Observed Rate Constants for the $[\text{Cr}(\text{NN})_3]^{3+}$ Systems at Various Temperatures:	
	i) $[\text{Cr}(\text{bipy})_3]^{3+}$ System	340
	ii) $[\text{Cr}(\text{phen})_3]^{3+}$ System	342
J.	Data for the Absorption Spectrum of:	
	i) $[\text{Cr}(\text{bipy})_3](\text{ClO}_4)_3 \cdot 1/2 \text{H}_2\text{O}$ in 0.1 M Hydrochloric Acid	346
	ii) $[\text{Cr}(\text{phen})_3](\text{ClO}_4)_3 \cdot 2\text{H}_2\text{O}$ in 0.1 M Hydrochloric Acid	349
K.	Data for the Absorption Spectrum of $[\text{Rh}(\text{bipy})_3]\text{Cl}_3 \cdot 4.5 \text{H}_2\text{O}$ in Methanol	352
L.	Data for the Absorption Spectrum of:	
	i) $[\text{Cr}(5\text{-Clphen})_3](\text{ClO}_4)_3 \cdot 2\text{H}_2\text{O}$ in 0.1 M Hydrochloric Acid	355
	ii) $[\text{Cr}(4,7\text{-Me}_2\text{phen})_3](\text{ClO}_4)_3 \cdot 2 \text{H}_2\text{O}$ in Methanol	358
	iii) $[\text{Cr}(4,7\text{-Ph}_2\text{phen})_3](\text{ClO}_4)_3 \cdot 4 \text{H}_2\text{O}$ in Methanol	361
	iv) $[\text{Cr}(4,4'\text{-Ph}_2\text{bipy})_3](\text{ClO}_4)_3 \cdot 2 \text{H}_2\text{O}$ in Methanol	364

## I. INTRODUCTION

Substitution reactions of octahedral transition metal complexes have been extensively studied over the years in an effort to elucidate the mechanism(s) by which they proceed. The general mechanisms for substitution reactions of such complexes have been classified by Langford and Gray [1,2] and Swaddle [3] as either associative (A or  $I_a$ ) or dissociative (D or  $I_d$ ). The most common substitution reaction is hydrolysis, whether in acidic (aquation) or basic media. Such reactions present an interesting challenge because the solvent also serves as the nucleophile.

More recently, there has been interest in the hydrolysis reactions of metal chelates of the type  $[M(NN)_x]^{n+}$ , where (NN) refers to some N-heterocyclic ligand and  $x = 2$  or 3. Racemization and dissociation studies of  $[Fe(bipy)_3]^{2+}$  [4,5,6,7] have shown that this iron(II) chelate undergoes acid hydrolysis via a dissociative (D) pathway to yield a pentacoordinate intermediate species. Analogous studies on the  $[Fe(phen)_3]^{2+}$  cation [5] suggest a dissociative pathway for this cation, although some doubt about the

plausibility of the rigid phenanthroline ligand acting as a unidentate ligand has arisen. A dissociative mechanism has also been ascribed to the aquation of iron(II) chelates with tridentate ligands, namely  $[\text{Fe}(\text{TPTZ})_2]^{2+}$  [8] and  $[\text{Fe}(\text{terpy})_2]^{2+}$  [9], in which successive Fe-N bond-rupture yields a pentacoordinate intermediate species <sup>a</sup>. Dissociation and racemization studies on the tris-bipyridyl and tris-phenanthroline complexes of nickel(II) [10,11,12] reveal that these also undergo hydrolysis via a dissociative pathway.

The anomalous behaviour of bipyridyl and phenanthroline complexes of some transition metal ions has prompted Gillard [13,14] to postulate a base hydrolysis mechanism involving nucleophilic attack by water or hydroxide ion on the carbon atom adjacent to the nitrogen atom of the ligand. The result of such an attack is the formation of a covalent hydrate which is capable of undergoing protonation, intramolecular hydroxyl shift, or deprotonation. This pathway, herein referred to as Gillard's mechanism, has been postulated for the base hydrolysis of  $[\text{Ru}(\text{bipy})_3]^{3+}$  [15].

---

<sup>a</sup> TPTZ = 2,4,6-tripyridyl-s-triazine; terpy = 2,2',2''-terpyridine.

The hydrolyses of tris-bipyridyl and tris-phenanthroline complexes of chromium(III) present an interesting challenge in view of Swaddle's contention [3] that cationic complexes of chromium(III) undergo substitution via an associative-type mechanism (A or  $I_a$ ) in those instances where an  $S_N1_{cb}$  mechanism is not applicable, and where the trans-effect [4] does not predominate. As the bipyridine and phenanthroline ligands do not possess any ionizable hydrogen atoms, an  $S_N1_{cb}$  pathway is implausible; further, the trans-effect is not operative in a tris-chelate. Maestri *et al.* [16] have investigated the hydrolysis of  $[Cr(bipy)_3]^{3+}$  in the pH range 0 - 10.7 at 11°C, and postulated several mechanisms to account for the observed kinetics. The two most likely pathways for this chromium(III) cation under the conditions of the experiment are an associative mechanism involving nucleophilic attack on the central metal ion to produce a heptacoordinate aquo-intermediate, and Gillard's mechanism involving nucleophilic attack on the  $C_6$  (or  $C_6'$ ) position of the bipyridine ring to yield a covalent hydrate. The former pathway was concluded [16] as more appropriate. The hydrolysis of  $[Cr(bipy)_3]^{3+}$  up to pH 14 at 11°C, and of  $[Cr(phen)_3]^{3+}$  from pH 0 - 14 at 31.1°C, have been investigated in an effort to further elucidate the most plausible mechanism(s) for the hydrolysis of each of

the two chromium(III) cations. Temperature-dependence studies have been carried out to determine the activation parameters for each system.

The current interest in tris-chelates prompted further investigation of complexes of other transition metal ions. The hydrolysis of the  $[\text{Rh}(\text{bipy})_2\text{Cl}_2]^+$  cation was studied [17] and the complex was found to be inert to substitution in both aqueous acidic and basic media at 80°C. Similar behaviour is exhibited by the rhodium(III) cation  $[\text{Rh}(\text{bipy})_3]^{3+}$  in acidic and basic media at 25°C. Thus, a kinetic investigation was not undertaken for this cation.

Presently, active research centers around the photochemistry of transition metal compounds, with concentrated efforts in the areas of transition metal hydrides and polypyridyl-chelates of transition metal ions. The photochemical and photophysical behaviour of chromium(III) chelates is receiving increased attention owing to the relatively long lifetimes of their lowest excited states and the high reactivity of these excited states toward redox quenchers. The photoreactivity of  $[\text{Cr}(\text{bipy})_3]^{3+}$  has been investigated [18]. Several new polypyridyl chelates of chromium(III) have been prepared for photochemical investigation, including  $[\text{Cr}(5\text{-Clphen})_3]^{3+}$ ,  $[\text{Cr}(4,7\text{-Me}_2\text{phen})_3]^{3+}$ ,  $[\text{Cr}(4,7\text{-Ph}_2\text{-phen})_3]^{3+}$ , and  $[\text{Cr}(4,4'\text{-Ph}_2\text{bipy})_3]^{3+}$ . The preparations

of these cationic species and absorption spectra are included in Sections II-F and III, respectively.

## II. EXPERIMENTAL

### A. Preparation of Compounds for Kinetic Measurements.

#### 1. Reagents and Solvents.

The following reagents were used as received from commercial suppliers without further purification: chromium(III) nitrate nonahydrate (Anachemia); anhydrous chromium(II) chloride, 98% (Alfa Products); 1,10-phenanthroline monohydrate (Sigma); 2,2'-bipyridine (Eastman); chlorine gas (Matheson); and oxygen gas (Matheson). Reagent grade absolute methanol (Anachemia) was used as supplied. Sodium hydroxide (5 M) was prepared from dilution of 50% (w/w) sodium hydroxide (Fisher Scientific); all nitric acid solutions were prepared by dilution of 70% (w/w) nitric acid (Baker Chemical); and perchloric acid solutions were prepared by dilution of reagent grade 70% (w/w) perchloric acid (Allied Chemical).

#### 2. General Techniques.

The syntheses of compounds, prepared with chromium(II) chloride, were carried out in a nitrogen-purged glove bag using deoxygenated solvents to avoid premature oxidation of the chromous complex. Thus, a stream of nitrogen gas was bubbled through the solvents for ca. 45 minutes immediately prior to use. All filtrations were performed using sintered-glass funnels connected

to a water aspirator. Oxidation of the chromous complexes by chlorine gas was carried out in a well-ventilated fumehood. Tygon tubing connected the lecture bottle to a sintered-glass dispersion tube, and the chlorine gas bubbled through the reaction solution until the solution was oxidized as noted by a change of colour from purple to yellow. Drying of the final product was carried out in vacuo.

### 3. Elemental Analyses.

Elemental analyses were performed by Galbraith Laboratories, Inc., Knoxville, Tennessee. In those preparations where elemental analyses were not performed, the ultraviolet absorption spectrum of the final product was recorded and compared with published spectra.

### 4. Tris(1,10-phenanthroline)chromium(III) Perchlorate.

This product was synthesized by a modified procedure of Hunt et al. [19]. In a nitrogen-purged glove bag, a solution of 1.08 g (8.79 mmol) chromium(II) chloride dissolved in 150 ml deoxygenated, distilled water containing a few drops of 70% perchloric acid was added to a solution of 5.17 g (26.1 mmol) 1,10-phenanthroline monohydrate in 50 ml deoxygenated methanol. The resulting dark olive green mixture was stirred for 15 minutes, after which it was removed from the glove bag and chlorine gas was bubbled through it for 40 minutes. During this time, 2 ml of a saturated sodium perchlorate



solution was added. The resulting yellow solution was filtered and the crude, solid yellow product collected. The crude product was recrystallized from hot, distilled water containing a few drops of concentrated hydrochloric acid. The hot solution was filtered, and the filtrate allowed to cool to induce crystallization. The solution was then filtered, and the yellow product was subsequently collected and dried. Recrystallization was repeated until the pure product,  $[\text{Cr}(\text{phen})_3](\text{ClO}_4)_3 \cdot 2\text{H}_2\text{O}$  was obtained. Yield 4.3 g (53% of theoretical).

Analysis: Calc<sup>d</sup> for  $\text{CrC}_{36}\text{H}_{28}\text{N}_6\text{Cl}_3\text{O}_{14}$ : C, 46.64; H, 3.04; N, 9.07; Found: C, 46.93; H, 3.02; N, 9.11.

#### 5. Tris(2,2'-bipyridyl)chromium(III) Perchlorate.

The compound was prepared by a modified method of Baker and Mehta [20]. A solution of 2.13 g (17.3 mmol) chromium(II) chloride dissolved in 150 ml deoxygenated  $10^{-2}$  M perchloric acid was added to a 100-ml suspension of 8.23 g (52.7 mmol) 2,2'-bipyridine in  $10^{-2}$  M perchloric acid in a nitrogen-purged glove bag. The resulting black mixture was stirred for 20 minutes, and subsequently 50 ml of a concentrated sodium perchlorate solution, 150 ml of distilled water, and 2 ml of 1 M perchloric acid were added to the solution. The solution was then removed from the glove bag and oxygen gas bubbled through it for 1.5 hours with stirring. The resulting yellow solution was filtered to yield a

solid yellow product, which was dissolved in 500 ml of hot  $10^{-4}$  M perchloric acid. The volume of the solution was reduced to about 50 ml by additional heating. On cooling, a yellow product formed which was collected, washed twice with 95% ethanol, once with chloroform, and twice with n-heptane. The yield of the product,  $[\text{Cr}(\text{bipy})_3](\text{ClO}_4)_3 \cdot 1/2\text{H}_2\text{O}$ , was 10.6 g (74% of theoretical). The purity of the product was determined by comparison of its absorption spectrum with that reported in the literature.[20].

6. Di aquobis(1,10-phenanthroline)chromium(III) Nitrate.

This compound was prepared by a modified procedure of Inskip and Bjerrum [21]. Thus, a solution of 4.00 g (10.0 mmol) chromium(III) nitrate nonahydrate and 7.21 g (36.4 mmol) of 1,10-phenanthroline monohydrate suspended in 100 ml of 0.4 M nitric acid was refluxed for 8 hours. After each hour of reflux, 5 M sodium hydroxide was added, as necessary, to maintain the pH of the reaction mixture at ca. 7. After the reflux was completed, concentrated nitric acid was added (ca. 4 ml) to adjust the pH to 1. The solution volume was reduced to one-half the original volume with heating. The hot solution was then filtered, allowed to cool to room temperature, and then stored in the cold ( $0^\circ\text{C}$ ) to induce crystallization of the crude product. The crude pinkish-red product was filtered and subsequently recrystallized

from 0.1 M nitric acid. The complex,  $[\text{Cr}(\text{phen})_2(\text{H}_2\text{O})_2](\text{NO}_3)_3 \cdot 3/2\text{H}_2\text{O}$  was collected (3.05 g, 46% of theoretical); and its purity ascertained by comparison of the ultraviolet absorption spectrum with that reported by Inskeep and Bjerrum [21].

## B. Kinetic Measurements.

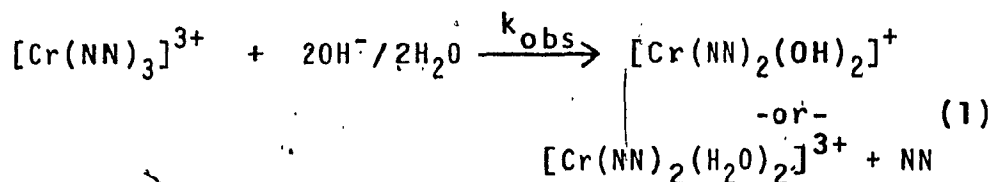
### 1. General Techniques.

Owing to the enhanced rate of ligand substitution in the presence of ordinary laboratory fluorescent lighting, all experiments were performed in dim, red light. Solutions were thermostated to  $\pm 0.1^\circ\text{C}$  in an electronic, constant-temperature water bath (Lauda, model K4R).

All absorption spectra were recorded on an AMINCO-Bowman DW-2 UV/VIS spectrophotometer, equipped with deuterium and tungsten-iodide lamps. Ultraviolet spectra were recorded in the range 210 - 360 nm, and visible spectra in the 350 - 650 nm range, unless otherwise noted. The spectrophotometer was calibrated as per the instructions [22] provided by the manufacturer, at 300 nm prior to use.

The observed rate constants for the hydrolysis of the  $[\text{Cr}(\text{phen})_3]^{3+}$  complex ion were determined at  $31.1 \pm 0.1^\circ\text{C}$ , and those for  $[\text{Cr}(\text{bipy})_3]^{3+}$  were determined at  $11 \pm 0.1^\circ\text{C}$ . The temperatures were chosen so that the reactions

had a convenient half-life. The overall reaction is



The course of the reaction was followed by extraction of the released polypyridine NN using hexanes (or n-heptane) from the acidic or basic aqueous solutions at various time intervals. The concentration of free NN was then determined from the appropriate calibration curve (see Section II-3,ab), or calculated from the slopes of the calibration plots.

2. Solvents, Solvent Systems, and Preparation of Solutions.

a. Solvents.

Hydrochloric acid solutions (or sodium hydroxide) were prepared by dilution of hydrochloric acid (or sodium hydroxide) concentrates, as supplied by Fisher Scientific. Reagent grade sodium chloride (Fisher Scientific) was used to maintain constant ionic strength. Boric acid (Fisher Scientific), reagent grade acetic acid (Fisher Scientific), and ortho-phosphoric acid (85% w/w, Fisher Scientific) were used to prepare the Britton-Robinson buffers [23]. Distilled water was used in all preparations. Spectroanalysed hexanes and n-heptane (Fisher Scientific) were used as supplied.

b. Preparation of Solutions.

i) Sodium chloride (4 M) was prepared by dissolving 233.8 g of reagent grade sodium chloride in one liter of distilled water.

ii) The Britton-Robinson stock solution was prepared according to the procedure of Mongay and Cerda [23]. Dilution of a mixture of 11.5 ml of acetic acid, 7.5 ml of ortho-phosphoric acid, and 12.4 g of boric acid to 1.00 liter gave a 0.20 M solution.

iii) Sodium hydroxide (1.000 ± 0.0005 M) and hydrochloric acid (0.1000 ± 0.0005 M) were prepared by dilution of the appropriate concentrations.

c. Solvent Systems for  $[\text{Cr}(\text{phen})_3]^{3+}$ .

i) In the pH range 4.66 - 12.17, the solvent systems contain 0.1000 ± 0.0005 M sodium hydroxide, 4 M sodium chloride, and 0.20 M Britton-Robinson stock solution in the volumes given in Table I. The pH of these solutions was measured using a Metrohm-Herisau E463 potentiograph, equipped with a combination glass-calomel (saturated potassium chloride) electrode.

ii) For sodium hydroxide concentrations of 0.10, 0.30, 0.50, and 0.80  $[\text{OH}^-]$ , it was necessary to use sodium chloride to maintain an ionic strength of 1.0 M. The volume of 1.000 ± 0.0005 M sodium hydroxide and weight of sodium chloride required for the appropriate  $[\text{OH}^-]$  used in this study are presented in Table II.

Table I

Preparation of Solvent Systems for  $[\text{Cr}(\text{bipy})_3]^{3+}$  and  
 $[\text{Cr}(\text{phen})_3]^{3+}$  Systems<sup>a</sup>

pH ( $\pm 0.05$ )	4 M NaCl (ml)	0.2 M BR <sup>b</sup> (ml)	0.1000 M NaOH (ml)
4.66	125.00	20.00	60.00
5.53	125.00	20.00	80.00
6.66	125.00	20.00	105.0
7.75	125.00	20.00	120.0
8.43	125.00	20.00	130.0
8.88	125.00	20.00	135.0
9.45	125.00	20.00	150.0
10.15	125.00	20.00	165.0
10.50	125.00	20.00	175.0
10.83	125.00	20.00	185.0
11.14	125.00	20.00	200.0
11.31	125.00	20.00	220.0
11.67	125.00	20.00	245.0
11.82	125.00	20.00	265.0
12.17	125.00	20.00	300.0

<sup>a</sup> Volume of solution is 500.0 ml

<sup>b</sup> BR = Britton-Robinson stock solution.

Table II

Preparation of Solvent Systems for  $[\text{Cr}(\text{bipy})_3]^{3+}$  and  
 $[\text{Cr}(\text{phen})_3]^{3+}$  Systems<sup>a</sup>

<u><math>[\text{OH}^-]</math></u>	<u>1.000 M NaOH (ml)</u>	<u>NaCl (g)</u>
0.10	50.00	26.302
0.30	167.0	20.458
0.50	250.0	14.612
0.80	400.0	5.845
1.00	500.0	---

<sup>a</sup> Volume of solution is 500.0 ml.

d. Solvent Systems for  $[\text{Cr}(\text{bipy})_3]^{3+}$ .

i) In the pH range 10.83 - 12.16, the volumes of sodium hydroxide ( $0.1000 \pm 0.005 \text{ M}$ ), sodium chloride ( $4 \text{ M}$ ), and Britton-Robinson stock solution ( $0.2 \text{ M}$ ) used are given in Table I. The pH of these solutions were measured in the same manner as previously mentioned for the  $[\text{Cr}(\text{phen})_3]^{3+}$  system.

ii) For sodium hydroxide concentrations of 0.10, 0.50, and 0.80  $[\text{OH}^-]$ , the volumes of sodium hydroxide and weight of sodium chloride required are presented in Table II.

3. Calibration Curves.

The reaction between  $[\text{Cr}(\text{phen})_3]^{3+}$  and water (or hydroxide ion) and that between  $[\text{Cr}(\text{bipy})_3]^{3+}$  and water (or hydroxide ion) was followed as mentioned earlier by measuring the amount of free 1,10-phenanthroline or free 2,2'-bipyridine released, respectively. Calibration curves were obtained for each system using the procedures outlined below.

a. Calibration Curves for  $[\text{Cr}(\text{phen})_3]^{3+}$ .

1,10-phenanthroline monohydrate (ca.  $1 \times 10^{-3}$  mole) was dissolved in 50.00 ml of solvent at the desired pH (or  $[\text{OH}^-]$ ). Three or four dilutions of the original solution were prepared to obtain solutions over the concentration range  $10^{-3} - 10^{-5} \text{ M}$ . Two ml of each solution was pipetted into a 25-ml screw-top, glass vial



containing exactly 5.00 ml of hexanes. The solution was shaken manually for exactly one minute, and allowed to stand for two minutes. With the aid of a Pasteur pipet, a sufficient volume of the upper non-aqueous phase containing 1,10-phenanthroline was transferred to a cuvet, and the ultraviolet absorption spectrum recorded in the range 210 - 290 nm. The concentrations of the 1,10-phenanthroline solutions and the absorbance maxima at 231 and 262 nm were recorded, and plotted to obtain the calibration curve. This procedure was followed for each of the following solutions of pH 5.53, 6.66, 7.75, 8.43, 8.88, 10.15, 11.14, and 0.80  $[OH^-]$ . The data and calibration curves are presented in Table III and Appendix A, respectively.

b. Calibration Curve for  $[Cr(bipy)_3]^{3+}$ .

The same general procedure was followed as that for the calibration curves for  $[Cr(phen)_3]^{3+}$  described above, except for the following alterations: (i) it was necessary to construct only one calibration curve, at pH 10.50, as the absorbance was constant over the entire pH range studied; (ii) n-heptane was used for the extraction procedure; (iii) the ultraviolet absorption spectrum was recorded in the 210 - 320 nm range for the upper non-aqueous phase; (iv) absorbance maxima at 237 and 282 nm were recorded and plotted against concentration of 2,2'-bipyridine to obtain the calibration

Table III

Data for the 1,10-phenanthroline Calibration Curves

a) pH = 5.53;  $C_0 = 1.1 \times 10^{-3}$  M.

No.	[PHEN] (M)	Absorbance <sup>a</sup>	
		231 nm	262 nm.
1	$1.099 \times 10^{-3}$	---	1.795
2	$4.399 \times 10^{-4}$	1.430	0.765
3	$2.199 \times 10^{-4}$	0.693	0.379
4	$1.099 \times 10^{-4}$	0.323	0.178

$$A_{231} = 3.233 \times 10^{+3} [\text{PHEN}]; \quad A_{262} = 1.644 \times 10^{+3} [\text{PHEN}]$$

b) pH = 6.66;  $C_0 = 1.28 \times 10^{-3}$  M.

No.	[PHEN] (M)	Absorbance <sup>a</sup>	
		231 nm	262 nm
1	$6.407 \times 10^{-4}$	---	1.370
2	$3.844 \times 10^{-4}$	1.435	0.768
3	$2.563 \times 10^{-4}$	0.970	0.545
4	$1.281 \times 10^{-4}$	0.503	0.272

$$A_{231} = 3.752 \times 10^{+3} [\text{PHEN}]; \quad A_{262} = 2.108 \times 10^{+3} [\text{PHEN}]$$

<sup>a</sup> error in absorbance is  $\pm 0.005$ .

Table III (cont'd) -18-

c) pH = 7.75;  $C_0 = 1.1 \times 10^{-3}$  M.

No.	[PHEN] (M)	Absorbance <sup>a</sup>	
		231 nm	262 nm
1	$5.484 \times 10^{-4}$	1.756	0.962
2	$4.387 \times 10^{-4}$	1.470	0.786
3	$3.290 \times 10^{-4}$	1.114	0.598
4	$1.097 \times 10^{-4}$	0.380	0.209

$$A_{231} = 3.272 \times 10^{+3} [\text{PHEN}]; \quad A_{262} = 1.773 \times 10^{+3} [\text{PHEN}]$$

d) pH = 8.43;  $C_0 = 1.3 \times 10^{-3}$  M.

No.	[PHEN] (M)	Absorbance <sup>a</sup>	
		231 nm	262 nm
1	$6.508 \times 10^{-4}$	---	1.365
2	$5.206 \times 10^{-4}$	1.944	1.105
3	$3.905 \times 10^{-4}$	1.589	0.854
4	$1.302 \times 10^{-4}$	0.538	0.293

$$A_{231} = 3.845 \times 10^{+3} [\text{PHEN}]; \quad A_{262} = 2.116 \times 10^{+3} [\text{PHEN}]$$

e) pH = 8.88;  $C_0 = 1.0 \times 10^{-3}$  M.

No.	[PHEN] (M)	Absorbance <sup>a</sup>	
		231 nm	262 nm
1	$5.156 \times 10^{-4}$	1.778	0.988
2	$4.125 \times 10^{-4}$	1.472	0.792
3	$3.094 \times 10^{-4}$	1.102	0.600
4	$2.062 \times 10^{-4}$	0.715	0.391
5	$4.125 \times 10^{-5}$	0.136	0.077

$$A_{231} = 3.504 \times 10^{+3} [\text{PHEN}]; \quad A_{262} = 1.921 \times 10^{+3} [\text{PHEN}]$$

Table III (cont'd)

-19-

f) pH = 10.15;  $C_0 = 9.7 \times 10^{-4}$  M.

No.	[PHEN] (M)	Absorbance <sup>a</sup>	
		231 nm	262 nm
1	$4.838 \times 10^{-4}$	1.396	0.758
2	$3.870 \times 10^{-4}$	1.234	0.669
3	$2.903 \times 10^{-4}$	0.993	0.538
4	$1.935 \times 10^{-4}$	0.606	0.320
5	$1.161 \times 10^{-4}$	0.356	0.191

$$A_{231} = 3.221 \times 10^{+3} [\text{PHEN}]; \quad A_{262} = 1.657 \times 10^{+3} [\text{PHEN}]$$

g) pH = 11.14;  $C_0 = 1.8 \times 10^{-3}$  M.

No.	[PHEN] (M)	Absorbance <sup>a</sup>	
		231 nm	262 nm
1	$5.509 \times 10^{-4}$	---	1.180
2	$3.673 \times 10^{-4}$	1.470	0.817
3	$2.204 \times 10^{-4}$	0.890	0.481
4	$1.469 \times 10^{-4}$	0.596	0.320

$$A_{231} = 4.013 \times 10^{+3} [\text{PHEN}]; \quad A_{262} = 2.165 \times 10^{+3} [\text{PHEN}]$$

h) 0.80 [OH<sup>-</sup>];  $C_0 = 1.1 \times 10^{-3}$  M.

No.	[PHEN] (M)	Absorbance <sup>a</sup>	
		231 nm	262 nm
1	$5.403 \times 10^{-4}$	1.924	1.140
2	$4.322 \times 10^{-4}$	1.674	0.916
3	$3.242 \times 10^{-4}$	1.240	0.668
4	$1.297 \times 10^{-4}$	0.470	0.252

$$A_{231} = 3.697 \times 10^{+3} [\text{PHEN}]; \quad A_{262} = 1.936 \times 10^{+3} [\text{PHEN}]$$

Table IV

Data for the 2,2'-bipyridine Calibration Curve at pH 10.5

pH = 10.5;  $C_0 = 1.84 \times 10^{-3}$  M.

No.	[BIPY] (M)	Absorbance <sup>a</sup>	
		237 nm	282 nm
1	$1.838 \times 10^{-4}$	0.820	1.046
2	$1.470 \times 10^{-4}$	0.658	0.821
3	$1.102 \times 10^{-4}$	0.484	0.606
4	$7.35 \times 10^{-5}$	0.324	0.409

<sup>a</sup> The error in the absorbance is  $\pm 0.005$ .

curve which is shown in Appendix B. The pertinent data are presented in Table IV.

4. Determination of the Observed Rate Constant,  
 $k_{obs}$ .

a.  $[\text{Cr}(\text{phen})_3]^{3+}$  System.

A 50.00 ml solution of  $[\text{Cr}(\text{phen})_3]^{3+}$  (ca.  $1 \times 10^{-3} \text{ M} = C_0$ ) of the desired pH (or  $[\text{OH}^-]$ ) was prepared and thermostated at the appropriate temperature. At various times, a 2.00-ml aliquot was pipetted into a screw-top, glass vial containing exactly 5.00 ml hexanes. The mixture was shaken manually for exactly one minute, and allowed to stand for two minutes. With the aid of a Pasteur pipet, a sufficient volume of the upper non-aqueous phase containing released 1,10-phenanthroline was transferred to a cuvet, and the ultraviolet absorption spectrum of the solution was recorded from 210 - 290 nm. The extraction procedure was repeated at various time intervals.

The above procedure was followed in solvent systems of pH 4.66 - 12.17, for  $[\text{OH}^-]$  of 0.10 - 1.00, and in 0.1 M hydrochloric acid. The data are presented in Appendix C.

b.  $[\text{Cr}(\text{bipy})_3]^{3+}$  System.

The same procedure as that for  $[\text{Cr}(\text{phen})_3]^{3+}$  was followed for the determination of the observed rate constant, except for the following alterations: (i) n-heptane was used in the extraction procedure rather than

hexanes; (ii) the absorption spectrum was recorded in the range 210 - 320 nm, for the released 2,2'-bipyridine; (iii) the procedure was carried out for solvent systems of pH 10.83 - 12.16, and 0.10 - 1.00  $[\text{OH}^-]$ .

The data are presented in Appendix D.

5. Isosbestic Points.

a.  $[\text{Cr}(\text{phen})_3]^{3+}$  System.

A buffered solution of  $[\text{Cr}(\text{phen})_3]^{3+}$  ( $3.128 \times 10^{-5} \text{ M} = C_0$ ) at pH 11.82 was prepared and thermostated at  $30.5 \pm 0.1^\circ\text{C}$ . The ultraviolet absorption spectrum of the solution was recorded over a period of fourteen hours. The solution was kept in the analysing cuvet over the entire period, with a water-jacketed cell mount attached to maintain constant temperature. The analysing beam was blocked between spectral scans to avoid possible decomposition.

b.  $[\text{Cr}(\text{bipy})_3]^{3+}$  System.

A buffered solution of  $[\text{Cr}(\text{bipy})_3]^{3+}$  ( $6.208 \times 10^{-5} \text{ M} = C_0$ ) at pH 11.82 and 0.50  $[\text{OH}^-]$  was prepared and thermostated at  $29.5 \pm 0.1^\circ\text{C}$ . The ultraviolet absorption spectrum was recorded over a period of 12.5 hrs. The same precautions as those described for the  $[\text{Cr}(\text{phen})_3]^{3+}$  system above were observed.

6. Kinetics in Oxygenated and Deoxygenated Solvents.

To determine whether or not the rate of hydrolysis was affected by the presence of oxygen, the reaction

was followed spectrophotometrically in oxygenated and deoxygenated solvent systems for  $[\text{Cr}(\text{bipy})_3]^{3+}$ . The following procedures were followed.

a. Oxygenated Solvent System.

Solutions of  $[\text{Cr}(\text{bipy})_3]^{3+}$  (ca.  $7 \times 10^{-5} \text{ M}$ ) at pH 11.82 and 0.50  $[\text{OH}^-]$  were prepared and thermostated at 29.5 and  $7.5 \pm 0.1^\circ\text{C}$ , respectively. Sufficient solution volume was transferred to a cuvet, and the ultraviolet absorption spectrum was recorded for a period of eight hours or longer. The solution was kept in the analysing cuvet for the entire time period, and the analysing beam was blocked between spectral scans to avoid possible rate enhancement by light. A water-jacketed cell mount was used to insure constant temperature.

b. Deoxygenated Solvent System.

Solvent systems of pH 11.82 and 0.50  $[\text{OH}^-]$  were deoxygenated for 1.5 hours by passing a stream of nitrogen gas through the solvent, stored in a nitrogen-purged glove bag, immediately prior to use. A solution of  $[\text{Cr}(\text{bipy})_3]^{3+}$  (ca.  $5 \times 10^{-5} \text{ M} = C_0$ ) of each solvent was prepared inside a nitrogen-purged glove bag. A sufficient volume of the chromium(III) complex solution was transferred to an analysing cuvet and sealed with a solid, pure gum rubber stopper. The ultraviolet absorption spectrum was recorded over a period of 8.5 hours.



or longer. At pH 11.82 and 0.50  $[\text{OH}^-]$ , the spectral scans were recorded at 29.5 and  $7.5 \pm 0.1^\circ\text{C}$ , respectively. The analysing beam was again blocked between spectral scans to avoid possible rate enhancement. Pertinent data are given in Appendices E and F; and the results of this experiments are tabled and discussed in Section III.

### 7. Temperature-dependence Studies.

The activation energies,  $E_a$ , and pre-exponential factors,  $A$ , were determined from the following temperature dependence experiments.

#### a. $[\text{Cr}(\text{phen})_3]^{3+}$ System.

Following the same procedure outlined in Section II-B-4a, the observed rate constants,  $k_{\text{obs}}$ , were determined in solvent systems of pH 10.10 and 12.17, and 0.80  $[\text{OH}^-]$  over the designated temperature range.

(i) at pH 10.10, the temperatures utilized were 31.1, 40.8, 50.8, 60.8, and  $71.0 \pm 0.1^\circ\text{C}$ ;

(ii) at pH 12.17, the temperatures utilized were 21.1, 31.1, 38.3, and  $48.1 \pm 0.1^\circ\text{C}$ ;

(iii) at 0.80  $[\text{OH}^-]$ , the temperatures utilized were 15.5, 20.8, 25.5, and  $30.6 \pm 0.1^\circ\text{C}$ .

The pertinent data are presented in Appendix G.

#### b. $[\text{Cr}(\text{bipy})_3]^{3+}$ System.

The observed rate constants,  $k_{\text{obs}}$ , were determined as per the procedure given in Section II-B-4b.

at pH 11.82 and 0.50  $[\text{OH}^-]$  for the following temperatures:

(i) at pH 11.82, the temperatures utilized were 11.1, 16.8, 23.1, and  $29.8 \pm 0.1^\circ\text{C}$ ;

(ii) at 0.50  $[\text{OH}^-]$ , the temperatures utilized were 5.5, 11.1, 17.5, and  $23.4 \pm 0.1^\circ\text{C}$ .

The pertinent data are presented in Appendix-G, and results and discussion are given in Section III-E.

#### 8. Electronic Spectra of the Chromium(III) Aqueous Products.

The absorption spectrum of the diaquo complex  $[\text{Cr}(\text{bipy})_2(\text{H}_2\text{O})_2]^{3+}$  is pH dependent, as reported by Bjerrum and Inskeep [21]. Depending on the pH of the solution, species present are  $[\text{Cr}(\text{bipy})_2(\text{H}_2\text{O})_2]^{3+}$ ,  $[\text{Cr}(\text{bipy})_2(\text{OH})_2]^+$ , or  $[\text{Cr}(\text{bipy})_2(\text{OH})(\text{H}_2\text{O})]^{2+}$ . The products of the hydrolysis of  $[\text{Cr}(\text{bipy})_3]^{3+}$  have been reported [16] as  $[\text{Cr}(\text{bipy})_2(\text{OH})_2]^+$  and bipy at pH  $\sim 8$ . The presence of  $[\text{Cr}(\text{bipy})_2(\text{OH})_2]^+$  was confirmed by the appearance of an increase in absorption near 518 nm [21]. The absorption spectra of  $[\text{Cr}(\text{bipy})_2(\text{H}_2\text{O})_2]^{3+}$  and  $[\text{Cr}(\text{bipy})_2(\text{OH})_2]^+$  have recently been reported [16] with maxima located at 311 and 492 nm for the diaquo complex, and at 247, 305, and 518 nm for the dihydroxo complex, respectively.

To determine the reaction products for the base hydrolysis of the analogous phenanthroline complex,  $[\text{Cr}(\text{phen})_3]^{3+}$ , the diaquo complex  $[\text{Cr}(\text{phen})_2(\text{H}_2\text{O})_2]^{3+}$

was prepared according to the procedure given in Section II-A-6. The following experiment was performed on the diaquo ion at ambient temperature in an effort to identify the hydrolysis products of  $[\text{Cr}(\text{phen})_3]^{3+}$ .

The following solution concentrations of  $[\text{Cr}(\text{phen})_2(\text{H}_2\text{O})_2]^{3+}$  were prepared in distilled water:

A:  $1.519 \times 10^{-2}$  M

B:  $1.215 \times 10^{-3}$  M

C:  $1.944 \times 10^{-5}$  M

D:  $7.776 \times 10^{-6}$  M

The above solutions (A - D) were used to record the following spectra in the range 210 - 360 nm:

1: spectrum of solution C;

2: spectrum of sample 1 plus two drops of 1 M nitric acid;

3: spectrum of sample 2 plus 3 drops of 1 M sodium hydroxide;

4: spectrum of solution C plus one drop of 1 M nitric acid;

5: spectrum of solution D;

6: spectrum of sample 5 plus 2 drops of 1 M sodium hydroxide;

7: spectrum of sample 6 plus one drop 1 M sodium hydroxide;

8: spectrum of solution D plus 2 drops of 1 M sodium hydroxide.

The solutions were also used to record the following spectra in the 350 - 650 nm range:

9: spectrum of solution A;

- 10: spectrum of sample 9 plus 2 drops of 1 M nitric acid;
- 11: spectrum of sample 10 plus 2 drops of 1 M sodium hydroxide;
- 12: spectrum of solution A plus 2 drops of 1 M sodium hydroxide;
- 13: spectrum of solution B;
- 14: spectrum of sample 13 plus 2 drops of 1 M nitric acid;
- 15: spectrum of sample 14 plus 2 drops of 1 M nitric acid;
- 16: spectrum of solution B plus one drop of 1 M sodium hydroxide.

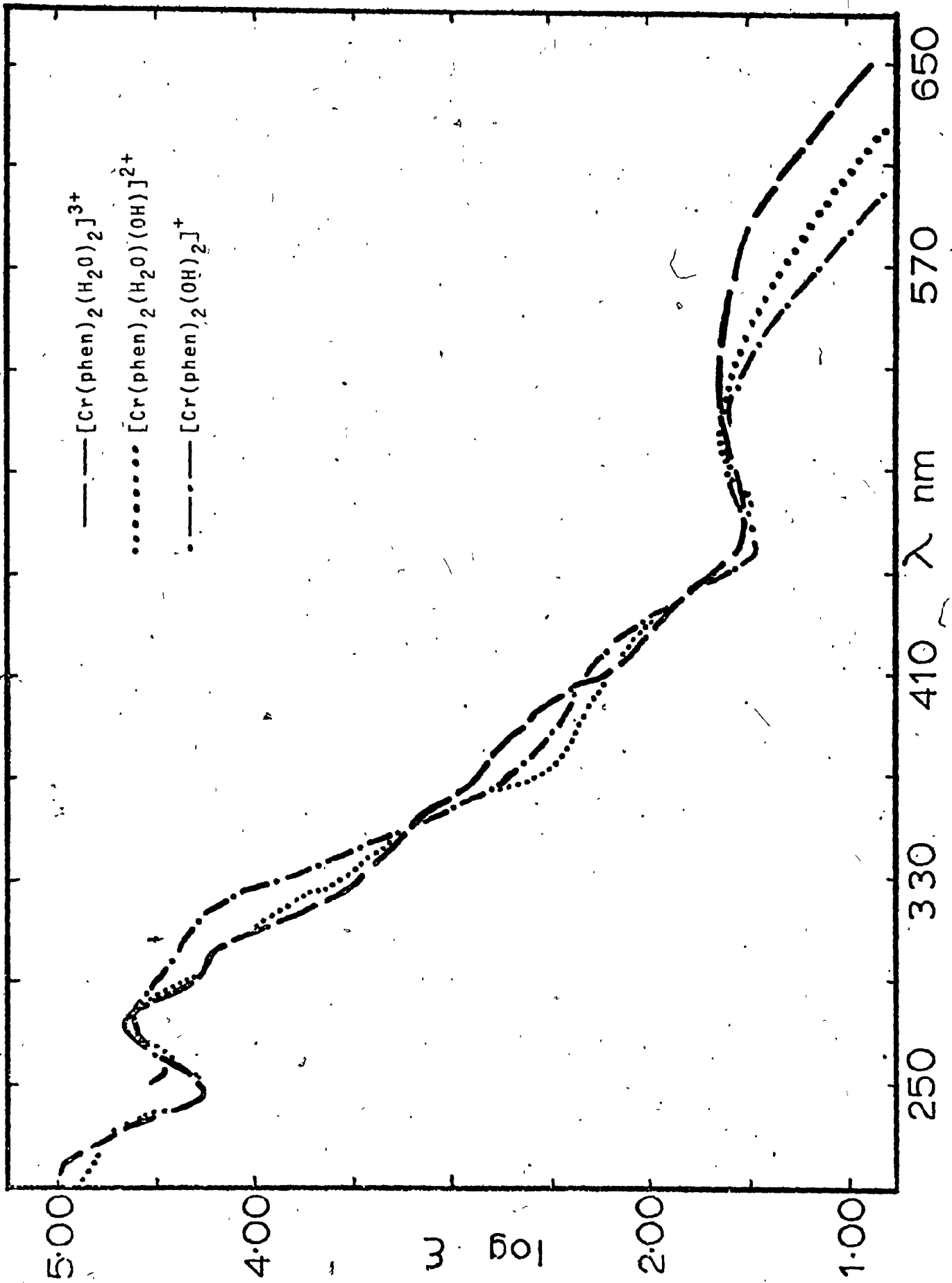
The spectral data are recorded in Appendix H, and the spectra are presented in Figure 1. In acid solution, the predominant species is  $[\text{Cr}(\text{phen})_2(\text{H}_2\text{O})_2]^{3+}$ ; in neutral solution,  $[\text{Cr}(\text{phen})_2(\text{H}_2\text{O})(\text{OH})]^{2+}$ ; and, in basic solution,  $[\text{Cr}(\text{phen})_2(\text{OH})_2]^+$ . Confirmation of the species was made by comparison of the spectra (Figure 1) with those of  $[\text{Cr}(\text{phen})_2(\text{H}_2\text{O})_2]^{3+}$  and  $[\text{Cr}(\text{phen})_2(\text{OH})_2]^+$  reported by Bjerrum and Inskeep [21].

### C. Calculations for Kinetic Studies.

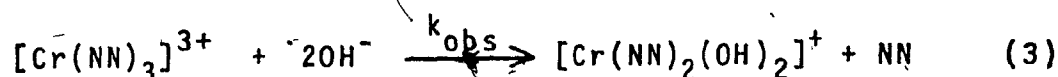
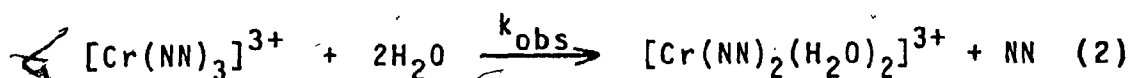
#### 1. Observed Rate Constant, $k_{\text{obs}}$ .

The reaction between  $[\text{Cr}(\text{bipy})_3]^{3+}$  and water (or hydroxide ion), and that between  $[\text{Cr}(\text{phen})_3]^{3+}$  and water (or hydroxide ion) follows pseudo first-order kinetics inasmuch as the nucleophiles ( $\text{H}_2\text{O}$  or  $\text{OH}^-$ ) are either present in excess or the concentration remains constant by the use of buffered solutions. The course of the

Figure 1. Absorption Spectra of  $[\text{Cr}(\text{phen})_2(\text{H}_2\text{O})_2]^{3+}$ ,  
 $[\text{Cr}(\text{phen})_2(\text{OH})_2]^+$ , and  $[\text{Cr}(\text{phen})_2(\text{H}_2\text{O})(\text{OH})]^{2+}$ .



hydrolysis reaction was followed by determining the concentration of free 2,2'-bipyridine or 1,10-phenanthroline released, NN, as a function of time, according to either reaction (2) or (3),



where NN represents 2,2'-bipyridine or 1,10-phenanthroline.

The rate of a first order reaction, in terms of the disappearance of the reactant is given by (4),

$$\text{Rate} = \frac{-d[\text{Cr(NN)}_3^{3+}]}{dt} \quad (4)$$

and the rate law by (5),

$$-d[C]/dt = k_{\text{obs}}[C] \quad (5)$$

where C represents the concentration, or some measurable quantity, of the reactant  $\text{Cr(NN)}_3^{3+}$ . In terms of the rate of appearance of the products, the overall rate and rate law, respectively, will be as in (6) and (7),

$$\text{Rate} = +d[\text{NN}]/dt \quad (6)$$

$$\frac{+d[\text{NN}]}{dt} = k_{\text{obs}} [\text{complex}]_t = k_{\text{obs}} \{C_0 - [\text{NN}]\} \quad (7)$$

where  $[\text{NN}]$  is the concentration of free polypyridine released,  $[\text{complex}]_t$  is the concentration of the complex at any time 't' during the reaction and is equal to the concentration of the reactant complex at initial time,  $C_0$ , less the concentration of free polypyridine released,  $[\text{NN}]$ . Rearrangement and integration of equation (7) yields

$$\int_0^t \frac{d[\text{NN}]}{\{C_0 - [\text{NN}]\}} = k_{\text{obs}} \int_0^t dt \quad (8)$$

$$-\ln \{C_0 - [\text{NN}]\} = k_{\text{obs}} t - \ln C_0 \quad (9)$$

$$\ln \{C_0 - [\text{NN}]\} = -k_{\text{obs}} t + \ln C_0 \quad (10)$$

$$\log \{C_0 - [\text{NN}]\} = (-k_{\text{obs}}/2.3026)t + \log C_0 \quad (11)$$

Hence, a plot of  $\log \{C_0 - [\text{NN}]\}$  versus time yields a slope equal to  $-k_{\text{obs}}/2.3026$  and intercept  $\log C_0$ . Since it is the concentration of  $[\text{NN}]$  that was measured as a function of time in the procedures outlined in Section



II-B-4, it is valid to plot  $\log \{C_0 - [NN]\}$  as a function of time. The concentration of free 2,2'-bipyridine [BIPY] released in the aquation reaction was read directly from the calibration plot (Appendix B), in the case of  $[\text{Cr}(\text{bipy})_3]^{3+}$ . For the corresponding phenanthroline cation, a series of calibration plots (Appendix A) were obtained at various pH values. The average of the slopes of these linear least-squares plots was used to determine the concentration of free phenanthroline released, [PHEN], into the bulk of the solution. At 231 nm, the slope is  $3.57 \pm 0.31 \times 10^3 \text{ A/M}$  and at 262 nm the average slope is  $1.94 \pm 0.22 \times 10^3 \text{ A/M}$ , where A is the optical density. The data given in Appendices C and D were utilized to construct plots of  $\log \{C_0 - [NN]\}$  versus time, which are presented in Section III.

## 2. Ionic Strength Calculations for Solvent Systems.

According to the Debye-Huckel theory, the activity coefficient ( $f_i$ ) of an ion may be related to its charge ( $z_i$ ) and the ionic strength ( $\mu$ ) by equation (12),

$$\log f_i = -Q z_i^2 (\mu)^{1/2} \quad (12)$$

where  $Q = 0.51$  at  $25^\circ\text{C}$ , and  $\mu_{\text{calc}} = 1/2 \sum_i z_i^2 C_i$  (13)

In equation (13),  $C_i$  is the concentration in mole-liter<sup>-1</sup>, and this equation was used to calculate all ionic strength values ( $\mu_{\text{calc}}$ ). However, in addition to the sodium

hydroxide present in the reaction solution, the ions present in the Britton-Robinson stock solution and the sodium chloride must also be accounted for. In the Britton-Robinson solution, the acid dissociation constants ( $K_a$ ) were used to determine the relative contribution of each ion to the ionic strength of the solvent system. The  $K_a$  values [23] are given in Table V for acetic, boric, and ortho-phosphoric acids. The ionic strength ( $\mu_{\text{calc}}$ ) was calculated from the formal concentrations and charge on the ions present in sodium hydroxide, sodium chloride, acetic acid, phosphoric acid, and boric acid. Table VI gives the values of  $\mu_{\text{calc}}$  at the indicated pH.

### 3. Activation Parameters.

The rate of a reaction is quite sensitive to changes in temperature, increasing with increasing temperature. The temperature dependence of the reaction rate, in terms of the observed rate constant, is given by the Arrhenius relation

$$k_{\text{obs}} = A e^{-E_a/RT} \quad (14)$$

or

$$\ln k_{\text{obs}} = \ln A - E_a/RT \quad (15)$$

where  $A$  is the pre-exponential factor,  $E_a$  the activation

Table V

Acid Dissociation Constants  $K_a$  for Acetic, o-phosphoric, and Boric Acids<sup>a</sup>

Acid	$K_1$	$K_2$	$K_3$
Acetic acid <sup>b</sup>	$1.76 \times 10^{-5}$	---	---
o-phosphoric acid <sup>b</sup>	$7.52 \times 10^{-3}$	$6.23 \times 10^{-8}$	$2.2 \times 10^{-13}$
Boric acid <sup>c</sup>	$7.3 \times 10^{-10}$	$1.8 \times 10^{-13}$	$1.6 \times 10^{-14}$

<sup>a</sup> Reference 23. <sup>b</sup> 25°C. <sup>c</sup> 20°C.

Table VI

pH Values for Solvent Systems  
and Calculated Ionic Strengths

<u>pH</u> <u>(±0.05)</u>	<u>Ionic Strength</u> <u>(<math>\mu_{\text{calc}}</math>) (M)</u>
4.66	1.02
5.53	1.02
6.66	1.03
7.75	1.04
8.43	1.04
8.88	1.04
9.45	1.04
10.15	1.05
10.50	1.05
11.14	1.05
11.67	1.06
12.17	1.09

energy,  $R$  is the gas constant, and  $T$  is the absolute temperature. A linear plot of  $\ln k_{\text{obs}}$  versus  $10^3/T$  yields a slope  $-E_a/R$  and intercept  $\log A$ .

By assuming [24] that there exists an equilibrium between the reactant and the activated complex, i.e.,



the rate constant of any reaction is given by the Eyring relation in (17),

$$k = (RT/Nh)K^\ddagger \quad (17)$$

where  $K^\ddagger$  is the equilibrium constant for reaction (16),  $N$  is Avogadro's number, and  $h$  is Planck's constant. Using the two thermodynamic relations in (18) and (19),

$$\Delta G^\circ = -RT \ln K \quad (18)$$

$$\Delta G^\circ = \Delta H^\circ - T\Delta S^\circ \quad (19)$$

the general expression given in equation (20) may be derived.

$$k = e^{-\Delta G^\circ/RT} = e^{\Delta S^\circ/R} e^{-\Delta H^\circ/RT} \quad (20)$$

An analogous equation (20) can be written for  $K^\ddagger$ , i.e.,

$$K^\ddagger = e^{-\Delta G^\ddagger/RT} = e^{\Delta S^\ddagger/R} e^{-\Delta H^\ddagger/RT} \quad (21)$$

Substitution of  $K^\ddagger$  into equation (17) yields

$$k = (RT/Nh) e^{-\Delta G^\ddagger/RT} = (RT/Nh) e^{\Delta S^\ddagger/R} e^{-\Delta H^\ddagger/RT} \quad (22)$$

where  $\Delta G^\ddagger$ ,  $\Delta H^\ddagger$ , and  $\Delta S^\ddagger$  are now the free energy of activation, enthalpy of activation, and entropy of activation, respectively, in going from the reactant to the activated complex. Substitution and rearrangement of equation (22) yields.

$$\Delta S^\ddagger = R [ \ln A - \ln RT/Nh ] - R \quad (23)$$

An equation analogous to (22) can be written for  $\Delta G^\ddagger$ ,

$$\Delta G^\ddagger = \Delta H^\ddagger - T\Delta S^\ddagger \quad (24)$$

and for  $\Delta H^\ddagger$ ,

$$\Delta H^\ddagger = E_a - RT \quad (25)$$

Thus, the activation energies and Arrhenius factors were determined from least-squares plots of  $\ln k_{\text{obs}}$  versus  $10^3/T$ ; and the activation parameters  $\Delta S^\ddagger$ ,  $\Delta G^\ddagger$ , and  $\Delta H^\ddagger$

were calculated from equations (23 - 25), respectively, or from least-squares plots of  $\ln k/T$  versus  $10^3/T$ , where [25]

$$R = 1.9872 \text{ cal-mol}^{-1}\text{K}^{-1} = 8.314 \times 10^7 \text{ erg-K}^{-1}\text{mol}^{-1}$$

$$h = 6.6252 \times 10^{-27} \text{ erg-sec}$$

$$N = 6.0226 \times 10^{23} \text{ mol}^{-1}$$

$$T = 298.16 \text{ K}$$

The pertinent data are presented in Appendix I, and the results are tabled, illustrated, and discussed in Section III.

#### 4. Kinetics in Oxygenated and Deoxygenated Solvents.

The procedure given in Section II-B-6 was performed in order to determine whether the presence of oxygen affected the observed rate constant. In order to ensure that the deoxygenated system remained air-free, the usual extraction procedure utilized to determine the observed rate constant was discarded in favour of the procedure described below.

The wavelength corresponding to the largest change in absorbance over the entire reaction time was 287 nm. Therefore, the absorbance at 287 nm was determined for the following species:

- a)  $[\text{Cr}(\text{bipy})_3]^{3+}$  at initial time,  $t_i$
- b) 2,2'-bipyridine
- c)  $[\text{Cr}(\text{bipy})_2(\text{OH})_2]^+$  at final time,  $t_f$

The absorbance values of a) - c) were determined from the extinction coefficients,  $\xi$ , of  $[\text{Cr}(\text{bipy})_3]^{3+}$  (Appendix J and Figure 8), of 2,2'-bipyridine [26], and from the concentration  $C_0$  of the reactant solution, according to the relation in (26).

$$\text{Absorbance} = \xi C_0 \text{ for } \lambda = 1 \text{ cm} \quad (26)$$

The absorbance value of  $[\text{Cr}(\text{bipy})_2(\text{OH})_2]^+$  at final time  $t_f$  was read directly from the spectrum. Therefore,

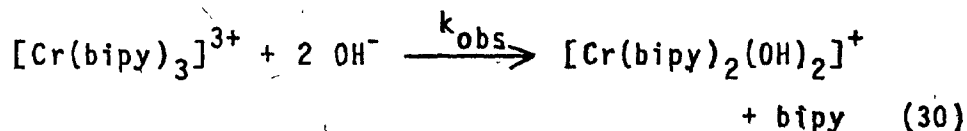
$$A_i = \xi_{287} \text{ of } [\text{Cr}(\text{bipy})_3]^{3+} \times C_0 \quad (27)$$

$$A_f = \{ \xi_{287} \text{ of } [\text{Cr}(\text{bipy})_2(\text{OH})_2]^+ \times C_0 \} + \{ \xi_{287} \text{ of bipy} \times C_0 \} \quad (28)$$

$$A_t = A_{287} \text{ of the sample solution} \quad (29)$$

At pH 11.82 and 0.50  $[\text{OH}^-]$ , the overall stoichiometry of the reaction is the same as found earlier [16],





Considering the following general reaction,



where P refers to all reaction products, the physical property chosen to follow the reaction was absorbance A. The absorbances of the reactant R and products P are, respectively,

$$A_R = \epsilon_R C_R \quad (\text{pathlength} = 1\text{cm}) \quad (32)$$

$$A_P = \epsilon_P C_P \quad (33)$$

At the start of the reaction, the total absorbance is that due to the reactant, i.e.,

$$A_i = A_R = \epsilon_R C_R \quad (34)$$

At any time 't' during the course of the reaction the absorbance is given by

$$A_t = \epsilon_R C_R - \epsilon_R C_P + \epsilon_P C_P = \epsilon_R (C_R - C_P) + \epsilon_P C_P \quad (35)$$

The absorbance at final time is

$$A_f = A_p = \epsilon_p C_p \quad (36)$$

Therefore,

$$A_f - A_t = (\epsilon_p C_p) - [\epsilon_R (C_R - C_p) + \epsilon_p C_p] \quad (37)$$

$$A_t - A_f = \epsilon_R (C_R - C_p) \quad (38)$$

which is a function of the concentration of reactant R at any time 't' during the reaction. Now, the overall rate of the reaction in terms of the disappearance of the reactant R is

$$\text{Rate} = \frac{-d[R]_t}{dt} = k_{\text{obs}} [R]_t \quad (39)$$

Rearrangement and integration of the rate law (39) yields

$$\int_0^t \frac{-d[R]_t}{dt} = k_{\text{obs}} \int_0^t dt \quad (40)$$

$$\ln [R]_t = -k_{\text{obs}} t + \ln [R]_i \quad (41)$$

$$\ln [R]_t / [R]_i = -k_{\text{obs}} t \quad (42)$$

In terms of the measured property, equation (42) becomes

$$\ln (C_R - C_P) / C_R = -k_{\text{obs}} t \quad (43)$$

$$\ln \epsilon_R (C_R - C_P) / \epsilon_R C_R = -k_{\text{obs}} t = \ln (A_t - A_f) / A_i \quad (44)$$

Rearrangement yields

$$\ln |(A_f - A_t)| = -k_{\text{obs}} t + \ln A_i \quad (45)$$

$$\log |(A_f - A_t)| = (-k_{\text{obs}} / 2.3026) t + \log A_i \quad (46)$$

A linear plot of  $\log |(A_f - A_t)|$  versus time yields a slope equal to  $-k_{\text{obs}} / 2.3026$  and intercept equal to  $\log A_i$ . The pertinent data are presented in Appendices E and F, and the results are discussed in Section III.

#### D. Preparation of Rhodium(III) Compound.

##### 1. Reagents and Solvents.

The following reagents were used without further purification: rhodium(III) chloride trihydrate (Fisher Scientific); 2,2'-bipyridine (Eastman).

Acetone (N.F., Fisher Scientific), 95% ethanol (Anachemia), and decolourizing charcoal (Anachemia) were used without further purification.

##### 2. Tris(2,2'-bipyridyl)rhodium(III) Chloride.

The compound was synthesized using a modified procedure of Harris and McKenzie [27]. Rhodium(III)

chloride trihydrate (0.482 g, 1.83 mmol) and 2,2'-bipyridine (1.07 g, 6.83 mmol) in a small porcelain crucible were heated in a silicone oil bath at ca. 220°C. Fusion of the two reactants initially produced a dark brown solid, which turned golden-brown upon further heating. More 2,2'-bipyridine (ca. 3 mmol) was added to the solid, and the resulting dark brown solution was stirred and heated. This solution subsequently solidified to a dark, brownish-green mass, and was allowed to cool; it was then transferred to a 50-ml round-bottom flask attached to a reflux condenser. The solid was dissolved in ca. 20 ml of 50% aqueous ethanol, yielding a clear orange solution, which was refluxed for ten hours.

Subsequently, decolourizing charcoal was added to the orange solution, and refluxed for another hour. This procedure was repeated three times (or, as necessary) until a clear filtrate was obtained upon filtration.

Acetone was added to the clear filtrate to precipitate the white product. The solution was filtered, the product collected and washed several times with acetone, and dried in the air for two hours. Yield 1.14 g (81% of theoretical). The purity of the product  $[\text{Rh}(\text{bipy})_3] \cdot \text{Cl}_3 \cdot 4.5 \text{H}_2\text{O}$  was checked by comparison of the absorption spectrum with that reported in the literature [27].

E. Experiments Performed on  $[\text{Rh}(\text{bipy})_3]^{3+}$ .

The  $[\text{Rh}(\text{bipy})_3]^{3+}$  cation was synthesized in an effort to determine its behaviour in aqueous acid and base.

1. Behaviour of  $[\text{Rh}(\text{bipy})_3]^{3+}$  in Acid Solution.

A solution of  $[\text{Rh}(\text{bipy})_3]^{3+}$  (ca.  $3 \times 10^{-5}$  M) in 6 M hydrochloric acid was prepared and thermostated at ca. 85°C. The ultraviolet absorption spectrum (220 - 360 nm) of the solution was recorded over a period of nine hours. The solution was kept in the analysing cuvet over the entire time period, with a water-jacketed cell mount to maintain constant temperature. The analysing beam was blocked between spectral scans to avoid possible decomposition.

After nine hours, a 2-ml aliquot of the rhodium-(III) solution was pipetted into a 25-ml screw-top glass vial containing exactly 5.00 ml of hexanes. The solution was shaken manually for exactly one minute and allowed to stand for two minutes. With the aid of a Pasteur pipet, a sufficient volume of the upper non-aqueous layer was transferred to a cuvet and the ultraviolet absorption (210 - 360 nm) recorded to determine whether or not any free 2,2'-bipyridine was released.

2. Behaviour of  $[\text{Rh}(\text{bipy})]^{3+}$  in Basic Solution.

A similar procedure to that in acid solution (see Section II-E-1) was performed for the rhodium(III) cation in 6 M sodium hydroxide over a period of eleven hours.

The results of these experiments are discussed in Section III.

F. Preparation of Substituted Phenanthroline and Bipyridyl Complexes of Chromium(III).

1. Reagents and Solvents.

The following reagents were used as supplied without further purification: anhydrous chromium(II) chloride, 98% (Alfa); 5-chloro-1,10-phenanthroline (G.F. Smith Chemical); 4,4'-diphenyl-2,2'-bipyridine and 4,7-dimethyl-1,10-phenanthroline (Chemical Procurements Laboratory); 4,7-diphenyl-1,10-phenanthroline (Eastman); chlorine gas (Matheson).

Tetrahydrofuran (Certified, Fisher Scientific), absolute methanol (Reagent, Anachemia), 95% ethanol (Reagent, Anachemia), were used as supplied.

Saturated sodium perchlorate solutions were prepared using purified sodium perchlorate (Fisher Scientific).

2. Elemental Analyses.

All elemental analyses of the chromium(III)

complexes were performed by Galbraith Laboratories, Inc., Knoxville, Tennessee.

3. Techniques.

In the syntheses of the chromium(III) complexes, the preparations were carried out in a nitrogen-purged glove bag using deoxygenated solvents to avoid premature oxidation of the chromous complex. Thus, a stream of nitrogen gas was bubbled through the solvents for ca. 45 minutes immediately prior to use. All filtrations were performed using sintered-glass funnels connected to a water aspirator. In procedures where it was necessary to treat the reaction solution with chlorine gas, a well-ventilated fumehood was used. Tygon tubing was connected between the lecture bottle and the sintered-glass dispersion tube, and the chlorine gas bubbled through the reaction solution. Drying of the final product was carried out in vacuo.

4. Tris(5-chloro-1,10-phenanthroline)chromium-(III) Perchlorate.

A solution of 0.762 g (6.20 mmol) of chromium-(II) chloride in 100 ml deoxygenated, distilled water containing one ml perchloric acid was added to a solution of 1.53 g (7.14 mmol) of 5-chloro-1,10-phenanthroline dissolved in 50 ml of deoxygenated, absolute methanol inside a nitrogen-purged glove bag. The resulting dark green solution was stirred for ten minutes. Subsequently,

the solution was removed from the glove bag, stirred in the air for ten minutes, and oxidized by bubbling chlorine gas through the reaction mixture for ca. 15 minutes.

The yellow solution was filtered to yield a greenish-yellow solid, and then dissolved in ca. 600 ml of hot distilled water. Approximately 3 ml of saturated sodium perchlorate solution was added, and the solution allowed to cool. The beige-yellow product was filtered, dried in air for ten minutes, and then in vacuo for two hours. Yield was 0.97 g (15% of theoretical)

Analysis: Calc<sup>d</sup> for  $\text{CrC}_{36}\text{H}_{25}\text{N}_6\text{Cl}_3\text{O}_{14}$ : C, 41.97; H, 2.44; N, 8.16; Cl, 20.64; Cr, 5.05. Found: C, 41.60; H, 2.20; N, 8.07; Cl, 20.60; Cr, 5.09.

Formula:  $[\text{Cr}(\text{5-Clphen})_3](\text{ClO}_4)_3 \cdot 2\text{H}_2\text{O}$

5. Tris(4,7-dimethyl-1,10-phenanthroline)chromium-(III) Perchlorate.

In a nitrogen atmosphere, a solution of 0.80 g (6.54 mmol) chromium(II) chloride dissolved in ca. 50 ml of deoxygenated, distilled water containing three drops of perchloric acid was added to 2.76 g (1.22 mmol) of 4,7-dimethyl-1,10-phenanthroline dissolved in ca. 30 ml of deoxygenated absolute methanol. The resulting dark brown solution was stirred for ten minutes in a nitrogen atmosphere, and subsequently in air for ten minutes.



Approximately 600 ml of distilled water containing 2 ml of saturated sodium perchlorate solution was added, and chlorine gas bubbled through the solution for ten minutes, whereupon the solution turned to a bright yellow colour within five minutes.

The solution was filtered, and the collected greenish-yellow solid was dissolved in ca. 500 ml of hot distilled water containing a few drops of concentrated hydrochloric acid. The hot solution was filtered, and the yellow filtrate allowed to cool. Approximately 2 ml of saturated sodium perchlorate solution was added to the filtrate to effect product precipitation. The solution was then filtered, the yellow product collected and washed with distilled water containing a small amount of sodium perchlorate solution. Drying in air for ten minutes and in vacuo for two hours yielded 1.50 g (23% of theoretical) of the product.

Analysis: Calc<sup>d</sup> for  $\text{CrC}_{42}\text{H}_{40}\text{N}_6\text{Cl}_3\text{O}_{14}$ : C, 49.86; H, 3.99; N, 8.31; Cl, 10.51; Cr, 5.14. Found: C, 49.51; H, 4.00; N, 8.26; Cl, 11.44; Cr, 5.30.

Formula:  $[\text{Cr}(4,7\text{-Me}_2\text{phen})_3](\text{ClO}_4)_3 \cdot 2\text{H}_2\text{O}$

6. Tris(4,7-diphenyl-1,10-phenanthroline)chromium(III) Perchlorate.

In a nitrogen-purged glove bag, a solution of 0.178 g (1.44 mmol) chromium(II) chloride dissolved in

100 ml of deoxygenated, distilled water containing a few drops of concentrated hydrochloric acid was added to a solution of 0.960 g (2.89 mmol) of 4,7-diphenyl-1,10-phenanthroline dissolved in 50 ml of deoxygenated tetrahydrofuran. The resulting dark purple solution was stirred in a nitrogen atmosphere for ca. 40 minutes, and then in the air for ten minutes. Approximately 150 ml of distilled water containing one ml of saturated sodium perchlorate solution was added to the reaction mixture, which was subsequently oxidized with chlorine gas. The solution was filtered to yield the crude yellow product which was extracted with ca. 100 ml of tetrahydrofuran. To the yellow filtrate was added 200 ml of distilled water containing one ml of the sodium perchlorate solution. The resulting solution was stirred for ten minutes, filtered, and the final product was collected, washed twice with distilled water and then dried in air for ten minutes and in vacuo for two hours. Yield was 0.60 g (29% of theoretical).

Analysis: Calc<sup>d</sup> for  $\text{CrC}_{72}\text{H}_{56}\text{N}_6\text{Cl}_3\text{O}_{16}$ : C, 60.91; H, 3.98; N, 5.92; Cl, 7.49; Cr, 3.66. Found: C, 60.70; H, 3.84; N, 5.80; Cl, 7.70; Cr, 3.59.

Formula:  $[\text{Cr}(4,7\text{-Ph}_2\text{phen})_3](\text{ClO}_4)_3 \cdot 2\text{H}_2\text{O}$

7. Tris(4,4'-diphenyl-2,2'-bipyridyl)chromium(III) Perchlorate.

In a nitrogen-purged glove bag, a solution of 0.377 g (3.07 mmol) chromium(II) chloride dissolved in 100 ml of deoxygenated, distilled water was added to a solution of 2.41 g (7.80 mmol) 4,4'-diphenyl-2,2'-bipyridine dissolved in 50 ml of deoxygenated tetrahydrofuran. The resulting dark purple solution was stirred for ca. 40 minutes in a nitrogen atmosphere; and subsequently removed from the glove bag and stirred for an additional ten minutes. Chlorine gas was bubbled through the solution for ca. ten minutes, resulting in a yellow solution.

The yellow solution was filtered, and the crude yellow product collected. The crude product was then dissolved in 50% hot, aqueous methanol. Approximately 3 ml of saturated sodium perchlorate solution was added, and the solution allowed to cool. Filtration afforded a yellow product, which was recrystallized from aqueous methanol, and 1.70 g (42% of theoretical) were collected after drying in vacuo for two hours.

Analysis: Calc<sup>d</sup> for  $\text{CrC}_{66}\text{H}_{52}\text{N}_6\text{Cl}_3\text{O}_{14}$ : C, 60.44; H, 4.00; N, 6.41; Cl, 8.11; Cr, 3.96. Found: C, 60.52; H, 3.97; N, 6.28; Cl, 8.02; Cr, 4.93.

Formula:  $[\text{Cr}(4,4'\text{-Ph}_2\text{bipy})_3](\text{ClO}_4)_3 \cdot 2\text{H}_2\text{O}$

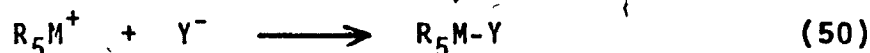
### III. RESULTS AND DISCUSSION

#### A. Octahedral Substitution Mechanisms.

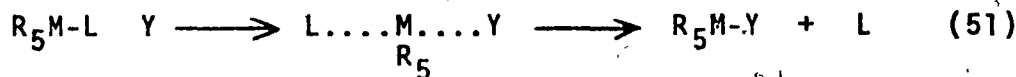
Substitution reactions of octahedral coordination compounds have been intensively investigated since the early 1950's when the relative reactivities of these compounds were rationalized in terms of valence bond theory [28]. Subsequently, molecular orbital theory [1] and crystal field theory [4] were used to explain the observed kinetics of such complexes. Substitution reactions in inorganic chemistry, which generally involve the replacement of one ligand by another in a coordination compound, are termed nucleophilic substitution (denoted,  $S_N$ ). These reactions may thus be considered as acid-base reactions, in which the positively charged metal ion serves as the Lewis acid and the ligands as the Lewis bases. Two different limiting pathways have been conceived for this acid-base reaction. These include displacement and dissociation, called  $S_N2$  and  $S_N1$ , respectively, by Hughes and Ingold [29]. A dissociative mechanism follows a two-step pathway: a slow unimolecular heterolytic dissociation,



followed by a fast coordination of the entering nucleophile  $Y^-$  to the metal ion,



In such a mechanism, the coordination number of the central metal ion decreases by one in the rate-controlling step (49) to form a pentacoordinate intermediate, and the leaving group L departs independently of the nature of the entering group Y. A displacement mechanism, on the other hand, involves a bimolecular rate-controlling step wherein the entering group Y displaces the leaving group L,



In the transition state, the coordination number of the central metal ion increases by one, producing a heptacoordinate species.

It has been recognized that very few complexes undergo substitution via a pure displacement or pure dissociative pathway. Hence, there might well be an intermediate pathway between the two limiting pathways, having characteristics of both. As a result, Basolo and Pearson [4] have proposed four classifications for inorganic nucleophilic substitution reactions, very

similar to those proposed for analogous organic reactions [30]. The classifications include:

- a)  $S_N1(lim)$ : a dissociative pathway for which evidence of a pentacoordinate intermediate exists;
- b)  $S_N1$ : a dissociative pathway which only involves rupture of the metal-leaving group bond as the rate-controlling step, and for which the intermediate is usually isolable;
- c)  $S_N2(lim)$ : a displacement pathway wherein the rate-controlling step involves only the formation of the bond between the metal atom and the entering group Y;
- d)  $S_N2$ : a displacement pathway in which the rate-controlling step involves simultaneously both bond-rupture between the metal and the leaving group, and bond-formation between the metal and the entering group.

An alternate system utilized to identify reaction mechanisms has been explained in terms of reactivities of the environment of the central metal ion. A metal ion with a positive charge of two or more, is believed [2] to be surrounded by four concentric zones:

- a) the first coordination sphere, where covalent bonds exist between the ligands and the metal ion;
- b) the solvation shell, which contains solvent molecules and electrostatically-bound anions;
- c) a region intermediate between the solvation

shell and the bulk solvent;

d) the bulk solvent.

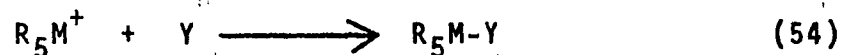
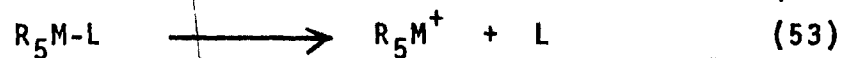
The structure of these zones will depend on the nature of the cation, anions, and solvent. Assuming such an environment about a metal ion, Langford and Gray [2,31] and Swaddle [3] have suggested three general mechanisms for octahedral substitution in solution: (i) associative (A); (ii) dissociative (D); and (iii) interchange (I), which may be either associative ( $I_a$ ) or dissociative ( $I_d$ ). For all three mechanisms, the substitution of the leaving group L by the entering group Y in the first coordination sphere must occur subsequent to the entry of Y into the solvation shell. This results in the formation of an 'encounter complex' [2,31].

An associative (A) mechanism implies the formation of a heptacoordinate intermediate species,

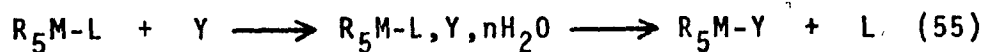


which is long-lived relative to the time required for ligand exchange between the solvation shell and the bulk solvent. In a dissociative (D) mechanism, the leaving group L leaves independently of the nature of the entering group Y, such that the pentacoordinate intermediate and its solvation shell are not influenced by L prior

to the formation of a bond between the metal and the entering group Y.



Such a situation may occur when the leaving group cannot stay in the solvation shell, and therefore moves rapidly into the bulk solvent; or when the pentacoordinate intermediate is relatively long-lived in comparison to the time necessary for ligand exchange between the solvation shell and the bulk solvent. The interchange (I) pathway is ascribed [2,3,31] to a reaction in which substitution of the leaving group L by the entering group Y occurs within the 'encounter complex'.



That is, bond-formation between the metal M and the entering group Y occurs to some extent prior to complete bond-rupture of M-L. More specifically, an associative interchange ( $I_a$ ) mechanism occurs when M-L bond-rupture and M-Y bond-formation are synchronous, yielding a heptacoordinate intermediate characteristic of both L and

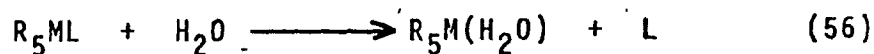


Y. A dissociative interchange ( $I_d$ ) pathway, on the other hand, is ascribed to M-Y bond-formation occurring subsequent to M-L bond-rupture but prior to the exit of L from the solvation shell. In such a case, the transient pentacoordinate intermediate  $R_5M$  occupies the first coordination sphere and the solvation shell.

B. Hydrolysis Reactions.

1. Introduction.

Hydrolysis reactions, predominantly those of cobalt(III) complexes, have been the most thoroughly investigated octahedral substitution reactions. The reaction involves the replacement of one or more coordinated ligands by a solvent molecule. Where the product of the reaction contains coordinated water molecules,

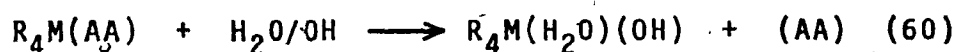
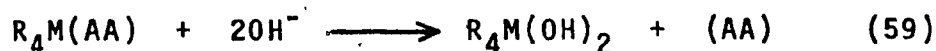
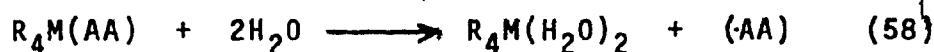


the reaction is termed 'acid hydrolysis' or 'aquation'; and where the product contains hydroxo-ligands, the reaction is termed 'base hydrolysis'.



Similar sequences may be written for complexes in which

bidentate ligands. (AA) are replaced by water or hydroxo-ligands.



Thus, the nature of the product is dependent on the solution pH.

Various attempts (see below) to elucidate the role of water and/or hydroxide ion in such hydrolyses reactions have been made.

## 2. Acid Hydrolysis.

The stepwise hydrolysis of  $[Cr(NH_3)_6]^{3+}$  in acid and base was studied by column chromatography [32,33]. The reaction sequence in 0.1 M nitric acid is presented in Figure 2. The aquation was found to be independent of hydrogen ion concentration, and the observed pseudo first-order rate constant was  $k_{obs} = 1.34 \times 10^{-6} \text{ sec}^{-1}$  at 25°C, with an activation energy  $E_a = 26 \text{ kcal/mole}$ . The reaction sequence in 0.1 M sodium hydroxide is given in Figure 3 with the appropriate rate constants. The rate of hydrolysis in base was observed to be only twice as fast as that in acid; and  $[Cr(NH_3)_5(H_2O)]^{3+}$

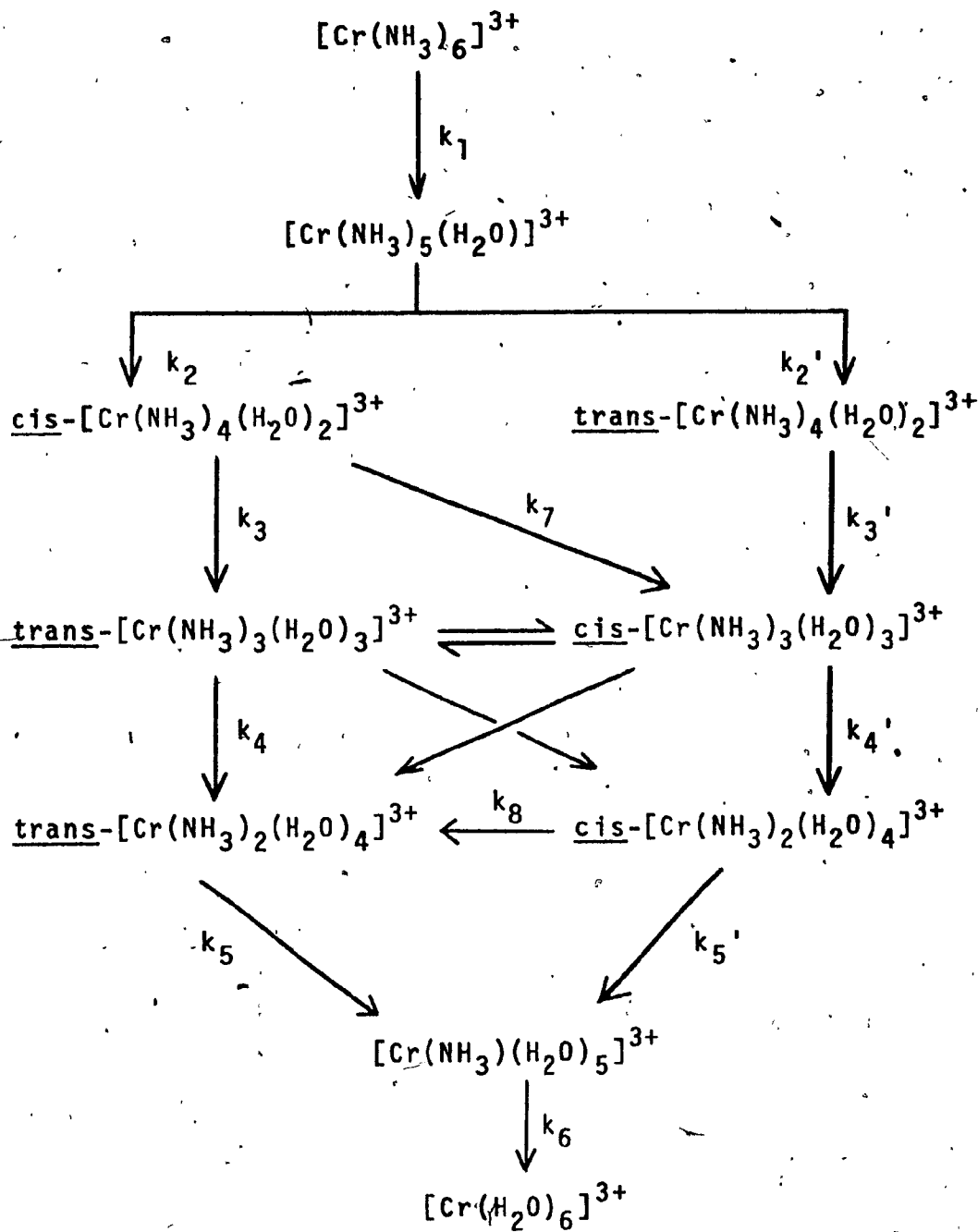
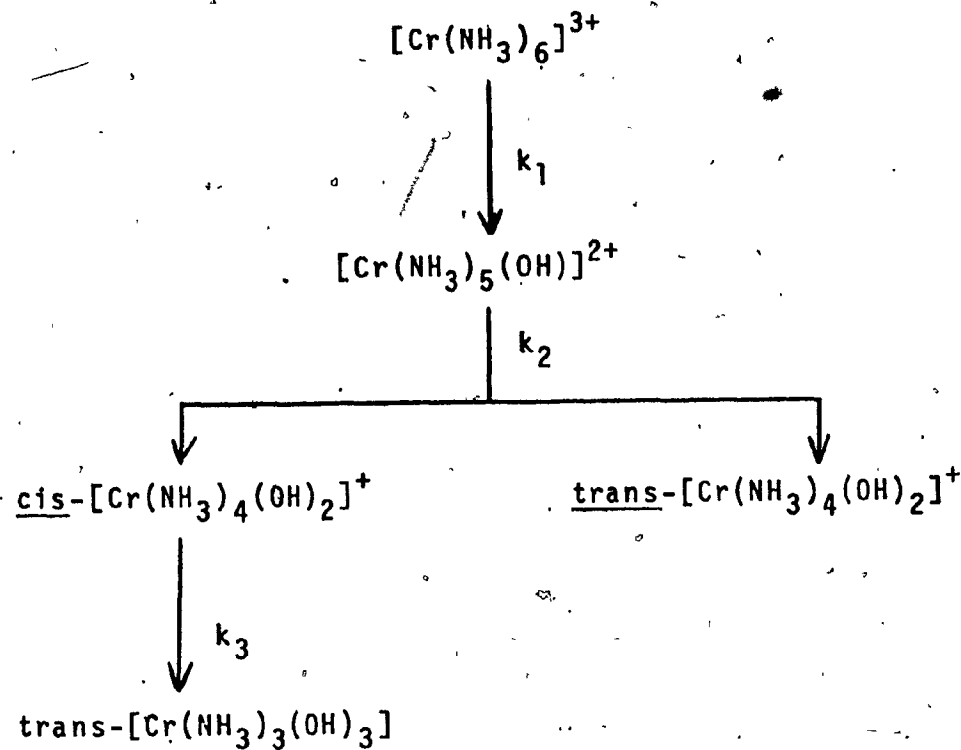


Figure 2: Hydrolysis of  $[\text{Cr}(\text{NH}_3)_6]^{3+}$  in 0.1 M Nitric Acid at 40°C.



where:

$$k_1 = 1 \times 10^{-2} \text{ hr}^{-1}$$

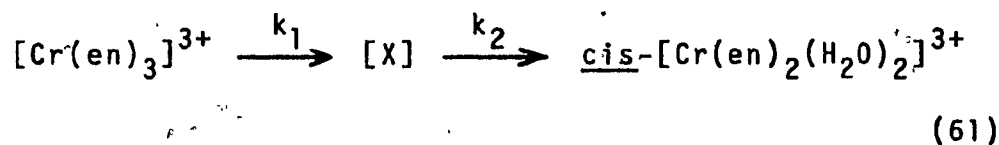
$$k_2 = 4 \times 10^{-2} \text{ hr}^{-1}$$

$$k_3 \sim 3 \text{ hr}^{-1}$$

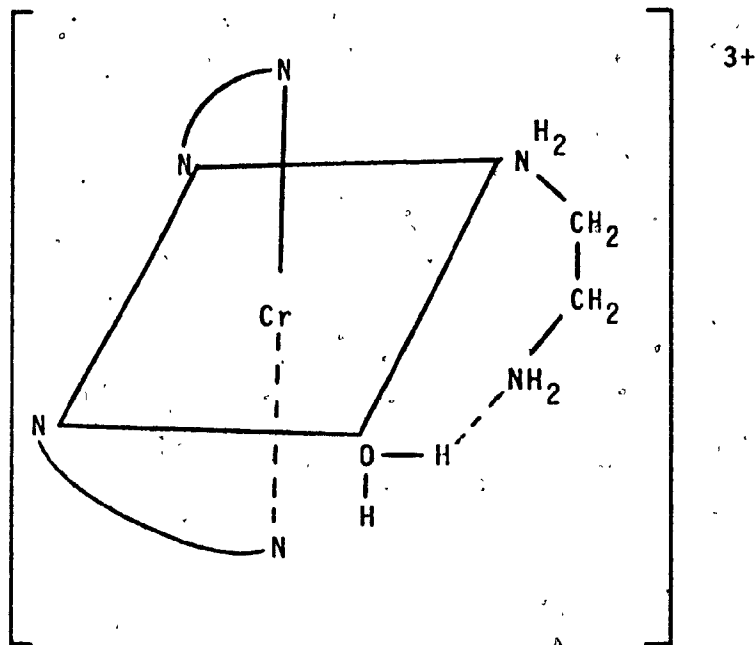
Figure 3: Hydrolysis of  $[\text{Cr}(\text{NH}_3)_6]^{3+}$  in 0.1 M Sodium Hydroxide at 40°C.

in acid was observed to react twice as fast as  $[\text{Cr}(\text{NH}_3)_5(\text{OH})]^{2+}$  in base. However, no mechanism was proposed [32,33]. The aquation of the analogous cobalt(III) complex,  $[\text{Co}(\text{NH}_3)_6]^{3+}$ , was observed [34] to be much slower than the chromium(III) complex.

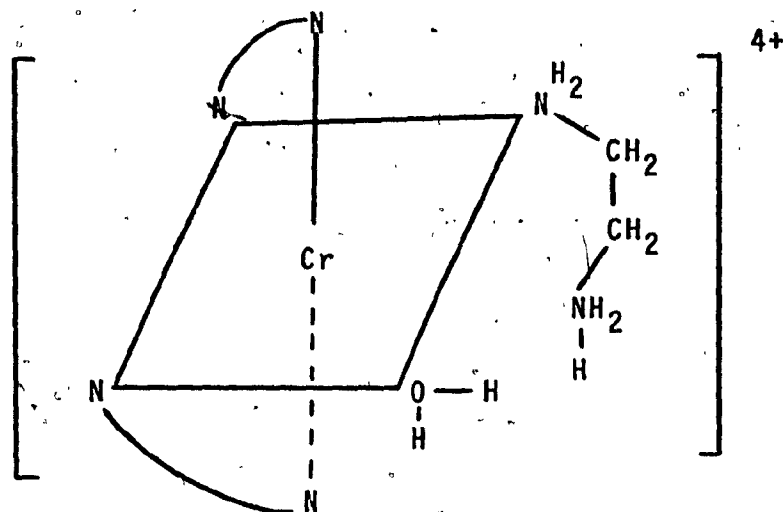
Schlafer and coworkers [35,36] have proposed the following general reaction sequence for the acid hydrolysis of  $[\text{Cr}(\text{en})_3]^{3+}$ ,



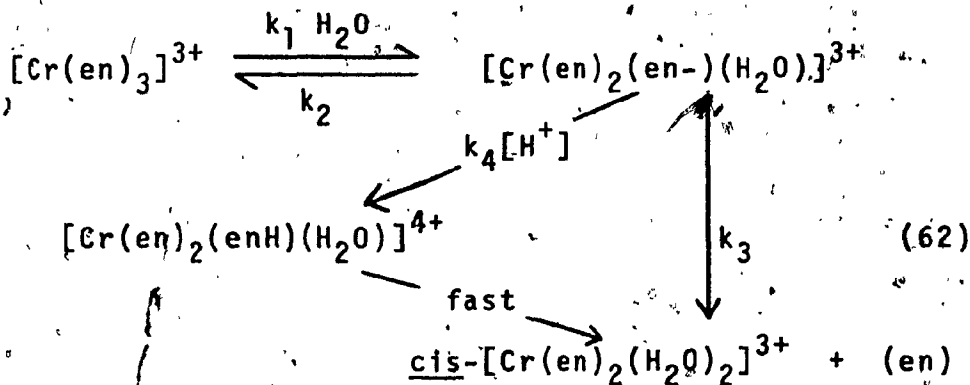
in which the liberation of one ethylenediamine-metal bond is the first step. Assuming that the rate was pseudo first-order, the intermediate species [X] was thought to have the structure



A reinvestigation by Jorgensen and Bjerrum [37] suggested that the first reaction product of the acid hydrolysis was an aquo-pentaammine ion with the structure

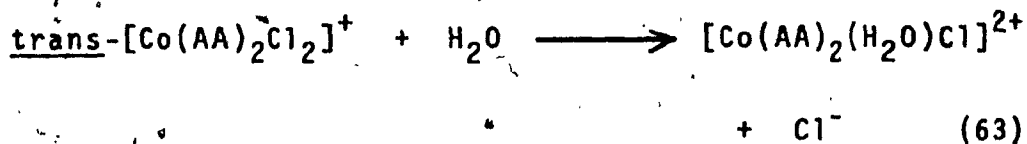


Such a species would be stabilized via hydrogen-ion-uptake by the displaced  $\text{-NH}_2$  group. The observed irregularities in the beginning of the racemization process of  $[\text{Cr}(\text{en})_3]^{3+}$  have led Schlafer and Seidel [35] to propose two competitive steps. These workers [35] attributed the faster step to direct racemization of  $[\text{Cr}(\text{en})_3]^{3+}$  and the slower step to racemization via aquation of an insoluble intermediate, while Jorgensen and Bjerrum [37] have attributed the faster step to a partially-hydrolysed species and the slower step to aquation of  $[\text{Cr}(\text{en})_3]^{3+}$ . Jorgensen and Bjerrum viewed the acid hydrolysis of this complex as that in (62).



In the above reaction scheme, the rate-determining step was described as the opening of the ethylenediamine ring via Cr-N bond rupture, since at high acid concentrations  $k_4[\text{H}^+]$  will be significantly greater than  $k_2$ . The scheme is similar to that proposed for the acid hydrolysis of  $[\text{Fe}(\text{bipy})_3]^{2+}$  [38,39] and  $[\text{Ni}(\text{bipy})_3]^{2+}$  [10,11] (see below). Hence, the rate would be expected to show similar inverse hydrogen ion dependence; however, pH dependence studies have not been performed on  $[\text{Cr}(\text{en})_3]^{3+}$ . The theory presented by Jorgensen and Bjerrum [37] suggests an intramolecular racemization pathway for  $[\text{Cr}(\text{en})_3]^{3+}$ , while Schlafer's theory does not preclude an intermolecular pathway, via water exchange. The racemization pathway may provide further insight into the hydrolysis mechanism of such complexes.

Basolo and coworkers [40] have determined the relative rates of aquation of several analogous cobalt(III) complexes, in which only the nature of the amine ligand was altered:



where (AA) represents ethylenediamine and C-methyl substituted ethylenediamines. The aquation rates were observed to increase with increasing size of the ammine ligands. Such an observation is consistent [40] with a dissociative mechanism, since the increased strain on the complex resulting from increased ligand size would be relieved by expulsion of a chloride ligand to form a pentacoordinate intermediate species. If a displacement mechanism were operative, a decreased aquation rate with increasing size would have been expected since the central metal ion would become less accessible to nucleophilic attack by the incoming water molecule.

In general, chromium(III) ammine complexes aquate faster than the analogous cobalt(III) complexes [1]. Some acid hydrolysis rate constants and activation energies are shown in Table VII. However, base hydrolysis of chromium(III) complexes is often many times slower than that for the analogous cobalt(III) complex. At 25°C,  $k_{\text{obs}} = 3.4 \times 10^{-4} \text{ sec}^{-1}$  for the aquation of cis- $[\text{Cr}(\text{en})_2\text{Cl}_2]^+$  and  $k_{\text{obs}} = 1.8 \times 10^{-4} \text{ sec}^{-1}$  for the analogous cobalt(III) complex. On the other hand,  $k_{\text{obs}} = 2.7 \times 10^{-2} \text{ M}^{-1}\text{sec}^{-1}$  for cis- $[\text{Cr}(\text{en})_2\text{Cl}]^+$  and  $k_{\text{obs}} = 1.0 \times 10^{-3} \text{ M}^{-1}\text{sec}^{-1}$  for the cobalt complex [41, 94]. It is



Table VII

Activation Energies and Rate Constants for Acid Hydrolysis at 25°C of Some Chromium(III) and Cobalt(III) Complexes

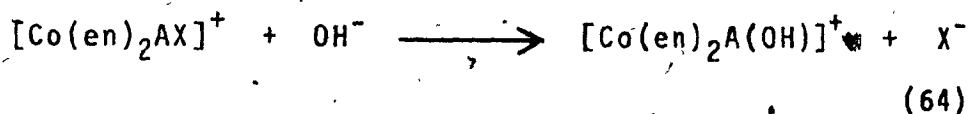
Complex	$k_{\text{obs}}$ ( $\text{sec}^{-1}$ )	$E_a$ (kcal/mol)
$[\text{Cr}(\text{NH}_3)_6]^{3+}$	$1.34 \times 10^{-6}$	26 <u>a</u>
$[\text{Cr}(\text{NH}_3)_5\text{Cl}]^{2+}$	$7.3 \times 10^{-6}$	24 <u>b</u>
$[\text{Cr}(\text{en})_3]^{3+}$	---	24.6 <u>c</u>
<u>cis</u> - $[\text{Cr}(\text{en})_2\text{Cl}_2]^+$	$3.4 \times 10^{-4}$	<u>d</u>
$[\text{Co}(\text{NH}_3)_6]^{3+}$	$10^{-10}$	<u>e</u>
$[\text{Co}(\text{NH}_3)_5\text{Cl}]^{2+}$	$1.7 \times 10^{-6}$	-9
<u>cis</u> - $[\text{Co}(\text{en})_2\text{Cl}_2]^+$	$1.8 \times 10^{-4}$	<u>d</u>

a see reference [32]; b see reference [92]; c see reference [42]; d see reference [93]; e see reference [34]..

thus quite difficult to reconcile a displacement or a dissociative mechanism to both complexes. Swaddle [3] has suggested that cobalt(III) complexes undergo ligand substitution reactions via a dissociative-type pathway; whereas chromium(III) complexes undergo substitution via an associative-type pathway. In support of Swaddle's contention, an increased aquation rate has been observed [40] for  $[\text{Co}(\text{MeNH}_2)_5\text{Cl}]^{2+}$  relative to that for  $[\text{Co}(\text{NH}_3)_5\text{Cl}]^{2+}$ ; while the opposite effect was observed [42] for the analogous chromium(III) complexes. Thus, for an associative-type mechanism to be operative, steric effects are thought to show up in the approach of the entering group, as opposed to the release of the leaving group in a dissociative-type mechanism. Therefore, larger ligands about the chromium(III) metal ion would restrict the approach of the entering nucleophile. The mechanism also depends on the relative electron import from the non-replaced ligands to the reaction site. Electron-releasing ligands promote a dissociative-type mechanism while electron-withdrawing ligands facilitate an associative-type mechanism. In complexes where each non-replaced ligand contributes equally to the mechanism, as do the tris-chelates, such a prediction as to the mechanism cannot be made.

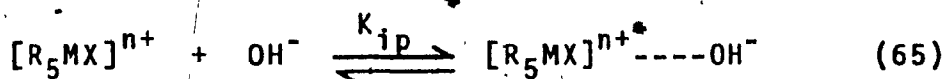
3. Base Hydrolysis.

Base hydrolysis was first thought to be a simple bimolecular substitution reaction at the metal centre [43] for cobalt(III) complexes of the type  $[\text{Co}(\text{en})_2\text{AX}]^+$ : The reaction showed second-order kinetics,



but the unique role of the hydroxide ion suggests a unique mechanism, as other potentially strong nucleophiles (like  $\text{CN}^-$ ) did not show similar behaviour [44]. This unique role of the hydroxide ion has been explained in terms of its mobility through the solvation shell of the complex via a Grotthus chain [45], regardless of the operating mechanism. Hence, hydroxide ion may be transported, via Grotthus-chain-conduction and proton transfer, to the solvation shell of the complex. The result is that the hydroxide ion will end up on some particular inner water molecule. If then this water molecule is positioned firmly among the ligands (e.g., by hydrogen-bonding to the ligand), its position may well facilitate the entry of the hydroxide ion.

A subsequent hypothesis was proposed [46] to account for the high reactivities observed, involving a pre-equilibrium ion-association between the complex cation and hydroxide ion,



where step (65) represents ion-association between the complex cation and hydroxide ion, and step (66) represents the rate-determining interchange process to form the products. The latter step could be either an associative ( $I_a$ ) or dissociative ( $I_d$ ) process. In support of such an ion-association mechanism, the effect of hydroxide ion on chloropentaamine-, cis-chloroamine-bis-ethylenediamine-, and cis-chloroaminetriethylenetetramine- cobalt(III) cations was investigated [47]. For one of the complexes, the overall reaction proposed is given in Figure 4. The observed rate constant for this reaction was given by equation (67).

$$k_{obs} = \frac{K_{ip}k[OH^-]}{1 + K_{ip}[OH^-]} \quad (67)$$

Deviation from linearity observed in plots of  $k_{obs}$  versus  $[OH^-]$  were explained in terms of equation (67), since  $(1 + K_{ip}[OH^-])$  will increase with increasing  $[OH^-]$ . A linear relationship was found to exist between  $1/k_{obs}$  and  $1/[OH^-]$ , with a slope  $k$  and intercept  $K_{ip}$ . In

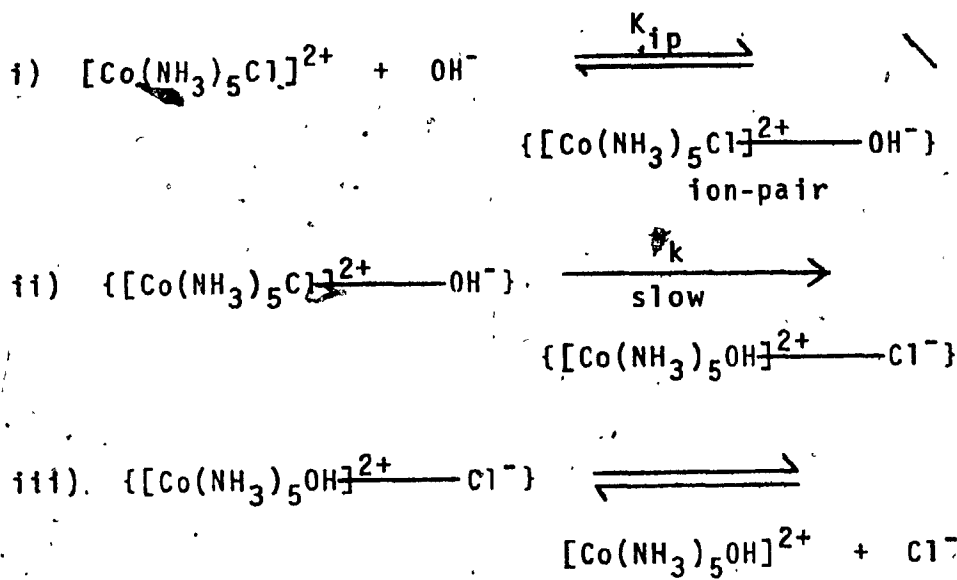


Figure 4: Base Hydrolysis of  $[\text{Co}(\text{NH}_3)_5\text{Cl}]^{2+}$  via an Ion-pair Pathway.

favour of such a mechanism was the prediction and observation [47] that increased complex size achieved by increased chelation yields a decrease in  $K_{ip}$ . Thus, if unidentate ammonia ligands are replaced by bidentate ethylenediamine ligands, the size of the complex does increase, and therefore ion-pair formation would be more difficult for the larger complex, denoted by a decrease in  $K_{ip}$ . However, Buckingham and coworkers [48] were unable to repeat the observations made above.

Gillard [49] has suggested that hydroxide ion is capable of acting as a reducing agent, and thus a mechanism involving an electron-transfer process was proposed for the base hydrolysis of some cobalt(III) complexes. The reaction is outlined in Figure 5. In reference to Figure 5, species I is an ion-pair, and species II, III, and V are radicals with the latter two associated in the primary solvation sphere with cobalt(II) cations. An electron is transferred, at least partly, from the hydroxide ion to the cobalt(III) cation to yield a radical species. The hydroxo-radical is trapped, and thus localized in the vicinity of the labile cobalt(II) species. The cobalt(II) species subsequently rearranges to give a more stable species, IV or VI. The constant  $k_2$  defines the rate-determining process, and  $k_4$  and  $k_6$  represent the combination of the hydroxo-radical with the cobalt(II) ion



to form a hydroxo-cobalt(III) product, IV or VI. In favour of this mechanism, the value of  $K_{ip} = 72.7$  for  $\{[\text{Co}(\text{NH}_3)_6], \text{OH}\}^{2+}$  has been cited [50]. It was later shown that [51] the concentration of this ion-pair is greater than the concentration of the conjugate base of  $[\text{Co}(\text{NH}_3)_6]^{3+}$ , i.e.,  $[\text{Co}(\text{NH}_3)_5(\text{NH}_2)]^{2+}$ . Thus, it was thought that hydroxide ion is indeed capable of acting as a reducing agent to form a cobalt(II) intermediate.

A catalytic role for the hydroxide ion effect has also been suggested [52], wherein the hydroxide ion abstracts a proton from the complex cation to form a dissociatively-reactive species. Assuming this idea, Basolo and Pearson [53] proposed the  $S_N1cb$  mechanism, for which 'cb' refers to conjugate-base. The reaction scheme presented in Figure 6 for  $[\text{Co}(\text{NH}_3)_5\text{Cl}]^{2+}$  was proposed, assuming that base hydrolysis in aqueous solution proceeds via specific catalysis by hydroxide ion. The first step involves the removal of a proton by  $\text{OH}^-$  in a rapid acid-base equilibrium to yield a complex B of lower charge. This latter complex then loses a chloride ligand more rapidly than the reactant complex because of its lower charge. The last step is relatively fast, and therefore the second step is rate-controlling. It is the conjugate-base B which undergoes the hydrolysis reaction. The rate law was given [53] as





$$\text{Rate} = k'(K_a/K_w)[\text{Co}(\text{NH}_3)_5\text{Cl}]^{2+}[\text{OH}^-] \quad (68)$$

wherein the observed rate constant is

$$k_{\text{obs}} = k'(K_a/K_w) \quad (69)$$

For the  $S_N1cb$  mechanism to be operative, the reactant must possess a moderately acidic proton.

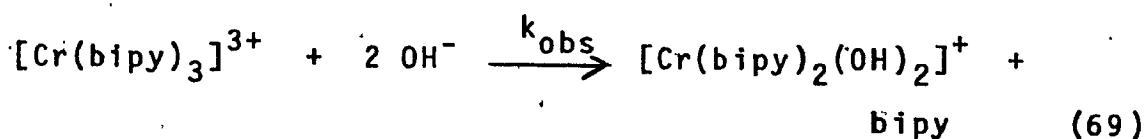
### C. Kinetics of Base Hydrolysis of $[\text{Cr}(\text{bipy})_3]^{3+}$ and $[\text{Cr}(\text{phen})_3]^{3+}$ .

#### 1. Introduction.

The N-heterocyclic molecules 2,2'-bipyridine and 1,10-phenanthroline are well known, and frequently used as ligands to form coordination compounds with transition metal ions. The structure and numbering systems for these molecules are shown in Figure 7. In the interest of brevity, 2,2'-bipyridine and 1,10-phenanthroline will be abbreviated as bipy and phen, respectively, when serving as ligands. Brandt *et al.* [54] have reviewed the complex chemistry of these and related ligands, as have Lindoy and Livingstone [55]. Because both molecules contain two nitrogen atoms their electronic absorption spectra show a pH dependence in the positions of the absorption bands. This pH dependence results from the following equilibria, as given

complex cation.

Four clearly-defined isosbestic points were observed for the  $[\text{Cr}(\text{bipy})_3]^{3+}$  reaction at 255, 263, 271, and 307 nm in 0.50  $[\text{OH}^-]$  at 7.5°C, and pH 11.82 at 29.5°C, as shown in Figure 10. These values are in good agreement with those reported by Maestri *et al.* [16] at 255, 263, 274, and 307 nm at pH 9.8 and 11°C. The spectral changes observed in Figure 10 are those expected for the overall reaction



The formation of the dihydroxo product is confirmed by an increase in absorbance near 518 nm, where only  $[\text{Cr}(\text{bipy})_2(\text{OH})_2]^+$  absorbs. Because of the close proximity of absorption maxima of free phenanthroline and  $[\text{Cr}(\text{phen})_3]^{3+}$ , it was difficult to obtain clearly-defined isosbestic points for the  $[\text{Cr}(\text{phen})_3]^{3+}$  reaction system. However, an attempt to locate these points at pH 11.82 at 30.5°C approximates their location at 235, 254, 287, and 304 nm. Confirmation of the overall reaction as

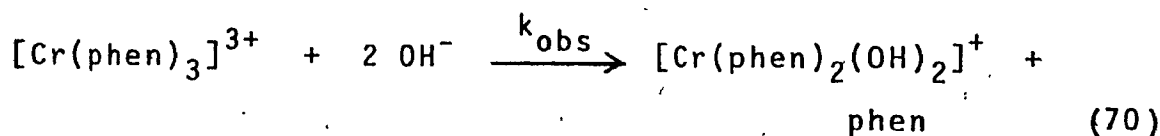
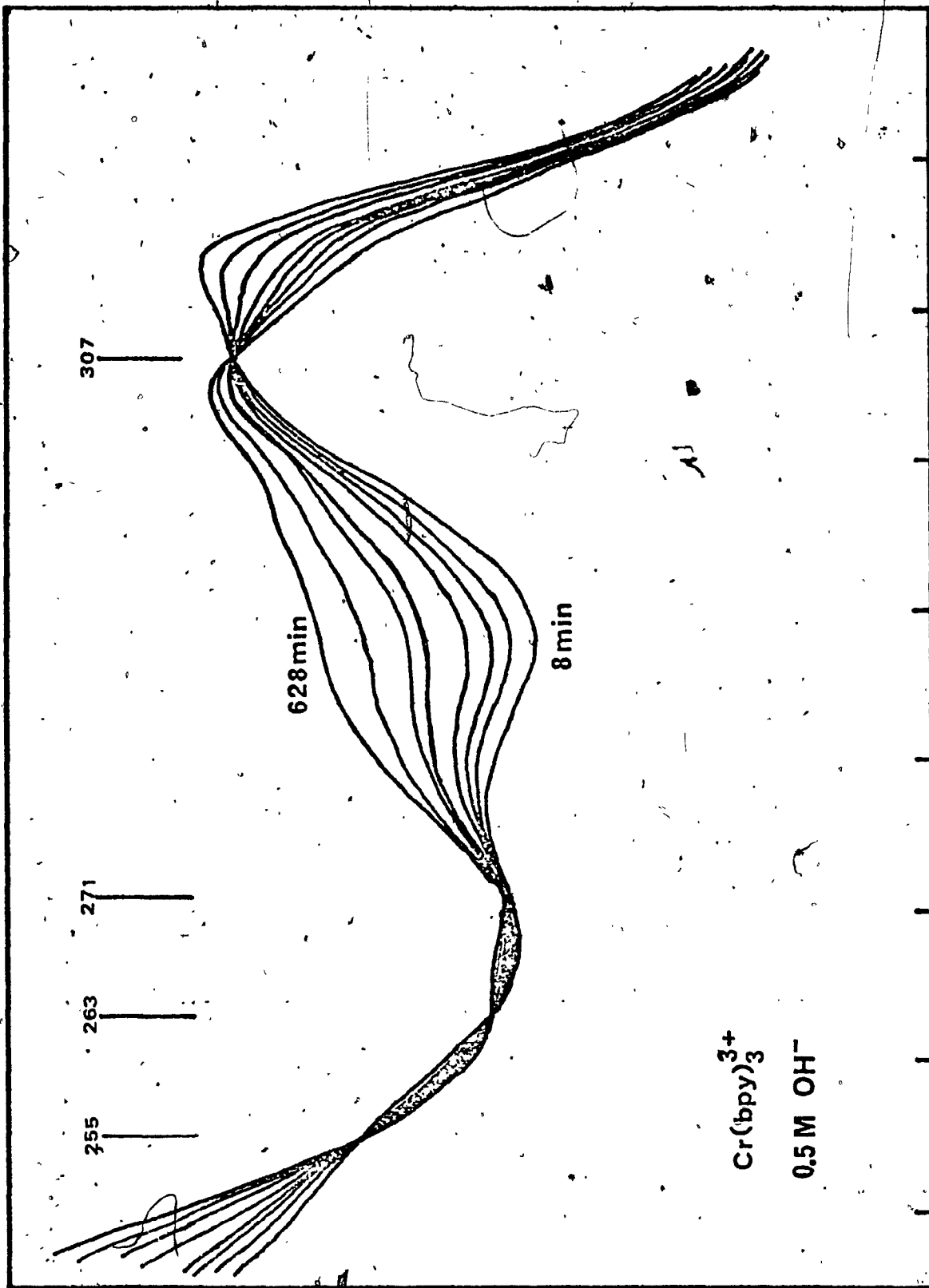


Figure 10. Ultraviolet Absorption Spectrum of  
 $[\text{Cr}(\text{bipy})_3]^{3+}$  at pH 11.82 and 29.5°C  
Depicting the Isosbestic Points.

---



O.D.

$\text{Cr}(\text{bpy})_3^{3+}$   
 $0.5 \text{ M OH}^-$

260 280 300 320  
nm →

was obtained by the observation of an increase in absorbance near 530 nm, where  $[\text{Cr}(\text{phen})_2(\text{OH})_2]^+$  absorbs, and  $[\text{Cr}(\text{phen})_3]^{3+}$  does not.

Pseudo first-order plots of  $\log \{C_0 - [\text{BIPY}]\}$  versus time have been reported [16] for the  $[\text{Cr}(\text{bipy})_3]^{3+}$  system at 11°C in the pH range 6.03 - 10.68, and are presented (with permission) in Figure 11. Subsequent investigation on this system at 11°C in the pH range 10.83 - 12.16 and 0.10 - 1.00 M sodium hydroxide yielded pseudo first-order plots as given in Figures 12 and 13, respectively. Table VIII gives the observed rate constants  $k_{\text{obs}}$  as a function of pH or  $[\text{OH}^-]$  at 11°C; and Figure 14 depicts the pH and  $[\text{OH}^-]$  dependence of  $k_{\text{obs}}$  for the hydrolysis of  $[\text{Cr}(\text{bipy})_3]^{3+}$  at 11°C. The same procedure was followed for the hydrolysis of  $[\text{Cr}(\text{phen})_3]^{3+}$  at 31.1°C. The pseudo first-order plots of  $\log \{C_0 - [\text{PHEN}]\}$  versus time are presented in Figures 15, 16, and 17 for the pH ranges 4.66 - 10.50, 11.14 - 12.17, and 0.10 - 1.00  $[\text{OH}^-]$ , respectively. Table IX gives the observed rate constants  $k_{\text{obs}}$  as a function of pH or  $[\text{OH}^-]$  at 31.1°C; and Figure 18 depicts the pH and  $[\text{OH}^-]$  dependence of  $k_{\text{obs}}$  for the hydrolysis of  $[\text{Cr}(\text{phen})_3]^{3+}$  at the same temperature.

It is immediately apparent from a comparison of the pH (or  $[\text{OH}^-]$ ) dependence of  $k_{\text{obs}}$  for the two systems (Figures 14 and 18) that their behaviour is very similar.

Figure 11. Plots of  $\log \{C_0 - [\text{BIPY}]\}$  versus time in  
the pH range 6.03 - 10.68: 11°C,  $C_0 \approx$   
 $1 \times 10^{-3}$  M,  $\mu = 1.0$  M.

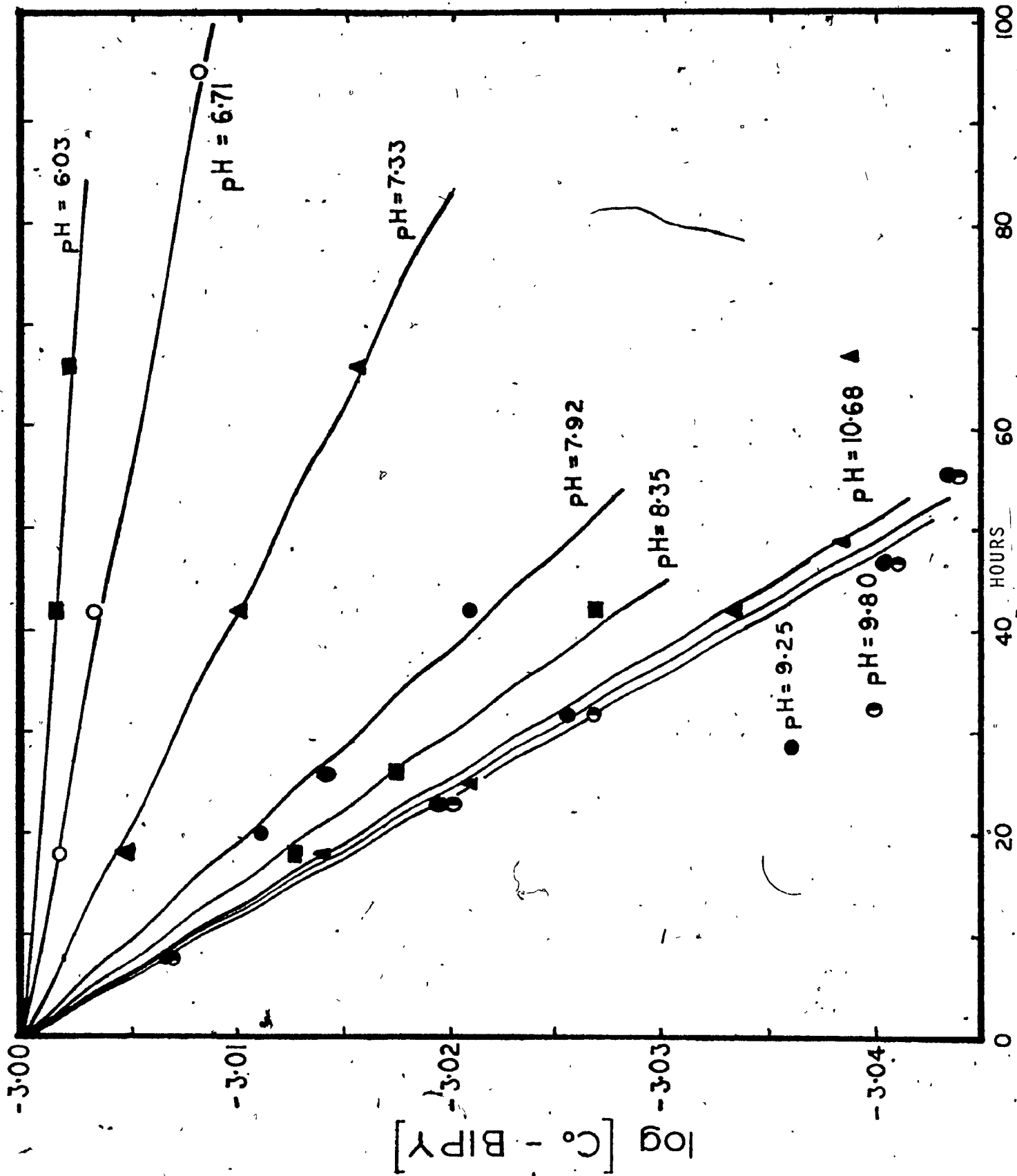




Figure 12. Plots of  $\log \{C_0 - [BIPY]\}$  versus time in the pH range 10.83 - 12.16: 11°C;  $C_0 \sim 1 \times 10^{-3}$  M;  $\mu = 1.0$  M.

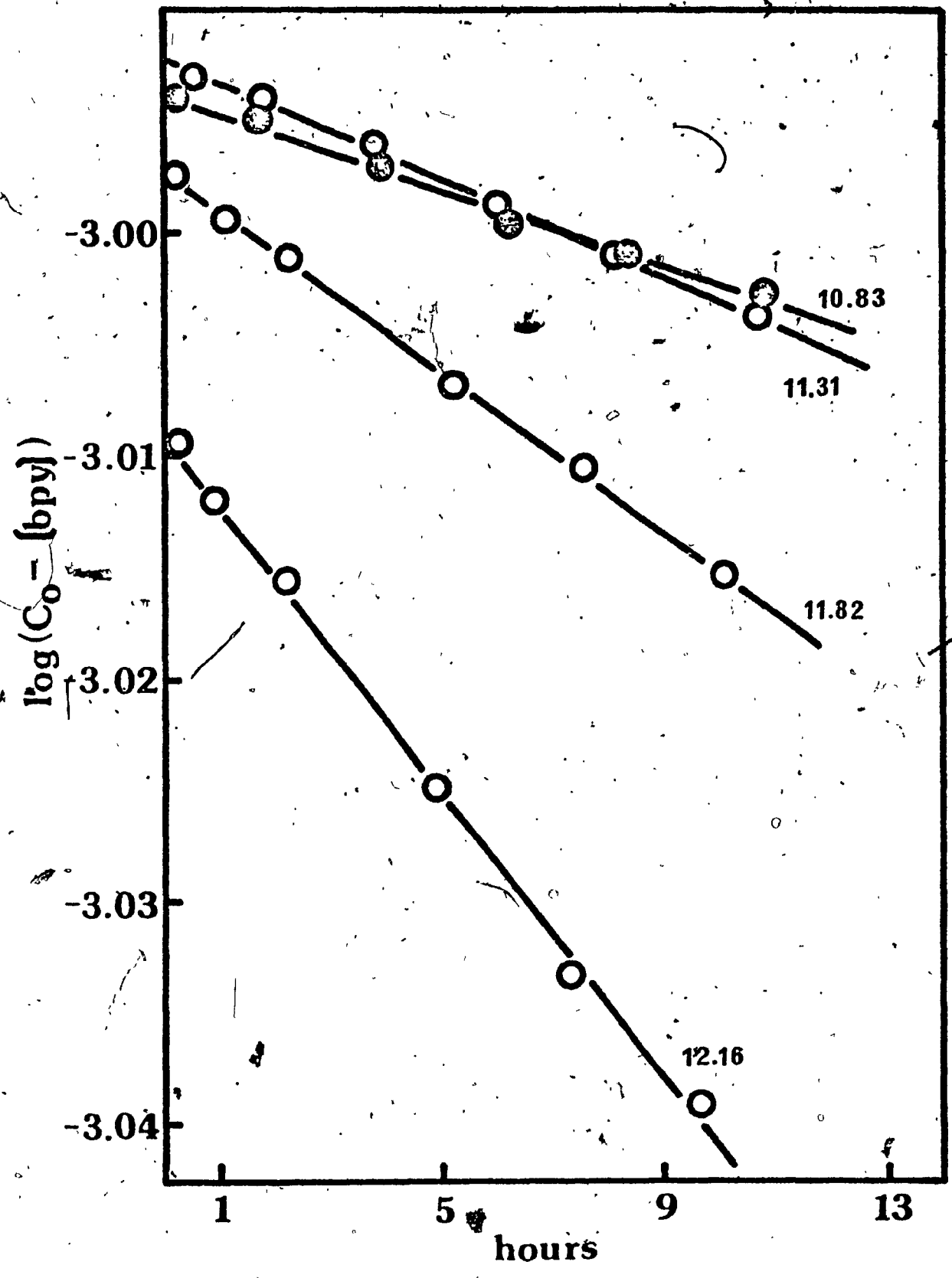


Figure 13. Plots of  $\log \{C_0 - [BIPY]\}$  versus time in the range 0.10 - 1.00  $[OH^-]$ : 11°C,  $C_0 \approx 1 \times 10^{-3}$  M;  $\mu = 1.0$  M.

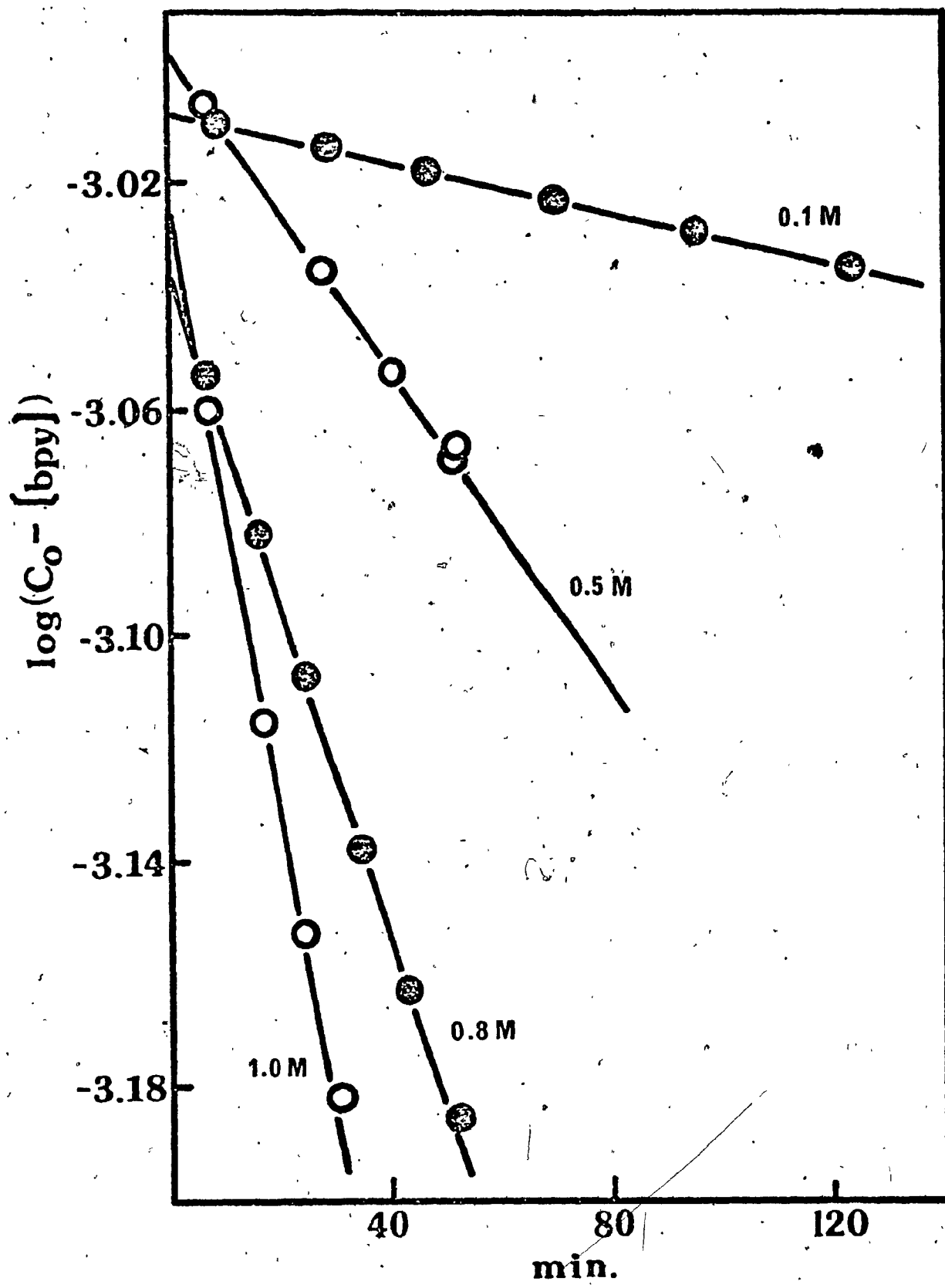


Table VIII

The Observed Rate Constants as a Function of pH or  $[\text{OH}^-]$  for  $[\text{Cr}(\text{bipy})_3]^{3+}$  at  $11^\circ\text{C}$ ,  $\mu = 1.0 \text{ M}^{\text{a}}$

pH ( $\pm 0.05$ )	$k_{\text{obs}} \times 10^{+7} \text{ (sec}^{-1}\text{)}$
0	$< 0.01^{\text{b}}$
6.71	0.59
7.33	1.5
7.92	3.2
8.35	4.1
9.25	5.1
9.80	5.2
10.68	5.1
10.83	$5.4 \pm 0.2$
11.31	$6.9 \pm 0.2$
11.82	$11.5 \pm 0.1$
12.16	$20.1 \pm 0.2$
$[\text{OH}^-]$	$k_{\text{obs}} \times 10^{+5} \text{ (sec}^{-1}\text{)}$
0.10	$0.30 \pm 0.1$
0.50	$5.3 \pm 0.1$
0.80	$11.0 \pm 0.2$
1.00	$19.7 \pm 0.6$

<sup>a</sup> Errors of  $k_{\text{obs}}$  reported as standard error.

<sup>b</sup> N. Serpone, personal communication for pH 0 - 10.68; the errors associated with the values of  $k_{\text{obs}}$  are estimated to be 10%.

Figure 14. Plot of pH and OH<sup>-</sup> Dependence of the Pseudo First-order Rate Constant for the Hydrolysis of [Cr(bipy)<sub>3</sub>]<sup>3+</sup> at 11°C,  $\mu = 1.0 \text{ M}$ .

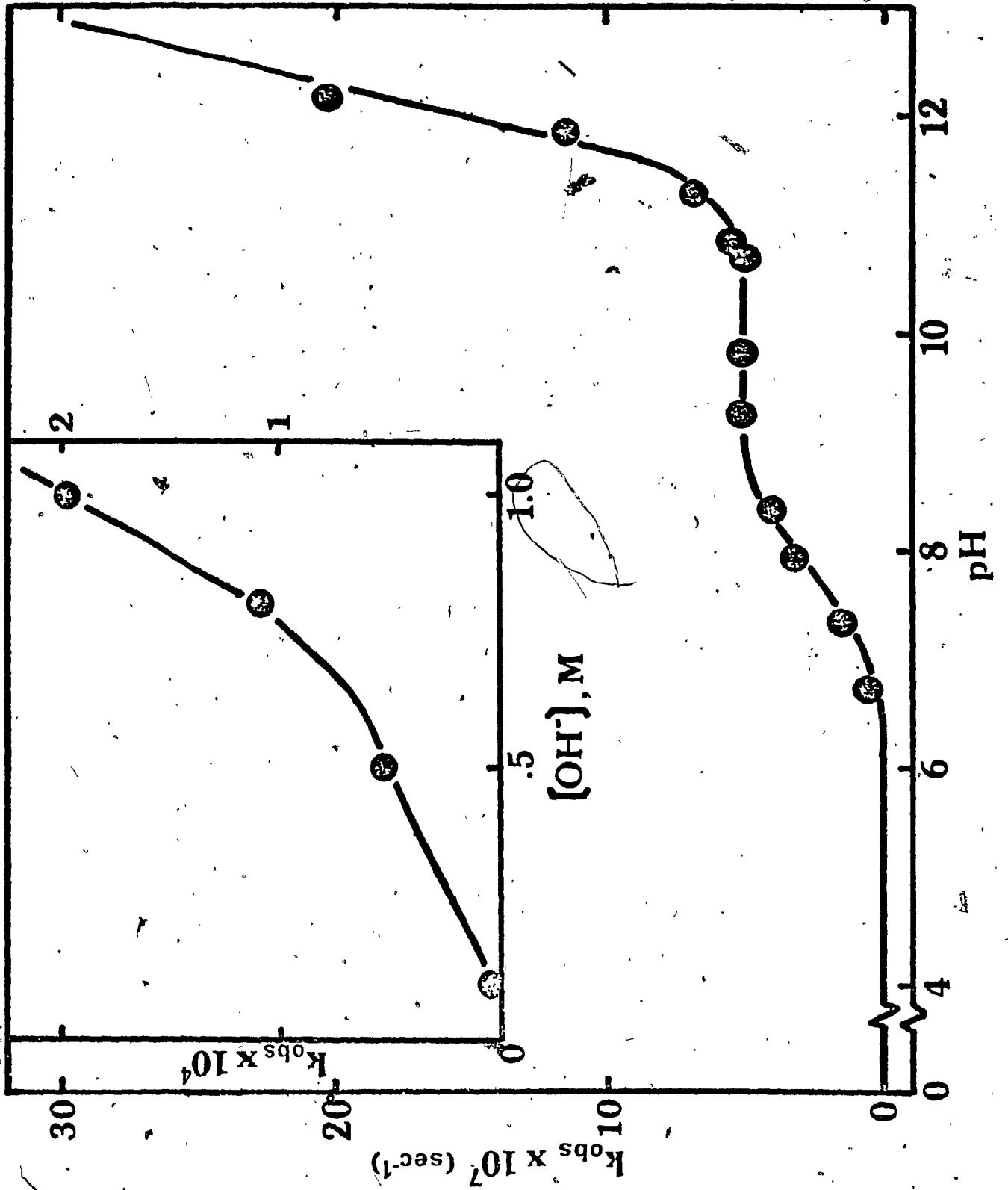


Figure 15. Plots of  $\log \{C_0 - [\text{PHEN}]\}$  versus time in  
the pH range 4.66 - 10.50: 31.1°C;  $C_0 \approx$   
 $1 \times 10^{-3}$  M;  $\mu = 1.0$  M.



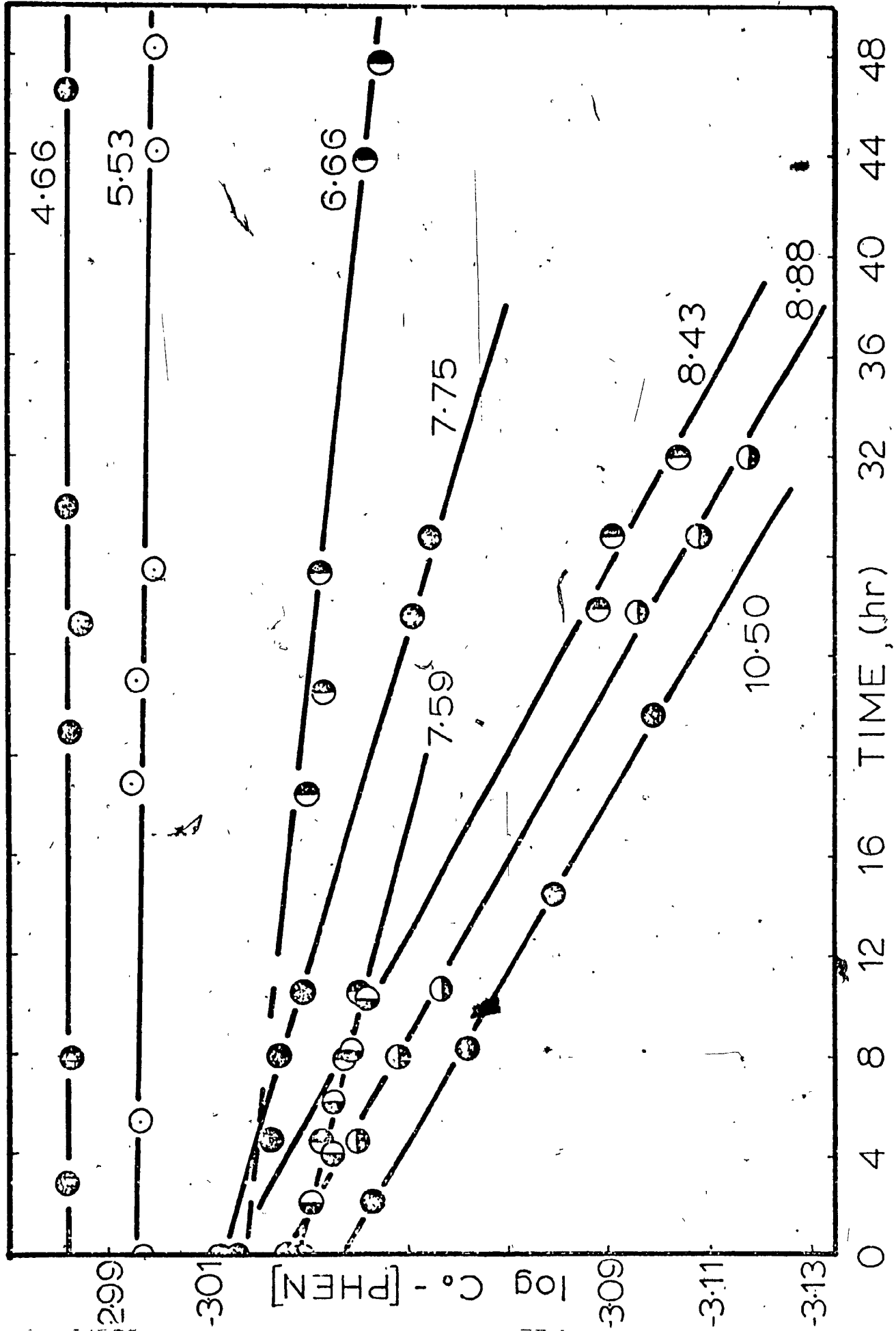
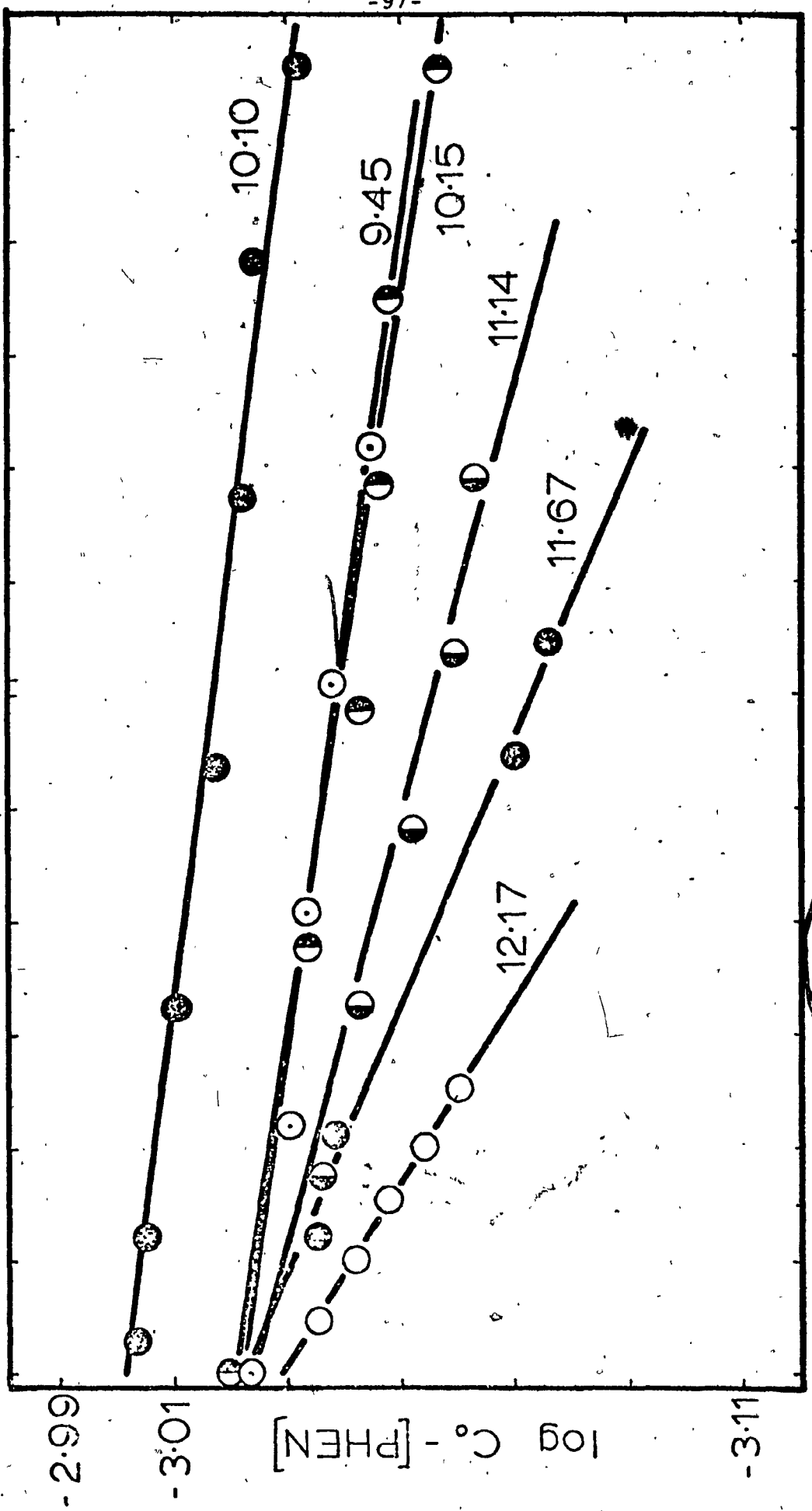


Figure 16. Plots of  $\log \{C_0 - [\text{PHEN}]\}$  versus time in the pH range 11.14 - 12.17: 31.1°C;  $C_0 = 1 \times 10^{-3}$  M;  $\mu = 1.0$  M.



TIME (hr) 8 10

T

Figure 17. Plots of  $\log \{C_0 - [\text{PHEN}]\}$  versus time in  
the range 0.10 - 1.00  $[\text{OH}^-]$ : 31.1°C;  
 $C_0 \sim 1 \times 10^{-3}$  M;  $\mu = 1.0$  M.

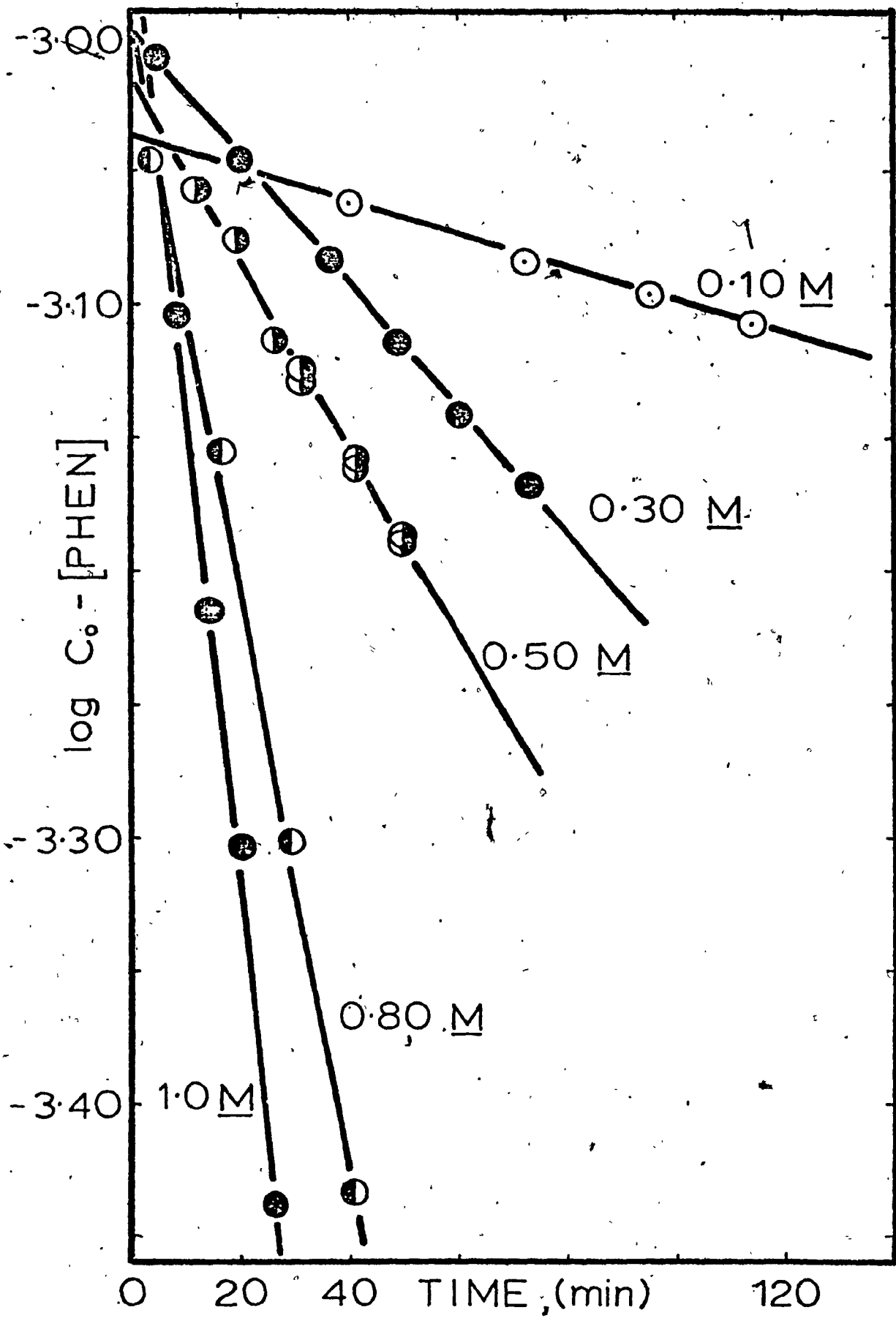


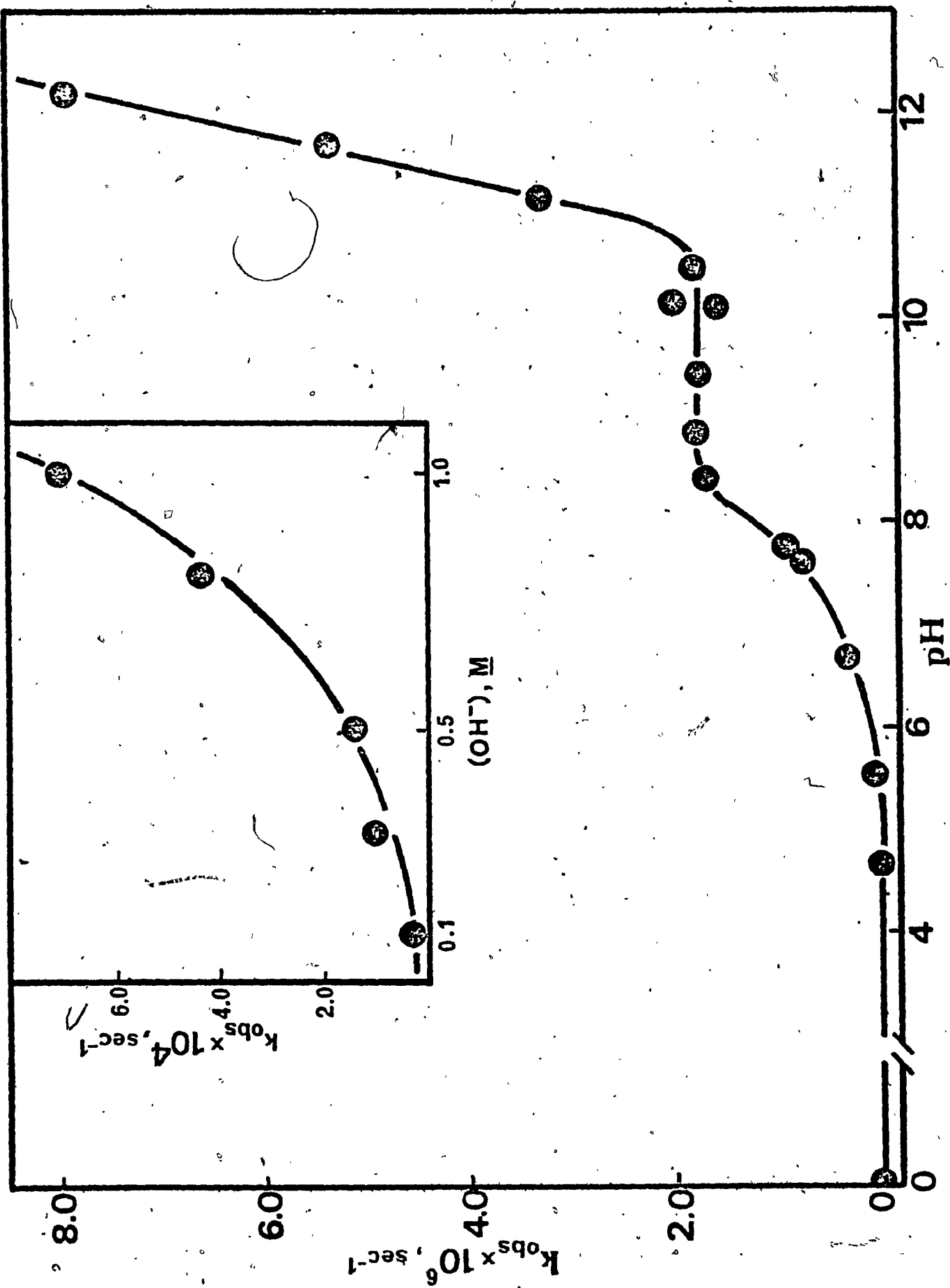
Table IX

The Observed Rate Constants as a Function of pH  
or  $[\text{OH}^-]$  for  $[\text{Cr}(\text{phen})_3]^{3+}$  at  $31.1^\circ\text{C}$ ,  $\mu = 1.0 \text{ M}^a$

pH ( $\pm 0.05$ )	$k_{\text{obs}} \times 10^6 \text{ (sec}^{-1}\text{)}$
0	<0.01
4.66	<0.01
5.53	$0.049 \pm 0.017$
6.66	$0.32 \pm 0.04$
7.59	$0.80 \pm 0.07$
7.75	$0.93 \pm 0.04$
8.43	$1.72 \pm 0.07$
8.88	$1.80 \pm 0.04$
9.45	$1.77 \pm 0.14$
10.10	$1.57 \pm 0.08$
10.15	$2.01 \pm 0.17$
10.50	$1.83 \pm 0.02$
11.14	$3.29 \pm 0.25$
11.67	$5.37 \pm 0.25$
12.17	$7.91 \pm 0.04$
$[\text{OH}^-]$	
0.10	$23.4 \pm 0.5$
0.30	$91.4 \pm 1.2$
0.50	$132.1 \pm 4.8$
0.80	$430 \pm 20$
1.00	$709 \pm 28$

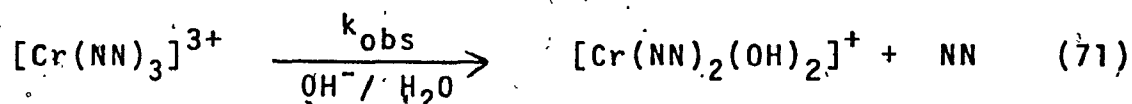
<sup>a</sup> Errors of  $k_{\text{obs}}$  reported as standard error.

Figure 18. Plot of pH and  $\text{OH}^-$  Dependence of the Pseudo First-order Rate Constant for the Hydrolysis of  $[\text{Cr}(\text{phen})_3]^{3+}$  at  $31.1^\circ\text{C}$ ,  $\mu = 1.0 \text{ M}$





The results show that at pH  $\geq$  6.03 for  $[\text{Cr}(\text{bipy})_3]^{3+}$  and  $\geq$  6.66 for  $[\text{Cr}(\text{phen})_3]^{3+}$ , the substitution of a bidentate ligand in the coordination sphere of the chromium(III) complex follows pseudo first-order kinetics, according to the overall stoichiometric reaction



wherein  $k_{\text{obs}}$  increases with increasing pH (and  $[\text{OH}^-]$ ). The relationships between  $k_{\text{obs}}$  and hydroxide ion concentration for each system will now be dealt with separately.

1. The  $[\text{Cr}(\text{bipy})_3]^{3+}$  system:

Region (a): in the pH range 6.03 - 10.68, the hydroxide ion concentration dependence of  $k_{\text{obs}}$  has been reported by Maestri *et al.* [16] as

$$1/k_{\text{obs}} = (B/[\text{OH}^-]) + A = 1/k_x \quad (72)$$

$$k_x = k_{\text{obs}} = [\text{OH}^-] / (B + A[\text{OH}^-]) \quad (73)$$

where B and A are the slope and intercept, respectively, of a linear least-squares plot of  $1/k_{\text{obs}}$  versus  $1/[\text{OH}^-]$ , and equal to  $0.82 \pm 0.02$  M-sec and  $2.1 \pm 0.2 \times 10^6$  sec at 11°C, respectively [16].

Region (b): in the pH range 10.83 - 12.16, a

plot of  $k_{\text{obs}}$  versus  $[\text{OH}^-]$  (Figure 19) is linear, related by the expression

$$k_{\text{obs}} = C[\text{OH}^-] + D = k_c \quad (74)$$

where  $C$  is the slope of the least-squares line and is equal to  $1.06 \pm 0.01 \times 10^{-4} \text{ M}^{-1} \text{ sec}^{-1}$ , and  $D$  is the intercept, and equal to  $4.6 \pm 0.1 \times 10^{-7} \text{ sec}^{-1}$  at  $11^\circ\text{C}$ .

Region (c): for  $0.10 - 1.00 [\text{OH}^-]$ ,  $k_{\text{obs}}$  shows second-order dependence on the hydroxide ion concentration, as given by the expression

$$k_{\text{obs}} = E[\text{OH}^-]^2 + F = k_E \quad (75)$$

where the slope  $E$  and intercept  $F$  of the least-squares plot of  $k_{\text{obs}}$  versus  $[\text{OH}^-]^2$  (Figure 20) are equal to  $1.9 \pm 0.1 \times 10^{-4} \text{ M}^{-2} \text{ sec}^{-1}$  and  $\sim 3 \times 10^{-7} \text{ sec}^{-1}$  at  $11^\circ\text{C}$ , respectively.

## 2. The $[\text{Cr}(\text{phen})_3]^{3+}$ system:

Region (a): in the pH range  $6.66 - 10.50$ , the dependence of the observed rate constant  $k_{\text{obs}}$  on the hydroxide ion concentration is given by the expression

$$k_{\text{obs}} = [\text{OH}^-] / (B' + A'[\text{OH}^-]) = k_x' \quad (76)$$

as obtained from the linear relationship between  $1/k_{\text{obs}}$  and  $1/[\text{OH}^-]$  (Figure 21). The slope  $B'$  is equal to  $2.8 \pm 0.1 \times 10^{-1} \text{ Msec}$ , and the intercept  $A'$  is equal to

Figure 19: Hydroxide Ion Dependence of  $k_{obs}$  in the Hydrolysis of  $[\text{Cr}(\text{bipy})_3]^{3+}$  in the pH Range 10.83 - 12.16 at 11°C.

Figure 20. Hydroxide Ion Dependence of  $k_{obs}$  in the Hydrolysis of  $[\text{Cr}(\text{bipy})_3]^{3+}$  in the Range 0.10 - 1.00  $[\text{OH}^-]$  at 11°C.

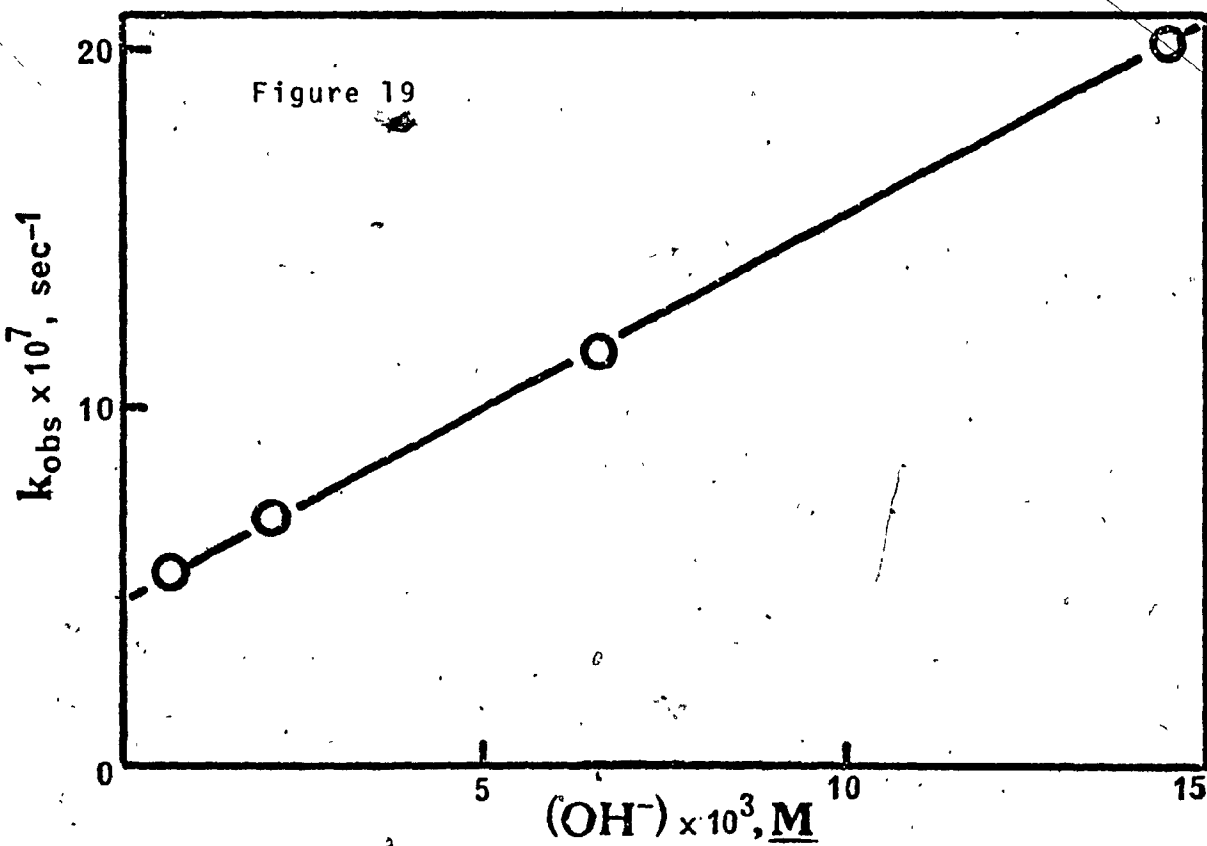
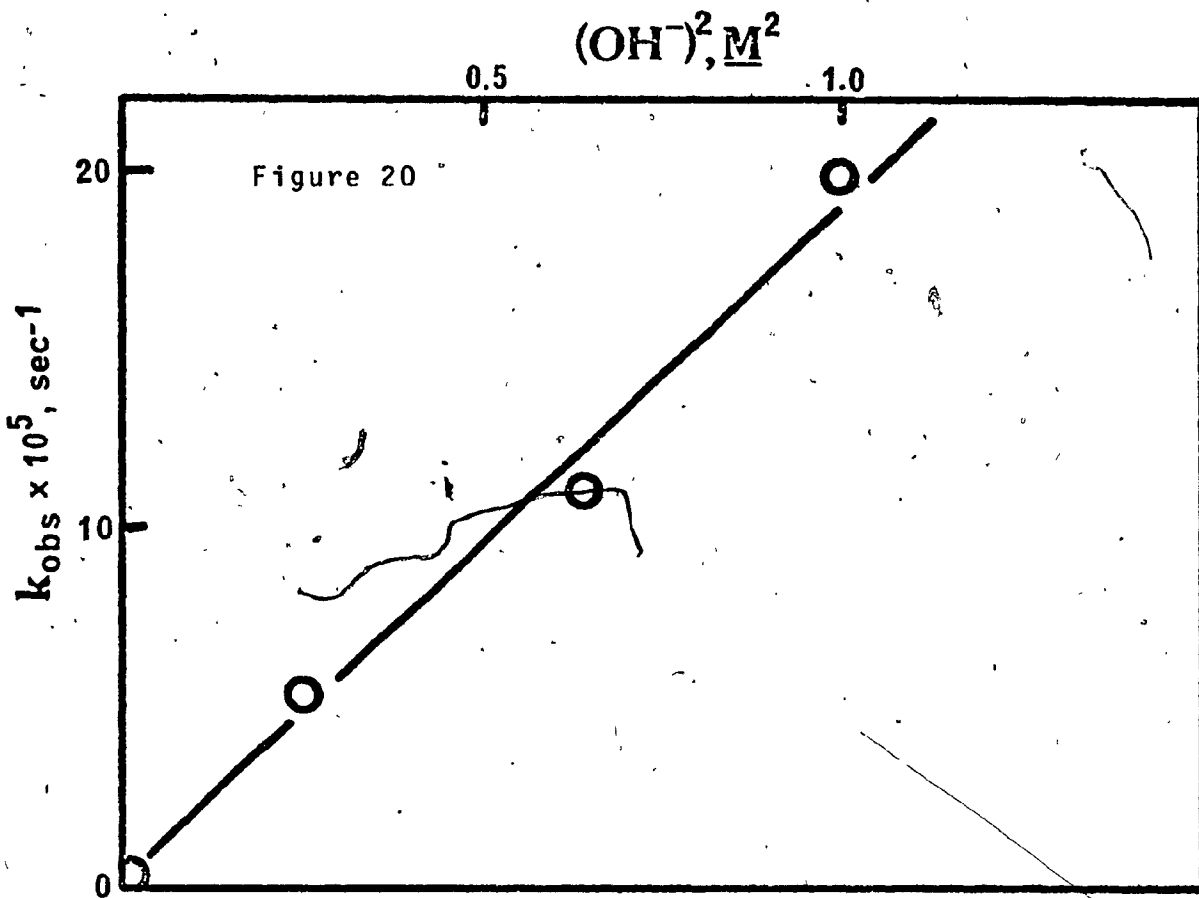


Figure 21. Hydroxide Ion Dependence of  $k_{obs}$  in the Hydrolysis of  $[\text{Cr}(\text{phen})_3]^{3+}$  in the pH Range 6.66 - 10.50 at 31.1°C.

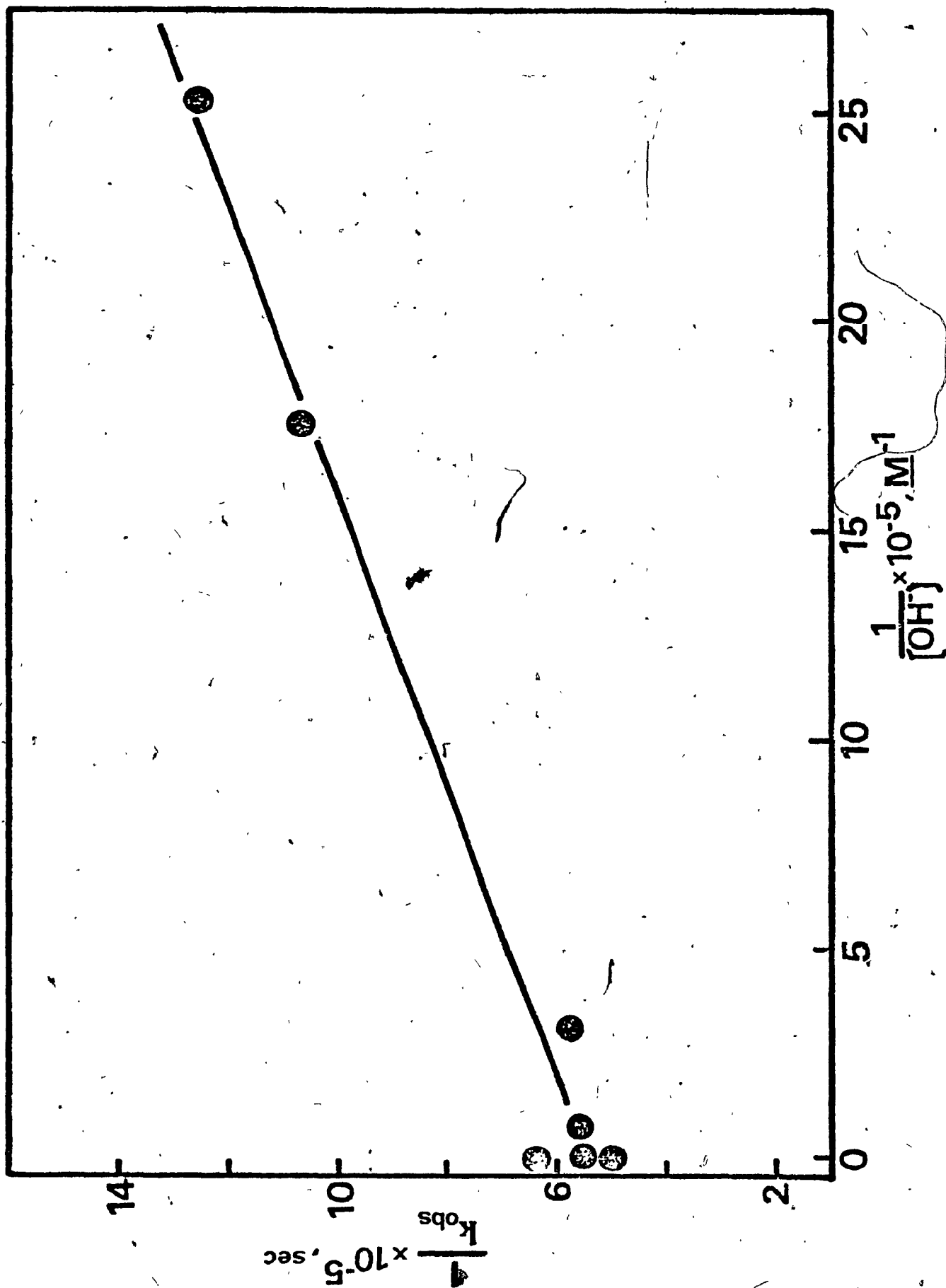
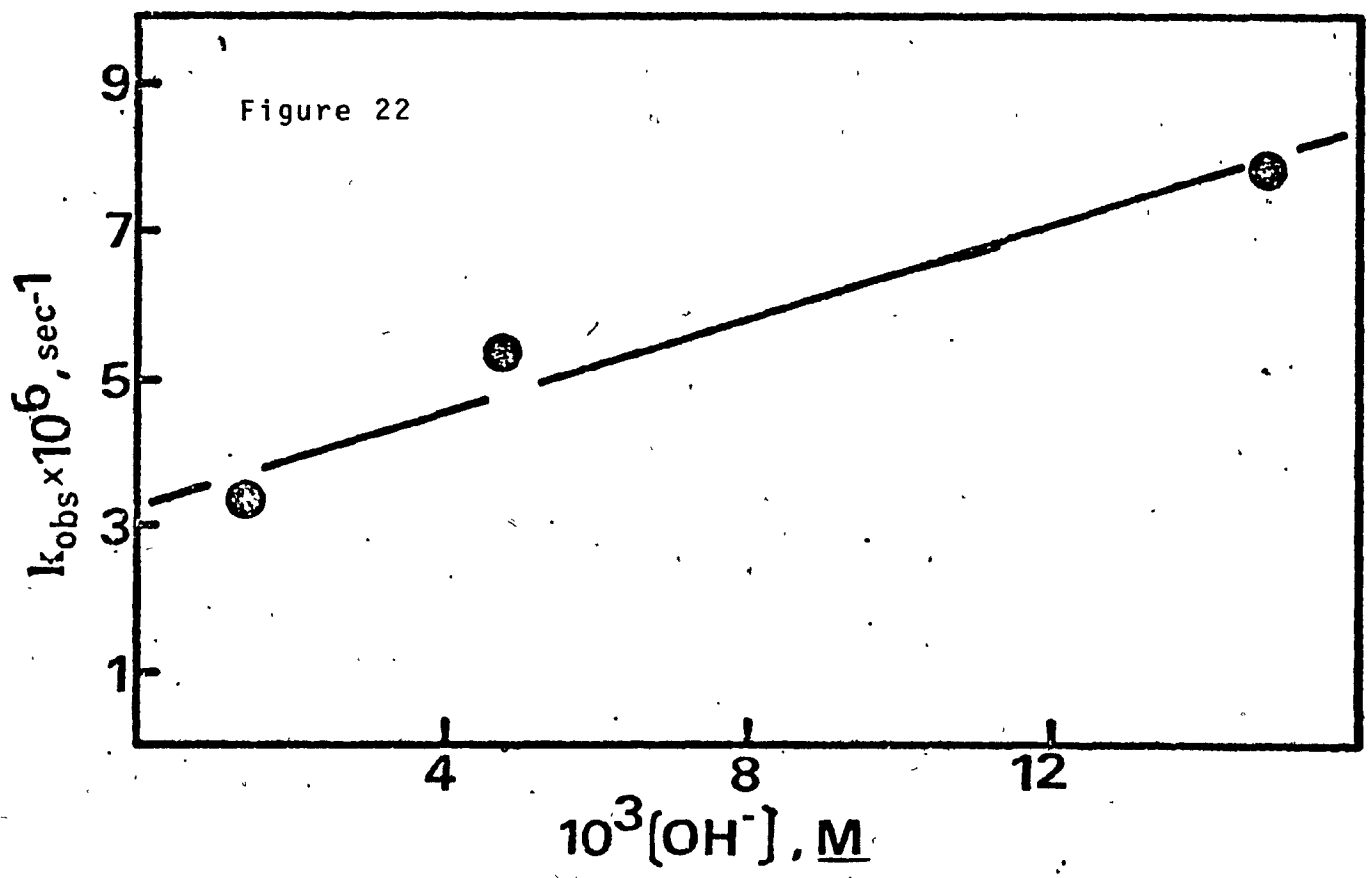
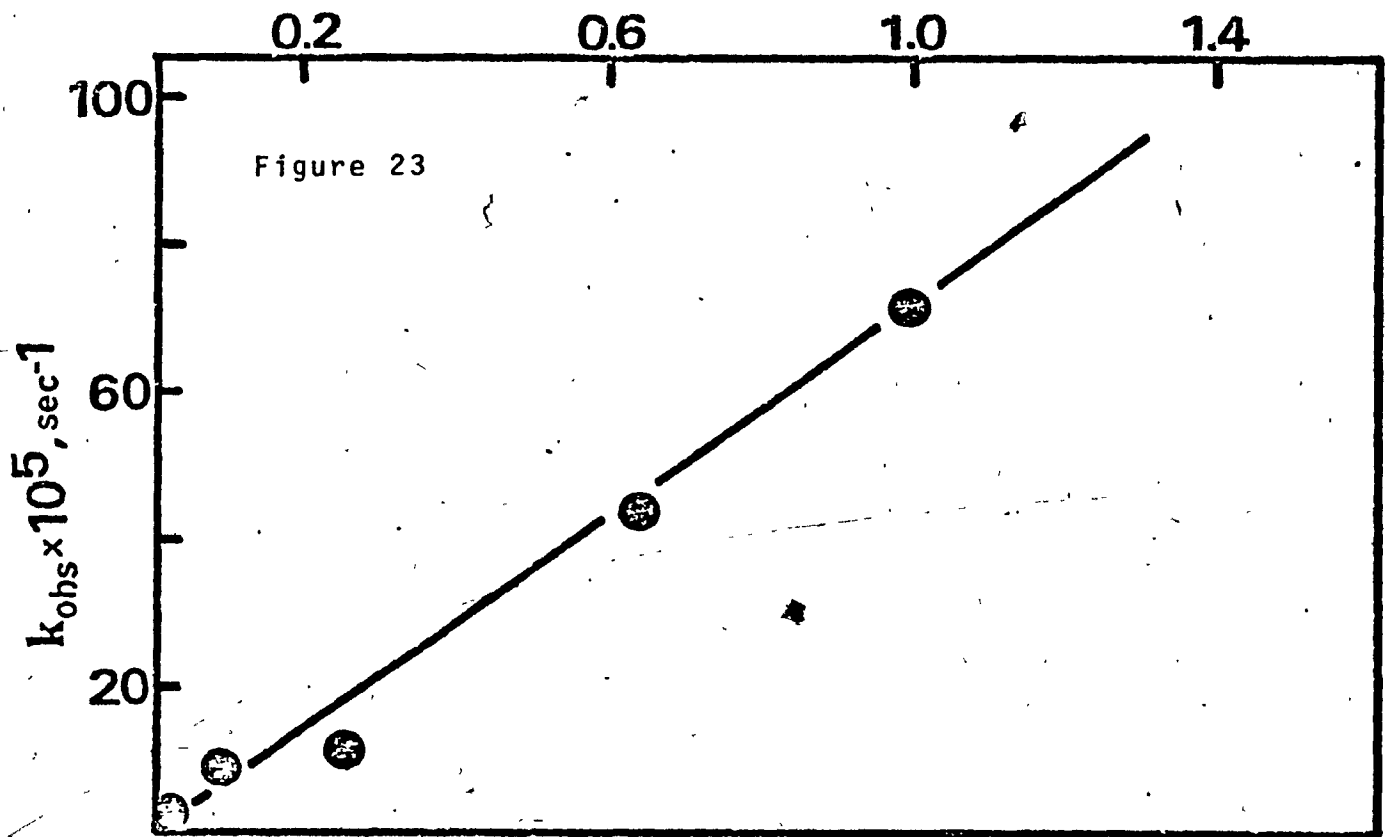


Figure 22. Hydroxide Ion Dependence of  $k_{obs}$  in the Hydrolysis of  $[\text{Cr}(\text{phen})_3]^{3+}$  in the pH Range 11.14 - 12.17 at 31.1°C.

Figure 23. Hydroxide Ion Dependence of  $k_{obs}$  in the Hydrolysis of  $[\text{Cr}(\text{phen})_3]^{3+}$  in the Range 0.10 - 1.00  $[\text{OH}^-]$  at 31.1°C.

$[\text{OH}^-]^2, \text{M}^2$





$5.4 \pm 0.3 \times 10^5$  sec at  $31.1^\circ\text{C}$ .

Region (b): in the pH range 11.14 - 12.17, a linear relationship exists between the observed rate constant and the hydroxide ion concentration (Figure 22) as given by the expression

$$k_{\text{obs}} = C'[\text{OH}^-] + D' = k_C' \quad (77)$$

where  $C'$  is the slope and equal to  $3.2 \pm 0.7 \times 10^{-4} \text{ M}^{-1} \text{ sec}^{-1}$ , and  $D'$  the intercept is equal to  $3.3 \pm 0.9 \times 10^{-6} \text{ sec}^{-1}$  at  $31.1^\circ\text{C}$  of a linear least-squares plot of  $k_{\text{obs}}$  versus  $[\text{OH}^-]$ .

Region (c): for 0.10 - 1.00  $[\text{OH}^-]$ , the observed rate constant shows a second-order dependence on the hydroxide ion concentration, as shown in the expression

$$k_{\text{obs}} = E'[\text{OH}^-]^2 + F' = k_E' \quad (78)$$

where  $E'$  and  $F'$  are the slope and intercept, respectively, of a least-squares plot of  $k_{\text{obs}}$  versus  $[\text{OH}^-]^2$  (Figure 23) and equal to  $6.9 \pm 0.4 \times 10^{-4} \text{ M}^{-2} \text{ sec}^{-1}$  and  $\sim 3 \times 10^{-6} \text{ sec}^{-1}$ , respectively, at  $31.1^\circ\text{C}$ .

From the above analysis of the hydroxide ion concentration dependence of the observed rate constant, it is apparent that each of the two chromium(III) complex cations has three distinct regions, (a), (b), and (c); and the

general relationship between  $k_{\text{obs}}$  and  $[\text{OH}^-]$  is the same for each complex, that is,

$$\text{region (a): } k_{\text{obs}} = [\text{OH}^-] / (B + A[\text{OH}^-]) = k_x \quad (79)$$

$$\text{region (b): } k_{\text{obs}} = C[\text{OH}^-] + D = k_c \quad (80)$$

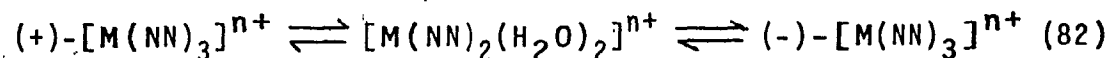
$$\text{region (c): } k_{\text{obs}} = E[\text{OH}^-]^2 + F = k_E \quad (81)$$

D. Mechanisms for the Base Hydrolysis of  $[\text{Cr}(\text{bipy})_3]^{3+}$  and  $[\text{Cr}(\text{phen})_3]^{3+}$ .

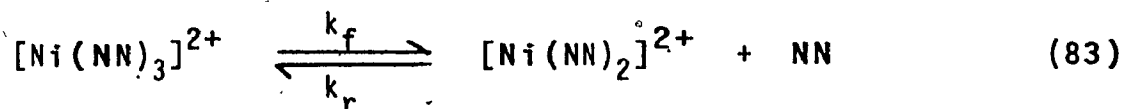
From the kinetic analysis given previously, it is obvious that a simple bimolecular reaction between the complex cation and hydroxide ion is not applicable to the hydrolysis of either chromium(III) cation under investigation. Maestri and coworkers [16] have proposed several possible mechanisms for the hydrolysis of  $[\text{Cr}(\text{bipy})_3]^{3+}$  in the pH range 6.03 - 10.68, including dissociative and associative pathways, an ion-pair mechanism, and Gillard's mechanism. At first glance, one can eliminate the feasibility of an  $S_N1_{\text{cb}}$  pathway, inasmuch as such a mechanism requires the presence of an acidic proton. Neither  $[\text{Cr}(\text{bipy})_3]^{3+}$  nor  $[\text{Cr}(\text{phen})_3]^{3+}$  possess such a proton. The possible pathways envisaged for the hydrolysis of these two cations are entertained separately in the following discussion.

1. Dissociative Pathway (D).

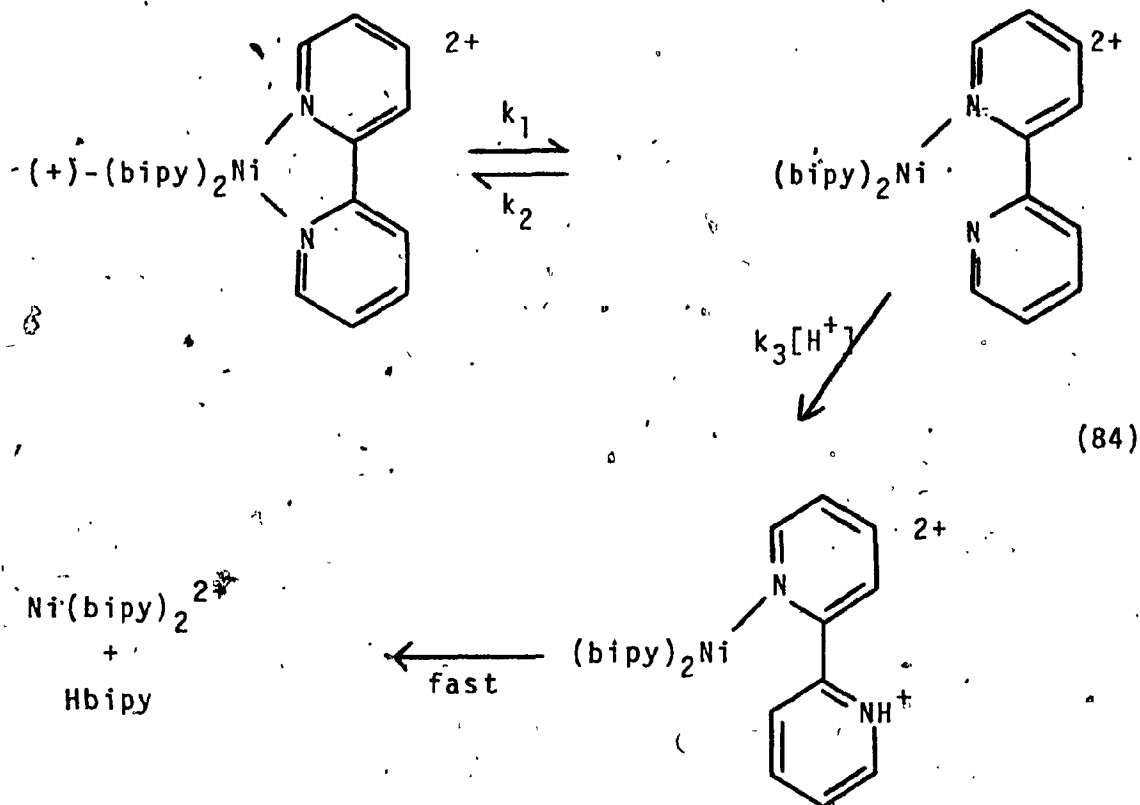
As previously discussed, a dissociative (D) pathway involves the formation of pentacoordinate intermediate species. Racemization studies have aided in the elucidation of operable mechanisms in bipyridyl and phenanthroline complexes of transition metal ions, most notably those of iron(II) and nickel(II). The two basic racemization pathways for octahedral complexes are intra- and inter-molecular racemization. The phenanthroline and bipyridine ligands have played an important role in both the development and differentiation of the two pathways. Racemization via an intermolecular pathway involves a ligand exchange process, in which the rate of ligand exchange is equal to or faster than the rate of racemization, and may be represented by the scheme (82).



$[Ni(bipy)_3]^{2+}$  and  $[Ni(phen)_3]^{2+}$  were originally thought to racemize via an intramolecular pathway [38, 60, 61] as the presence of excess ligand did not alter the rate of racemization. It was thought that excess ligand should favour the reformation of the tris-complex via an intermolecular process ( see (83)), that is,  $k_r \gg k_f$ . However, if the  $[Ni(NN)_2]^{2+}$  species is symmetrical or loses optical activity rapidly, then excess



ligand would not be expected to alter the racemization rate. Basolo et al. [10] have proposed an intermolecular racemization pathway for the two nickel(II) complex cations, based on spectrophotometric studies on the rates of racemization and dissociation. The two rates in acid solution were found to be equal within experimental error. Similar activation energies were observed for the dissociation in acid and racemization in water, suggesting a similar mechanism in acid and neutral media. The only significant difference between the two nickel(II) complexes was the observation that while the racemization rate of  $[\text{Ni}(\text{phen})_3]^{2+}$  varies only slightly with changing acidity, there is a significant rate increase with increasing acidity for  $[\text{Ni}(\text{bipy})_3]^{2+}$ . The same observations were made by Wilkins and Williams [11]. The discrepancy was rationalized in terms of the more flexible bipyridine ligand being capable of facile protonation. Thus, at low acidities the reaction was envisaged [10] as that in (84), wherein ring closure ( $k_2$ ) would theoretically be capable of competing with protonation ( $k_3$ ) and consequential release of the protonated bipyridine ligand. This might suggest different rates for the dissociation and racemization. At higher acidities, the two rates should be equal, with rapid protonation of the



free end of the bipyridine ligand ( $k_3$ ) followed by liberation of the protonated species. However, since the two rates were observed to be equal, within experimental error, over the entire acid concentration range, the bipyridine ring must necessarily open and close with retention of configuration.

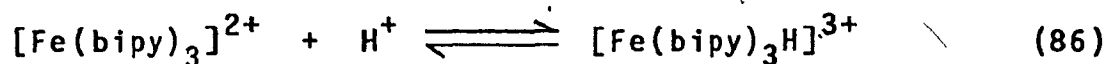
In basic media, the rate of racemization of  $[\text{Ni}(\text{phen})_3]^{2+}$  showed a slight increase with increasing hydroxide ion concentration up to 1.5 M  $\text{OH}^-$  [12]. The same trend was observed [12] for the dissociation of  $[\text{Ni}(\text{phen})_3]^{2+}$  in basic solution, according to the reaction in (85).



Intramolecular racemization occurs in octahedral complexes when the rate of racemization is faster than the rate of dissociation. Various investigations [5, 6, 38, 39] have indicated that  $[\text{Fe}(\text{phen})_3]^{2+}$  and  $[\text{Fe}(\text{bipy})_3]^{2+}$  racemize, at least partly, via an intramolecular pathway. The racemization and dissociation behaviour of these iron(II) complexes differ significantly from that of the nickel(II) complexes noted above. First of all, a comparison of the dissociation [38, 39] and racemization [38] rates shows that racemization is significantly faster than dissociation for the iron(II) cations. Thus, an intermolecular pathway is inoperable. Basolo et al. [5] have made the following observations concerning the iron(II) complexes: i) the dissociation rate of  $[\text{Fe}(\text{bipy})_3]^{2+}$  increases with increasing acidity up to a limiting rate in 1 M hydrochloric acid, in agreement with results reported by other investigators [6]; ii) the dissociation of  $[\text{Fe}(\text{phen})_3]^{2+}$  is acid-independent, as was observed for the nickel(II) complex cations; iii) the racemization rate of  $[\text{Fe}(\text{bipy})_3]^{2+}$  increases with increasing acidity up to a limiting rate in 1 M hydrochloric acid, while that of  $[\text{Fe}(\text{phen})_3]^{2+}$  is acid-independent.

Baxendale and George [6] have explained the acid

dependence of the dissociation rate of  $[\text{Fe}(\text{bipy})_3]^{2+}$  on the basis of the following equilibrium

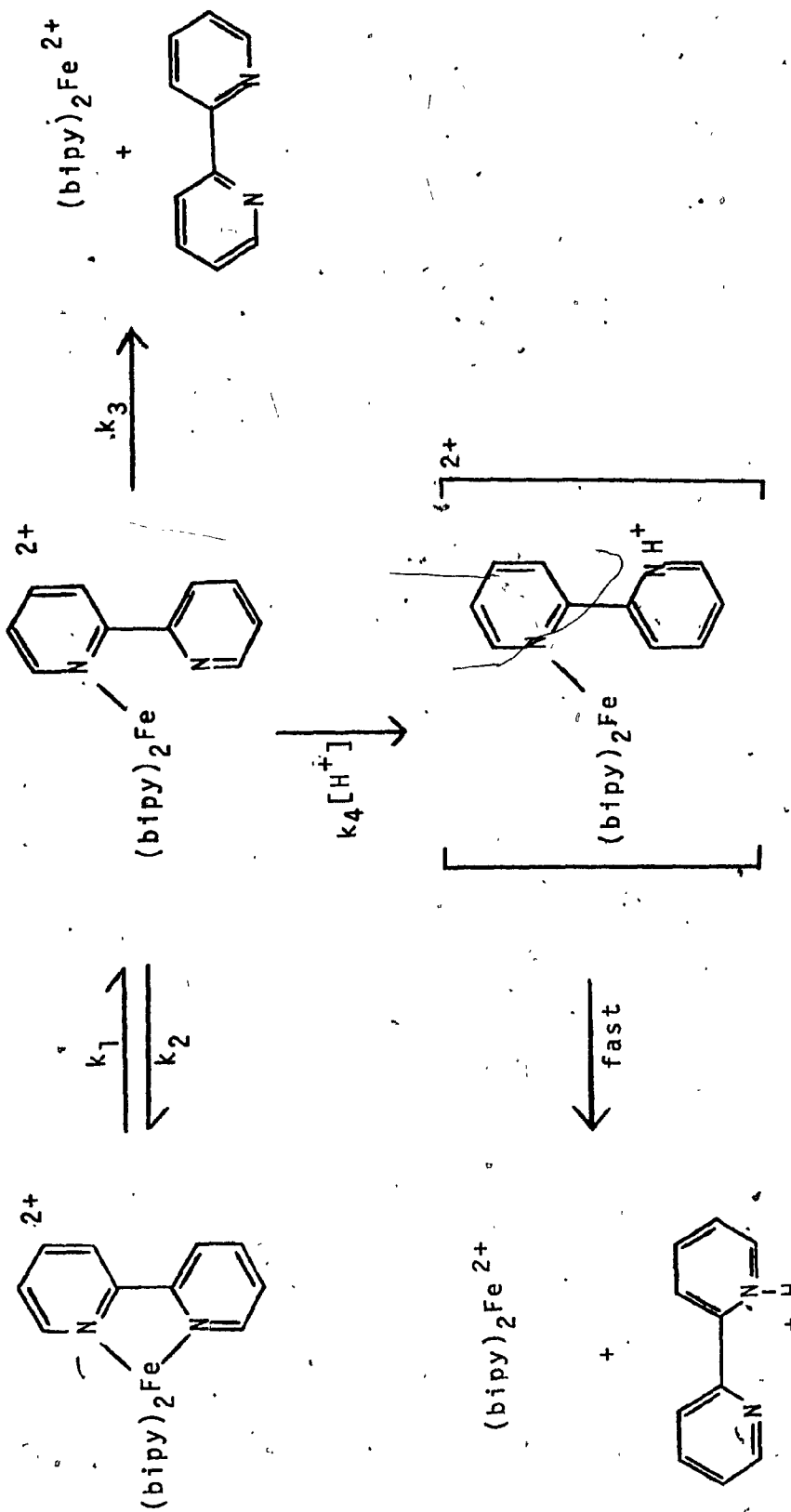


suggesting that  $[\text{Fe}(\text{bipy})_3\text{H}]^{3+}$  is more reactive than  $[\text{Fe}(\text{bipy})_3]^{2+}$ ; and, as such, the protonated species would predominate at high acidities. If this were the case, a change in the absorption spectrum should have been observed on going from the unprotonated  $[\text{Fe}(\text{bipy})_3]^{2+}$  to the protonated  $[\text{Fe}(\text{bipy})_3\text{H}]^{3+}$  species in concentrated acid solution. No such spectral changes were observed. Therefore the acid dependence shown by  $[\text{Fe}(\text{bipy})_3]^{2+}$  can only be explained kinetically in that the protonated species does not achieve a significant concentration in the course of the reaction. The dissociation of  $[\text{Fe}(\text{bipy})_3]^{2+}$  was thought to proceed through a mechanism similar to that of  $[\text{Ni}(\text{bipy})_3]^{2+}$ , with the notion that the bipyridine ligand is capable of acting as a unidentate ligand. The dissociation in acid is depicted in Figure 24 for the iron(II) complex  $[\text{Fe}(\text{bipy})_3]^{2+}$ . The observed rate constant  $k_{\text{obs}}$  for the dissociation was reported [6] as

$$k_{\text{obs}} = k_1 \left[ \frac{k_3 + k_4[\text{H}^+]}{k_2 + k_3 + k_4[\text{H}^+]} \right] \quad (87)$$

Figure 24. Acid Hydrolysis of  $[\text{Fe}(\text{bipy})_3]^{2+}$  via a  
Dissociative Pathway.





At low acid concentrations, then,

$$k_{\text{obs}} = \frac{k_1 k_3}{k_2 + k_3} = k_0 \quad (88)$$

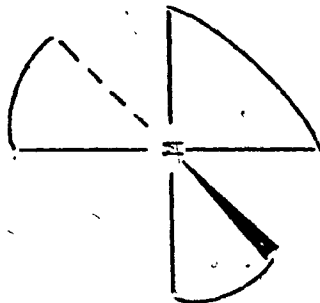
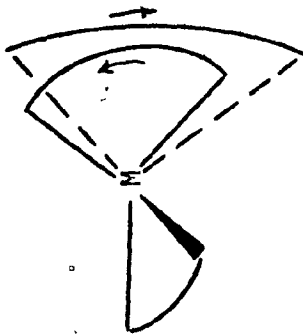
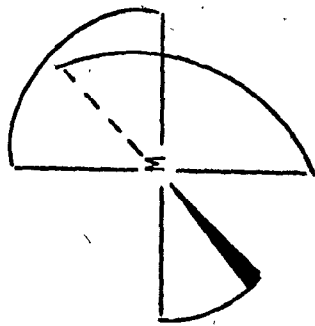
and at high acid concentrations;

$$k_{\text{obs}} = k_1 = k_{\infty} \quad (89)$$

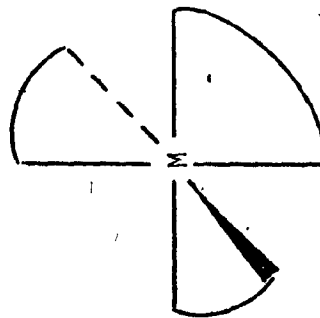
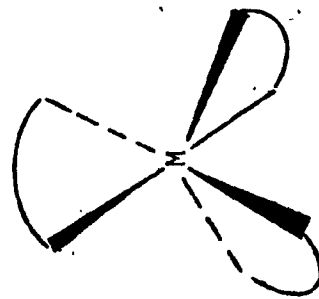
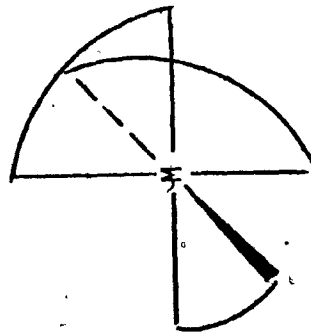
The ratio  $k_0/k_{\infty}$  was found to be 0.16 [5]. The inference here is that at low acid concentration, each time an Fe-N bond ruptures, that bond will reform 84% of the time; while only 16% of the time will the second Fe-N bond rupture to yield complete dissociation. The corresponding  $[\text{Fe}(\text{phen})_3]^{2+}$  cation behaves differently in acid solution, inasmuch as its dissociation was found to be only slightly acid-dependent [5]. This difference was rationalized in terms of the reduced flexibility of the phenanthroline ligand.

With regard to the  $[\text{Fe}(\text{phen})_3]^{2+}$  cation, it seemed highly unlikely that the chelate ring would open in a manner similar to that of the bipyridyl complex. This was attributed to the rigid planar structure of the phenanthroline ligand. It seemed unlikely that the phenanthroline ligand would be capable of behaving as a unidentate ligand. These conclusions lead one to assume that the racemization of the phenanthroline complex proceeds through an intramolecular pathway via movement

Figure 25. Possible Twist Pathways for the Racemization of  $[\text{Fe}(\text{phen})_3]^{2+}$ .

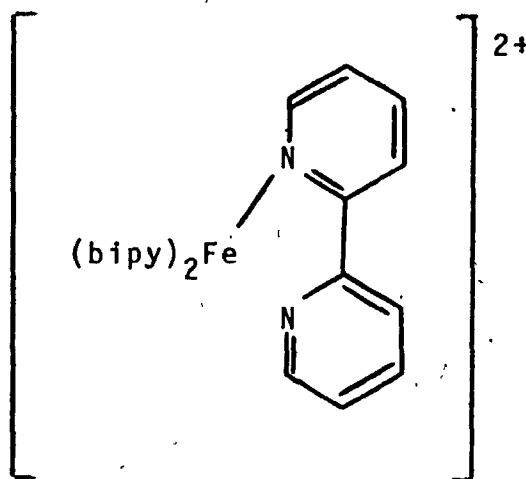


RHOMBIC TWIST



TRIGONAL TWIST

of the phenanthroline ligand about the central iron(II) atom (probably through a rhombic or trigonal twist) [62, 63]. Such twist pathways are expected to show acid independence, as was observed [5] for the total racemization rate and the dissociation rate of  $[\text{Fe}(\text{phen})_3]^{2+}$ . The two twist paths possible for this complex are presented in Figure 25. However, recent evidence [64] suggests that the phenanthroline ligand, as rigid as it might be, can act as a unidentate ligand. Basolo [5] has further suggested that the bipyridyl complex  $[\text{Fe}(\text{bipy})_3]^{2+}$  may also racemize via one of these twist mechanisms, or via racemization of the species



Both intramolecular pathways are plausible for  $[\text{Fe}(\text{bipy})_3]^{2+}$ , though the latter seems unlikely for  $[\text{Fe}(\text{phen})_3]^{2+}$ . Table X summarizes the processes, rate constants, and activation parameters for the nickel(II) and iron(II)

Table X

Rates for Processes Leading to Racemization at 25° for  $[M(NN)_3]^{2+}$  <sup>a</sup>

COMPLEX	Intramolecular Racemization			Intermolecular Racemization		
	k (min <sup>-1</sup> )	E <sub>a</sub> (kcal/mol)	ΔS <sup>‡</sup> (eu)	k (min <sup>-1</sup> )	E <sub>a</sub> (kcal/mol)	ΔS <sup>‡</sup> (eu)
[Fe(phen) <sub>3</sub> ] <sup>2+</sup>	3.9 × 10 <sup>-2</sup>	29 ± 2	21 ± 7	0.42 × 10 <sup>-2</sup>	32.1 ± 0.5	28 ± 2
[Fe(bipy) <sub>3</sub> ] <sup>2+</sup>	1.6 × 10 <sup>-2</sup>	26 ± 2	12 ± 7	4.7 × 10 <sup>-2</sup>	27.4 ± 0.5	17 ± 1
[Ni(phen) <sub>3</sub> ] <sup>2+</sup>	<6.0 × 10 <sup>-5</sup>	---	---	6.0 × 10 <sup>-4</sup>	25.0 ± 0.5	2 ± 2
[Ni(bipy) <sub>3</sub> ] <sup>2+</sup>	<1.4 × 10 <sup>-2</sup>	---	---	1.1	21.8 ± 0.5	6 ± 2

<sup>a</sup> reference 5.

complexes discussed above.

The effect of hydroxide ion on the dissociation rate of  $[\text{Fe}(\text{phen})_3]^{2+}$  has been investigated [65], and it was observed that, in basic solution, the rate was dependent on solution pH, and was faster than that in acidic solution. The first-order rate was given [65] by expression (90),

$$\frac{-d[\text{Fe}(\text{phen})_3^{2+}]}{dt} = k_{\text{obs}} [\text{Fe}(\text{phen})_3^{2+}] \quad (90)$$

wherein  $k_{\text{obs}}$  is a function of hydroxide ion concentration, ionic strength, and temperature. The observed rate constant increases with increasing hydroxide ion concentration, and decreasing ionic strength. At low hydroxide ion concentrations, the rate constant is given by

$$k_{\text{obs}} = k_d + k_1[\text{OH}^-] \quad (91)$$

where  $k_d$  is the observed rate constant in neutral solution, and  $k_1$  is the slope of a plot of  $k_{\text{obs}}$  versus  $[\text{OH}^-]$ . As the hydroxide ion concentration increases,  $k_{\text{obs}}$  becomes more dependent on  $[\text{OH}^-]$ , and the two are related by

$$k_{\text{obs}} = k_d + k_1[\text{OH}^-] + k_2[\text{OH}^-]^2 \quad (92)$$

At yet higher hydroxide ion concentrations, a third-order dependence is observed, and  $k_{\text{obs}}$  and  $[\text{OH}^-]$  are related by expression (93).

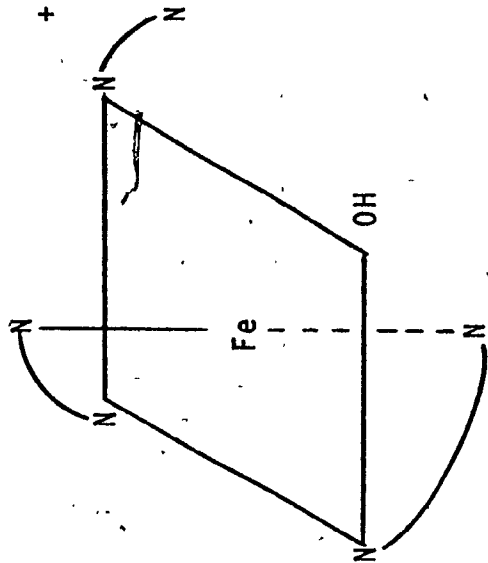
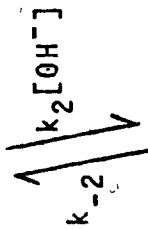
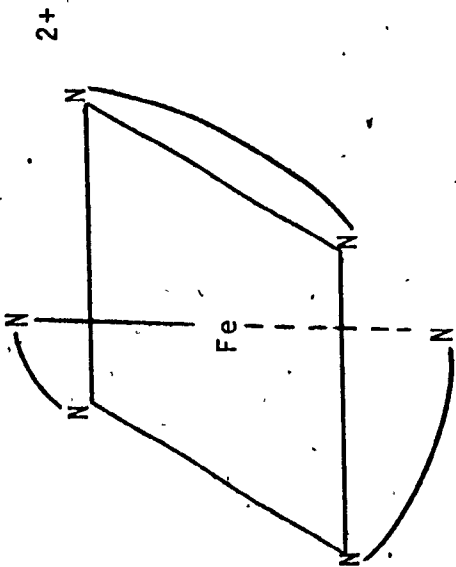
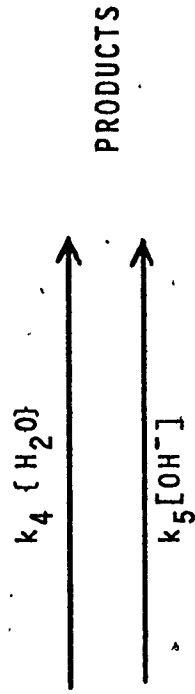
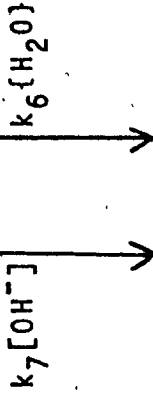
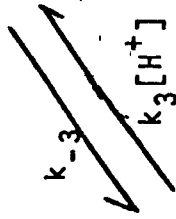
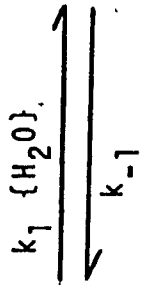
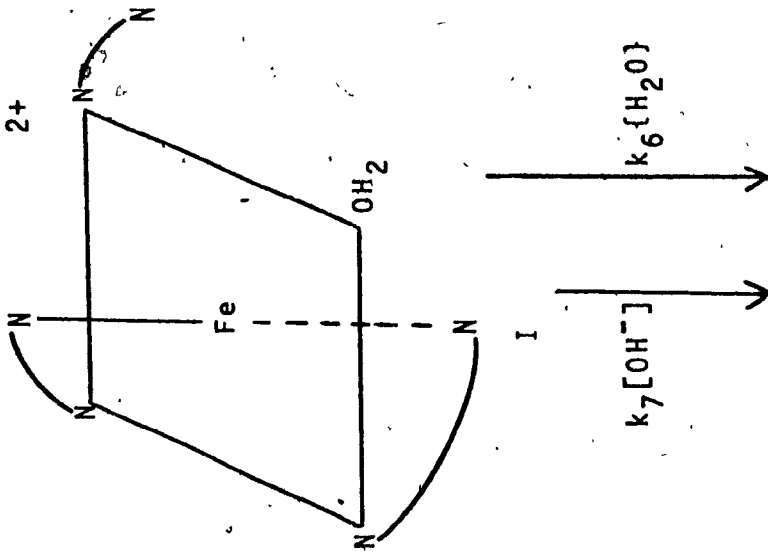
$$k_{\text{obs}} = k_d + k_1[\text{OH}^-] + k_2[\text{OH}^-]^2 + k_3[\text{OH}^-]^3 \quad (93)$$

An interesting observation concerns the reaction products of this system, that being that no absorbing species were detected after 85% of the reaction had gone to completion [65]. The only product that was detected was hydrated ferric oxide; thus, the formation of the predicted products,  $[\text{Fe}(\text{phen})_2(\text{OH})_2]$ ,  $[\text{Fe}(\text{phen})_2(\text{H}_2\text{O})_2]^{2+}$ , or  $[\text{Fe}(\text{phen})_2(\text{H}_2\text{O})(\text{OH})]^+$ , was insignificant.

Two mechanisms were originally postulated [65] to account for the kinetic results observed, one involving nucleophilic attack by water or hydroxide ion, and the other involving hydroxide ion catalysis. The former is shown in Figure 26, as this pathway was thought to be more favourable. In such a mechanism, it was assumed that the Fe-N bonds do not rupture simultaneously, and that nucleophilic attack by water and/or hydroxide ion produces species I and/or III, respectively, depending on the solution pH. Once species I is formed, it is expected to undergo rapid equilibration with species III by proton transfer. Subsequently, either I or III can reform  $[\text{Fe}(\text{phen})_3]^{2+}$  or lose the activated phenanthroline



Figure 26. Hydrolysis of  $[\text{Fe}(\text{phen})_3]^{2+}$  via Nucleophilic  
Attack by Water or Hydroxide Ion.

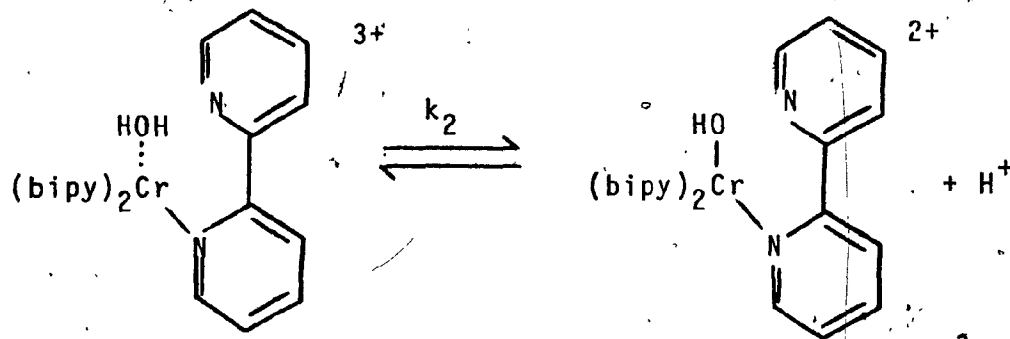


molecule via attack by another molecule of water or hydroxide ion. The observed rate constant was derived from the mechanism depicted in Figure 26 and reported to be equal to

$$k_{\text{obs}} = \frac{k_1 k_6}{k_{-1}} + \frac{k_1 k_7 + k_1 k_4 k_3}{k_{-1}} [\text{OH}^-] + \frac{k_1 k_7 k_3}{k_{-1}} [\text{OH}^-]^2 \quad (94)$$

The above expression (94) corresponds to the observed first- and second-order dependence on hydroxide ion concentration.

A dissociative pathway for the  $[\text{Cr}(\text{bipy})_3]^{3+}$  and  $[\text{Cr}(\text{phen})_3]^{3+}$  systems in which the Cr-N bond ruptures to yield a pentacoordinate intermediate  $\lambda$  is illustrated in Figures 27 and 28. The vacant coordination site in species  $\lambda$  is most likely occupied by a molecule of water. As such, the step described by  $k_2$  may be viewed as the acid-base reaction (shown below for  $[\text{Cr}(\text{bipy})_3]^{3+}$ )



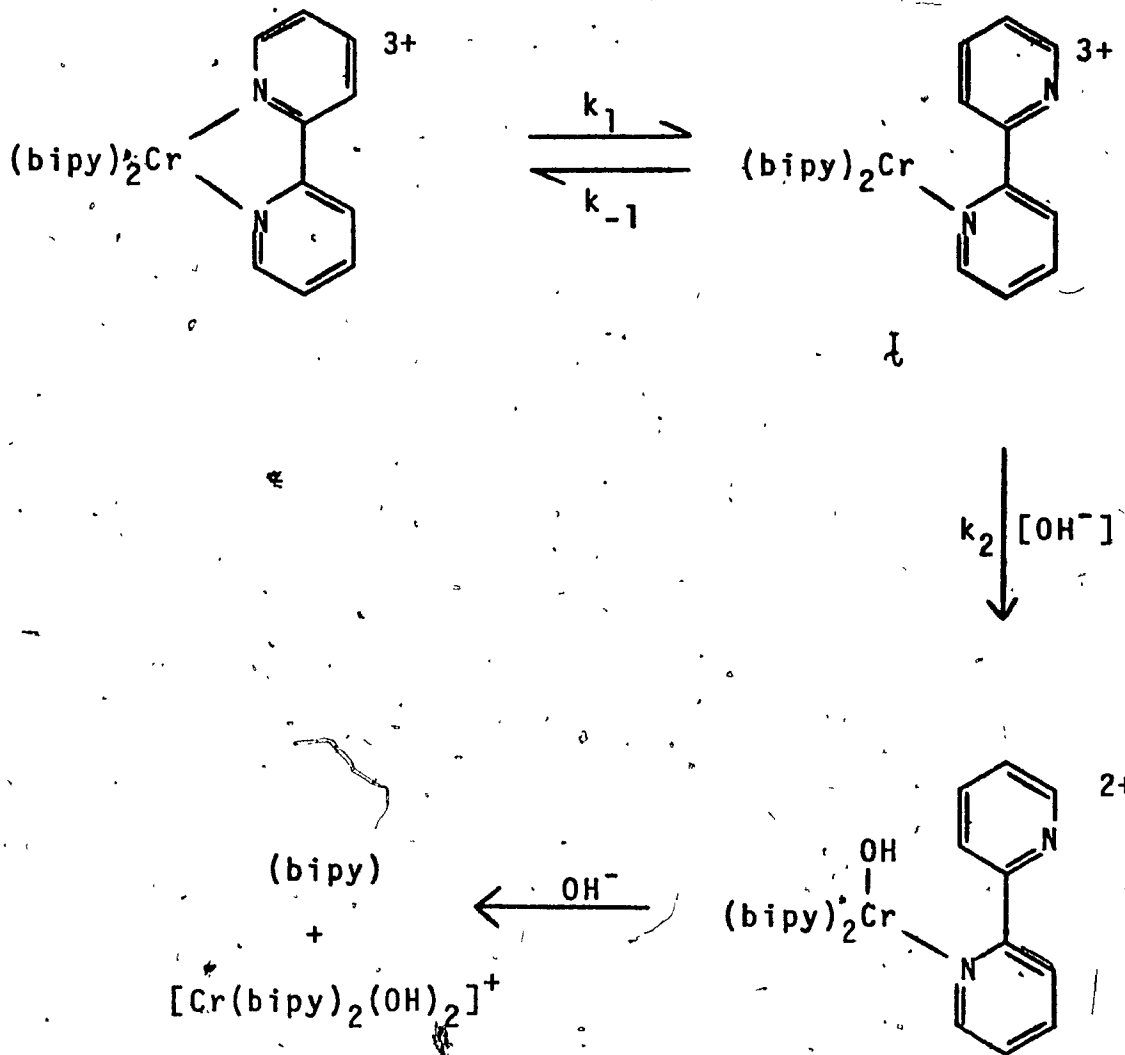


Figure 27. Hydrolysis of  $[\text{Cr}(\text{bipy})_3]^{3+}$  via a Dissociative Mechanism.

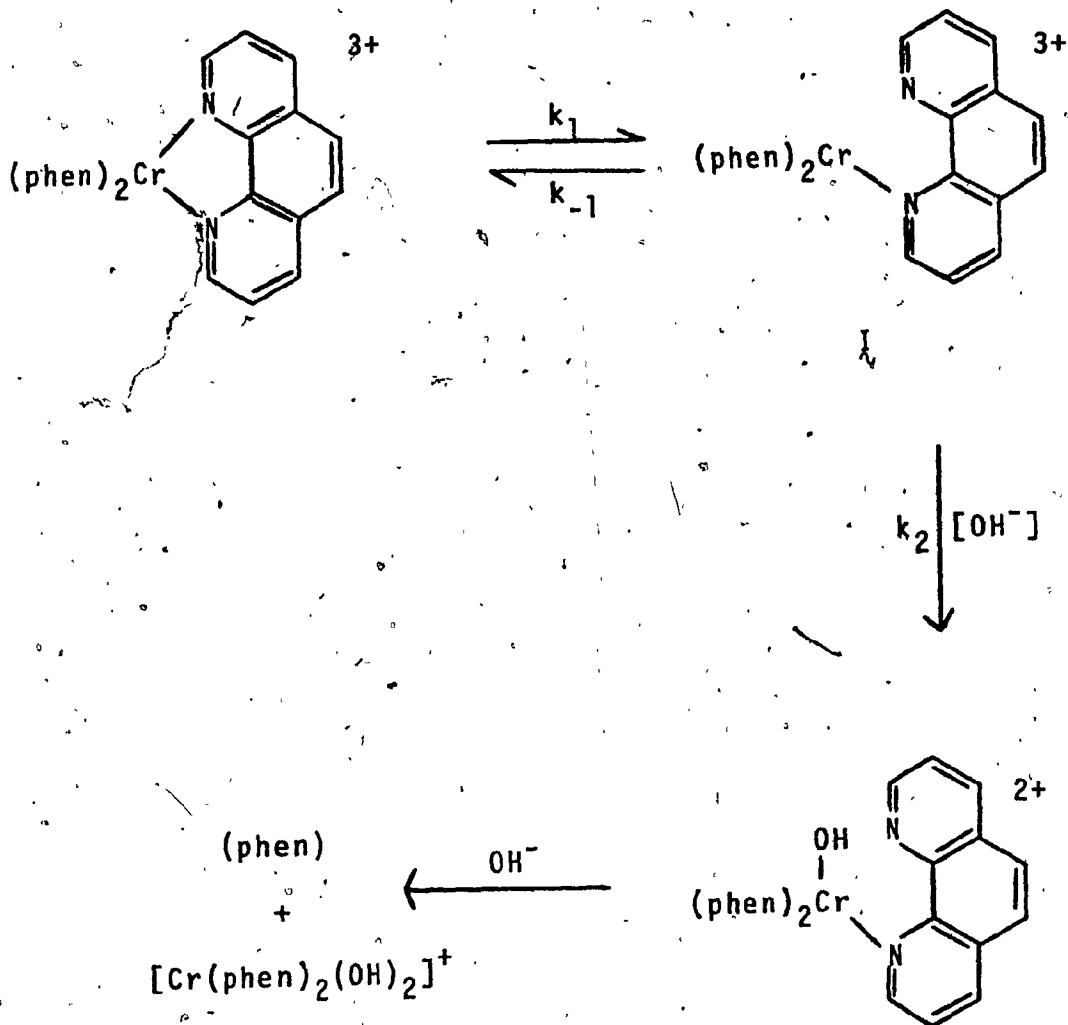


Figure 28. Hydrolysis of  $[\text{Cr}(\text{phen})_3]^{3+}$  via a Dissociative Mechanism.

or substitution of the water ligand by the more nucleophilic hydroxide ion.

The rate of disappearance of the reactant will be

$$\frac{-d[\text{Cr}(\text{NN})_3]^{3+}}{dt} = k_1[\text{Cr}(\text{NN})_3^{3+}] - k_{-1}[\text{I}] \quad (96)$$

and the rate of formation of the intermediate species  $\text{I}$  is given by the expression

$$\frac{+d[\text{I}]}{dt} = k_1[\text{Cr}(\text{NN})_3^{3+}] - k_{-1}[\text{I}] - k_2[\text{I}][\text{OH}^-] \quad (97)$$

A steady-state treatment on the concentration of  $\text{I}$ , i.e.,  $+d[\text{I}]/dt \cong 0$ , yields

$$[\text{I}] = \frac{k_1[\text{Cr}(\text{NN})_3^{3+}]}{k_{-1} + k_2[\text{OH}^-]} \quad (98)$$

as the concentration of the intermediate  $\text{I}$ . Subsequent substitution of expression (98) into (96) yields

$$\frac{-d[\text{Cr}(\text{NN})_3^{3+}]}{dt} = \frac{k_1 k_2 [\text{Cr}(\text{NN})_3^{3+}] [\text{OH}^-]}{k_{-1} + k_2 [\text{OH}^-]} \quad (99)$$

Inasmuch as the kinetics of hydrolysis were carried out at constant  $[\text{OH}^-]$ , the rate law for the hydrolysis of

$[\text{Cr}(\text{NN})_3]^{3+}$  allows one to set expression (99) equal to  $k_{\text{obs}}[\text{Cr}(\text{NN})_3]^{3+}$ , wherefrom the observed rate constant is given by

$$k_{\text{obs}} = \frac{k_1 k_2 [\text{OH}^-]}{k_{-1} + k_2 [\text{OH}^-]} \quad (100)$$

Expression (100) and the values of A and B from a plot of  $1/k_{\text{obs}}$  versus  $1/[\text{OH}^-]$  have yielded  $k_1 = 4.7 \times 10^{-7} \text{ sec}^{-1}$  and  $k_1 k_2 / k_{-1} = 1.2 \text{ M}^{-1} \text{ sec}^{-1}$  for  $[\text{Cr}(\text{bipy})_3]^{3+}$  in region (a) at  $11^\circ\text{C}$  [16]. When  $k_2 [\text{OH}^-]$  is much greater than  $k_{-1}$ ,  $k_{\text{obs}} = k_1 = 4.7 \times 10^{-7} \text{ sec}^{-1}$ . Thus, in the pH range 9 - 10.7, a first-order pH-independent rate is expected. In fact, a limiting rate  $k_{\text{obs}} = 5.1 \pm 0.2 \times 10^{-7} \text{ sec}^{-1}$  was observed [16] in this plateau of region (a), which was independent of hydroxide ion concentration. If on the other hand,  $k_2 [\text{OH}^-]$  is much less than  $k_{-1}$ , the observed rate constant at low pH will be

$$k_{\text{obs}} = \frac{k_1 k_2 [\text{OH}^-]}{k_{-1}} \quad (101)$$

Under the conditions where  $k_2 [\text{OH}^-] > k_{-1}$ , the rate-determining step is thought to be the rupture of the Cr-N bond in  $[\text{Cr}(\text{bipy})_3]^{3+}$ , described by  $k_1$ . A similar

analysis of the  $[\text{Cr}(\text{phen})_3]^{3+}$  system predicts a limiting rate constant  $k_{\text{obs}} = k_1 = 1.8 \times 10^{-6} \text{ sec}^{-1}$ , which agrees well with the experimental value of  $1.78 \pm 0.14 \times 10^{-6} \text{ sec}^{-1}$ .

Although the mechanism shown in Figures 27 and 28 for a dissociative pathway is consistent with the observed kinetic results in region (a), a dissociative-type mechanism is not thought probable in view of Swaddle's contention [3] that most chromium(III) centres undergo substitution via an associative-type pathway. Also, a dissociative pathway has been assigned to the effect of hydroxide ion on the complex cation  $[\text{Fe}(\text{phen})_3]^{2+}$  [65]. Its behaviour, as discussed above, is not analogous to either  $[\text{Cr}(\text{bipy})_3]^{3+}$  or  $[\text{Cr}(\text{phen})_3]^{3+}$ . Acid catalysis has been observed for the tris-bipyridyl and phenanthroline complexes of iron(II) and nickel(II) [5]. As no acid catalysis was observed for either chromium(III) cation in 0.1 or 1.0 M hydrochloric acid, a dissociative-type pathway does not appear plausible for the systems investigated and reported herein.

## 2. Ion-Pair Pathway (I).

An alternate mechanism which may be applicable to the base hydrolysis of the two chromium(III) complex cations under investigation may involve the formation of ion-pairs between the cation and hydroxide ion.



The hydrolysis behaviour may be explained by invoking ion-pair formation in regions (a) and (c), as shown in Figures 29 and 30. The ion-pair formation constant  $K_{ip}$  describes the equilibrium between the reactants  $[\text{Cr}(\text{NN})_3]^{3+}$  and  $\text{OH}^-$ , and the ion-pair  $\{[\text{Cr}(\text{NN})_3]^{3+}, \text{OH}^-\}$ .

With reference to region (a) and Figures 29 and 30,  $K_{ip}$  is defined by expression (102),

$$K_{ip} = \frac{\{[\text{Cr}(\text{NN})_3]^{3+}, \text{OH}^-\}_t}{[\text{Cr}(\text{NN})_3]^{3+}_t [\text{OH}^-]} \quad (102)$$

where  $[\text{Cr}(\text{NN})_3]^{3+}_t$  is the concentration of the reactant at time 't'. The concentration of the ion-pair then becomes

$$\{[\text{Cr}(\text{NN})_3]^{3+}, \text{OH}^-\}_t = K_{ip} [\text{Cr}(\text{NN})_3]^{3+}_t [\text{OH}^-] \quad (103)$$

The rate of the reaction is given by equations (104) and (105).

$$\text{Rate} = k_1 \{[\text{Cr}(\text{NN})_3]^{3+}, \text{OH}^-\}_t \quad (104)$$

$$= k_1 K_{ip} [\text{Cr}(\text{NN})_3]^{3+}_t [\text{OH}^-] \quad (105)$$

A material balance on the concentration of the reactant at time 't' (assuming no product formation) yields

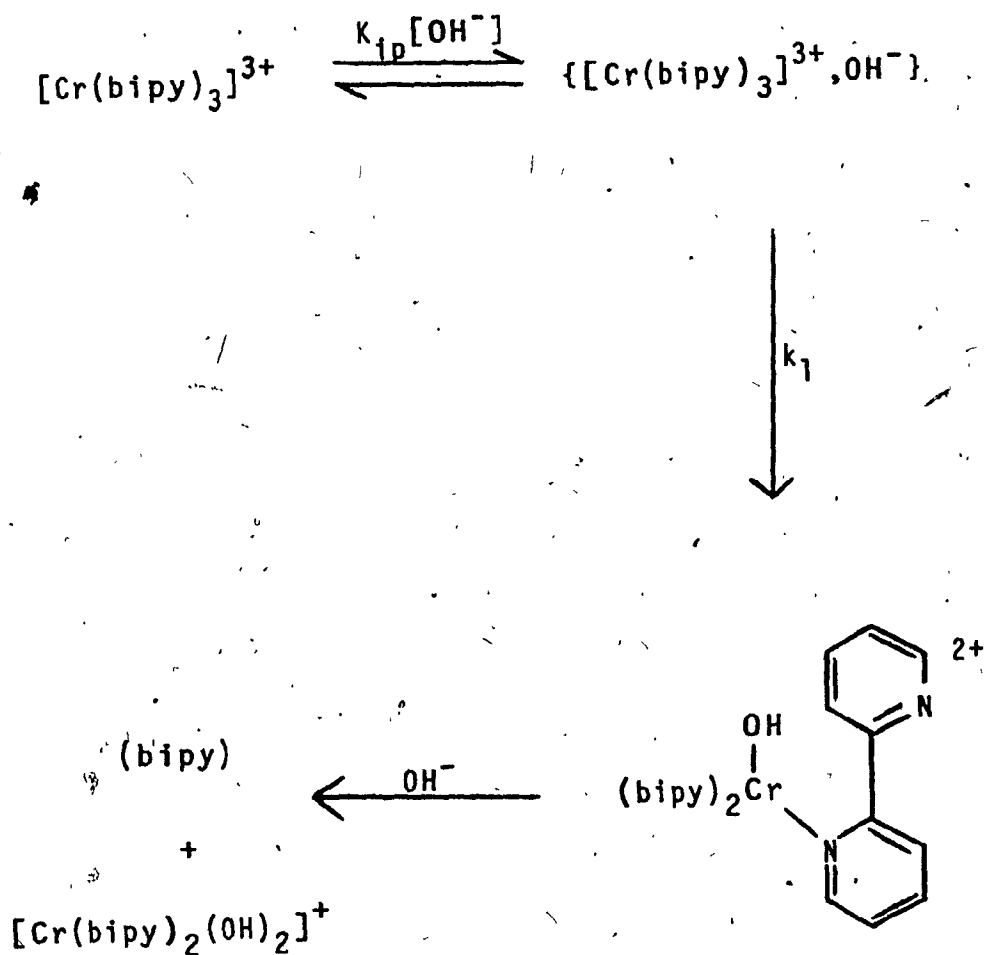
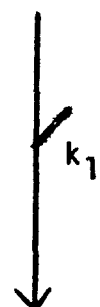
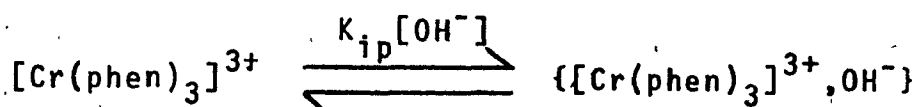


Figure 29. Hydrolysis of  $[\text{Cr}(\text{bipy})_3]^{3+}$  via an Ion-pair Pathway.



(phen)

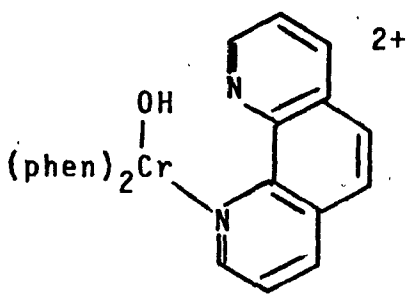
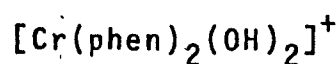
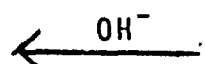


Figure 30. Hydrolysis of  $[\text{Cr}(\text{phen})_3]^{3+}$  via an Ion-pair Pathway.

$$[\text{Cr}(\text{NN})_3^{3+}]_t = [\text{Cr}(\text{NN})_3^{3+}] - \{[\text{Cr}(\text{NN})_3^{3+}, \text{OH}^-]_t \quad (106)$$

$$= [\text{Cr}(\text{NN})_3^{3+}] - K_{ip} [\text{Cr}(\text{NN})_3^{3+}]_t [\text{OH}^-] \quad (107)$$

Rearrangement of expression (107) gives the initial reactant concentration as

$$[\text{Cr}(\text{NN})_3^{3+}] = [\text{Cr}(\text{NN})_3^{3+}]_t + K_{ip} [\text{Cr}(\text{NN})_3^{3+}]_t [\text{OH}^-] \quad (108)$$

$$= [\text{Cr}(\text{NN})_3^{3+}]_t (1 + K_{ip} [\text{OH}^-]) \quad (109)$$

whence  $[\text{Cr}(\text{NN})_3^{3+}]_t = [\text{Cr}(\text{NN})_3^{3+}] / (1 + K_{ip} [\text{OH}^-])$ , and by substitution the rate law becomes that given in expression (110) at constant  $[\text{OH}^-]$ .

$$\begin{aligned} \text{Rate} &= k_1 K_{ip} [\text{Cr}(\text{NN})_3^{3+}] [\text{OH}^-] / (1 + K_{ip} [\text{OH}^-]) \\ &= k_{\text{obs}} [\text{Cr}(\text{NN})_3^{3+}] \end{aligned} \quad (110)$$

The observed rate constant is thus

$$k_{\text{obs}} = k_1 K_{ip} [\text{OH}^-] / (1 + K_{ip} [\text{OH}^-]) \quad (111)$$

At pH values greater than 9,  $K_{ip} [\text{OH}^-]$  will be much greater than unity, and  $k_{\text{obs}}$  becomes

$$k_{\text{obs}} = \frac{k_1 K_{\text{ip}} [\text{OH}^-]}{K_{\text{ip}} [\text{OH}^-]} = k_1 \quad (112)$$

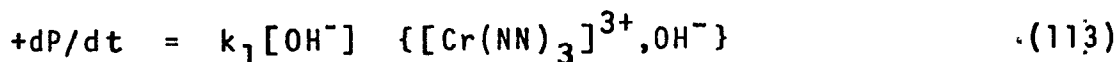
As such, a limiting rate is predicted at  $\text{pH} > 9$ , as is experimentally observed for  $[\text{Cr}(\text{bipy})_3]^{3+}$  [16] and  $[\text{Cr}(\text{phen})_3]^{3+}$  systems in region (a). Equation (111) and the values of A and B from a plot of  $1/k_{\text{obs}}$  versus  $1/[\text{OH}^-]$  yield  $k_1 = 4.7 \times 10^{-7} \text{ sec}^{-1}$  and  $K_{\text{ip}} = 2.6 \times 10^6 \text{ M}^{-1}$  for the  $[\text{Cr}(\text{bipy})_3]^{3+}$  system at  $11^\circ\text{C}$ ; equation (111) and the values of A' and B' from a similar plot yield  $k_1 = 1.8 \times 10^{-6} \text{ sec}^{-1}$  and  $K_{\text{ip}} = 2.0 \times 10^6 \text{ M}^{-1}$  for the  $[\text{Cr}(\text{phen})_3]^{3+}$  system at  $31.1^\circ\text{C}$ . (see Figure 21).

Although the relationship for  $k_{\text{obs}}$  given in expression (111) conforms to the experimental results observed in region (a), the formation of ion-pairs between  $[\text{Cr}(\text{NN})_3]^{3+}$  and  $\text{OH}^-$  is not considered to occur to any significant degree in region (a). The ion-pair constants  $K_{\text{ip}}$  calculated for the two chromium(III) cations are much larger than normal constants observed for coordination compounds [3,13,66].

To affirm that the various ions present in the buffer solution do not significantly affect the observed rate constant, the concentration of the Britton-Robinson stock solution was tripled, from 0.008 to 0.024 M. Under similar conditions of temperature ( $31.1^\circ\text{C}$ ) and pH (10.48), the observed rate constants  $k_{\text{obs}}$  were observed

to be equal to  $1.8 \pm 0.0 \times 10^{-6}$  and  $3.3 \pm 0.1 \times 10^{-6}$   $\text{sec}^{-1}$  for 0.008 and 0.024 M Britton-Robinson stock solution, respectively, for the  $[\text{Cr}(\text{phen})_3]^{3+}$  system. The variance in the two values of  $k_{\text{obs}}$  is probably insignificant. Maestri et al. [16] have also noted that the pseudo first-order rate constants are neither dependent on the nature of the buffer nor its concentration for the  $[\text{Cr}(\text{bipy})_3]^{3+}$  system.

In view of the above arguments and experimental results, an ion-pair mechanism is not considered plausible for the two chromium(III) cationic complexes in region (a), most importantly because the calculated values of  $K_{\text{ip}}$  are unreasonably large. However, as the hydroxide ion concentration is increased, ion-pair formation seems inevitable. In region (c), where  $k_{\text{obs}}$  is linearly dependent on  $[\text{OH}^-]^2$ , such a pathway may be a valid one. One plausible explanation involves initial formation of the ion-pair  $\{[\text{Cr}(\text{NN})_3]^{3+}, \text{OH}^-\}$ , followed by hydroxide ion attack on the ion-pair to form a heptacoordinate intermediate species, as shown in Figure 31. The ion-pair formation constant  $K_{\text{ip}}$  may be defined by expression (112), and the rate of formation of the products P is given in expression (113).



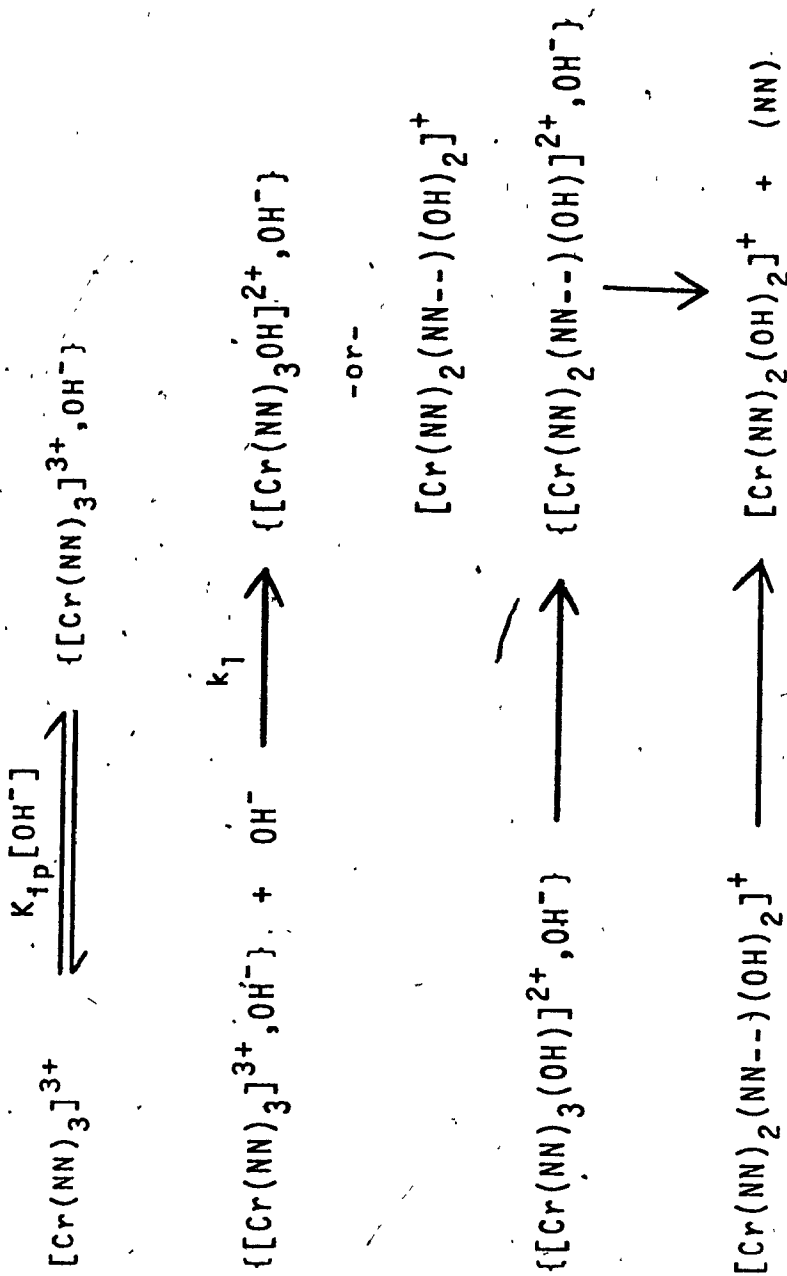


Figure 31. Hydrolysis of  $[\text{Cr}(\text{NN})_3]^{3+}$  in Region (c) via an Ion-pair Pathway.

Since  $\{[\text{Cr}(\text{NN})_3]^{3+}, \text{OH}^-\} = K_{ip}[\text{OH}^-][\text{Cr}(\text{NN})_3^{3+}]$ , expression (113) becomes

$$+dP/dt = k_1 K_{ip} [\text{Cr}(\text{NN})_3^{3+}] [\text{OH}^-]^2 = k_{obs} [\text{Cr}(\text{NN})_3^{3+}] \quad (114)$$

and the observed rate constant  $k_{obs}$  is equal to

$$k_{obs} = k_1 K_{ip} [\text{OH}^-]^2 \quad (115)$$

The slope of the least-squares plots of  $k_{obs}$  versus  $[\text{OH}^-]^2$  in region (c) is equal to  $k_1 K_{ip} = 1.9 \times 10^{-4} \text{ M}^{-2} \text{ sec}^{-1}$  for  $[\text{Cr}(\text{bipy})_3]^{3+}$  at 11°C (see Figure 20), and  $k_1 K_{ip} = 6.9 \times 10^{-4} \text{ M}^{-2} \text{ sec}^{-1}$  for  $[\text{Cr}(\text{phen})_3]^{3+}$  at 31.1°C (see Figure 23). For the bipy system, it is not unreasonable to assume that  $k_1$  in Figure 31 is of the order of  $10^{-4} - 10^{-5} \text{ M}^{-1} \text{ sec}^{-1}$  since  $k_3 = 1.1 \times 10^{-4} \text{ M}^{-1} \text{ sec}^{-1}$  (of Figures 42 and 45), and therefore  $K_{ip}$  will be of the order of 2 - 20  $\text{M}^{-1}$ . In the case of the  $[\text{Cr}(\text{phen})_3]^{3+}$  system,  $k_1$  is also  $\sim 10^{-4} - 10^{-5} \text{ M}^{-1} \text{ sec}^{-1}$  inasmuch as the corresponding  $k_3 = 3.2 \times 10^{-4} \text{ M}^{-1} \text{ sec}^{-1}$ ; hence  $K_{ip}$  is of the order of 7 - 70. Such values for the ion-pair formation constants are reasonable compared to those reported in the literature [3, 13, 66] for analogous ion-pairs.



### 3. Gillard's Pathway (covalent hydrate).

In organic chemistry it is generally believed that the 2-position of quaternized pyridines is accessible to nucleophilic attack. As a consequence, Gillard [13] has recently used this argument to explain the anomalous behaviour of tris-phenanthroline and tris-bipyridyl metal complexes. In the case of 1,10-phenanthroline, calculations [68] have shown that the carbon atoms adjacent to the nitrogen atoms (i.e., the 2- and 9-positions) are the most susceptible to nucleophilic attack. When phenanthroline is complexed to a metal ion such as iron(II) or ruthenium(II), a high-field shift of the resonance signal of the 2- and 9-protons was observed in the nmr spectrum [69]. This shift on complexation is much more pronounced for the 2- and 9-proton signals than for signals attributed to the other protons, and was observed to be more pronounced as the size of the central metal ion decreased. This observation was rationalized in two ways, according to Miller and Prince [69]: i) movement of electrons in the C<sub>9</sub>-H (or C<sub>2</sub>-H) bond towards the proton, due to the electric field of the central metal ion or the field due to water molecules in the solvation sphere; or ii) as a metal-hydrogen interaction similar to that observed in transition metal hydrides. The metal-C<sub>9</sub> (or C<sub>2</sub>) hydrogen distance is of the order of 2.8 - 2.9 Å, and so the only

atoms which could affect this hydrogen atom are the carbon atoms (C<sub>2</sub> and C<sub>9</sub>) to which it is attached and the metal ion. This latter metal-non bonded hydrogen interaction is thought [69] responsible for the observed proton shift. As the size of the central metal ion decreases, the metal-hydrogen distance also decreases, and the proton shift is more pronounced.

Based on the above character of these heterocyclic ligands, Gillard [13] views the quaternary character of such metal complexes in terms of the equilibria shown in Figure 32, in which K<sub>s</sub> describes the equilibrium between the unsolvated Q and the covalent hydrate HA,

$$K_s = \frac{[HA]}{[Q] [H_2O]} \quad (116)$$

and K<sub>A</sub> denotes the acid dissociation between the covalent hydrate HA and its conjugate base CB,

$$K_A = \frac{[CB] [H^+]}{[HA]} \quad (117)$$

In acid solution where the concentration of the conjugate base is unimportant, the concentration of the unsolvated Q will be inversely proportional to the activity of water,

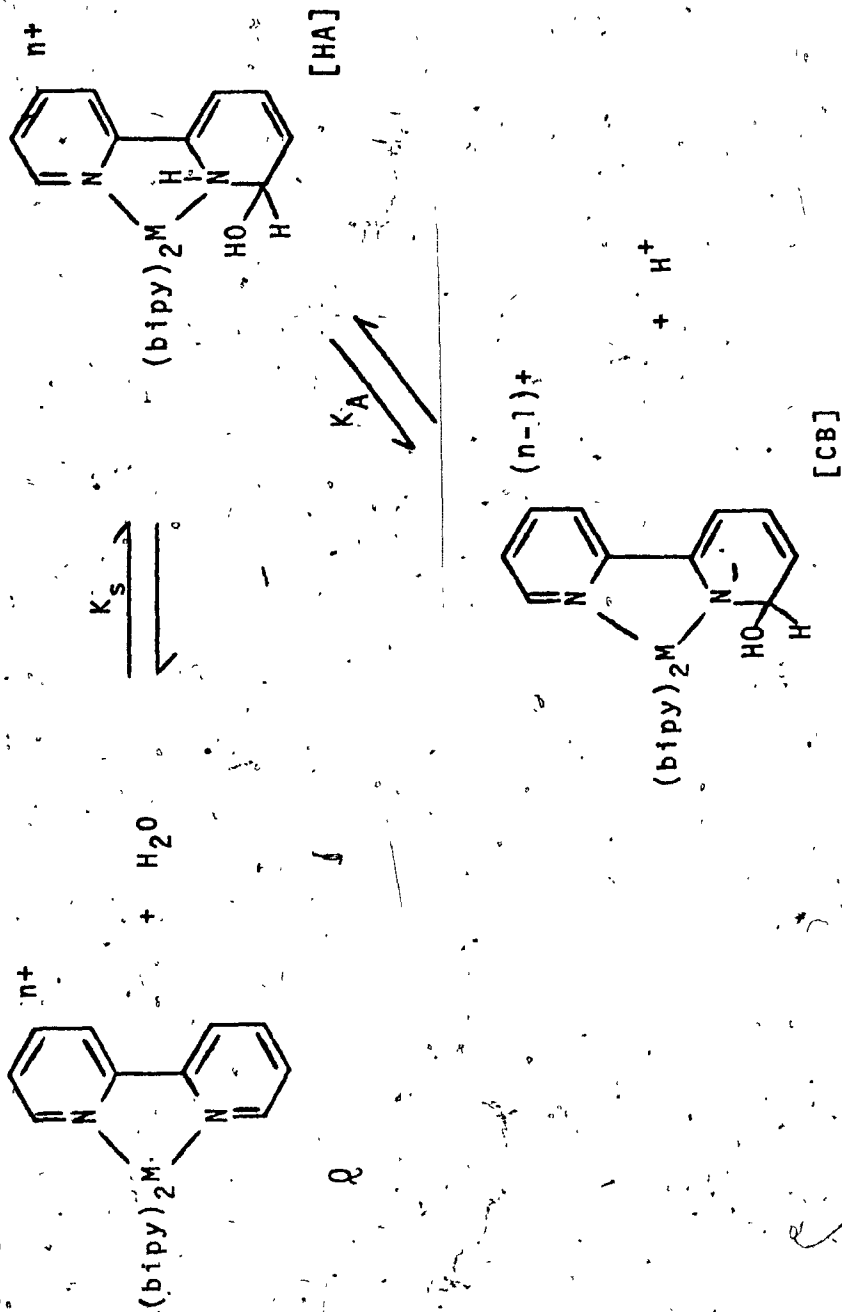


Figure 32. Equilibria of Polypyridyl Complexes Depicting Their Quaternary Character.

$$[Q] = [HA] / K_s \{H_2O\} \quad (118)$$

In the presence of hydroxide ion, the reaction scheme envisaged for complexes of the type  $[M(NN)_3]^{2+}$  is shown in Figure 33. The intermediate covalent hydrate HA, which is produced via attack on the  $C_6$  or  $C_6'$  atom ( $NN = \text{bipy}$ ) by the nucleophile, can react either by i) protonation to yield the conjugate acid CA and then undergo intramolecular water shift from  $C_6$  (or  $C_6'$ ) to the metal, ii) by an intramolecular hydroxyl shift within the covalent hydrate HA, or iii) by deprotonation with hydroxide to yield the conjugate base CB, which then reacts via an intramolecular hydroxyl shift from  $C_6$  (or  $C_6'$ ) to the metal centre.

For trivalent metal complexes, Gillard [13] has suggested reduction of  $M^{3+}$  as the operating reaction mode, as a result of their instability in basic solution. For  $[Ru(\text{bipy})_3]^{3+}$ , reduction is thought to occur via intramolecular contact of the metal ion with the  $C_6$ -hydroxyl group, as depicted in Figure 34. A comparison of the reaction schemes presented in Figures 33 and 34 shows that the covalent hydrate HA and base intermediates are the same except for the oxidation state of the metal. Addition of hydroxide to aqueous solutions of  $[Fe(NN)_3]^{3+}$  [70] and  $[Ru(NN)_3]^{3+}$  [71] proceed according to the general reaction in (119).

Figure 33: Gillard's Mechanism Applied to  $[M(NN)_3]^{2+}$   
Complexes in the Presence of Hydroxide Ion.

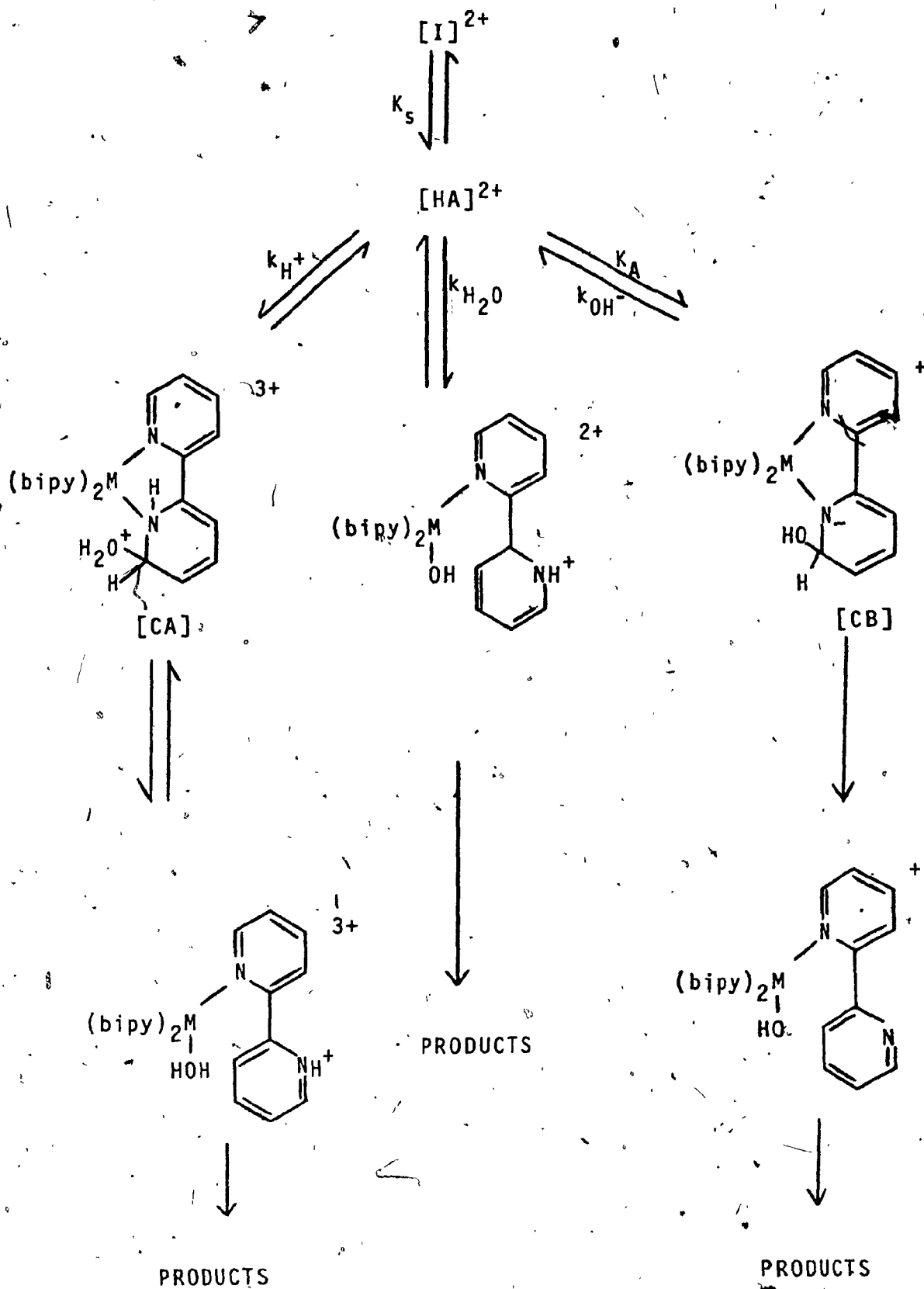
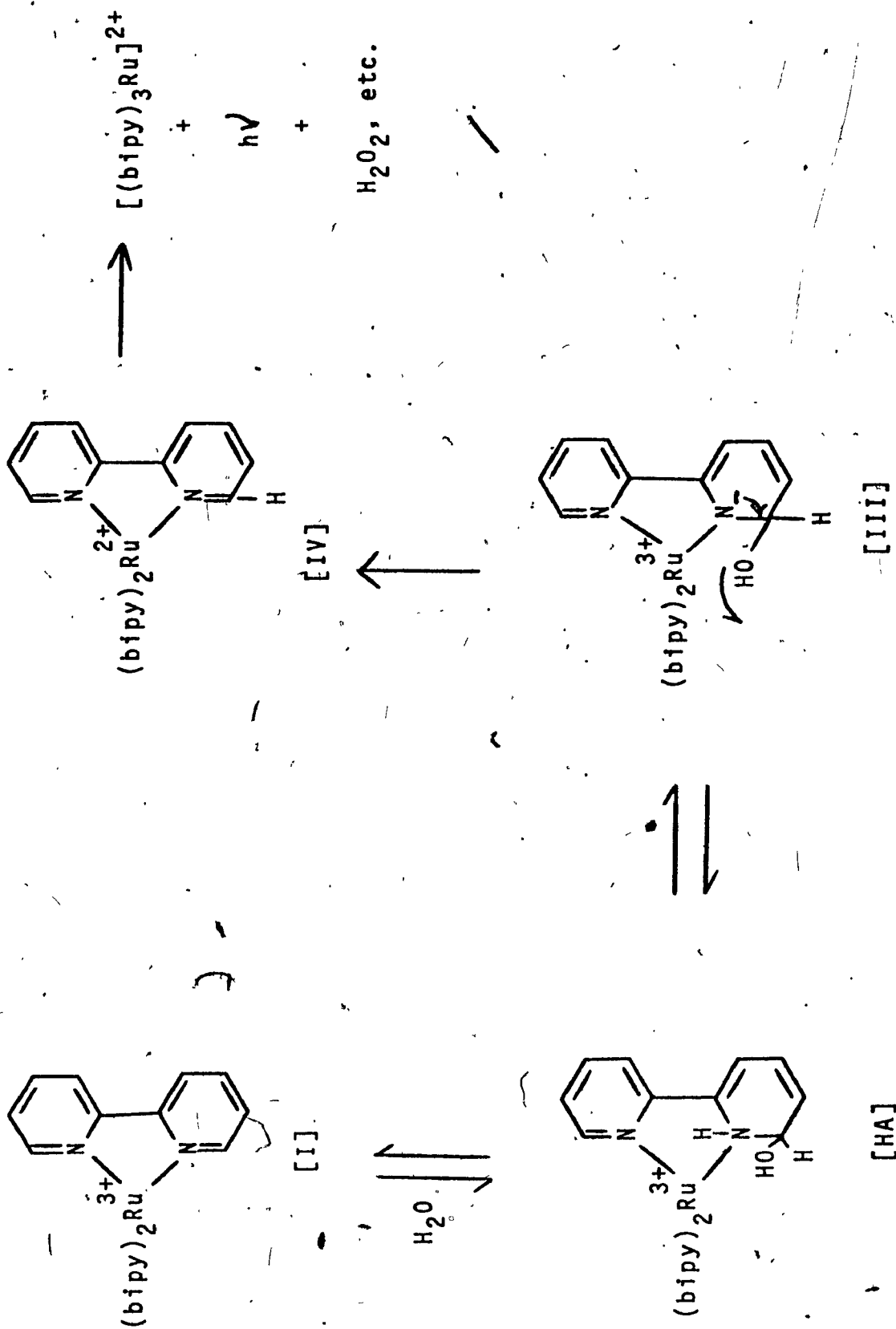
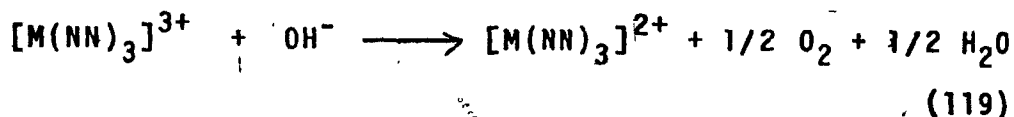


Figure 34. Reaction Sequence of  $[\text{Ru}(\text{bipy})_3]^{3+}$  in  
Base via Gillard's Mechanism.







The mechanism proposed for  $[Fe(bipy)_3]^{3+}$  [72] is presented in Figure 35. The hydroxide ion attacks the carbon atom adjacent to the ligand nitrogen atom in the rate-determining step to yield a radical intermediate B, which then reacts rapidly with hydroxide ion to eventually give the observed products. In terms of increased conjugation of the phenanthroline ligand over the bipyridine ligand, the radical intermediate can explain the observation that phenanthroline complexes react more rapidly than the analogous bipyridyl complexes.

In the case of the iron(III) [72] and ruthenium(III) [15], the metal centre is capable of oxidizing the hydroxide ion. The standard reduction potentials  $E^\circ$  for the  $[M(NN)_3]^{3+} / [M(NN)_3]^{2+}$  couples are given in expressions (120 - 122).

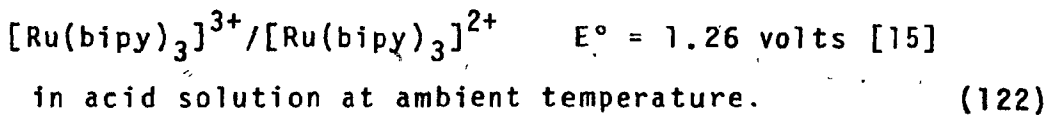
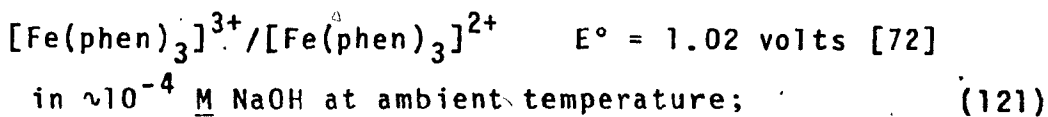
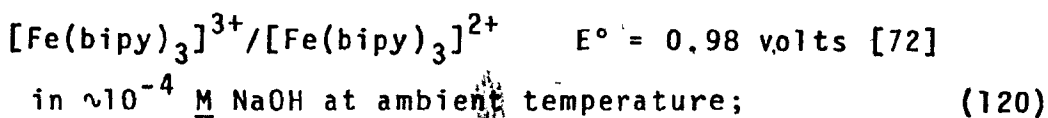
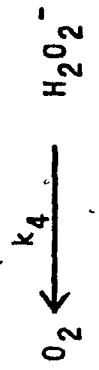
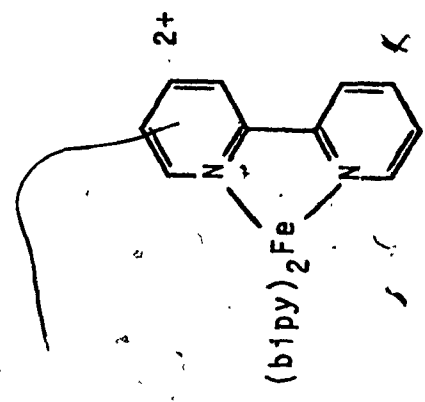
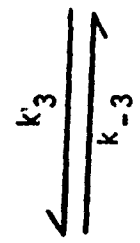
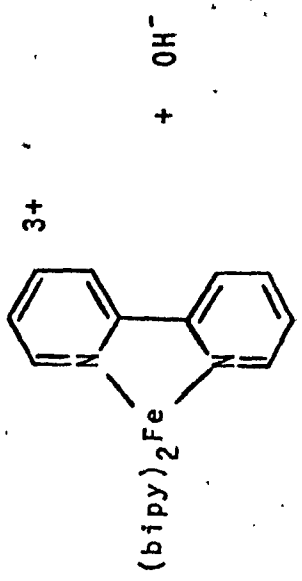
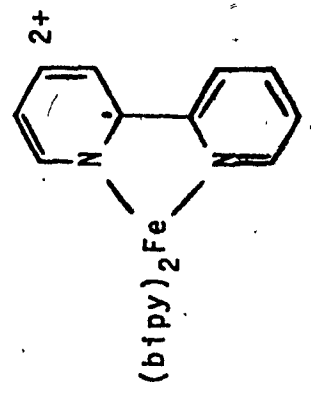
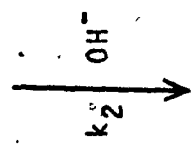
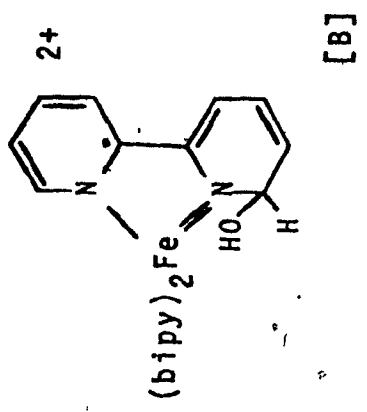


Figure 35. Reaction Sequence Between  $[\text{Fe}(\text{bipy})_3]^{3+}$  and Hydroxide Ion via Gillard's Mechanism.



However, this is not the case with chromium(III), where the  $E^\circ$  value does not favour such a reduction reaction. For the  $[\text{Cr}(\text{bipy})_3]^{3+}/[\text{Cr}(\text{bipy})_3]^{2+}$  couple,  $E^\circ = -0.25$  volts in aqueous acid solution [20]. Thus, a reaction pathway similar to that in Figure 35 for  $[\text{Fe}(\text{bipy})_3]^{3+}$  is applicable to neither  $[\text{Cr}(\text{bipy})_3]^{3+}$  nor  $[\text{Cr}(\text{phen})_3]^{3+}$ . To confirm the absence of reduction of these two chromium(III) cations, the reaction between  $[\text{Cr}(\text{bipy})_3]^{3+}$  and  $\text{OH}^-$  was followed spectrophotometrically at pH 11.82 and 0.50 M  $\text{OH}^-$ , at 29.5 and 7.5°C, respectively, in oxygenated and deoxygenated solvent systems. Table XI gives the results of this investigation, and confirms the suspicion that chromium(II) is not an intermediate species produced during the reaction. Had such a species been produced, different values for  $k_{\text{obs}}$  would have been expected in the early stages of the reaction. However, at both pH 11.82 and 0.50  $[\text{OH}^-]$ ,  $k_{\text{obs}}$  remained essentially constant in oxygenated and deoxygenated solvent systems.

Electrochemical investigations of catalytic ligand exchange in  $[\text{Cr}(\text{phen})_3]^{3+}$  [73] and  $[\text{Cr}(\text{bipy})_3]^{3+}$  [74] have suggested a reductive pathway. In aqueous acid solution, the following reaction sequence has been proposed [74] for  $[\text{Cr}(\text{bipy})_3]^{3+}$ .

Table XI

Observed Rate Constants at Various pH or  $[\text{OH}^-]$  in Oxygenated and Deoxygenated Solvents for the Hydrolysis of  $[\text{Cr}(\text{bipy})_3]^{3+}$  a, b

---

I. At pH 11.82,  $T = 29.5 \pm 0.1^\circ\text{C}$ .

a) deoxygenated solvent:  $k_{\text{obs}} = 1.27 \pm 0.02 \times 10^{-5} \text{ sec}^{-1}$ .

b) oxygenated solvent:  $k_{\text{obs}} = 1.16 \pm 0.03 \times 10^{-5} \text{ sec}^{-1}$ .

II. At 0.50  $[\text{OH}^-]$ ,  $T = 7.5 \pm 0.1^\circ\text{C}$ .

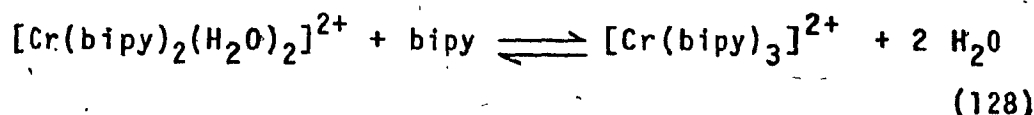
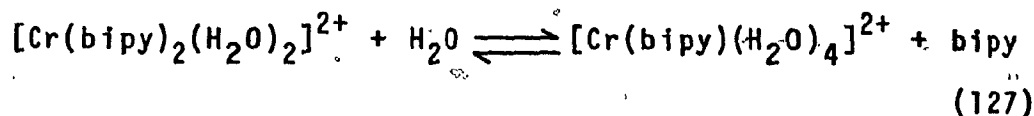
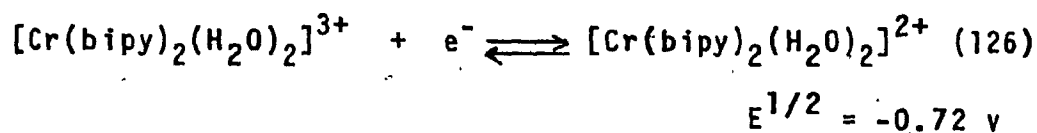
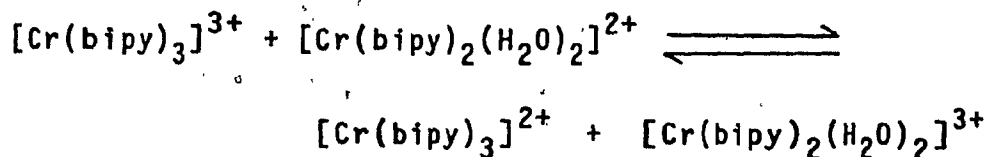
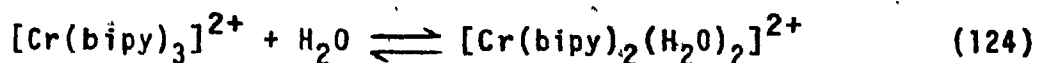
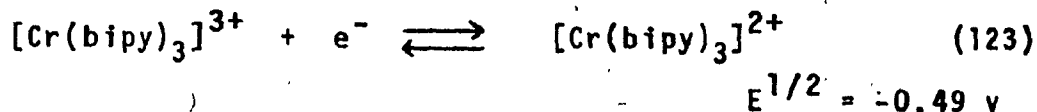
a) deoxygenated solvent:  $k_{\text{obs}} = 3.74 \pm 0.05 \times 10^{-5} \text{ sec}^{-1}$ .

b) oxygenated solvent:  $k_{\text{obs}} = 4.07 \pm 0.05 \times 10^{-5} \text{ sec}^{-1}$ .

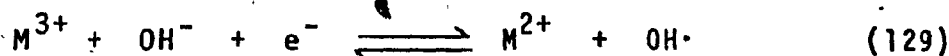
---

a Errors reported for  $k_{\text{obs}}$  as standard error.

b  $\mu_{\text{calc}} = 1.0 \text{ M}$ .



A similar reaction sequence has been proposed for  $[\text{Cr}(\text{phen})_3]^{3+}$  [73] in 50% aqueous ethanol. Obviously the ease of reduction of the trivalent metal will be the dominant factor in determining whether or not such a mechanism is plausible, that is



Whereas the above equilibrium (129) will lie to the right for cobalt(III), iron(III), and ruthenium(III), it will lie to the left for chromium(III). And, for any

trivalent metal ion, the reduction pathway becomes less probable as the ligand field strength increases if no other effects predominate.

Based on experimental results from the reaction between hydroxide ion and the bis-phenanthroline and bis-bipyridyl complexes of platinum(II) [75], Gillard has found support for nucleophilic attack by hydroxide ion through intermediates in which the hydroxyl group is linked to the carbon atom adjacent to the nitrogen atom in the N-heterocyclic ligand, the reaction scheme being given in Figure 36. In this scheme, if  $k_{\text{intra}}$  is large, it is thought that the concentration of the conjugate base CB will be negligible, and thus it will not be observed experimentally.

Gillard's pathway may be applied to the base hydrolysis of both  $[\text{Cr}(\text{bipy})_3]^{3+}$  and  $[\text{Cr}(\text{phen})_3]^{3+}$ , as schematized in Figures 37 and 38, respectively, for region (a). Nucleophilic attack on the  $C_6$  (or  $C_6'$ ) position of the bipy ligand, or the  $C_2$  (or  $C_9$ ) position of the phen ligand, of the reactant A produces the hydrated species CA. This species may then deprotonate at the quaternary nitrogen atom to give the conjugate base CB. Intramolecular shift of the hydroxyl group to the chromium(III) centre subsequently yields the observed products. In the reaction schemes,  $K_s$  denotes the equilibrium between the reactant and the covalent hydrate CA.

Figure 36. Reaction of Hydroxide Ion with  $[M(NN)_2]^{2+}$   
Complexes via Gillard's Mechanism.



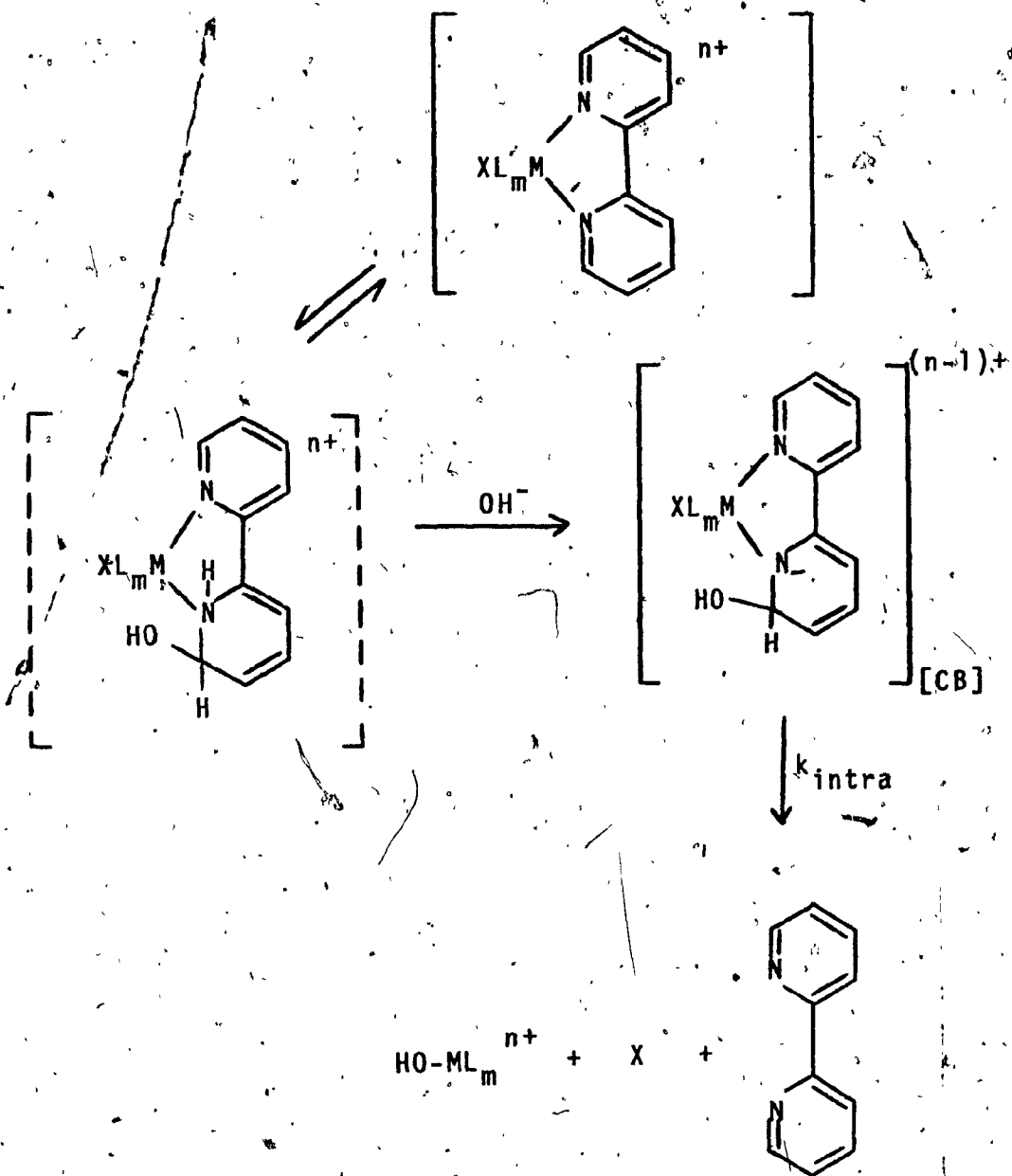
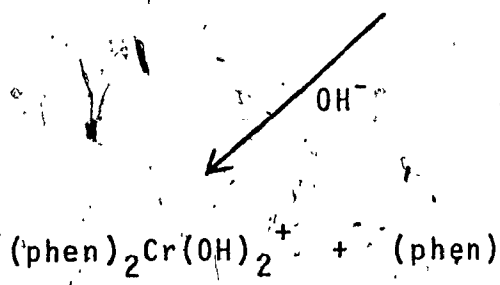
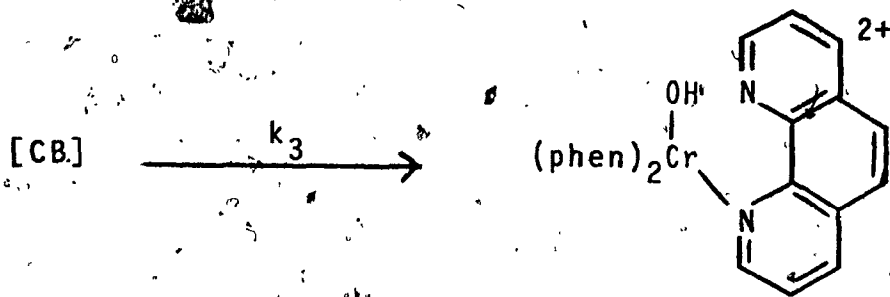
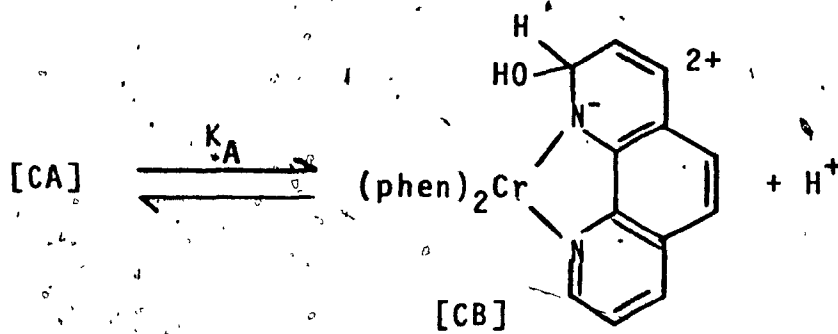
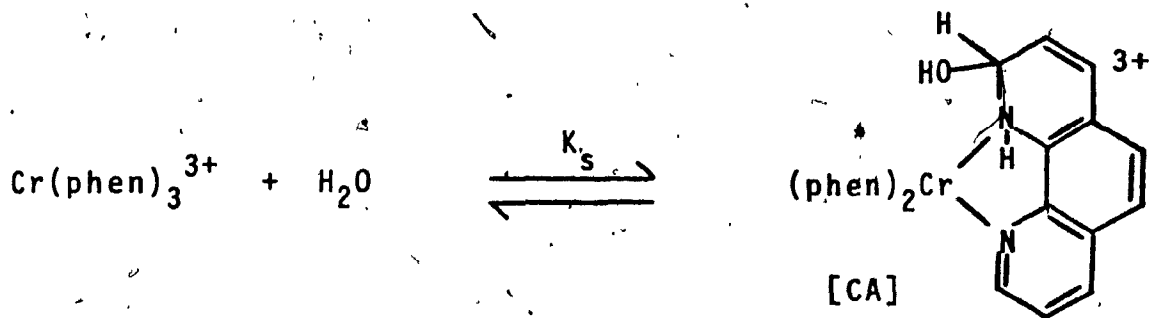


Figure 37. Hydrolysis of  $[\text{Cr}(\text{bipy})_3]^{3+}$  via  
Gillard's Mechanism.



Figure 38. Hydrolysis of  $[\text{Cr}(\text{phen})_3]^{3+}$  via  
Gillard's Mechanism.



$$K_s = \frac{[CA]}{[Cr(NN)_3^{3+}] [H_2O]} \quad (130)$$

The acid dissociation constant  $K_A$  is ascribed to the protonation-deprotonation equilibrium between CA and CB.

$$K_A = \frac{[H_2O] [CB]}{[OH^-] [CA]} \quad (131)$$

The overall rate of reaction is given by

$$\text{Rate} = k_3 [CB] = k_3 K_A [CA] [OH^-] \quad (132)$$

since  $[CB] = K_A [OH^-] [CA]$  from expression (131). The concentration of the hydrated species CA at any time 't' during the reaction (taking the activity of water as unity) is

$$[CA] = K_s [Cr(NN)_3^{3+}]_t \quad (133)$$

and the rate will then be given by

$$\text{Rate} = k_3 K_A K_s [Cr(NN)_3^{3+}]_t [OH^-] \quad (134)$$

A material balance on the concentration of  $[Cr(NN)_3^{3+}]$

yields

$$[\text{Cr}(\text{NN})_3^{3+}]_i = [\text{Cr}(\text{NN})_3^{3+}]_t + [\text{CA}] + [\text{CB}] \quad (135)$$

where the subscript 'i' refers to the initial concentration. Using previous equations, expression (135) may be rewritten as

$$[\text{Cr}(\text{NN})_3^{3+}]_i = [\text{Cr}(\text{NN})_3^{3+}]_t + K_s [\text{Cr}(\text{NN})_3^{3+}]_t + K_s K_A [\text{Cr}(\text{NN})_3^{3+}]_t [\text{OH}^-] \quad (136)$$

Rearrangement of expression (136) gives the concentration of  $[\text{Cr}(\text{NN})_3^{3+}]_t$  at time 't' as

$$[\text{Cr}(\text{NN})_3^{3+}]_t = \frac{[\text{Cr}(\text{NN})_3^{3+}]_i}{1 + K_s + K_A K_s [\text{OH}^-]} \quad (137)$$

Expression (132) for the rate then becomes

$$\text{Rate} = \frac{k_3 K_A K_s [\text{Cr}(\text{NN})_3^{3+}]_i [\text{OH}^-]}{(1 + K_s) + K_A K_s [\text{OH}^-]} \quad (138)$$

again if it is assumed that the activity of water is unity. The observed rate constant is therefore given by expression (139).

$$k_{\text{obs}} = \frac{k_3 K_A K_S [\text{OH}^-]}{(1 + K_S) + K_A K_S [\text{OH}^-]} \quad (139)$$

From the ratio of the intercept B to the slope A of a linear least-squares plot of  $1/k_{\text{obs}}$  versus  $1/[\text{OH}^-]$  in region (a), the acid dissociation constant  $K_A$  is equal to  $2.6 \times 10^6 (1 + K_S) / K_S$  for the  $[\text{Cr}(\text{bipy})_3]^{3+}$  system at  $11^\circ\text{C}$ . Use of the values of B' and A' from a similar plot yield  $K_A = 1.9 \times 10^6 (1 + K_S) / K_S$  for the  $[\text{Cr}(\text{phen})_3]^{3+}$  system at  $31.1^\circ\text{C}$ . As the ratio of  $(1 + K_S) / K_S$  is greater than unity, the lower limit for  $K_A$  will be  $2.6 \times 10^6$  and  $1.9 \times 10^6$  for the bipyridyl and phenanthroline systems, respectively. These  $K_A$  values correspond to  $\text{p}K_A$  values (upper limits) of -6.4 and -6.3, respectively, for the hydrated species CA.

The mechanism just described clearly implies a pH-dependent equilibrium, often evidenced by reversible spectral changes as the pH is changed [13]. However, no spectral changes were encountered for either complex investigated. The mechanism just described would necessitate the conjugate base concentration to be very small (less than 1%) with respect to  $[\text{Cr}(\text{NN})_3]^{3+}$  at hydroxide ion concentrations less than  $1 \times 10^{-10} \text{ M}$  ( $\text{pH} < 4$ ); and the same species would necessarily predominate (greater than 99%) at hydroxide ion concentrations greater than  $1 \times 10^{-5} \text{ M}$  ( $\text{pH} > 9$ ). Also, the



$pK_A$  values of -6.4 and -6.3 appear unlikely in view of the expected  $pK_A$  of about zero for trivalent metal complexes [13]. However, such an equilibrium need not be the operating pathway for Gillard's mechanism to be applicable. Instead, a more general treatment of Gillard's mechanism is shown in Figure 39 for  $[\text{Cr}(\text{bipy})_3]^{3+}$ . The overall rate is still given by

$$\text{Rate} = k_3[\text{CB}] \quad (140)$$

The rate of formation of the hydrated species CA is

$$\frac{+d[\text{CA}]}{dt} = k_1[\text{Cr}(\text{NN})_3^{3+}]\{\text{H}_2\text{O}\} - k_{-1}[\text{CA}] + k_{-2}[\text{CB}]\{\text{H}_2\text{O}\} - k_2[\text{CA}][\text{OH}^-] \quad (141)$$

A steady-state treatment on the concentration of CA yields

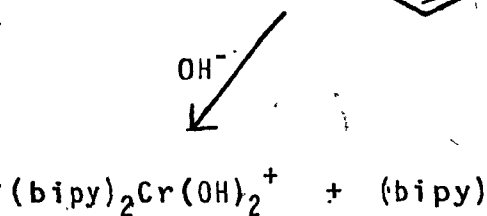
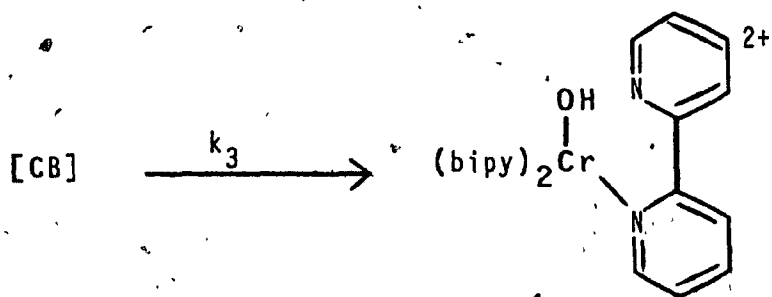
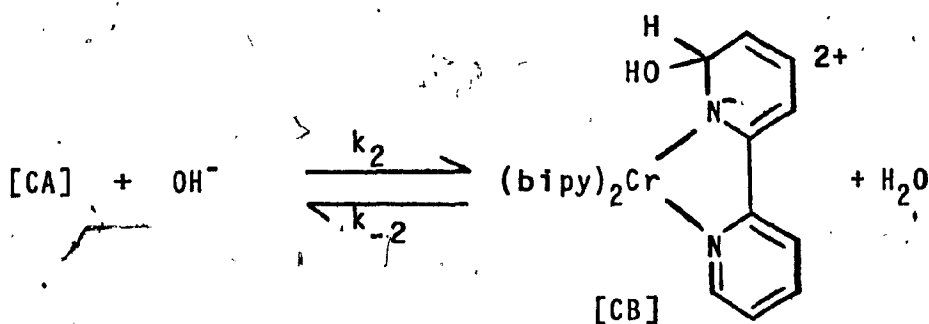
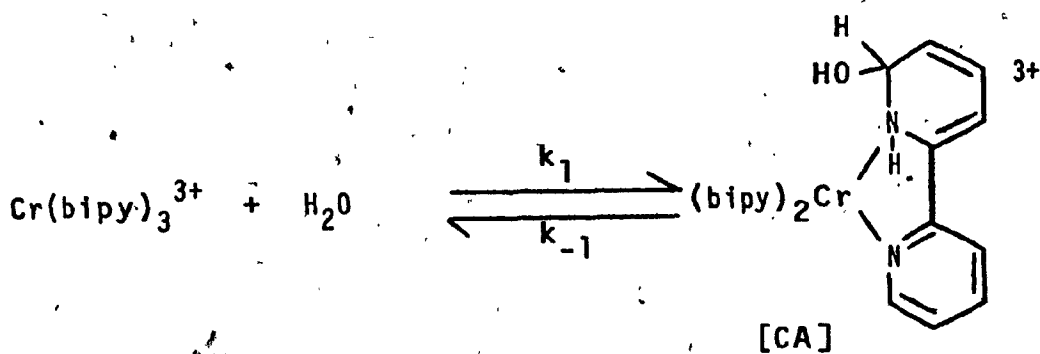
$$[\text{CA}] = \frac{k_1[\text{Cr}(\text{NN})_3^{3+}]\{\text{H}_2\text{O}\} + k_{-2}[\text{CB}]\{\text{H}_2\text{O}\}}{k_{-1} + k_2[\text{OH}^-]} \quad (142)$$

The rate of formation of the conjugate base CB is

$$+d[\text{CB}]/dt = k_2[\text{CA}][\text{OH}^-] - k_{-2}[\text{CB}]\{\text{H}_2\text{O}\} - k_3[\text{CB}] \quad (143)$$

Substitution of [CA] from expression (142) into expression

Figure 39. Hydrolysis of  $[\text{Cr}(\text{bipy})_3]^{3+}$  via a General Treatment of Gillard's Mechanism.



(143) and a steady-state treatment on the concentration of CB yields

$$[CB] = \frac{k_1' k_2 [Cr(NN)_3^{3+}] [OH^-]}{k_{-1}(k_{-2}' + k_3) + k_2 k_3 [OH^-]} \quad (144)$$

where  $k_1' = k_1 [H_2O]$ . The rate of disappearance of the reactant is

$$-d[Cr(NN)_3^{3+}]/dt = k_{obs} [Cr(NN)_3^{3+}] = k_3 [CB] \quad (145)$$

Thus, the observed rate constant is

$$k_{obs} = \frac{k_1' k_2 k_3 [OH^-]}{k_{-1}(k_{-2}' + k_3) + k_2 k_3 [OH^-]} \quad (146)$$

Using the values of A and B determined from the intercept and slope of the plot of  $1/k_{obs}$  versus  $1/[OH^-]$  in region (a) and expression (146),  $k_1' = 4.7 \times 10^{-7} \text{ sec}^{-1}$  and  $(k_1' k_2 k_3)/k_{-1}(k_{-2}' + k_3) = 1.2 \text{ M}^{-1} \text{ sec}^{-1}$  for the  $[Cr(bipy)_3]^{3+}$  system at 11°C. [16]. For the  $[Cr(phen)_3]^{3+}$  system at 31.1°C, the values of A' and B' from a similar plot and expression (146) yield  $k_1' = 1.8 \times 10^{-6} \text{ sec}^{-1}$  and  $(k_1' k_2 k_3)/k_{-1}(k_{-2}' + k_3) = 3.5 \text{ M}^{-1} \text{ sec}^{-1}$ . In the limit that  $k_2 k_3 [OH^-]$  is significantly greater than  $k_{-1}(k_{-2}' + k_3)$ , expression (146) reduces to

where  $k_1' = k_1\{H_2O\}$ . Use of the values of A and B determined from the intercept and slope of a linear least-squares plot of  $1/k_{obs}$  versus  $1/[OH^-]$  in region (a) and equation (155) yields  $k_1' = 4.7 \times 10^{-7} \text{ sec}^{-1}$  and  $(k_1'k_2k_3)/k_{-1}(k_{-2}' + k_3) = 1.2 \text{ M}^{-1}\text{sec}^{-1}$  [16] for the  $[Cr(bipy)_3]^{3+}$  system at  $11^\circ\text{C}$ . At high pH, where  $k_2k_3[OH^-]$  is much greater than  $k_{-1}(k_{-2}' + k_3)$ , a limiting rate is predicted, and equation (155) reduces to

$$k_{obs} = \frac{k_1'k_2k_3[OH^-]}{k_2k_3[OH^-]} = k_1' \quad (156)$$

If, on the other hand,  $k_{-1}(k_{-2}' + k_3)$  is much greater than  $k_2k_3[OH^-]$ , then equation (155) becomes

$$k_{obs} = \frac{k_1'k_2k_3[OH^-]}{k_{-1}(k_{-2}' + k_3)} \quad (157)$$

and the limiting rate shows dependence on the hydroxide ion concentration. As observed in Figure 14, the value of  $k_{obs}$  is pH-dependent up to ca. pH 9, at which point it becomes pH-independent to pH ca. 11 where  $k_{obs} = 5.1 \pm 0.2 \times 10^{-7} \text{ sec}^{-1}$  [16]. At high pH, where  $k_2k_3[OH^-] \gg k_{-1}(k_{-2}' + k_3)$ ,  $k_{obs} = k_1' = 4.7 \times 10^{-7} \text{ sec}^{-1}$  [16], which agrees well with the rate constant observed experimentally on the plateau of region (a). The same

general behaviour is observed for the  $[\text{Cr}(\text{phen})_3]^{3+}$  system (see Figure 18) in the pH range 0 - 10.5. The same reaction scheme as for  $[\text{Cr}(\text{bipy})_3]^{3+}$  is envisaged, as depicted in Figure 41. Use of the values of A' and B' determined for the phenanthroline system (see Figure 21) and equation (155) yields  $k_1' = 1.8 \times 10^{-6} \text{ sec}^{-1}$  and  $k_1'k_2k_3 / k_{-1}(k_{-2}' + k_3) = 3.5 \text{ M}^{-1} \text{ sec}^{-1}$ . A limiting rate, independent of hydroxide ion concentration, is attained where  $k_{\text{obs}} = 1.78 \pm 0.14 \times 10^{-6} \text{ sec}^{-1}$ . The experimental value agrees well with the calculated value of  $k_1'$  ( $1.8 \times 10^{-6} \text{ sec}^{-1}$ ).

A closer look at the detailed mechanism depicted in Figures 40 and 41 suggests that  $k_2$  and  $k_{-2}$  might well be quite large as they represent a deprotonation-protonation equilibrium. Also, the reaction step involving the rupture of the Cr-N bond in the heptacoordinate species C to yield the reaction products ( $k_3$ ) is thought to be relatively fast due to the extremely crowded situation in C. Thus, the formation of the aquo-intermediate B ( $k_1$ ) is considered the slowest step in this mechanism; and the assumption that  $k_2k_3[\text{OH}^-] / k_{-1}(k_{-2}' + k_3)$  is not unreasonable.

The observation of only one plateau (region (a)) over the entire reaction profile up to pH 14 may be indicative of some specific kinetic phenomenon. One possibility is a limiting kinetic step, for which  $k_{\text{obs}} = k_1'$ .

An associative-type reaction sequence which accounts for the observed kinetics in the plateau of region (a), and regions (b) and (c) is shown in Figure 42 for the  $[\text{Cr}(\text{NN})_3]^{3+}$  cation. The rate constant  $k_1$  describes the attack by water to yield a heptacoordinate aquo-species B, which can react in one of three modes: i) deprotonate ( $k_{-4}$ ) to form the heptacoordinate hydroxyl-species C; ii) react with water ( $k_2$ ) to yield some species D; iii) or react with hydroxide ion ( $k_6$ ) to eventually yield the observed reaction products. At high hydroxide ion concentrations ( $[\text{OH}^-] \geq 0.10$ ), the hydroxide ion may directly attack the reactant ( $k_3$ ) to yield the hydroxyl-species C. Species C may then react with water ( $k_5$ ) or hydroxide ion ( $k_7$ ) to yield the observed reaction products. The reaction with water ( $k_5$ ) will be negligible at high hydroxide ion concentrations since the  $\text{pK}_A$  of  $[\text{Cr}(\text{bipy})_3]^{3+}$  is 6.1 [21].

The reaction scheme presented in Figure 42 may be simplified to the following steps (158 - 164).

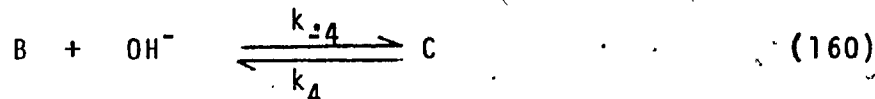
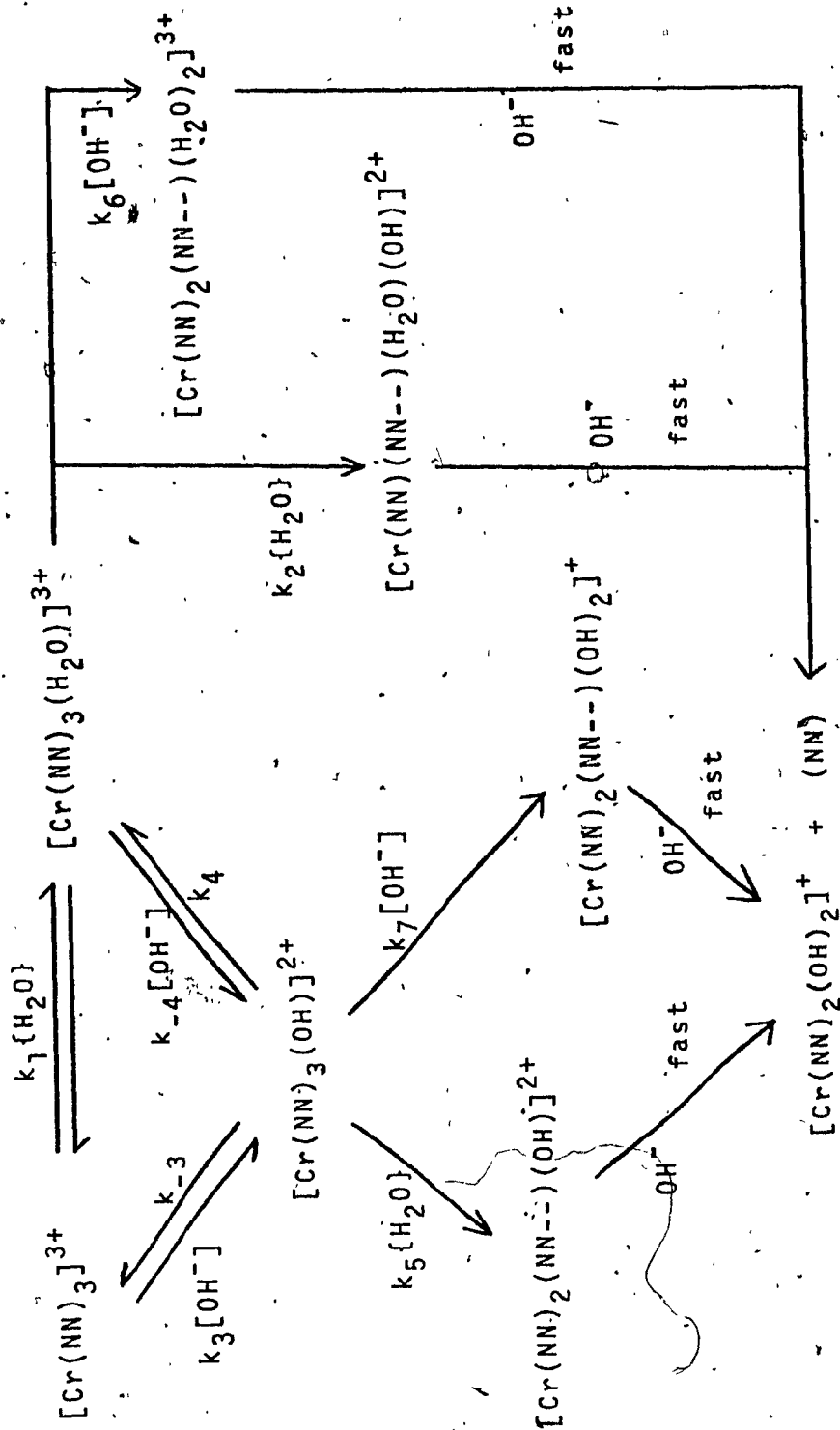
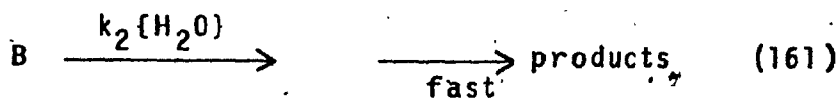


Figure 42. Hydrolysis of  $[\text{Cr}(\text{NN})_3]^{3+}$  via an Associative Pathway which Accounts for the Observed Kinetics.







The rate of disappearance of reactant A is given by equation (165),

$$\frac{-d[A]}{dt} = k_1[A] + k_3[A][OH^-] - k_{-1}[B] - k_{-3}[C] \quad (165)$$

and the rate of formation of the two heptacoordinate intermediate species B and C by the expressions (166 - 167),

$$\frac{+d[B]}{dt} = k_1[A] - k_{-1}[B] - k_{-4}[B][OH^-] + k_4[C] - k_2[B] - k_6[B][OH^-] \quad (166)$$

$$\frac{+d[C]}{dt} = k_3[A][OH^-] - k_{-3}[C] + k_{-4}[B][OH^-] - k_4[C] - k_7[C][OH^-] \quad (167)$$

Use of expressions (166 - 167) and a steady-state approximation to assume that  $(+d[B]/dt + d[C]/dt) = 0$  yields

$$\begin{aligned}
 &k_1[A] - k_{-1}[B] - k_{-4}[B][OH^-] + k_4[C] - k_2[B] - \\
 &k_6[B][OH^-] + k_3[A][OH^-] - k_{-3}[C] + k_{-4}[B][OH^-] - \\
 &k_4[C] - k_7[C][OH^-] = 0
 \end{aligned} \tag{168}$$

The acid-base equilibrium between the aquo- and hydroxyl-intermediates B and C is defined by the equilibrium constant  $K_4$ , as per equation (169),

$$K_4 = k_{-4}/k_4 = [C]/[B][OH^-] \tag{169}$$

wherefrom the concentration of C is given by

$$[C] = K_4[B][OH^-] \tag{170}$$

Substitution of the concentration of C (equation (170)) into expression (168) and subsequent cancellation of terms yields expression (171).

$$\begin{aligned}
 &k_1[A] - k_{-1}[B] - k_2[B] - k_6[B][OH^-] + k_3[A][OH^-] - \\
 &k_{-3}K_4[B][OH^-] - k_7K_4[B][OH^-]^2 = 0
 \end{aligned} \tag{171}$$

The concentration of the heptacoordinate aquo-intermediate species B is then given by expression (172).

$$[B] = \frac{k_1[A] + k_3[A][OH^-]}{k_{-1} + k_2 + k_6[OH^-] + k_4[OH^-](k_{-3} + k_7[OH^-])} \quad (172)$$

Expression (165) may be rewritten as per (173),

$$-d[A]/dt = k_1[A] + k_3[A][OH^-] - k_{-1}[B] - k_{-3}k_4[B][OH^-] \quad (173)$$

since  $[C] = k_4[B][OH^-]$  from equation (170). Subsequently, substitution of [B] (equation (172)) into equation (173) yields equations (174 - 177).

$$\frac{-d[A]}{dt} = \frac{k_1[A] + k_3[A][OH^-] - k_{-1} \frac{k_1[A] + k_3[A][OH^-]}{k_{-1} + k_2 + k_6[OH^-] + k_4[OH^-](k_{-3} + k_7[OH^-])} - k_{-3}k_4[OH^-] \frac{k_1[A] + k_3[A][OH^-]}{k_{-1} + k_2 + k_6[OH^-] + k_4[OH^-](k_{-3} + k_7[OH^-])}}{k_{-1} + k_2 + k_6[OH^-] + k_4[OH^-](k_{-3} + k_7[OH^-])} \quad (174)$$

$$\frac{-d[A]}{dt} = \frac{k_1[A] + k_3[A][OH^-] - k_{-1}k_1[A] + k_{-1}k_3[A][OH^-]}{k_{-1} + k_2 + k_6[OH^-] + k_4[OH^-](k_{-3} + k_7[OH^-])}$$

(175)

$$\frac{k_1k_{-3}k_4[A][OH^-] + k_3k_{-3}k_4[A][OH^-]^2}{k_{-1} + k_2 + k_6[OH^-] + k_4[OH^-](k_{-3} + k_7[OH^-])}$$

$$\frac{-d[A]}{dt} = \frac{k_1k_2[A][OH^-] + k_1k_6[A][OH^-] + k_3k_6[A][OH^-]^2 + k_1k_7k_4[A][OH^-]^2 + k_3k_7k_4[A][OH^-]^3}{k_{-1} + k_2 + k_6[OH^-] + k_4[OH^-](k_{-3} + k_7[OH^-])}$$

(176)

$$\frac{-d[A]}{dt} = \frac{k_1 + k_3[OH^-] [k_2 + k_6[OH^-] + k_7k_4[OH^-]^2] [A]}{k_{-1} + k_2 + k_6[OH^-] + k_4[OH^-](k_{-3} + k_7[OH^-])}$$

(177)

$$k_{obs} = (k_1 + k_3[OH^-]) \left[ \frac{k_2 + k_6[OH^-] + k_4k_7[OH^-]^2}{k_{-1} + k_2 + k_6[OH^-] + k_4[OH^-](k_{-3} + k_7[OH^-])} \right]$$

(178)

From expression (177) the observed rate constant becomes that given in (178). In expression (178), the numerator and denominator of the second term are identical, except for the  $k_{-1}$  and  $k_{-3}K_4[\text{OH}^-]$  terms. In order for this mechanism to agree with the observed hydroxide ion dependence, the  $[k_{-1} + k_{-3}K_4[\text{OH}^-]]$  term must be greater than the remaining terms in the denominator of expression (178). That is to say, the steps described by  $k_2$ ,  $k_6$ , and  $k_7$  would be rate-determining, and the heptacoordinate intermediate species B and C are in equilibrium with reactant A. Consequently, the equilibrium constant  $K_4$  becomes equal to  $(k_{-1}k_3)/(k_1k_{-3})$ , and thus

$$[k_{-1} + k_{-3}K_4[\text{OH}^-]] = (k_{-1}/k_1)[k_1 + k_3[\text{OH}^-]] \quad (179)$$

Expression (179) may be rearranged such that

$$\frac{k_1}{k_{-1}} = \frac{k_1 + k_3[\text{OH}^-]}{k_{-1} + k_{-3}K_4[\text{OH}^-]} \quad (180)$$

Using the above assumptions, the observed rate constant is then given by (181) and (182),

$$k_{\text{obs}} = \frac{(k_1 + k_3[\text{OH}^-]) [k_2 + k_6[\text{OH}^-] + K_4k_7[\text{OH}^-]]}{k_{-1} + k_{-3}K_4[\text{OH}^-]} \quad (181)$$

$$k_{\text{obs}} = (k_1/k_{-1}) \left[ k_2 + k_6[\text{OH}^-] + K_4 k_7 [\text{OH}^-]^2 \right] \quad (182)$$

The preceding expression for  $k_{\text{obs}}$  may be rearranged to

$$k_{\text{obs}} = \frac{k_1 k_2}{k_{-1}} + \frac{k_1 k_6}{k_{-1}} [\text{OH}^-] + \frac{k_1 K_4 k_7}{k_{-1}} [\text{OH}^-]^2 \quad (183)$$

which may then be rewritten in the more general form of equation (184),

$$k_{\text{obs}} = k_x + k_c [\text{OH}^-] + k_E [\text{OH}^-]^2 \quad (184)$$

where

$$k_x = k_1 k_2 / k_{-1} \quad (185)$$

$$k_c = k_1 k_6 / k_{-1} \quad (186)$$

$$k_E = k_1 k_7 K_4 / k_{-1} \quad (187)$$

Expression (184) accounts for the observed hydroxide ion dependence in the pH range 9 - 12.2 and 0.10 - 1.00  $[\text{OH}^-]$  for both the bipyridyl and phenanthroline systems. The observed rate constant in the plateau of region (a) is then equal to  $k_x = k_1 k_2 / k_{-1} = k_{\text{obs}}$ . For the  $[\text{Cr}(\text{bipy})_3]^{3+}$  system,  $k_x = 5.1 \pm 0.2 \times 10^{-7} \text{ sec}^{-1}$  at 11°C [16], and  $k_x = 1.78 \pm 0.14 \times 10^{-6} \text{ sec}^{-1}$  at 31.1°C for the  $[\text{Cr}(\text{phen})_3]^{3+}$  system. In region (b) the linear relationship

between  $k_{\text{obs}}$  and  $[\text{OH}^-]$ , in terms of expressions (183-184) is

$$k_{\text{obs}} = \frac{k_1 k_2}{k_{-1}} + \frac{k_1 k_6}{k_{-1}} [\text{OH}^-] = k_x + k_{c_1} [\text{OH}^-] \quad (188)$$

A plot of  $k_{\text{obs}}$  versus  $[\text{OH}^-]$  (see Figure 19) yields a slope  $k_{c_1} = k_1 k_6 / k_{-1} = 1.06 \times 10^{-4} \text{ M}^{-1} \text{ sec}^{-1}$  for  $[\text{Cr}(\text{bipy})_3]^{3+}$  at  $11^\circ\text{C}$ , and intercept  $k_{x_1} = k_1 k_2 / k_{-1} = 4.6 \times 10^{-7} \text{ sec}^{-1}$  under the same conditions. For the  $[\text{Cr}(\text{phen})_3]^{3+}$  system at  $31.1^\circ\text{C}$ , an analogous plot (see Figure 22) yields a slope  $k_{c_2} = k_1 k_6 / k_{-1} = 3.2 \times 10^{-4} \text{ M}^{-1} \text{ sec}^{-1}$ , and intercept  $k_{x_2} = 3.3 \times 10^{-6} \text{ sec}^{-1}$ . Tables XII and XIII give the values of  $k_{\text{obs}}$  calculated from expression (188) and those experimentally observed for the two chromium(III) cations in region (b). The results show that the observed and calculated values are in good agreement.

In region (c) (i.e.,  $0.10 - 1.00 \text{ M OH}^-$ ), where a linear relationship exists between  $k_{\text{obs}}$  and  $[\text{OH}^-]^2$ , expressions (183) and (184) show the observed kinetics, i.e.,

$$k_{\text{obs}} = \frac{k_1 k_2}{k_{-1}} + \frac{k_1 k_6}{k_{-1}} [\text{OH}^-] + \frac{k_1 k_7 K_4}{k_{-1}} [\text{OH}^-]^2 \quad (189)$$

$$k_{\text{obs}} = k_x + k_c [\text{OH}^-] + k_E [\text{OH}^-]^2 \quad (190)$$



Table XII  
 Observed And Calculated Rate Constants for  $[\text{Cr}(\text{bipy})_3]^{3+}$  in  
 Region (b) as Determined from Equation (188)

pH ( $\pm 0.05$ )	$[\text{OH}^-]$ (M)	$k_{\text{obs}}^a$ ( $\text{sec}^{-1}$ )	$k_{\text{calc}}$ ( $\text{sec}^{-1}$ )
10.83	$6.76 \times 10^{-4}$	$5.4 \pm 0.2 \times 10^{-7}$	$5.8 \times 10^{-7}$
11.31	$2.04 \times 10^{-3}$	$6.9 \pm 0.2 \times 10^{-7}$	$7.3 \times 10^{-7}$
11.82	$6.61 \times 10^{-3}$	$1.2 \pm 0.0 \times 10^{-6}$	$1.2 \times 10^{-6}$
12.16	$1.45 \times 10^{-2}$	$2.0 \pm 0.0 \times 10^{-6}$	$2.0 \times 10^{-6}$

<sup>a</sup> Errors reported as standard error.

Table XIII  
 Observed and Calculated Rate Constants for  $[\text{Cr}(\text{phen})_3]^{3+}$  in  
 Region (b) as Determined from Equation (188)

pH. ( $\pm 0.05$ )	$[\text{OH}^-]$ (M)	$k_{\text{obs}}^a$ ( $\text{sec}^{-1}$ )	$k_{\text{calc}}$ ( $\text{sec}^{-1}$ )
11.14	$1.38 \times 10^{-3}$	$3.3 \pm 0.2 \times 10^{-6}$	$3.7 \times 10^{-6}$
11.67	$4.68 \times 10^{-3}$	$5.4 \pm 0.2 \times 10^{-6}$	$4.8 \times 10^{-6}$
12.17	$1.48 \times 10^{-2}$	$7.9 \pm 0.0 \times 10^{-6}$	$8.0 \times 10^{-6}$

<sup>a</sup> Errors reported as standard error.

A plot of  $k_{\text{obs}}$  versus  $[\text{OH}^-]^2$  (see Figures 20 and 23) in the region 0.10 - 1.00  $[\text{OH}^-]$  yields a slope  $E = 1.9 \times 10^{-4}$  and  $6.9 \times 10^{-4} \text{ M}^{-2} \text{ sec}^{-1}$  for  $[\text{Cr}(\text{bipy})_3]^{3+}$  at  $11^\circ\text{C}$  and  $[\text{Cr}(\text{phen})_3]^{3+}$  at  $31.1^\circ\text{C}$ , respectively. Rearrangement of expression (190) yields

$$\frac{k_{\text{obs}} - k_x}{[\text{OH}^-]} = k_c + k_E[\text{OH}^-] \quad (191)$$

Thus, a plot of  $(k_{\text{obs}} - k_x)/[\text{OH}^-]$  versus  $[\text{OH}^-]$  should give a straight line with slope  $k_E$  and intercept  $k_c$ . The intercept  $k_c$  should be in agreement with the slope of a plot of  $k_{\text{obs}}$  versus  $[\text{OH}^-]$  in region (b). Plots of  $(k_{\text{obs}} - k_x)/[\text{OH}^-]$  versus  $[\text{OH}^-]$  for the  $[\text{Cr}(\text{bipy})_3]^{3+}$  and  $[\text{Cr}(\text{phen})_3]^{3+}$  systems in the range 0.10 - 1.00  $[\text{OH}^-]$  are presented in Figures 43 and 44. Tables XIV and XV present the pertinent data. A linear least-squares analysis of the plots of  $(k_{\text{obs}} - k_x)/[\text{OH}^-]$  versus  $[\text{OH}^-]$  yields

- i) for the  $[\text{Cr}(\text{bipy})_3]^{3+}$  system in region (c):  
 slope =  $k_{E1} = k_1 k_7 K_4 / k_{-1} = 1.8 \times 10^{-4} \text{ M}^{-2} \text{ sec}^{-1}$   
 intercept =  $k_{c3} = 7 \times 10^{-4} \text{ M}^{-1} \text{ sec}^{-1}$ ;
- ii) for the  $[\text{Cr}(\text{phen})_3]^{3+}$  system in region (c):  
 slope =  $k_{E2} = k_1 k_7 K_4 / k_{-1} = 5.3 \times 10^{-4} \text{ M}^{-2} \text{ sec}^{-1}$   
 intercept =  $k_{c4} = 1.5 \times 10^{-4} \text{ M}^{-1} \text{ sec}^{-1}$ .

Figure 43. Plot of  $(k_{\text{obs}} - k_x) / [\text{OH}^-]$  versus  $[\text{OH}^-]$  for the Hydrolysis of  $[\text{Cr}(\text{bipy})_3]^{3+}$  in the Range 0.10 - 1.00  $[\text{OH}^-]$  at 11°C.

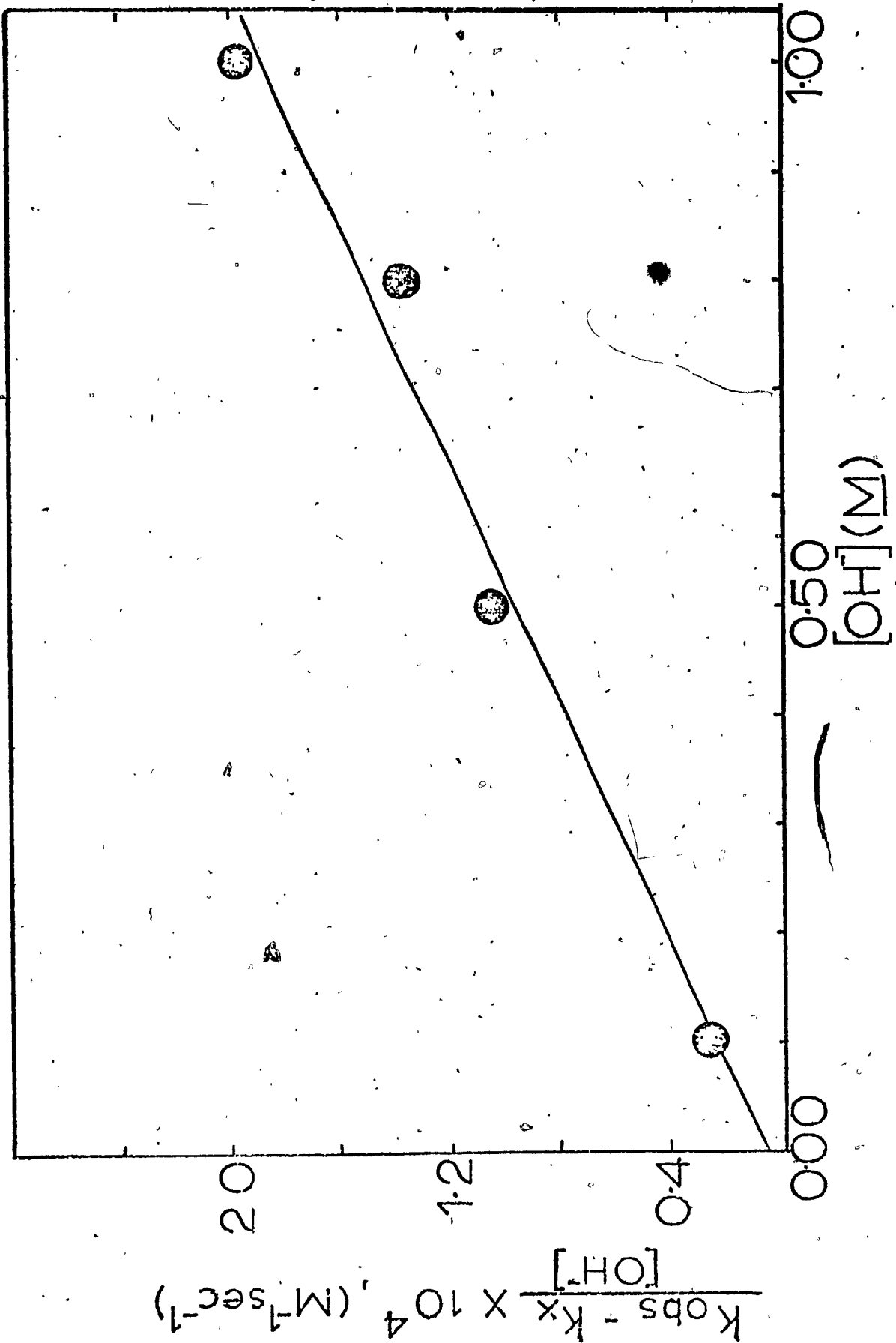


Figure 44. Plot of  $(k_{\text{obs}} - k_x) / [\text{OH}^-]$  versus  $[\text{OH}^-]$  for the Hydrolysis of  $[\text{Cr}(\text{phen})_3]^{3+}$  in the Range 0.10 - 1.00  $[\text{OH}^-]$  at 31.1°C.

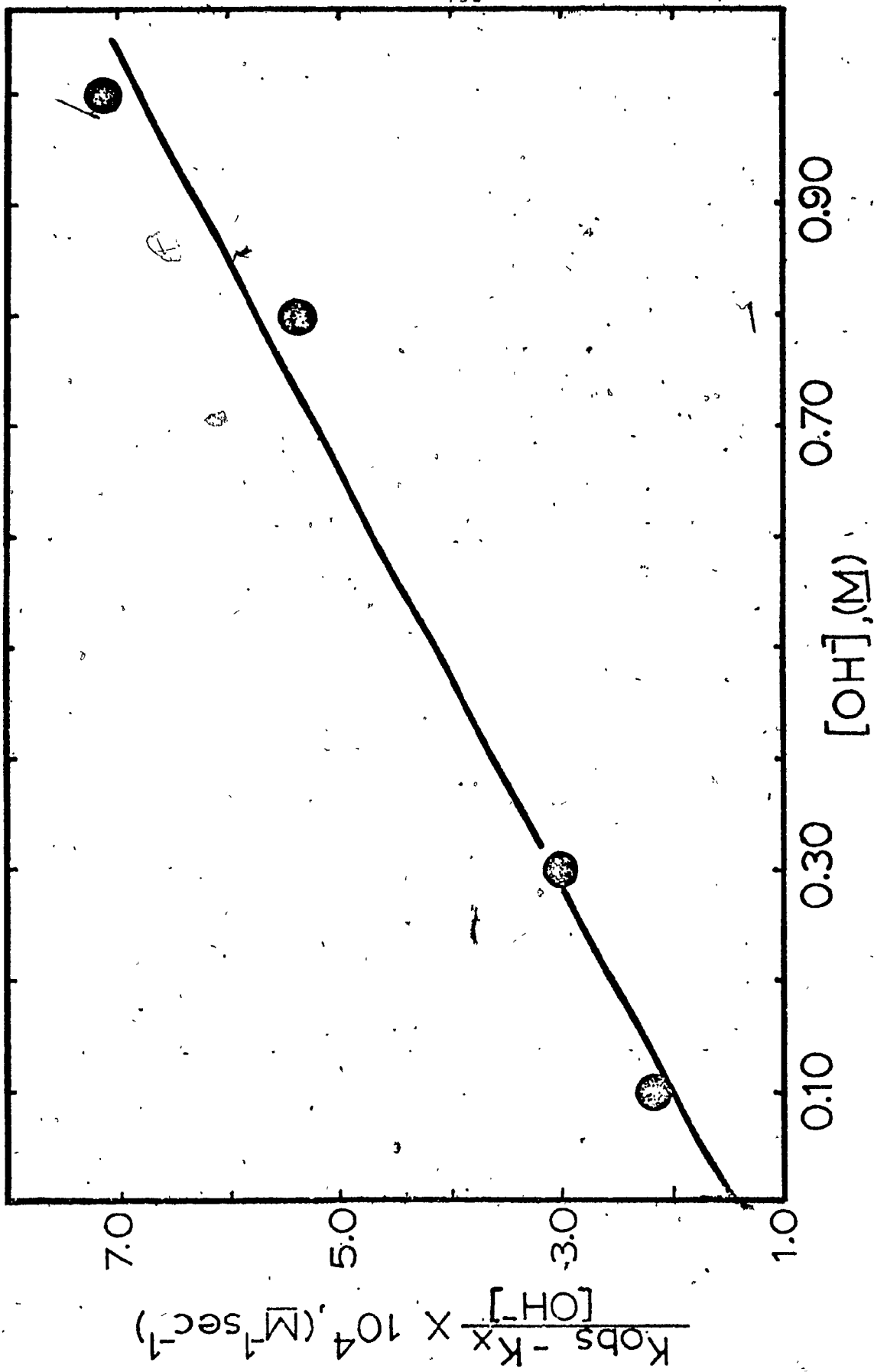


Table XIV  
 Comparison of Observed and Calculated Rate Constants in Region  
 (c) for the  $[\text{Cr}(\text{bipy})_3]^{3+}$  System

$[\text{OH}^-]$ (M)	$\frac{(k_{\text{obs}} - k_x)^a}{[\text{OH}^-]}$	$k_{\text{obs}}$ ( $\text{sec}^{-1}$ )	b, c
0.10	$2.51 \times 10^{-5}$	$0.30 \pm 0.01 \times 10^{-5}$	
0.50	$1.04 \times 10^{-4}$	$0.53 \pm 0.01 \times 10^{-4}$	
0.80	$1.37 \times 10^{-4}$	$1.10 \pm 0.02 \times 10^{-4}$	
1.00	$1.96 \times 10^{-4}$	$1.97 \pm 0.06 \times 10^{-4}$	

a  $k_x = 5.1 \pm 0.2 \times 10^{-7} \text{ sec}^{-1}$  at  $11^\circ\text{C}$  [16].

b Errors reported as standard error.

c  $k_{\text{obs}}$  at  $11^\circ\text{C}$ .



Table XV  
 Comparison of Observed and Calculated Rate Constants in Region  
 (c) for the  $[\text{Cr}(\text{phen})_3]^{3+}$  System

$[\text{OH}^-]$ (M)	$(k_{\text{obs}} - k_x) \frac{a}{[\text{OH}^-]}$	$k_{\text{obs}} \frac{b,c}{(\text{sec}^{-1})}$
0.10	$2.16 \times 10^{-4}$	$23.4 \pm 0.5 \times 10^{-6}$
0.30	$2.99 \times 10^{-4}$	$91.4 \pm 1.2 \times 10^{-6}$
0.50	$2.60 \times 10^{-4}$	$132 \pm 5 \times 10^{-6}$
0.80	$5.35 \times 10^{-4}$	$430 \pm 20 \times 10^{-6}$
1.00	$7.07 \times 10^{-4}$	$709 \pm 28 \times 10^{-6}$

a  $k_x = 1.8 \times 10^{-6} \text{ sec}^{-1}$  at  $31.1^\circ\text{C}$ .

b Errors reported as standard error.

c  $k_{\text{obs}}$  at  $31.1^\circ\text{C}$ .

The data in Tables XIV and XV indicates that between 0.80 and 1.00  $[\text{OH}^-]$ , there is good correlation between the experimental and calculated values; however, the values in the range 0.10 - 0.50  $[\text{OH}^-]$  do not correspond very well. This latter deviation may be due to the error associated with the small difference between  $k_{\text{obs}}$  and  $k_x$  in this region. A comparison of the intercepts  $k_{c_3}$  and  $k_{c_4}$  of plots of  $(k_{\text{obs}} - k_x)/[\text{OH}^-]$  versus  $[\text{OH}^-]$  in region (c) and the slopes  $k_{c_1}$  and  $k_{c_2}$  of plots of  $k_{\text{obs}}$  versus  $[\text{OH}^-]$  in region (b) is justifiable if inherent error in the method of obtaining  $k_{c_3}$  and  $k_{c_4}$  is taken into account. The pertinent values are given below:

i) for the  $[\text{Cr}(\text{bipy})_3]^{3+}$  system at  $11^\circ\text{C}$ ,

$$k_{c_1} = 1.06 \pm 0.01 \times 10^{-4} \text{ M}^{-1} \text{ sec}^{-1}$$

$$k_{c_3} = 7. \pm 14 \times 10^{-4} \text{ M}^{-1} \text{ sec}^{-1};$$

ii) for the  $[\text{Cr}(\text{phen})_3]^{3+}$  system at  $31.1^\circ\text{C}$ ,

$$k_{c_2} = 3.2 \pm 0.6 \times 10^{-4} \text{ M}^{-1} \text{ sec}^{-1}$$

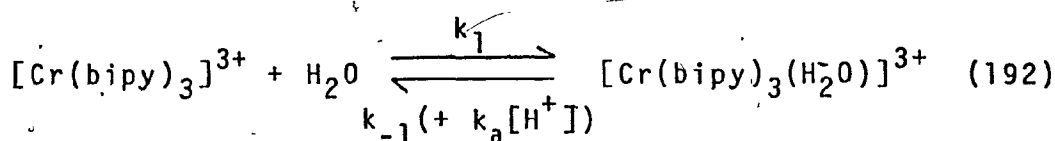
$$k_{c_4} = 1.5 \pm 0.3 \times 10^{-4} \text{ M}^{-1} \text{ sec}^{-1}.$$

##### 5. The Operative Pathway.

A dissociative pathway for the hydrolysis of either chromium(III) complex cation (see Figures 27 and 28) appears unlikely most importantly because acid hydrolysis was not observed. Furthermore; activation

energies for the two chromium(III) cations (see Tables XVII and XVIII) are more in line with an associative-type pathway, than with those of dissociation [76]. Gillard's mechanism involving covalent hydrate formation is also thought to be inapplicable to  $[\text{Cr}(\text{bipy})_3]^{3+}$  and  $[\text{Cr}(\text{phen})_3]^{3+}$  because no spectral variations were observed, even in very alkaline media. However, such a mechanism has been ascribed to the hydroxide reduction of  $[\text{Ru}(\text{bipy})_3]^{3+}$  [15] and of various substituted polypyridyl complexes of iron(III) and osmium(III) [72]. It has been shown (Table XI) that the two chromium(III) complexes do not undergo reduction to chromium(II).

Thus, the pathway believed to be operative for both  $[\text{Cr}(\text{bipy})_3]^{3+}$  and  $[\text{Cr}(\text{phen})_3]^{3+}$  is shown in Figure 45. The reaction scheme combines the associative pathway in regions (a) and (b), and an ion-pair pathway in region (c). At  $\text{pH} < 6$ , the observed rate constant is very small and independent of solution pH for both complexes (see Figures 14 and 18). This observation has been explained [18] for the  $[\text{Cr}(\text{bipy})_3]^{3+}$  cation in terms of the relaxation of the initially-formed  $[\text{Cr}(\text{bipy})_3(\text{H}_2\text{O})]^{3+}$  intermediate back to  $[\text{Cr}(\text{bipy})_3]^{3+}$  via acid-dependent ( $k_a = 4 \times 10^5 \text{ M}^{-1} \text{ sec}^{-1}$ ) and acid-independent ( $k_{-1} \leq 10 \text{ sec}^{-1}$ ) paths.



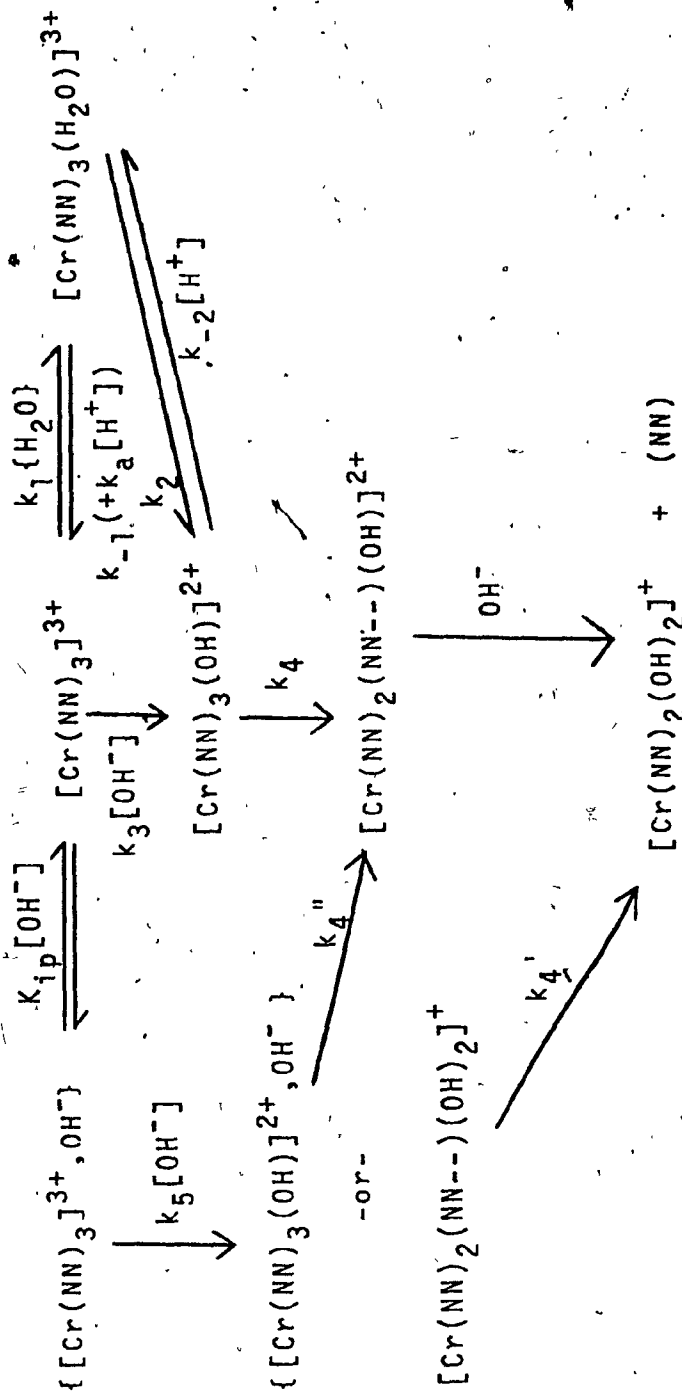
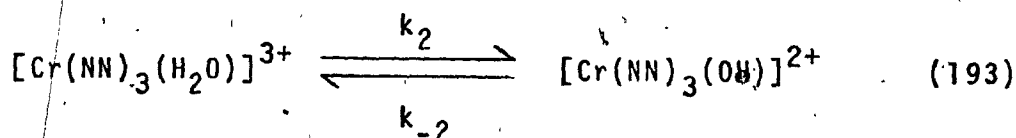
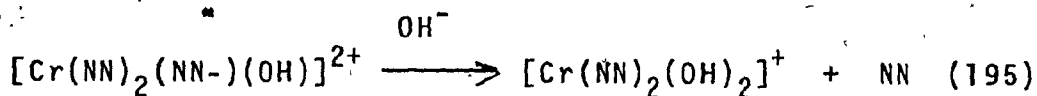
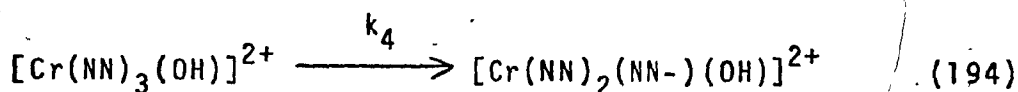


Figure 45. The Thermal Hydrolysis of  $[\text{Cr}(\text{NN})_3]^{3+}$  in Acidic and Basic Solution.

The similarity between the shape of the curve of region (a) and the common S-shaped titration curve suggests that the inflection point represents the deprotonation of the heptacoordinate intermediate species  $[\text{Cr}(\text{NN})_3(\text{H}_2\text{O})]^{3+}$  to form  $[\text{Cr}(\text{NN})_3(\text{OH})]^{2+}$ .



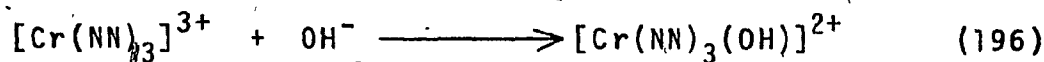
The hydroxyl-intermediate, known to be short-lived in the case of the bipyridyl complex [18], will subsequently undergo ring-opening, followed by irreversible loss of the unidentate (NN-) ligand.



The plateau of region (a) then reflects the complete titration of the heptacoordinate intermediate species  $[\text{Cr}(\text{NN})_3(\text{H}_2\text{O})]^{3+}$ , such that the observed rate constant  $k_{\text{obs}}$  in this plateau represents the rate constant for the direct attack of water on the substrate  $[\text{Cr}(\text{NN})_3]^{3+}$ , ( $k_1$ ).

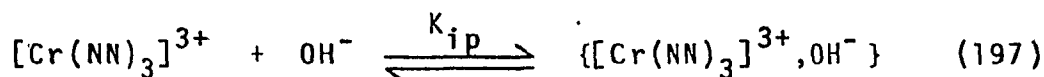
In region (b),  $k_{\text{obs}}$  increases rapidly with increasing pH, and is linearly dependent on hydroxide ion

concentration for both  $[\text{Cr}(\text{bipy})_3]^{3+}$  and  $[\text{Cr}(\text{phen})_3]^{3+}$  (see Figures 19 and 22). As shown in Section III-D-4, the slope of the plot of  $k_{\text{obs}}$  versus  $[\text{OH}^-]$  in region (b) is identified with the rate constant ( $k_3$ ) for the direct attack of hydroxide ion on the substrate,

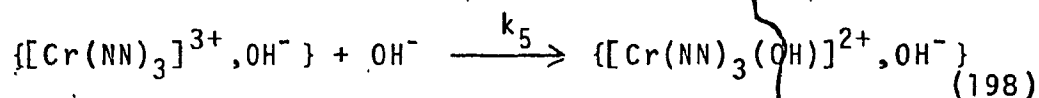


The heptacoordinate hydroxyl-species then yields the observed via reactions (194) and (195).

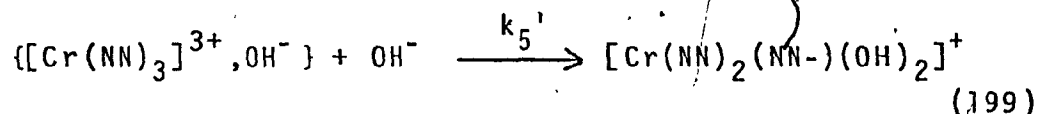
In region (c), where the observed rate constant shows a linear second-order dependence on hydroxide ion concentration (see Figures 20 and 23), it seems inevitable that ion-pairs (or outer-sphere complexes) will form between the chromium(III) substrate and hydroxide ion, as per (197).



Subsequent attack by a second hydroxide ion yields either



or



The two heptacoordinate species of (198) and (199) then

irreversibly lead to the release of the unidentate (NN-) ligand. The kinetic treatment presented in Section III-D-2 (equations 113 - 115) becomes that in equation (200),

$$k_{\text{obs}} = k_5 K_{\text{ip}} [\text{OH}^-]^2 \quad (200)$$

where  $k_5 K_{\text{ip}} = 1.9 \times 10^{-4} \text{ M}^{-2} \text{ sec}^{-1}$  for  $[\text{Cr}(\text{bipy})_3]^{3+}$  at  $11^\circ\text{C}$ , and  $k_5 K_{\text{ip}} = 6.9 \times 10^{-4} \text{ M}^{-2} \text{ sec}^{-1}$  for  $[\text{Cr}(\text{phen})_3]^{3+}$  at  $31.1^\circ\text{C}$ . Again, under the assumption that  $k_5$  is of the order of  $10^{-4} - 10^{-5} \text{ M}^{-1} \text{ sec}^{-1}$ ,  $K_{\text{ip}} \sim 2 - 20$  for the bipyridyl system and  $K_{\text{ip}} \sim 7 - 70$  for the corresponding phenanthroline system.

From Figure 45 and the above analysis, the expression for the observed rate constant  $k_{\text{obs}}$  becomes

$$k_{\text{obs}} = \frac{k_1' k_2 k_4 [\text{OH}^-]}{k_{-1} (k_{-2}' + k_4) + k_2 k_4 [\text{OH}^-]} + k_3 [\text{OH}^-] + k_5 K_{\text{ip}} [\text{OH}^-]^2 \quad (201)$$

A reconsideration of reactions (197 - 199) raises suspicions as to the applicability of expression (113), since the rate refers to the instantaneous rate at any time 't' during the reaction. Thus, expression (113) is applicable if it is assumed that the equilibrium in reaction (197) is rapid, and that  $k_5$  (or  $k_5'$ ) is much

slower than the reverse reaction in (197); i.e.,  $k_{-ip}$ . If in the case that  $k_5$  is of the same order of magnitude as the reverse reaction in (197), the ion-pair  $\{[\text{Cr}(\text{NN})_3]^{3+}, \text{OH}^-\}$  must necessarily be treated as a steady-state intermediate.

A material balance on the concentration of  $[\text{Cr}(\text{NN})_3]^{3+}$  in the rate law

$$\text{Rate} = k_5 k_{ip} [\text{Cr}(\text{NN})_3]^{3+} [\text{OH}^-]^2 \quad (202)$$

yields

$$[\text{Cr}(\text{NN})_3]^{3+} = [\text{Cr}(\text{NN})_3]^{3+}_0 - \{[\text{Cr}(\text{NN})_3]^{3+}, \text{OH}^-\} - [\text{P}] \quad (203)$$

where  $[\text{Cr}(\text{NN})_3]^{3+}_0$  is the initial concentration of the reactant, and  $[\text{P}]$  is the concentration of reactant present as products. Therefore,

$$[\text{Cr}(\text{NN})_3]^{3+} = [\text{Cr}(\text{NN})_3]^{3+}_0 - k_{ip} [\text{Cr}(\text{NN})_3]^{3+} [\text{OH}^-] - [\text{P}] \quad (204)$$

from which the concentration of  $[\text{Cr}(\text{NN})_3]^{3+}$  becomes that in expression (205).

$$[\text{Cr}(\text{NN})_3]^{3+} = \frac{[\text{Cr}(\text{NN})_3]^{3+}_0 - [\text{P}]}{1 + k_{ip} [\text{OH}^-]} \quad (205)$$



Thus, the rate law in (202) becomes

$$\text{Rate} = k_5 K_{ip} [\text{OH}^-]^2 \left[ \frac{[\text{Cr}(\text{NN})_3^{3+}]_0 - [\text{P}]}{1 + K_{ip} [\text{OH}^-]} \right] \quad (206)$$

If initial rates are assumed, then the [P] term in (206) will be equal to zero since there will be no appreciable product formed, and (206) becomes

$$(\text{Rate})_0 = \frac{k_5 K_{ip} [\text{Cr}(\text{NN})_3^{3+}]_0 [\text{OH}^-]^2}{1 + K_{ip} [\text{OH}^-]} \quad (207)$$

wherefrom the observed rate constant will be given by equation (208).

$$k_{\text{obs}} = \frac{k_5 K_{ip} [\text{OH}^-]^2}{1 + K_{ip} [\text{OH}^-]} \quad (208)$$

Rearrangement of expression (208) yields

$$\frac{[\text{OH}^-]}{k_{\text{obs}}} = \frac{1}{k_5 K_{ip} [\text{OH}^-]} + \frac{1}{k_5} \quad (209)$$

A plot of  $[\text{OH}^-]/k_{\text{obs}}$  versus  $1/[\text{OH}^-]$  is linear for the

$[\text{Cr}(\text{bipy})_3]^{3+}$  system at  $11^\circ\text{C}$  in region (c), where the slope of such a plot is equal to  $1/k_5 K_{ip} = 3.0 \pm 0.1 \times 10^3 \text{ M}^2 \text{ sec}$ , and the intercept is equal to  $1/k_5 = 3.0 \pm 0.6 \times 10^3 \text{ M-sec}$ . Thus,  $k_5 \sim 3.4 \times 10^{-4} \text{ M}^{-1} \text{ sec}^{-1}$  and  $K_{ip} \sim 1 \text{ M}^{-1}$ . Although such a plot for the bipyridyl system appears linear, it must be borne in mind that when one plots reciprocals, the data is compressed and the scatter of the points is minimized. Thus, it is rather difficult to be sure that in fact such a plot is linear.

Expressions (207 - 209) are not physically applicable to the systems under investigation as the expressions assume that initial rates were measured; and in fact, those rates experimentally-determined were instantaneous rates obtained from reactions where up to 35% product formation occurred. Thus, initial rates are not meaningful since this would imply that  $[P] = 0$  or negligibly small. However, expression (200) for the observed rate constant is applicable both at the beginning of the reaction and at any time 't' during the reaction.

If it is assumed that reaction (197) does not achieve rapid equilibrium, a steady-state treatment of the concentration of  $\{[\text{Cr}(\text{NN})_3]^{3+}, \text{OH}^-\}$  yields

$$\text{Rate} = k_5 \{ [\text{Cr}(\text{NN})_3]^{3+}, \text{OH}^- \} [\text{OH}^-] \quad (210)$$

$$\frac{+d \{[\text{Cr}(\text{NN})_3]^{3+}, \text{OH}^- \}}{dt} = k_{ip} [\text{Cr}(\text{NN})_3^{3+}] [\text{OH}^-] -$$

$$k_5 \{[\text{Cr}(\text{NN})_3]^{3+}, \text{OH}^- \} [\text{OH}^-] - k_{-ip} \{[\text{Cr}(\text{NN})_3]^{3+}, \text{OH}^- \} \quad (211)$$

$$\{[\text{Cr}(\text{NN})_3]^{3+}, \text{OH}^- \} = \frac{k_{ip} [\text{Cr}(\text{NN})_3^{3+}] [\text{OH}^-]}{k_{-ip} + k_5 [\text{OH}^-]} \quad (212)$$

$$\text{Rate} = \frac{k_{ip} k_5 [\text{Cr}(\text{NN})_3^{3+}] [\text{OH}^-]^2}{k_{-ip} + k_5 [\text{OH}^-]} \quad (213)$$

and the observed rate constant will then become

$$k_{\text{obs}} = \frac{k_{ip} k_5 [\text{OH}^-]^2}{k_{-ip} + k_5 [\text{OH}^-]} \quad (214)$$

wherein  $k_{ip}$  and  $k_{-ip}$  are the rate constants for the forward and reverse reactions, respectively, in expression (197). Two cases of (214) arise, those being (i) where  $k_5 [\text{OH}^-] \gg k_{-ip}$ , and (ii) where  $k_{-ip} \gg k_5 [\text{OH}^-]$ . In the first case, the observed rate constant will be given by

$$k_{\text{obs}} = k_{ip} [\text{OH}^-] \quad (215)$$

The observed rate constant becomes

$$k_{\text{obs}} = \frac{k_5 k_{\text{ip}}}{k_{-\text{ip}}} [\text{OH}^-]^2 = k_5 K_{\text{ip}} [\text{OH}^-]^2 \quad (216)$$

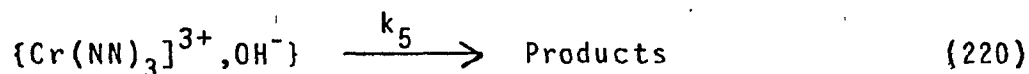
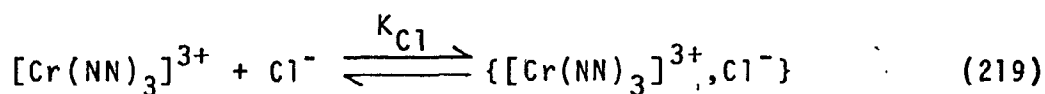
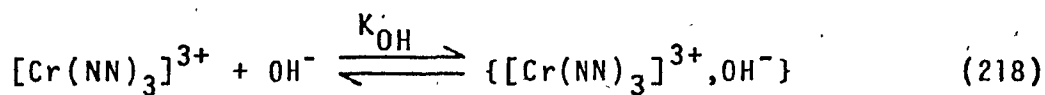
in the case where  $k_{-\text{ip}} \gg k_5 [\text{OH}^-]$ . In the latter case, the observed rate constant agrees with that given in expression (200). Thus, it becomes unnecessary to carry out a material balance. Rearrangement of (214) yields

$$\frac{[\text{OH}^-]}{k_{\text{obs}}} = \frac{k_{-\text{ip}}}{k_{\text{ip}} k_5 [\text{OH}^-]} + \frac{1}{k_{\text{ip}}} \quad (217)$$

For the  $[\text{Cr}(\text{bipy})_3]^{3+}$  system at  $11^\circ\text{C}$  in region (c),  $k_{\text{ip}} = 3.4 \times 10^{-4} \text{ M}^{-1} \text{ sec}^{-1}$  from a plot of  $[\text{OH}^-]/k_{\text{obs}}$  versus  $1/[\text{OH}^-]$ . Also, the slope of such a plot is equal to  $k_{-\text{ip}}/k_{\text{ip}} k_5 = 3.0 \pm 0.6 \times 10^3 \text{ M}^2 \text{ sec}$ . Thus,  $k_{-\text{ip}}$  will be approximately equal to  $k_5$  since  $k_{-\text{ip}}/k_{\text{ip}} k_5 = 1/k_5 K_{\text{ip}}$  from expression (216). The value of  $3.4 \times 10^{-4} \text{ M}^{-2} \text{ sec}^{-1} = k_5 K_{\text{ip}}$  agrees reasonably well with the value of  $1.9 \times 10^{-4} \text{ M}^{-2} \text{ sec}^{-1}$  given as the slope of the linear plot of  $k_{\text{obs}}$  versus  $[\text{OH}^-]^2$  in region (c) for this system.

From the above analysis, then, it appears reasonable to utilize expression (200) for the  $[\text{OH}^-]$  dependence of the observed rate constant in region (c).

Changes in the solution medium, as occurs above pH 13, can also explain the apparent second-order dependence of  $k_{obs}$  on  $[OH^-]$ . It has been brought to our attention by T.W. Swaddle that if major fractions of  $[Cr(NN)_3]^{3+}$  are present as hydroxide ion-pairs in region (c), then it is also possible that ion-pairs involving chloride ion may be important, according to Beck's [66] compilation of  $K_{ip}$ . Indeed, if the formation constant for the chloride ion-pair  $\{[Cr(NN)]^{3+}, Cl^-\}$  were significantly larger than that for the hydroxide analogue, the apparent increase in the reaction order with respect to  $[OH^-]$  above 0.10 M could then be rationalized without invoking attack of  $OH^-$  on  $\{[Cr(NN)_3]^{3+}, OH^-\}$  ion-pair (see reactions (198) and (199)). It can be argued, for instance, that hydrolysis occurs exclusively by reaction within the hydroxide ion-pair throughout the pH range 11 - 14, i.e., regions (b) and (c). Considering the following the reactions,



the rate of the reaction will be  $\text{Rate} = k_5 \{[Cr(NN)_3]^{3+}, OH^-\}$ .

From reactions (218 - 219) and  $[\text{Cr}(\text{NN})_3^{3+}]_0 = [\text{Cr}(\text{NN})_3^{3+}] + [\{\text{Cr}(\text{NN})_3^{3+}, \text{OH}^-\}] + [\{\text{Cr}(\text{NN})_3^{3+}, \text{Cl}^-\}]$ , where  $[\text{Cr}(\text{NN})_3^{3+}]_0$  is the total concentration of  $[\text{Cr}(\text{NN})_3^{3+}]$  complex,

$$[\{\text{Cr}(\text{NN})_3^{3+}, \text{OH}^-\}] = \frac{k_{\text{OH}}[\text{OH}^-] [\text{Cr}(\text{NN})_3^{3+}]_0}{1 + K_{\text{OH}}[\text{OH}^-] + K_{\text{Cl}}[\text{Cl}^-]} \quad (221)$$

whence

$$\text{Rate} = \frac{k_5 k_{\text{OH}}[\text{OH}^-] [\text{Cr}(\text{NN})_3^{3+}]_0}{1 + K_{\text{OH}}[\text{OH}^-] + K_{\text{Cl}}[\text{Cl}^-]} \quad (222)$$

and

$$k_{\text{obs}} = \frac{k_5 k_{\text{OH}}[\text{OH}^-]}{1 + K_{\text{Cl}} + (K_{\text{OH}} - K_{\text{Cl}})[\text{OH}^-]} \quad (223)$$

with  $([\text{OH}^-] + [\text{Cl}^-]) \sim 1.0 \text{ M}$ . Equation (223) indicates that at low  $[\text{OH}^-]$  ( $< 0.1 \text{ M}$ ) and  $[\text{Cl}^-] \sim 1.0 - 0.9 \text{ M}$ , the complex probably exists largely as chloride ion-pairs in near-constant concentration, thus leading to the first-order kinetics in  $[\text{OH}^-]$ . At lower  $[\text{Cl}^-]$ , where  $[\text{OH}^-] > 0.1 \text{ M}$ , the concentration of the chloride ion-pairs falls markedly as  $[\text{OH}^-]$  increases, thereby leading to an apparent order greater than one with respect to  $[\text{OH}^-]$ , inasmuch as  $k_{\text{obs}}$  increases faster than  $[\text{OH}^-]$  in region (c) when  $[\text{OH}^-]$  is comparable to one and  $K_{\text{Cl}} > 1$  and  $\gg K_{\text{OH}}$  in equation (223). It should be noted, however,

that  $k_{\text{obs}}$  is linearly dependent on  $[\text{OH}^-]^2$  in region (c) which a priori would not be expected if this second-order dependence were attributable to solution medium effects. Thus, it is concluded that in region (c) (0.10 - 1.00  $[\text{OH}^-]$ ), the thermal aquation of  $[\text{Cr}(\text{NN})_3]^{3+}$  follows second-order kinetics in  $[\text{OH}^-]$ .

E. Activation Parameters.

1. Energy of Activation,  $E_a$ .

One of the principal reasons that chromium(III) complexes aquate more rapidly than analogous cobalt(III) complexes is the difference in the contribution to the activation energy of the change in crystal field stabilization energy (CFSE) resulting from conversion of the reactant octahedral state to the intermediate activated state. If it is assumed that the observed activation energy  $E_a$  for a substitution reaction of an octahedral complex is predominantly dependent on the energy required to form an intermediate of penta- or hepta-coordination, then it may be plausible to compare the observed  $E_a$  with calculated CFSE values in an effort to predict the geometry of the intermediate.

If the intermediate species is formed via a mechanism which principally involves bond-rupture as a first step, it will most likely be pentacoordinate; while a heptacoordinate intermediate is produced from a mechanism

which principally involves bond formation. A pentacoordinate intermediate will possess either a square pyramidal or trigonal bipyramidal geometry, whereas a pentagonal bipyramidal or trapezoidal octahedral geometry is favoured for a heptacoordinate intermediate [76]. Spees et al. have predicted the more likely intermediate geometries for  $d^3$  and  $d^6$  octahedral reactant complexes, assuming that changes in CFSE and interelectronic repulsion energy are the two principal factors determining the geometry of the intermediate. Table XVI gives calculated and observed activation energies for several chromium(III) aquation reactions. It was concluded [76] that the observed  $E_a$  values are near those calculated for a heptacoordinate intermediate species for chromium(III), inasmuch as those calculated for a pentacoordinate species were so large. Arrhenius plots of  $\log k_{obs}$  versus  $10^3/T$  yield a slope  $-E_a/R$ , from which the activation energies  $E_a$  were obtained for  $[Cr(bipy)_3]^{3+}$  and  $[Cr(phen)_3]^{3+}$  systems. These plots are collected in Figures 46 and 47 for the bipyridyl system, and in Figures 48 - 50 for the phenanthroline system. Tables XVII and XVIII present the activation energies determined from these Arrhenius plots for both systems. The  $E_a$  values obtained therein are in closer agreement with those for a heptacoordinate species, as opposed to a pentacoordinate



Table XVI  
 Calculated and Observed Activation Energies for Several Chromium(III)  
 Aquation Reactions <sup>a</sup>

COMPLEX	ACTIVATION ENERGY (kcal/mol)				Observed
	Dissociative		Associative		
	C <sub>4v</sub>	D <sub>3h</sub>	D <sub>5h</sub>	C <sub>2v</sub>	
[Cr(NH <sub>3</sub> ) <sub>6</sub> ] <sup>3+</sup>	49.1	59.6	27.9	34.3	26.0
[Cr(NH <sub>3</sub> ) <sub>5</sub> Cl] <sup>2+</sup>	47.3	56.8	28.2	33.9	22.4
[Cr(en) <sub>3</sub> ] <sup>3+</sup>	48.1	58.7	26.5	33.0	24.6
cis[Cr(en) <sub>2</sub> (H <sub>2</sub> O) <sub>2</sub> ] <sup>3+</sup>	48.3	58.5	28.0	34.1	23.7
[Cr(H <sub>2</sub> O) <sub>6</sub> ] <sup>3+</sup>	47.3	55.7	30.1	35.2	28.0
[Cr(urea) <sub>6</sub> ] <sup>3+</sup>	45.4	58.9	29.5	34.2	27.0
[Cr(C <sub>2</sub> O <sub>4</sub> ) <sub>3</sub> ] <sup>3-</sup>	45.4	54.0	28.1	33.3	22.1

<sup>a</sup> see reference 76

Figure 46. Arrhenius Plot ( $\log k_{\text{obs}}$  versus  $1/T$ ) for  
 $[\text{Cr}(\text{bipy})_3]^{3+}$  at pH 11.82.

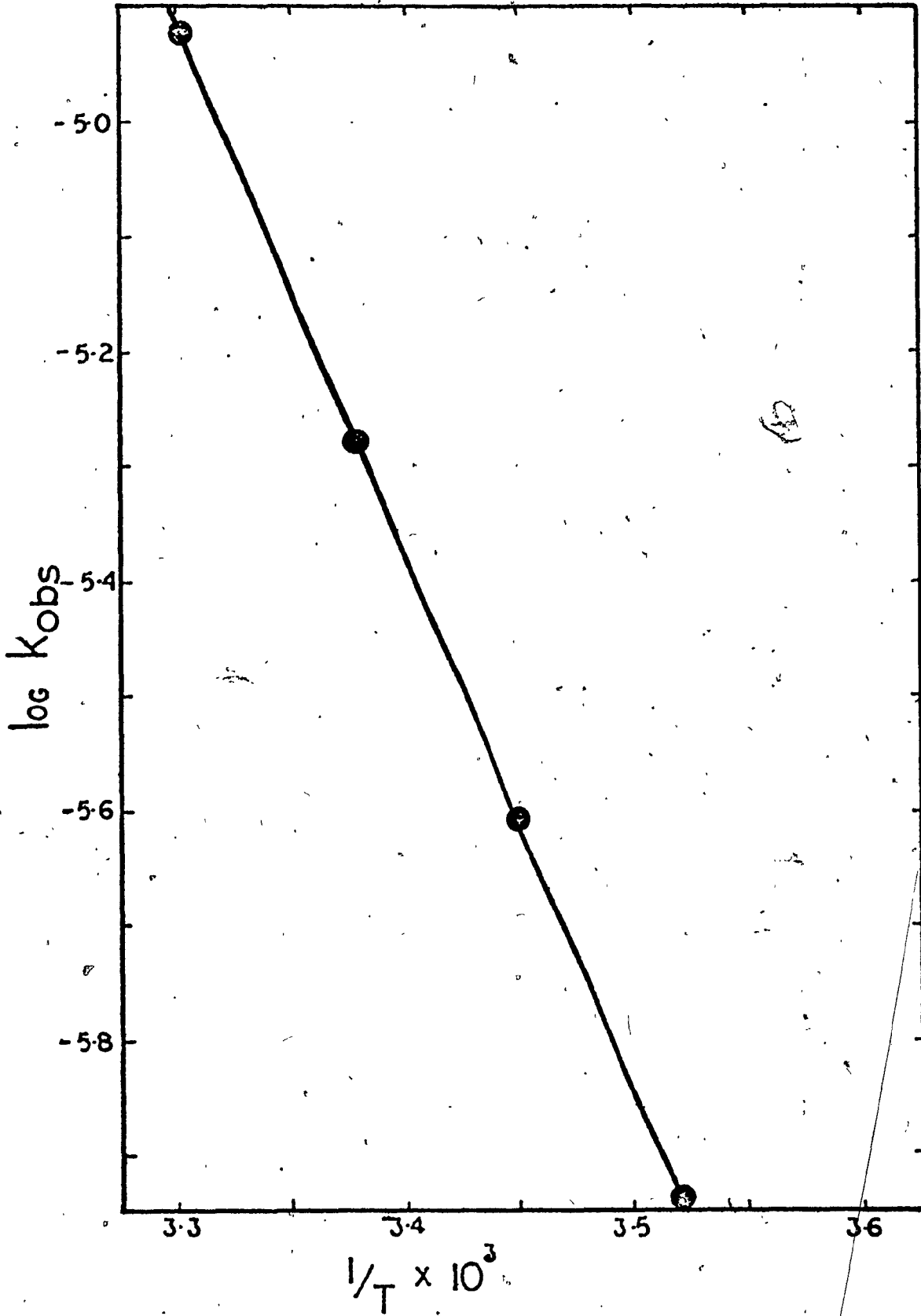


Figure 47. Arrhenius Plot (  $\log k_{\text{obs}}$  versus  $1/T$ ) for  $[\text{Cr}(\text{bipy})_3]^{3+}$  at  $0.50 [\text{OH}^-]$ .

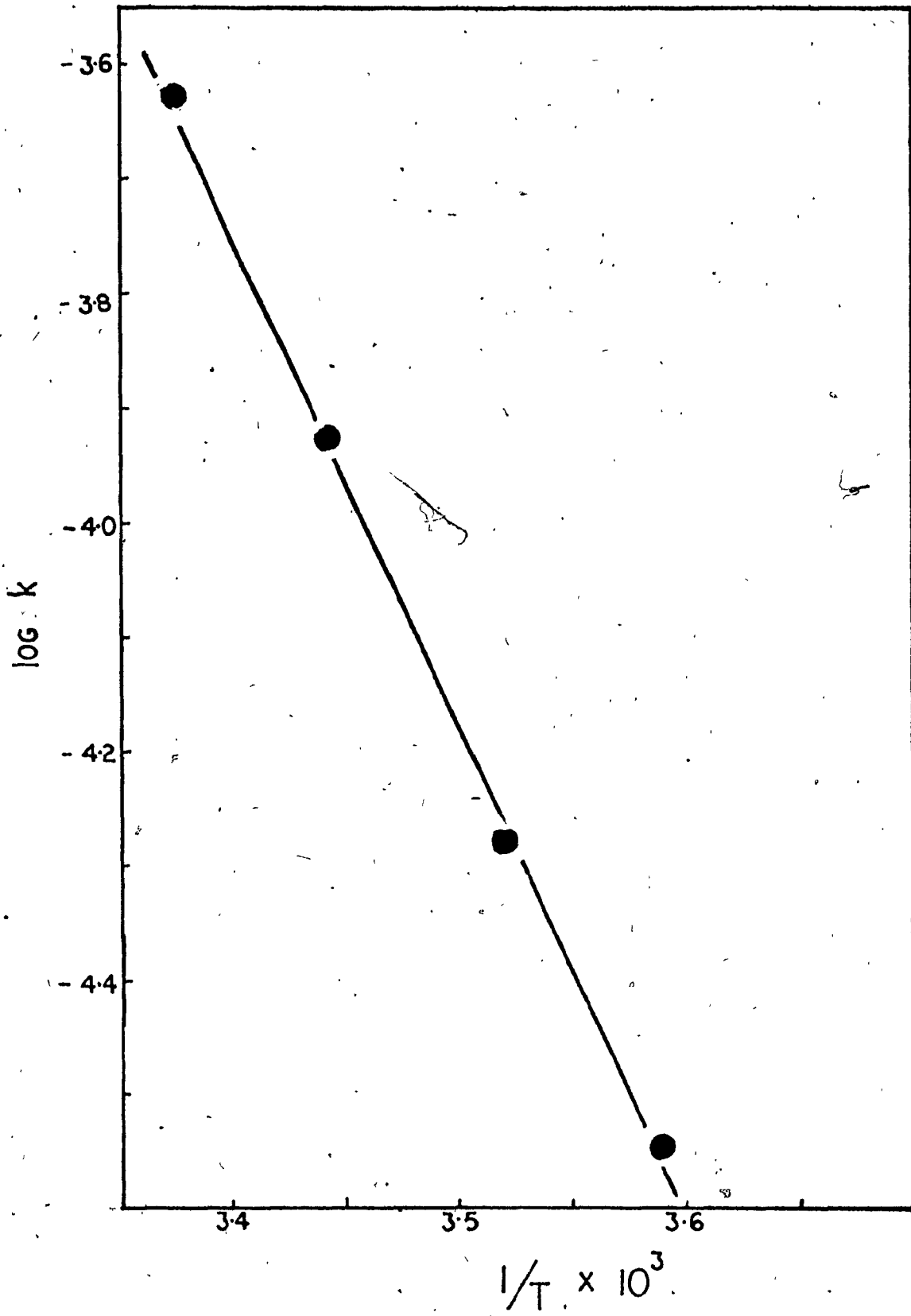


Figure 48. Arrhenius Plot ( $\log k_{\text{obs}}$  versus  $1/T$ )  
for  $[\text{Cr}(\text{phen})_3]^{3+}$  at pH 10.10.

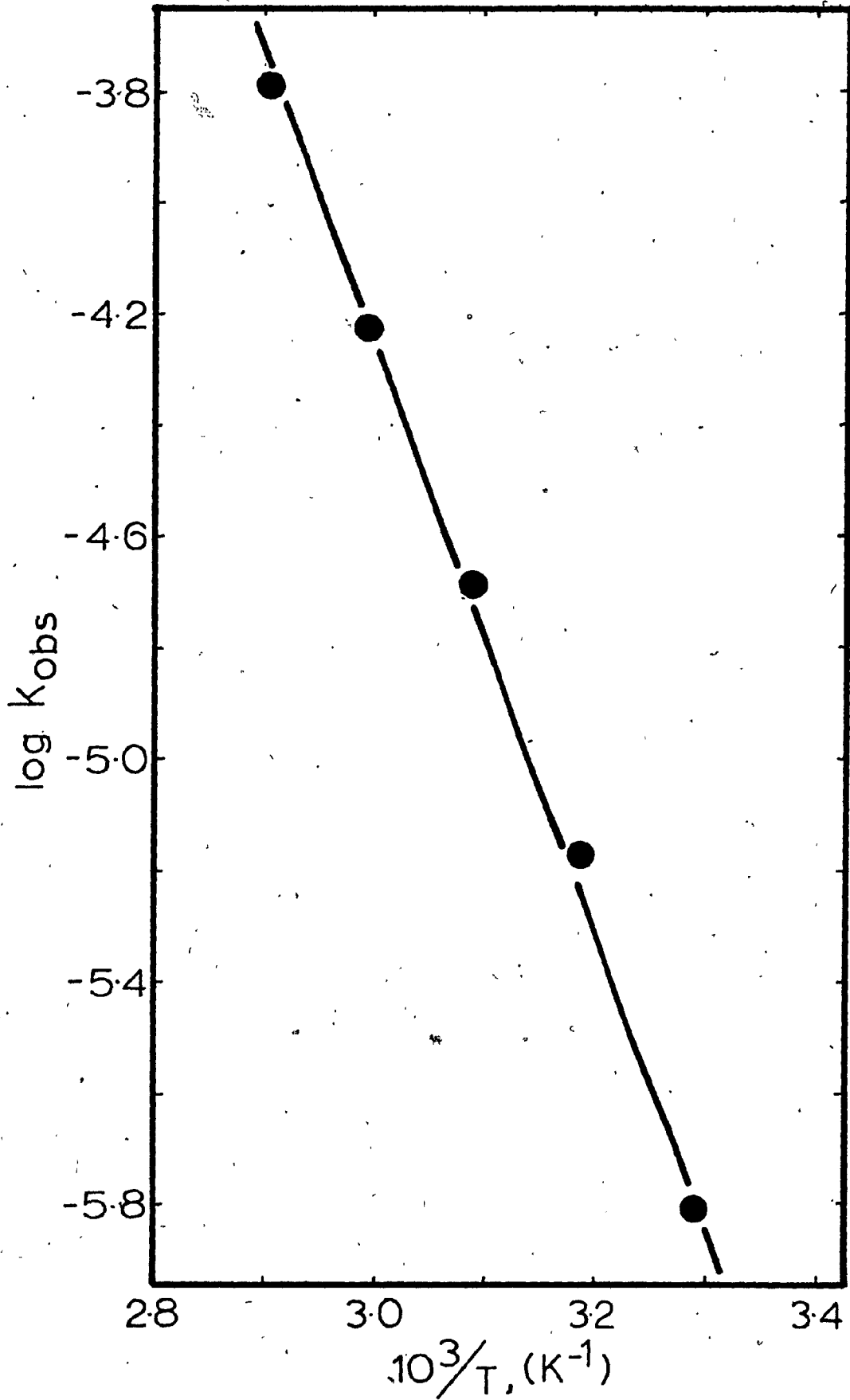


Figure 49. Arrhenius Plot (  $\log k_{\text{obs}}$  versus  $1/T$  ) for  
 $[\text{Cr}(\text{phen})_3]^{3+}$  at pH 12.17.



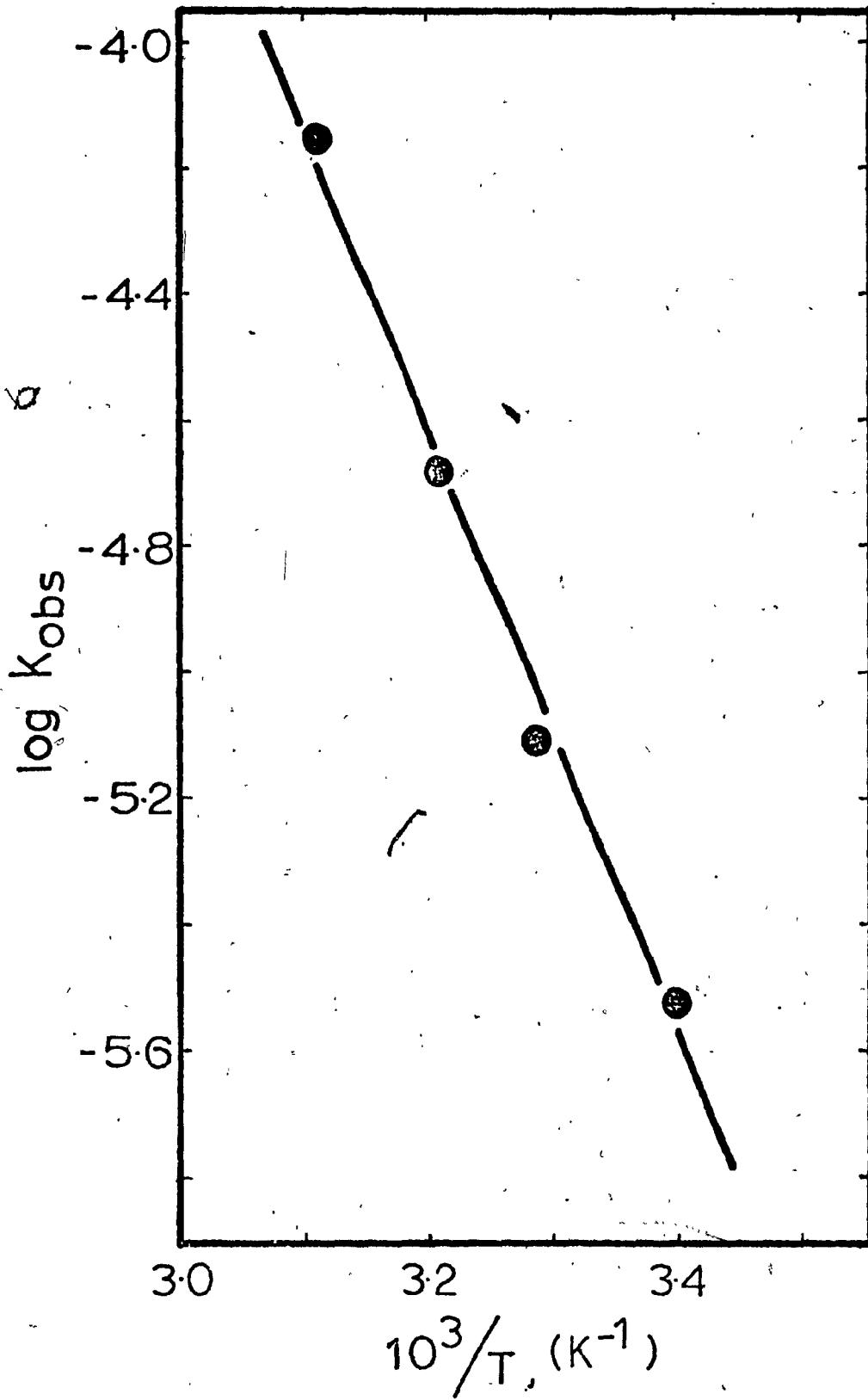


Figure 50. Arrhenius Plot ( $\log k_{\text{obs}}$  versus  $1/T$ ) for  $[\text{Cr}(\text{phen})_3]^{3+}$  at  $0.80 [\text{OH}^-]$ .

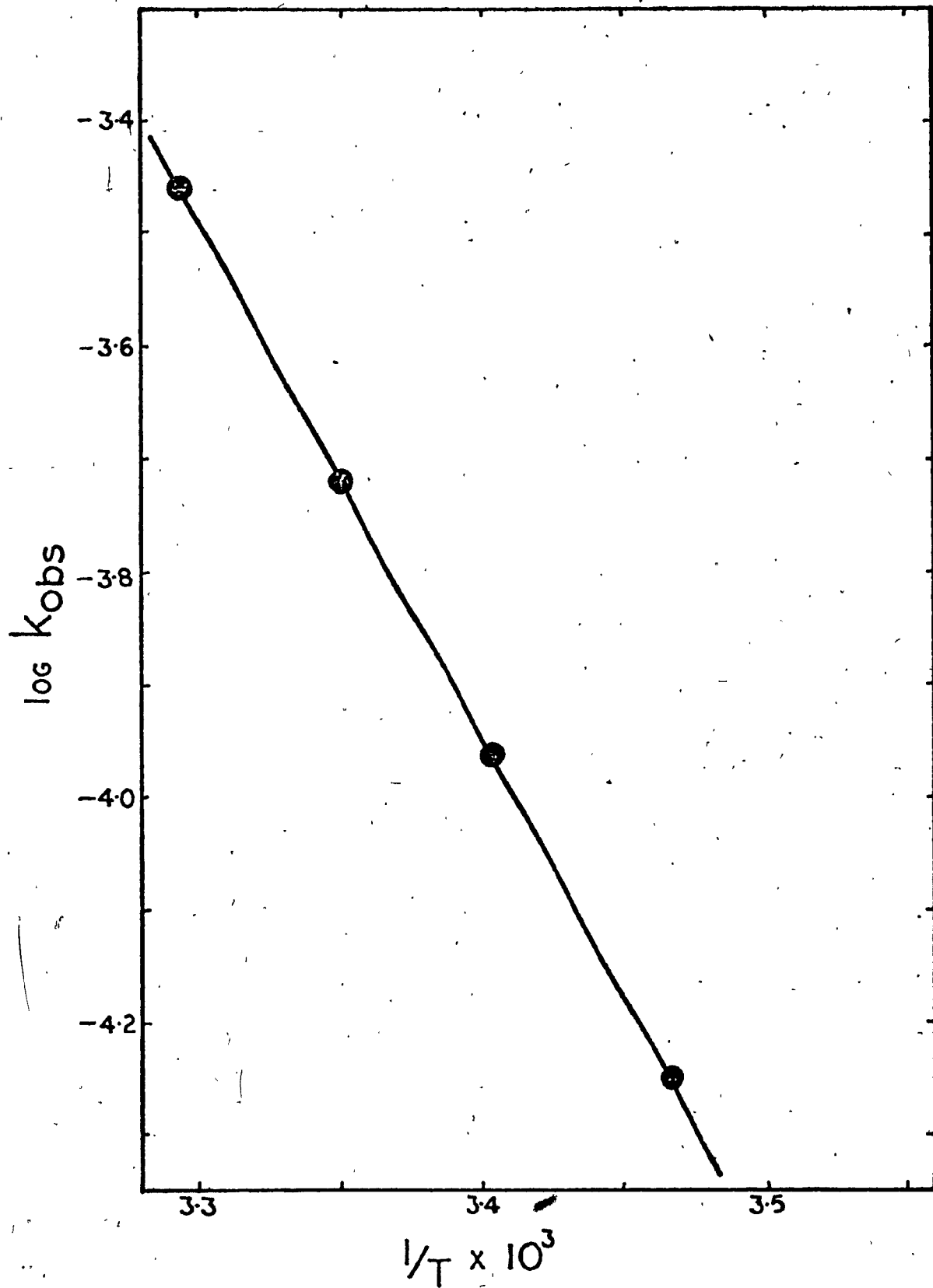


Table XVII  
Arrhenius and Eyring Activation Parameters for the Hydrolysis  
of  $[\text{Cr}(\text{bipy})_3]^{3+}$  <sup>a</sup>

	$\overline{\text{pH}}$	$[\text{OH}^-], \text{M}^c$
	9.8 <sup>b</sup>	0.50
	11.82	
$E_a$ , kcal/mol	$22.0 \pm 0.2$	$19.5 \pm 0.5$
$\Delta H_{298}^\ddagger$ , kcal/mol	$22.3 \pm 0.2$	$18.9 \pm 0.5$
$\ln A$	$26.1 \pm 0.1$	$24.8 \pm 0.9$
$\Delta S_{298}^\ddagger$ , eu	$-8.8 \pm 0.6$	$-11 \pm 2$
$\Delta G_{298}^\ddagger$ , kcal/mol	$24.9 \pm 0.3$	$22.2 \pm 1.1$
$k_{298}$ , sec <sup>-1</sup>	$3.3 \times 10^{-6}$	$2.9 \times 10^{-4}$
	$6.9 \times 10^{-6}$	

<sup>a</sup> Britton-Robinson buffer;  $\mu = 1.0 \text{ M}$  (NaCl); standard errors. <sup>b</sup> Reference (16). <sup>c</sup> NaOH solution;  $\mu = 1.0 \text{ M}$  (NaCl).

Table XVIII  
 Arrhenius and Eyring Activation Parameters for the Hydrolysis  
 of  $[\text{Cr}(\text{phen})_3]^{3+}$  <sup>a</sup>

	pH	$[\text{OH}^-], \text{M}$ <sup>b</sup>
	10.10	0.80
$E_a$ , kcal/mol	$23.9 \pm 0.7$	$21.5 \pm 0.4$
$\Delta H_{298}^\ddagger$ , kcal/mol	$23.3 \pm 0.7$	$20.9 \pm 0.4$
$\ln A$	$26.3 \pm 1.1$	$27.7 \pm 0.6$
$\Delta S_{298}^\ddagger$ , eu	$-8.4 \pm 2.3$	$-5.4 \pm 1.2$
$\Delta G_{298}^\ddagger$ , kcal/mol	$25.8 \pm 0.9$	$22.5 \pm 0.5$
$k_{298}$ , $\text{sec}^{-1}$	$7.9 \times 10^{-7}$	$1.9 \times 10^{-4}$

<sup>a</sup> Britton-Robinson buffer;  $\mu = 1.0 \text{ M}$  (NaCl); standard errors. <sup>b</sup> NaOH solution;  $\mu = 1.0 \text{ M}$  (NaCl).

species. However, it should be borne in mind that the most important factor in determining the activation energy is the bond strength between the central chromium(III) ion and the leaving group, and that crystal field effects play only a small role in that bond strength. Perhaps the only comparison that can be made in terms of CFSE alone is one between complexes which differ only in the central metal ion, as Basolo and Pearson [4] have pointed out.

However, it should be noted that  $E_a$  decreases slightly with increasing  $[\text{OH}^-]$ . This is not an unexpected result inasmuch as the  $\text{OH}^-$  is a better nucleophile than  $\text{H}_2\text{O}$ , and the  $\text{Cr-OH}$  bond is stronger than the  $\text{Cr-OH}_2$  bond in the heptacoordinate intermediate species. From Tables XVII and XVIII it is concluded that both  $[\text{Cr}(\text{bipy})_3]^{3+}$  and  $[\text{Cr}(\text{phen})_3]^{3+}$  react via similar transition states, as in each region the observed  $E_a$  values correspond reasonably well. Furthermore, the pH reaction profile for both complexes is nearly identical.

The above analysis, together with Swaddle's inferences [3] that chromium(III) substitution reactions proceed via associative pathways, Langford's recent findings that photoanation reactions of  $[\text{Cr}(\text{Me}_2\text{SO})_6]^{3+}$  with  $\text{N}_3^-$  and  $\text{NCS}^-$  ions occur via an associative mechanism, and Henry and Hoffman's [96] that the photosolvolysis reaction of  $[\text{Cr}(\text{bipy})_3]^{3+}$  is quenched by  $\text{H}^+$  in

0.2 mole fraction DMF in H<sub>2</sub>O suggesting that, also, the photoreaction occurs by an associative mechanism, lend further credence for the proposed associative mechanism and for the formation of heptacoordinate intermediate species in the hydrolysis of [Cr(NN)<sub>3</sub>]<sup>3+</sup>.

## 2. Entropy and Enthalpy of Activation.

The entropy of activation,  $\Delta S_{298}^{\ddagger}$ , is a measure of the increase in "randomness" in going from the reactant state to the transition state [3]. Some comparative information may be deduced from the  $\Delta S_{298}^{\ddagger}$  values of similar complexes. Tables XVII and XVIII show the  $\Delta S_{298}^{\ddagger}$  values for the [Cr(bipy)<sub>3</sub>]<sup>3+</sup> and [Cr(phen)<sub>3</sub>]<sup>3+</sup> systems, respectively, at various pH (or [OH<sup>-</sup>]) calculated from expression (224) [77], or from plots of  $\ln k_{\text{obs}}/T$  versus  $10^3/T$ .

$$\Delta S_{298}^{\ddagger} = R [ \ln A - \ln RT/Nh ] - R \quad (224)$$

Additional support for an associative-type mechanism is afforded by the near similarity in the values of  $\Delta S_{298}^{\ddagger}$ , and by the negative values of  $\Delta S_{298}^{\ddagger}$ . In the absence of strong solvent effects, dissociative mechanisms are expected to show positive  $\Delta S^{\ddagger}$  values [95]. The slightly more positive values of  $\Delta S_{298}^{\ddagger}$  on the plateau of region (a) probably reflects differences between [Cr(NN)<sub>3</sub>(OH)]<sup>2+</sup> and [Cr(NN)<sub>3</sub>(H<sub>2</sub>O)]<sup>3+</sup>.

The enthalpies of activation,  $\Delta H_{298}^{\ddagger}$ , as determined from equation (225),

$$\Delta H_{298}^{\ddagger} = E_a - RT = RT \ln RT/Nh + T\Delta S^{\ddagger} - RT \ln A + E_a \quad (225)$$

are given in Tables XVII and XVIII along with all the activation parameters calculated from the temperature-dependence studies. The close proximity of the  $\Delta H_{298}^{\ddagger}$  values supports a common mechanism in the plateau of region (a), and regions (b) and (c).

#### F. Conclusions.

The extraordinary similarity in the behaviour of  $[\text{Cr}(\text{bipy})_3]^{3+}$  and  $[\text{Cr}(\text{phen})_3]^{3+}$  in aqueous solution suggests that the two chelates undergo hydrolysis via a common pathway. A comparison of the two complexes shows that: i) neither complex cation undergoes acid hydrolysis. It is primarily because of this observation that a dissociative-type mechanism is rejected. ii) Neither cation is capable of undergoing base hydrolysis via an  $S_N1_{cb}$  mechanism as no ionizable protons are available. iii) Both chelates show similar hydroxide ion dependence, as evidenced by three distinct regions:

(a)  $1/k_{\text{obs}}$  is proportional to  $1/[\text{OH}^-]$ .

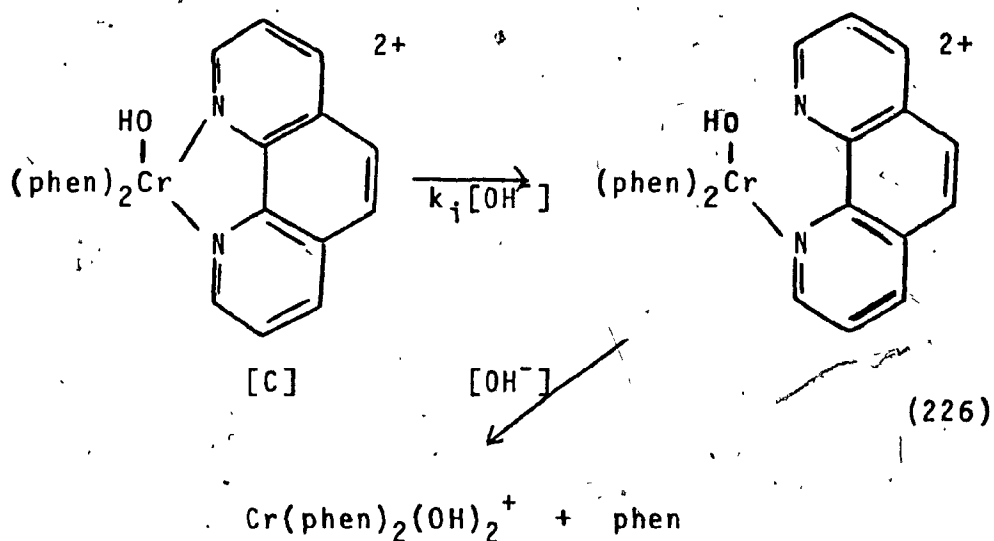
(b)  $k_{\text{obs}}$  is proportional to  $[\text{OH}^-]$

(c)  $k_{\text{obs}}$  is proportional to  $[\text{OH}^-]^2$ .



iv) In each of the above regions, the activation energies, determined from temperature-dependence studies, are very similar, suggesting a common transition state or intermediate species for both cations.

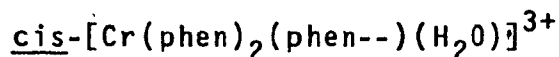
A major objection to the two complexes undergoing hydrolysis via a common mechanism concerns the rigid planar structure of the phenanthroline ligand. The different behaviour of  $[\text{Fe}(\text{bipy})_3]^{2+}$  and  $[\text{Fe}(\text{phen})_3]^{2+}$  in acid was attributed to the inability of the phen ligand to act as a unidentate ligand because of its inherent rigidity. However, a recent report [64] suggests that the phen ligand can act as a unidentate ligand. Also, optical isomers of 4,5,8-trisubstituted phenanthrenes have been observed [78]. Phenanthrene has a structure similar to that of 1,10-phenanthroline. The optical isomers observed [78] for 4,5,8-trimethyl-1-phenanthryl-acetic acid were attributed to the methyl groups on the 4- and 5-positions being bent out of the plane of the aromatic ring. Since it is possible for such a compound to exhibit a certain degree of nonplanarity it is not inconceivable that the 1,10-phenanthroline ligand can as well be nonplanar. If indeed the phenanthroline ligand can assume non-planarity, then the strained heptacoordinate hydroxyl-intermediate can undergo bond-rupture of the Cr-N bond to yield the products:



As a result, the 1,10-phenanthroline ligand can act as a unidentate ligand, though previously believed [62,63] unlikely for  $[\text{Fe}(\text{NN})_3]^{2+}$  chelates. The existence of complexes containing unidentate bipyridine ligands has recently been demonstrated in complexes of iridium(III) and ruthenium(II) [79]. Since the two chromium(III) chelates possess similar behaviour, not observed in the case of the iron(II) analogues, the assumption is further justified.

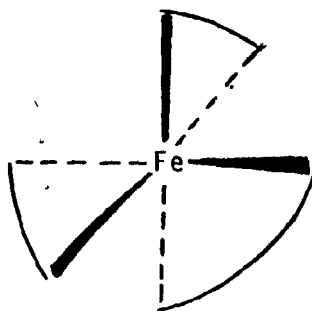
The photoracemization of  $(+)\text{-}[\text{Cr}(\text{phen})_3]^{3+}$  has been investigated by Kane-Maguire and Langford [80]. In acid media ( $\text{pH} < 7$ ), the final product observed was  $(\pm)\text{-}[\text{Cr}(\text{phen})_2(\text{H}_2\text{O})_2]^{3+}$ . An intramolecular racemization was envisaged inasmuch as the presence of iron(II) yielded no free 1,10-phenanthroline after 2.5 lifetimes of racemization. The negative ferroin colour test [80]

suggested that an intermolecular pathway was not likely. However, intramolecular racemization involving dissociation of one end of the phen ligand was also thought improbable owing to the rigid structure of the ligand. The result of such a pathway would be ring closure and retention of configuration. The observed decrease in phosphorescence intensity after 25 lifetimes could neither be attributed to photoaquation nor to a twist pathway, and thus partial racemization was thought to occur via the intermediacy of the ring-opened species



The two most plausible pathways for the base hydrolysis of  $[\text{Cr}(\text{bipy})_3]^{3+}$  and  $[\text{Cr}(\text{phen})_3]^{3+}$  are Gillard's general mechanism and an associative mechanism (see Sections III-D-3,4,5). The presently available data do not afford an unequivocal delineation between these two pathways. It would appear that one of the deciding factors as to whether or not Gillard's mechanism is applicable concerns the "approachability" of the incoming nucleophile. The feasibility of attack on the carbon atom adjacent to the nitrogen atom of the N-heterocyclic ligand will depend on the distance of closest approach between the nucleophile and the reactant chelate. Although the x-ray crystal structures of the two chromium

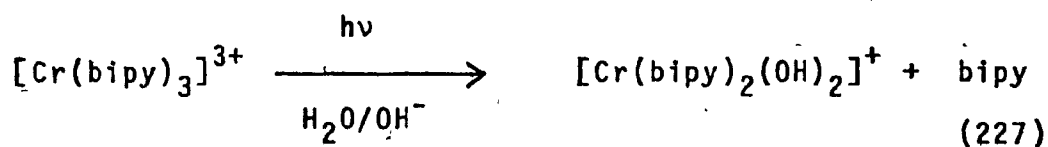
(III) chelates are not available, some inference may be taken from those complexes for which the crystal structures are known. That of  $[1\text{-Fe(phen)}_3][(\text{d-C}_4\text{H}_2\text{O}_6)_2\text{Sb}^{2+}]$  has been reported [81], in which the  $[\text{Fe(phen)}_3]^{2+}$  cation consists of an iron(II) atom complexed by three planar phenanthroline ligands forming a "three-bladed propellor".



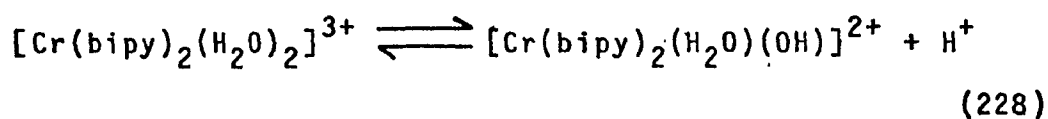
As such, there are three V-shaped "pockets" situated between the ligands, each of which is large enough to accommodate two small molecules such as water or hydroxide ion. The maximum distance between the centre of the complex and the edge of the ligands was reported [82] to be ca. 7 Å. Similar structures have been determined for  $[\text{Cu(phen)}_3]^{2+}$  [84] and  $[\text{Cu(bipy)}_3]^{2+}$  [81], wherein the distorted octahedron results from Jahn-Teller distortion. This type of distortion is not expected for low-spin iron(II) complexes. With regard to the structure of  $[\text{Cu(phen)}_3]^{2+}$ , small molecules in the three "pockets" are thought [81] to be capable of approaching to within

at least 3 Å of the central copper(II) ion. A similar distance is envisaged for the  $[\text{Fe}(\text{phen})_3](\text{ClO}_4)_2$  complex [82]. Proton nuclear magnetic resonance studies of tris-chelates of chromium(II) [83] suggest that water molecules can enter into these "pockets" to within 5 Å of the central chromium(II) ion in  $[\text{Cr}(4,7\text{-Me}_2\text{phen})_3]^{2+}$ . In view of these findings, it is reasonable to assume that water molecules and/or hydroxide ions are capable of entering these "pockets" in both  $[\text{Cr}(\text{bipy})_3]^{3+}$  and  $[\text{Cr}(\text{phen})_3]^{3+}$ . The more rigid structure of the phenanthroline complex may allow more facile approach of these nucleophiles, thus accounting for the slight rate enhancement of this complex ion over that of the analogous bipyridyl complex.

Additional support for an associative mechanism involving direct nucleophilic attack on the metal centre comes from results of a photochemical investigation of the  $[\text{Cr}(\text{bipy})_3]^{3+}$  ion [18] in aqueous solution. Continuous photolysis at 313, 365, 405, and 464 nm of solutions of  $[\text{Cr}(\text{bipy})_3]^{3+}$  in the pH range 7.3 - 10.7 (ionic strength = 1.0 M) yielded spectral changes and the formation of free 2,2'-bipyridine. Isosbestic points at 255, 263, 274, and 307 nm were recorded subsequent to irradiation; the location of these points is in good agreement with those cited for the thermal reaction. The overall photochemical reaction, then, is (pH > 7)



As in the thermal reaction, irradiation in somewhat acidic solution (pH 6.03 - 6.71) produced changes in the absorption spectrum different from those observed in basic media. These were ascribed to the same acid-base equilibrium as in the thermal reaction, that is,



The excited state thought [18] responsible for the observed photoreaction is the doublet ( $^2E$ ) state. The pH-dependence of the quantum yield of the photoreaction was found to be the same as the pH dependence of  $k_{\text{obs}}$  in region (a) of the thermal reaction [16]. This observation suggests that common, pH-dependent intermediates occur in both the thermal and photoreactions. Maestri et al. [18] have proposed two mechanisms to account for the photochemical behaviour of  $[\text{Cr}(\text{bipy})_3]^{3+}$ , one involving direct nucleophilic attack on the chromium-(III) centre to produce a heptacoordinate intermediate species, the other involving nucleophilic attack on the  $C_6$  (or  $C_6'$ ) carbon atom of the bipy ligand to form a covalent hydrate. The two pathways are presented in Figures 51 and 52, respectively. Of the two paths, direct attack on the metal centre is favoured [18] over

Figure 51

Associative Interchange Pathway for the Photochemical Reaction Between  $[\text{Cr}(\text{bipy})_3]^{3+}$  and Hydroxide Ion

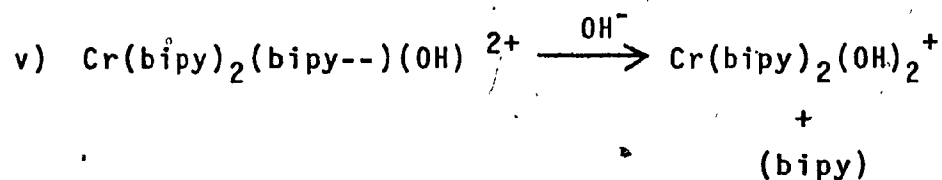
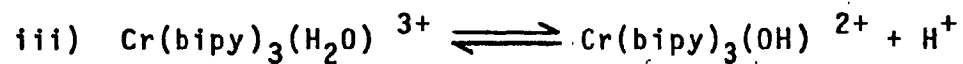
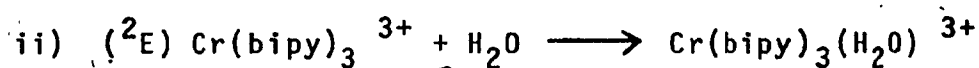
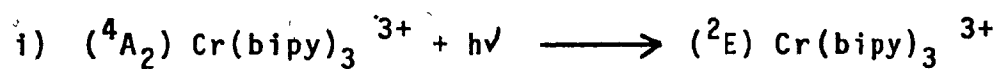
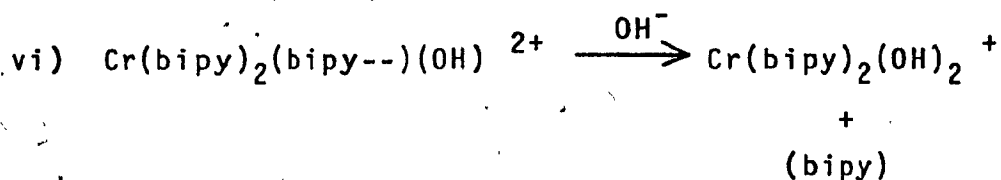
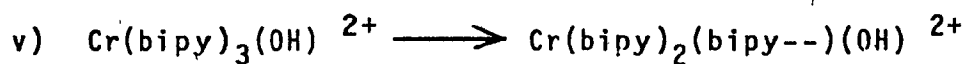
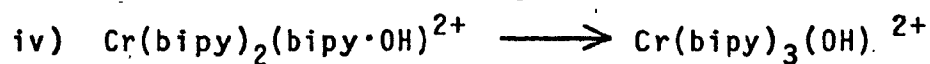
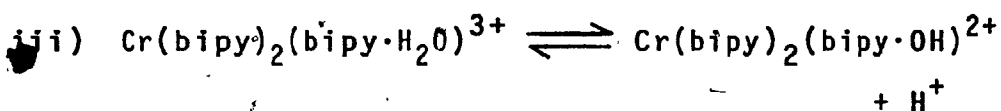
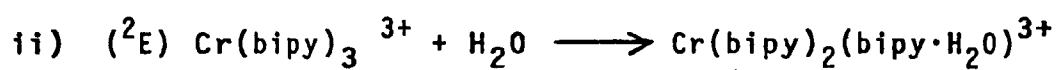
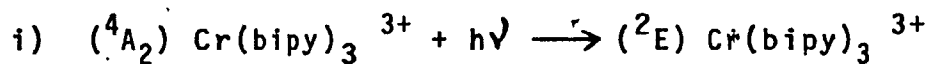


Figure 52

Gillard's Pathway for the Photochemical Reaction  
Between  $[\text{Cr}(\text{bipy})_3]^{3+}$  and Hydroxide Ion

---





covalent hydrate formation, based on characteristics of the doublet excited state. There is support for direct participation of the  $^2E$  state in the photosolvation of trans- $[\text{Cr}(\text{en})_2(\text{NCS})_2]^+$  [85]. Gillard's mechanism is not applicable to this particular system. Direct nucleophilic attack on the metal would be favoured by a metal-centred excited state, whereas a ligand-to-metal charge-transfer excited state would favour reaction via covalent hydrate formation. However, such a charge-transfer state is much too high in energy to efficiently participate in the reaction of the  $[\text{Cr}(\text{bipy})_3]^{3+}$  cation. The  $^2E$  state is essentially a metal-centred state, and has been described [18] as the excited state responsible for the observed photoreaction. Therefore, an associative-type mechanism is favoured for the reaction between hydroxide ion and  $[\text{Cr}(\text{bipy})_3]^{3+}$  from pH 0 - 10.7. A similar mechanism is consistent with experimental results in region (b), though no photochemical results are available. The similarity between the  $[\text{Cr}(\text{bipy})_3]^{3+}$  and  $[\text{Cr}(\text{phen})_3]^{3+}$  cations over the entire pH range investigated suggests that the associative mechanism is the most plausible one for both cations. However, at high hydroxide ion concentrations, there certainly must be formation of outer-sphere complexes between  $[\text{Cr}(\text{NN})_3]^{3+}$  and  $\text{OH}^-$ .

It is concluded that a covalent hydrate mechanism may be inconsequential in the thermal hydrolysis of the

two chromium(III) cations for the following reasons:

- i) The rate constant analogous to  $k_1$  in Figure 39 has been identified by Nord and Wernberg [72] as the rate-determining step in the  $\text{OH}^-$  reduction of  $[\text{Fe}(\text{bipy})_3]^{3+}$  and  $[\text{Os}(\text{bipy})_3]^{3+}$  with  $k_1 = 8 \text{ M}^{-1} \text{ sec}^{-1}$  and  $2 \text{ M}^{-1} \text{ sec}^{-1}$ , respectively. The rate constant for the first-order dependence of  $k_{\text{obs}}$  on  $[\text{OH}^-]$  (i.e., region (b)) in the hydrolysis of  $[\text{Cr}(\text{bipy})_3]^{3+}$  is  $\sim 10^{-3} \text{ M}^{-1} \text{ sec}^{-1}$ . Inasmuch as  $[\text{Cr}(\text{bipy})_3]^{3+}$  is quite similar to  $[\text{Fe}(\text{bipy})_3]^{3+}$  in terms of charge and size, it is difficult to explain why the rate constants differ by as much as four orders of magnitude if the same covalent hydrate is formed in the initial step of the reduction of  $[\text{Fe}(\text{bipy})_3]^{3+}$  and of the hydrolysis of  $[\text{Cr}(\text{NN})_3]^{3+}$ .
- ii) No spectral variations in solutions of  $[\text{Cr}(\text{bipy})_3]^{3+}$  were observed, even in very alkaline solutions, as would have been expected if the covalent hydrate  $[\text{Cr}(\text{bipy})_2(\text{bipy-OH})]^{2+}$  were the intermediate in the hydrolysis reaction. Also, as originally proposed by Gillard [13], covalent hydrates are rapidly formed in aqueous solution.
- iii) It is noteworthy that the nearly identical values of the activation parameters in Tables XVII and XVIII across the pH range 6 - 14 for each system preclude a sudden shift in mechanism throughout regions (a - c); and, insofar as the covalent hydrate mechanism does not

appear plausible for the hydrolysis at  $\text{pH} > 11$ , this pathway is also not considered likely at  $\text{pH} < 11$ . Thus, the reaction scheme depicted in Figure 45 is believed the operative pathway for the thermal hydrolysis of tris-2,2'-bipyridyl- and tris-1,10-phenanthroline-chromium(III).

#### G. Investigation of Rhodium(III) Cations.

##### 1. General Behaviour of Rhodium(III) Cationic Complexes.

Rhodium(III) ammine complexes might be expected to undergo substitution reactions similar to those of cobalt(III), as both ions have a  $d^6$  electron configuration. Table XIX presents some rates of acid hydrolysis of rhodium(III) ammine complexes, for which the observed rate constant is for the first-order approach to equilibrium and represents the sum of rate constants for the forward (aquation) and reverse (anation) reactions. In general, the rhodium(III) complex ions aquate more slowly than analogous cobalt(III) complex ions [17].

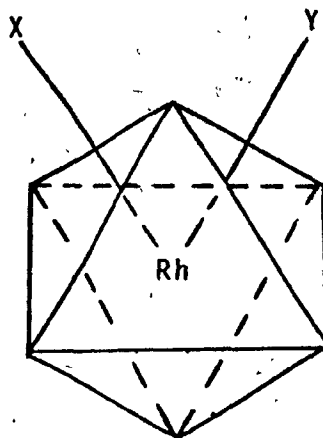
Basolo and coworkers [17] have proposed a general mechanism for the hydrolysis of rhodium(III) complexes involving a heptacoordinate transition state in which five inert ligands remain at just about their original positions in a square pyramidal geometry. The other two ligands, the leaving and entering groups, are

Table XIX  
 Rates of Acid Hydrolysis of Some Rhodium (III)  
 Complexes in 0.1 M Nitric Acid <sup>a</sup>

Complex	T (°C)	$k_{\text{obs}} \times 10^{+5}$ (sec <sup>-1</sup> )
$[\text{Rh}(\text{NH}_3)_5\text{Cl}]^{2+}$	80	6.2
<u>trans</u> - $[\text{Rh}(\text{NH}_3)_4\text{Cl}_2]^+$	80	12.1
<u>trans</u> - $[\text{Rh}(\text{en})_2\text{Cl}_2]^+$	80	10.4
<u>cis</u> - $[\text{Rh}(\text{en})_2\text{Cl}_2]^+$	80	85
<u>trans</u> - $[\text{Rh}(\text{bipy})_2\text{Cl}_2]^+$	80	---

<sup>a</sup> see reference 17.

located above the base of the square pyramid, as shown below.



An associative-type mechanism is favoured [17] for such complexes owing to the slower rates and insensitivity to complex charge exhibited by these complex ions, relative to those of cobalt(III). Although Langford and Gray [1] support a dissociative (D) or dissociative interchange ( $I_d$ ) pathway for rhodium(III) complexes, an associative interchange ( $I_a$ ) pathway is probably more likely. That is, a mechanism in which bond-formation is more important than bond-rupture. Alkyl substituents on ethylenediamine (AA) ligands in complexes of the type  $\text{trans-[M(AA)}_2\text{Cl}_2]^+$  augment the rate of reaction for both cobalt(III) and rhodium(III), although the effect is less for the latter. This observation [17] is consistent with a dissociative mechanism. However, the effect of complex charge on the aquation rate is different for cobalt(III) and rhodium(III) complexes.

$[\text{Co}(\text{NH}_3)_5\text{Cl}]^{2+}$  aquates approximately  $10^3$  times slower

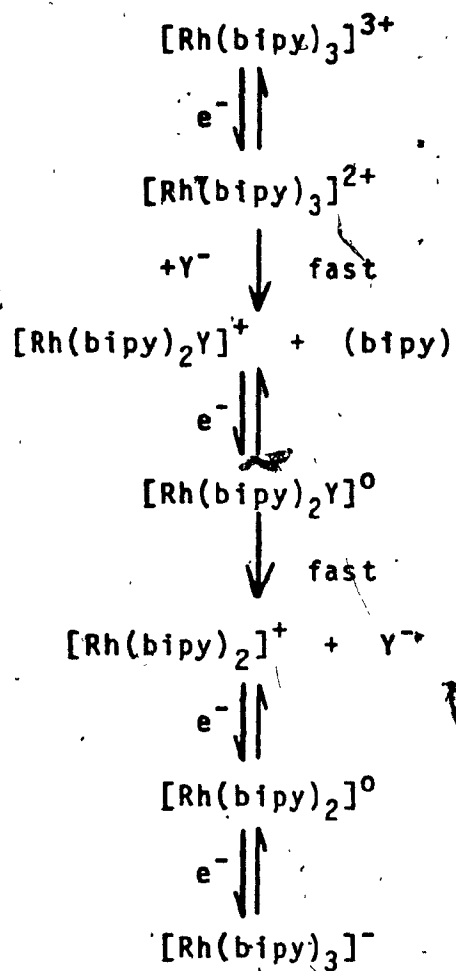
than does trans- $[\text{Co}(\text{NH}_3)_4\text{Cl}_2]^+$  [86], which is consistent with a dissociative-type mechanism wherein the larger cationic charge makes the Co-Cl bond-rupture more difficult. In contrast,  $[\text{Rh}(\text{NH}_3)_5\text{Cl}]^{2+}$  and trans- $[\text{Rh}(\text{NH}_3)_4\text{Cl}_2]^+$  aquate at very nearly the same rates [17], attributed to opposing effects of charge neutralization and charge separation. Thus, an associative-type pathway is favoured for rhodium(III) cations, as is observed for platinum(II) cations for which an associative mechanism is indeed operative [87].

The trans- $[\text{Rh}(\text{bipy})_2\text{Cl}_2]^+$  cation was observed [17] to be quite resistant to hydrolysis at 80°C in 0.1 M nitric acid and at pH 12.7. In comparison, trans- $[\text{Co}(\text{bipy})_2\text{Cl}_2]^+$  undergoes rapid hydrolysis [88]. This latter observation is attributed [17] to the greater steric strain in the bipy ring of the smaller cobalt(III) complex ion. The strain will be less for the larger rhodium(III) complex, and thereby may be responsible for its inert character.

DeArmond et al. [89] have investigated the electrochemistry of  $[\text{Rh}(\text{bipy})_3]^{3+}$  in acetonitrile, and proposed the reaction sequence shown in Figure 53. The sequence suggests that the liberation of 2,2'-bipyridine occurs in or after the first electron transfer.

Figure 53  
Electrochemical Reaction Sequence Proposed for  $[\text{Rh}(\text{bipy})_3]^{3+}$  in Acetonitrile

---



2. Behaviour of  $[\text{Rh}(\text{bipy})_3]^{3+}$ .

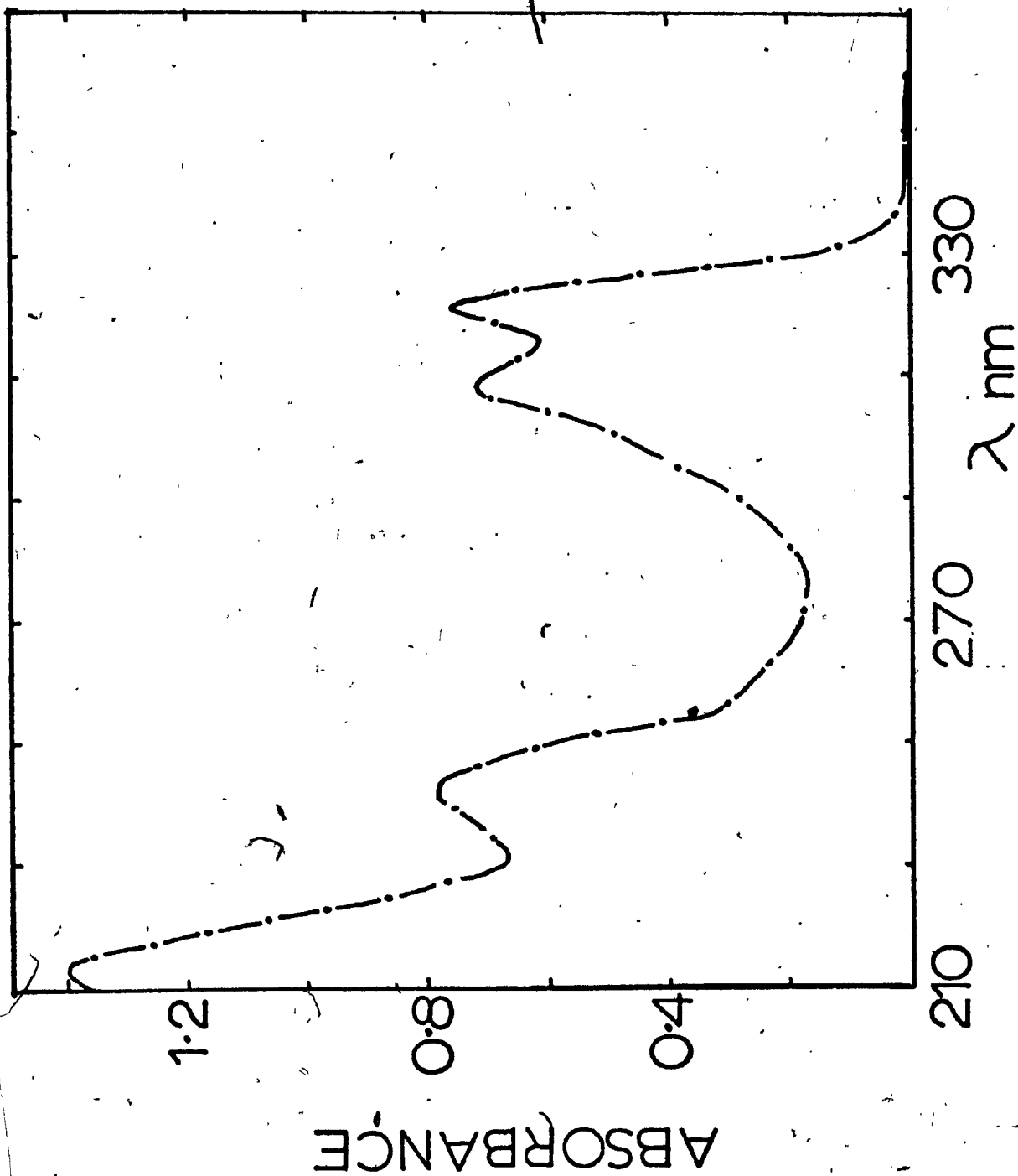
The behaviour of the  $[\text{Rh}(\text{bipy})_3]^{3+}$  cation was investigated in aqueous acid and base media in an effort to determine its reactivity towards hydrolysis. The absorption spectrum is presented in Figure 54, with relevant spectral data in Appendix K. With regard to the solubility of this complex ion, it was found to be very soluble in distilled water, 6 M hydrochloric acid, 11 M perchloric acid, and 2 M sodium hydroxide. However, in 0.5 M sodium hydroxide and 1 M perchloric acid, the rhodium(III) cation is not very soluble.

The reaction between  $[\text{Rh}(\text{bipy})_3]^{3+}$  and hydroxide ion (in 0.5 M and 2 M  $\text{OH}^-$ ) was followed spectrophotometrically at ca. 25°C. Over a period of six hours, no significant spectral changes were observed; that is, no shifts in absorption maxima nor any isosbestic points were discernable. After six hours no free bipyridine was detected by extraction with hexanes. In acidic media (1 M perchloric acid at ca. 22°C for 20 hours, and 6 M hydrochloric acid at ca. 60°C for 12 hours) neither isosbestic points nor shifts in absorption maxima were observed. The hexanes extract showed no absorption due to free 2,2'-bipyridine. From the latter observation, it is concluded that even in acidic media, neither free protonated bipyridine nor unprotonated bipyridine is present, as no absorption was observed in the



Figure 54. Absorption Spectrum of  $[\text{Rh}(\text{bipy})_3\text{Cl}_3 \cdot 4.5\text{H}_2\text{O}]$   
in Methanol:

$$c = 1.899 \times 10^{-5} \text{ M.}$$



2d

range 210 - 360 nm. However, it may be that the released bipyridine, if there is any, remains in the bulk solvent such that it cannot be extracted with hexanes.

From these experiments, it is concluded that  $[\text{Rh}(\text{bipy})_3]^{3+}$  is relatively inert to hydrolysis, both in acidic and basic media. Similar observations have been made for  $[\text{Co}(\text{phen})_3]^{3+}$  and  $[\text{Co}(\text{bipy})_3]^{3+}$  [90] in acid solution. The inert behaviour of these low-spin, diamagnetic rhodium- and cobalt(III) cations may be explained in terms of their crystal field stabilization energies (CFSE). Firstly, a tripositive metal ion possesses a larger CFSE than a dipositive ion because the metal ion will draw the ligands in more closely. The bipyridine and phenanthroline ligands are high in the spectrochemical series and contribute to an increase in the CFSE via back  $\pi$ -bonding from the metal to the ligand. In addition, a rhodium(III) complex cation will likely be more inert than an analogous cobalt(III) cation because the CFSE greatly increases as one transcends a given group of transition metal ions.

#### H. Preparation of Substituted Polypyridyl Chromium(III) Complexes.

When a transition metal complex absorbs a photon of light, and undergoes an electronic transition, an excited state of the complex results. This excited state differs

from the ground state in two ways: its energy is higher than that of the ground state, and its electron distribution may vary from that of the ground state. The higher energy of this excited state offers higher reactivity relative to that of the ground state, though the lifetime of the former may be too short for a chemical reaction to occur. Photoexcitation results in excited states possessing sufficiently high energy so as to be capable of undergoing radiative and non-radiative processes inaccessible to thermally-excited states.

Substituted-bipyridyl and -phenanthroline complexes of ruthenium(II) have been investigated in an effort to elucidate the quenching mechanism of the luminescent state of  $[\text{Ru}(\text{NN})_3]^{2+}$  complexes. The quenchers studied include iron(II), chromium(III) and europium(III), as investigated by Lin et al. [91]. The complexes chosen were those where (NN) was 4,4'-dimethylphenanthroline, bipyridine, 3,4,7,8-tetramethylphenanthroline, 3,5,6,8-tetramethylphenanthroline, phenanthroline, 4,7-dimethylphenanthroline, 5-methylphenanthroline, 5-chlorophenanthroline, 5-phenylphenanthroline, and 5-bromophenanthroline. The experimental results [91] indicate that neither the absorption nor emission spectra of the ruthenium(II) chelates alter significantly upon substitution of the bipyridine or phenanthroline ligands. However, the lifetimes of the emitting states and the reduction

potentials of the complexes are quite sensitive to variation in substituent: Phenyl substitution at the 4,7-positions of phenanthroline results in an increased emission lifetime, whereas 4,7-methyl substitution has no significant effect on the lifetimes. Methyl substitution at the 4,4'-positions of bipyridine reduces the emission lifetime relative to that of unsubstituted bipyridine. Phenyl substitution on both phenanthroline and bipyridine exhibits an increase in the emission lifetime over that of the respective unsubstituted ligand.

The photochemical and photophysical behaviour of chromium(III) chelates has recently received much attention because their lowest photoexcited states have relatively long lifetimes and show high reactivity toward redox quenchers. Therefore, four substituted polypyridyls of chromium(III) have been prepared such that future photochemical investigations may be undertaken.

These four cations include:

- 1)  $[\text{Cr}(5\text{-Clphen})_3](\text{ClO}_4)_3 \cdot 2\text{H}_2\text{O}$
- 2)  $[\text{Cr}(4,7\text{-Me}_2\text{phen})_3](\text{ClO}_4)_3 \cdot 2\text{H}_2\text{O}$
- 3)  $[\text{Cr}(4,7\text{-Ph}_2\text{phen})_3](\text{ClO}_4)_3 \cdot 4\text{H}_2\text{O}$
- 4)  $[\text{Cr}(4,4'\text{-Ph}_2\text{bipy})_3](\text{ClO}_4)_3 \cdot 2\text{H}_2\text{O}$

The syntheses are presented in Section II-F-4,5,6,7, and their absorption spectra with relevant data in Figures 55 - 58 and Appendix L for the complexes 1) - 4), respectively.

Figure 55. Absorption Spectrum of  $[\text{Cr}(5\text{-Clphen})_3]\text{-}(\text{ClO}_4)_3 \cdot 2\text{H}_2\text{O}$  in 0.01 M Hydrochloric Acid:

(a)  $6.871 \times 10^{-4}$  M;

(b)  $1.374 \times 10^{-4}$  M;

(c)  $1.649 \times 10^{-5}$  M.

*Handwritten mark*

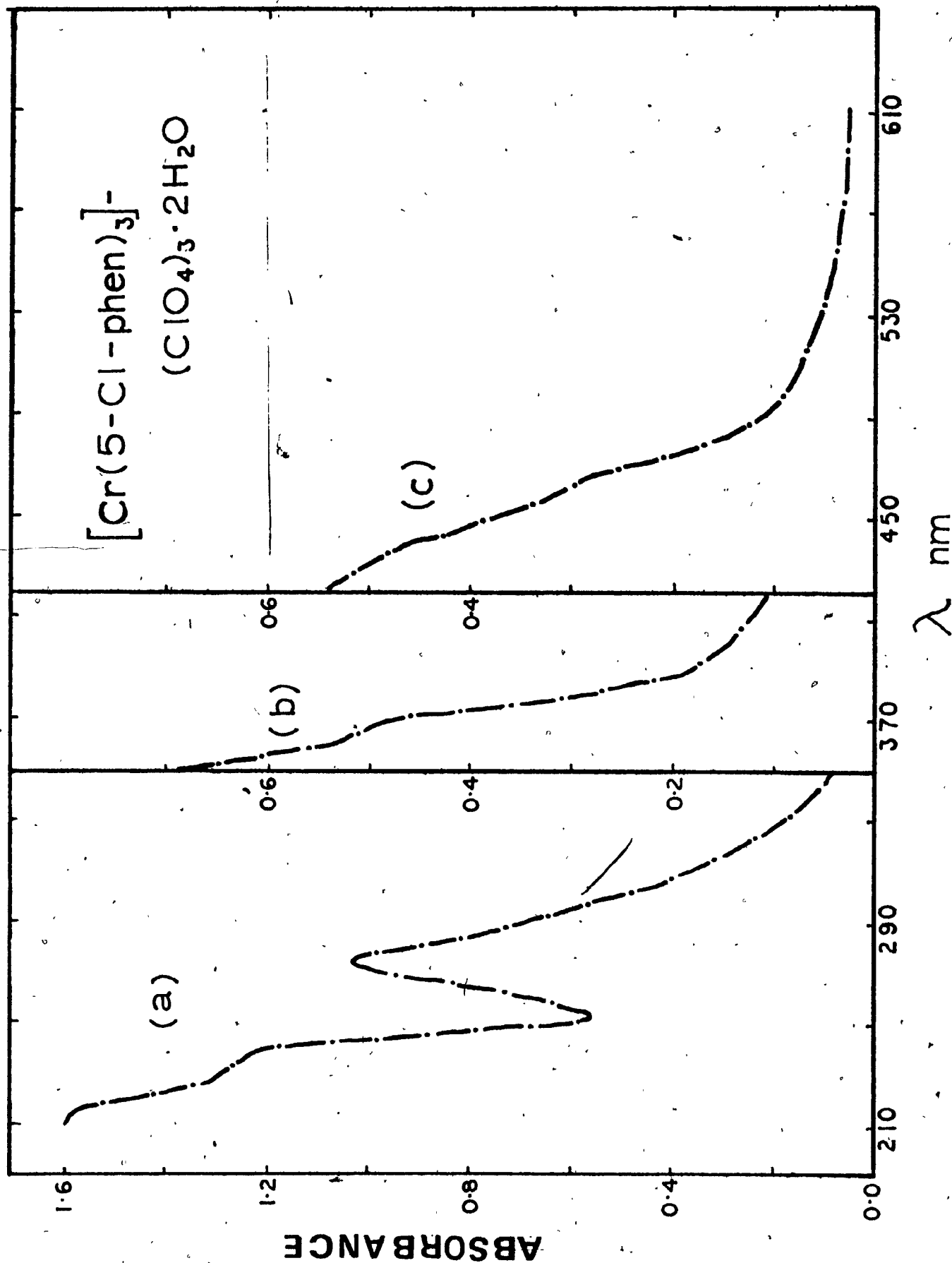


Figure 56. Absorption Spectrum of  $[\text{Cr}(4,7\text{-Me}_2\text{phen})_3]^{3+}$   
 $(\text{ClO}_4)_3 \cdot 2\text{H}_2\text{O}$  in Methanol:

(a)  $1.038 \times 10^{-3} \text{ M}$ ;

(b)  $2.077 \times 10^{-4} \text{ M}$ ;

(c)  $1.661 \times 10^{-5} \text{ M}$ .



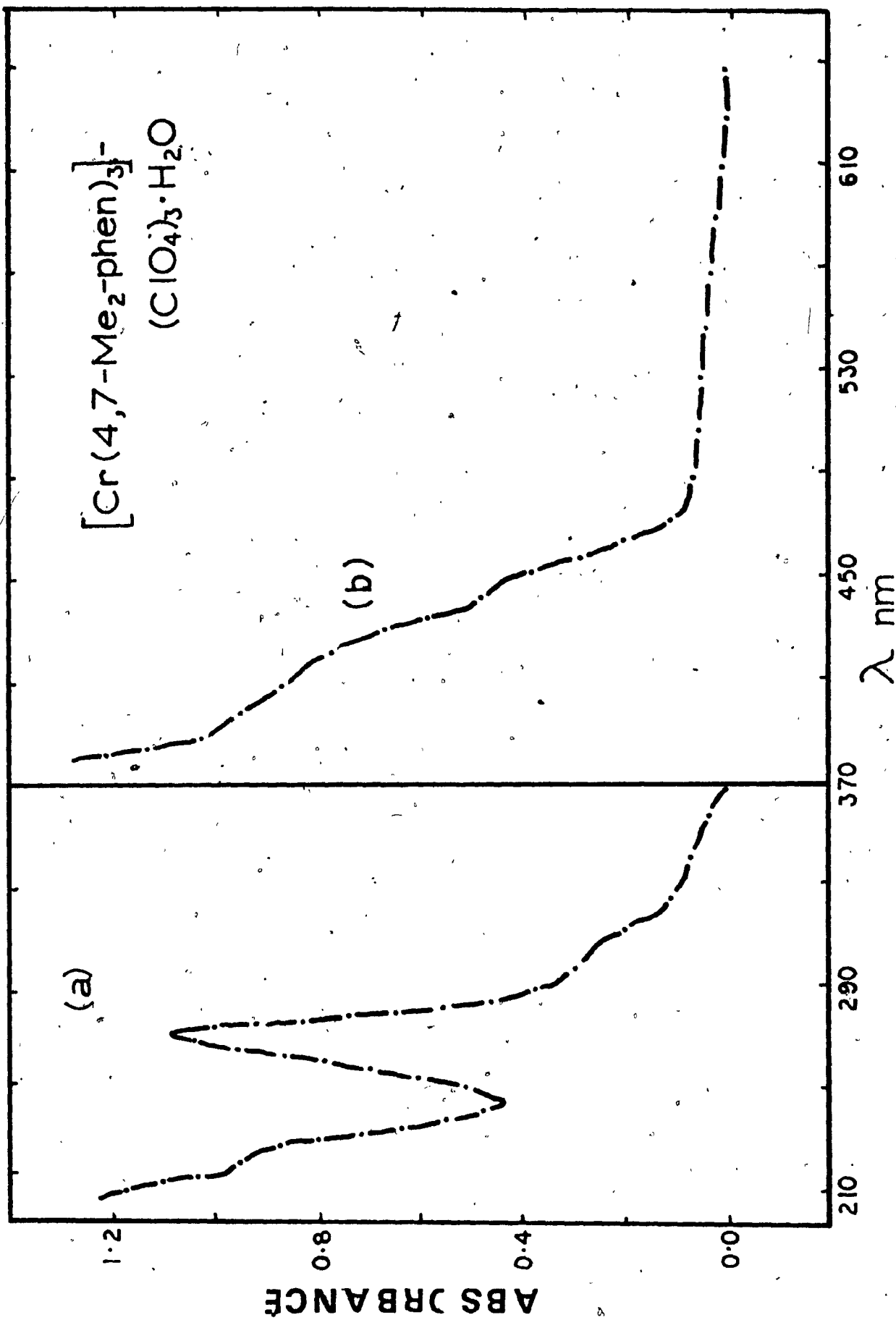




Figure 57. Absorption Spectrum of  $[\text{Cr}(4,7\text{-Ph}_2\text{phen})_3]\text{-(ClO}_4)_3 \cdot 4\text{H}_2\text{O}$  in Methanol:

- (a)  $7.537 \times 10^{-4} \text{ M}$ ;
- (b)  $1.206 \times 10^{-4} \text{ M}$ ;
- (c)  $2.412 \times 10^{-5} \text{ M}$ ;
- (d)  $9.648 \times 10^{-6} \text{ M}$ .

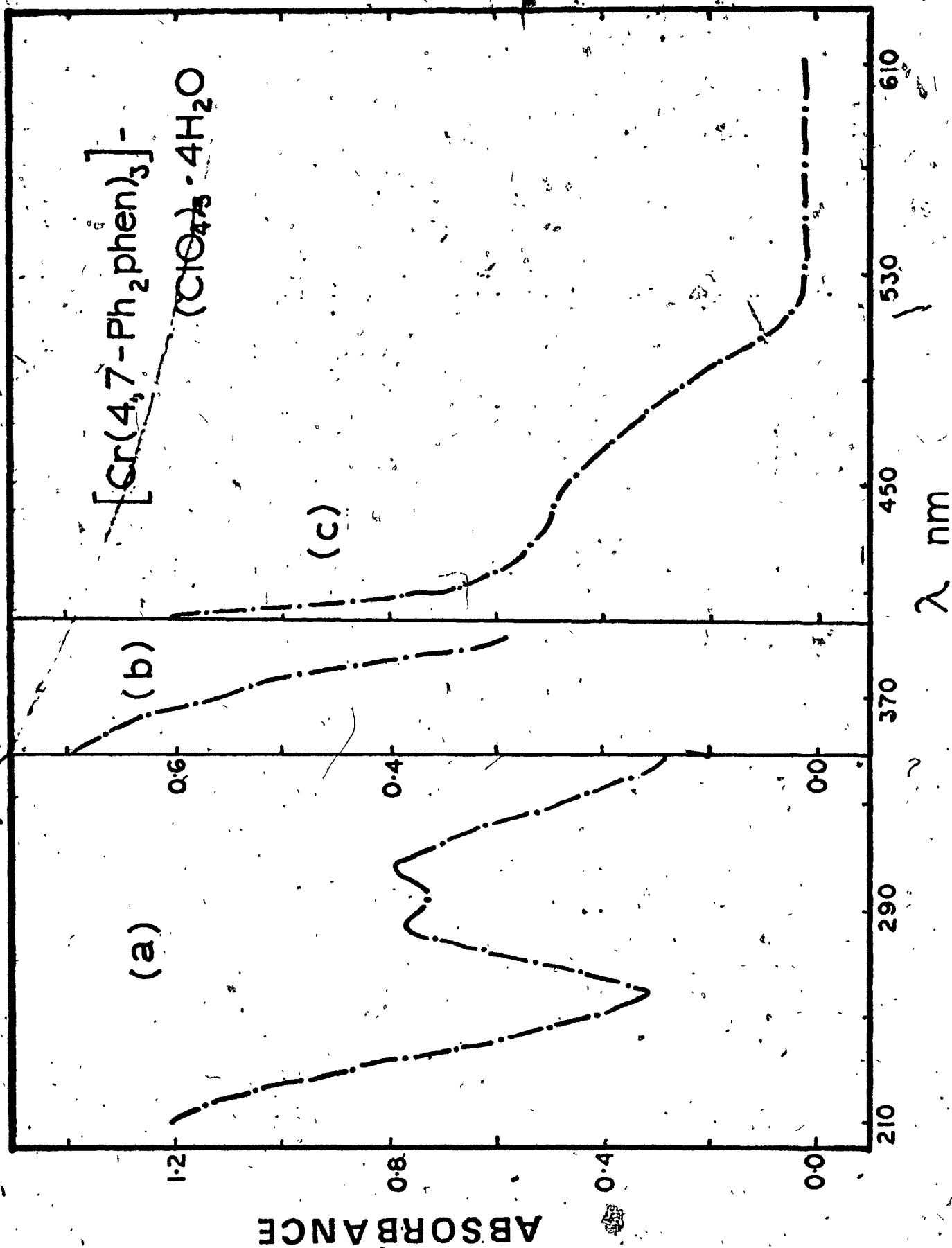
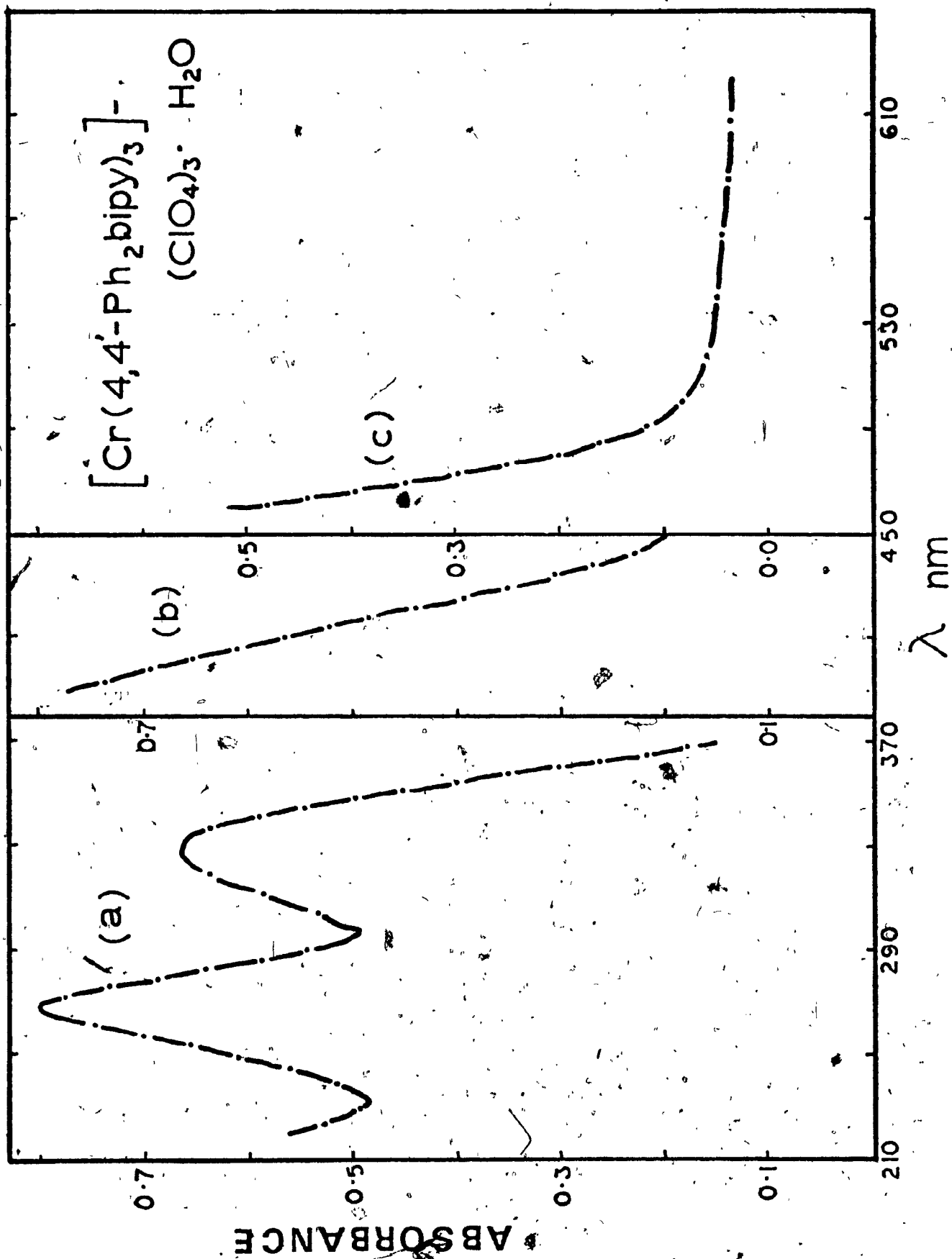


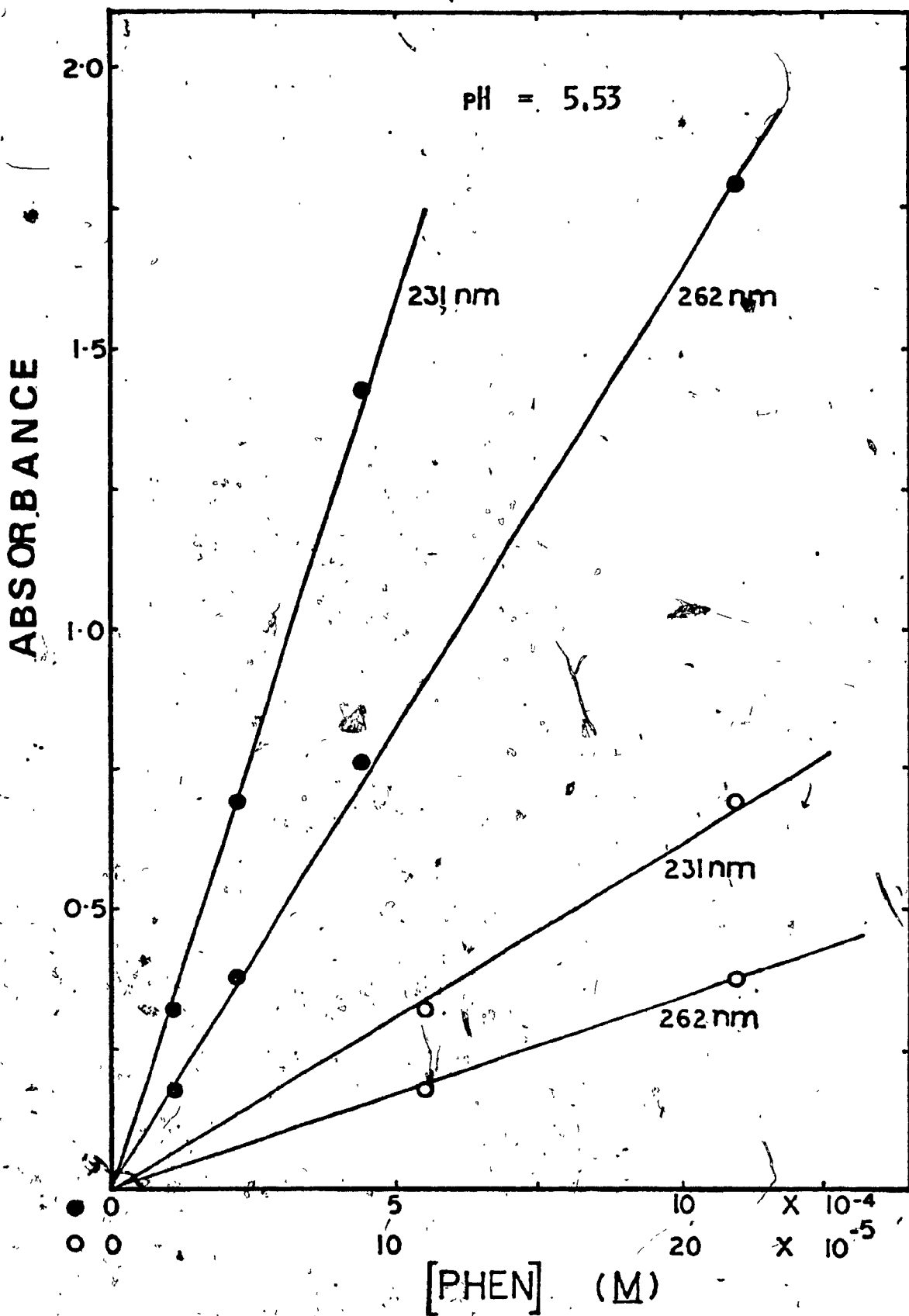
Figure 58. Absorption Spectrum of  $[\text{Cr}(4,4'\text{-Ph}_2\text{bipy})_3]\text{(ClO}_4)_3 \cdot 2\text{H}_2\text{O}$  in Methanol:

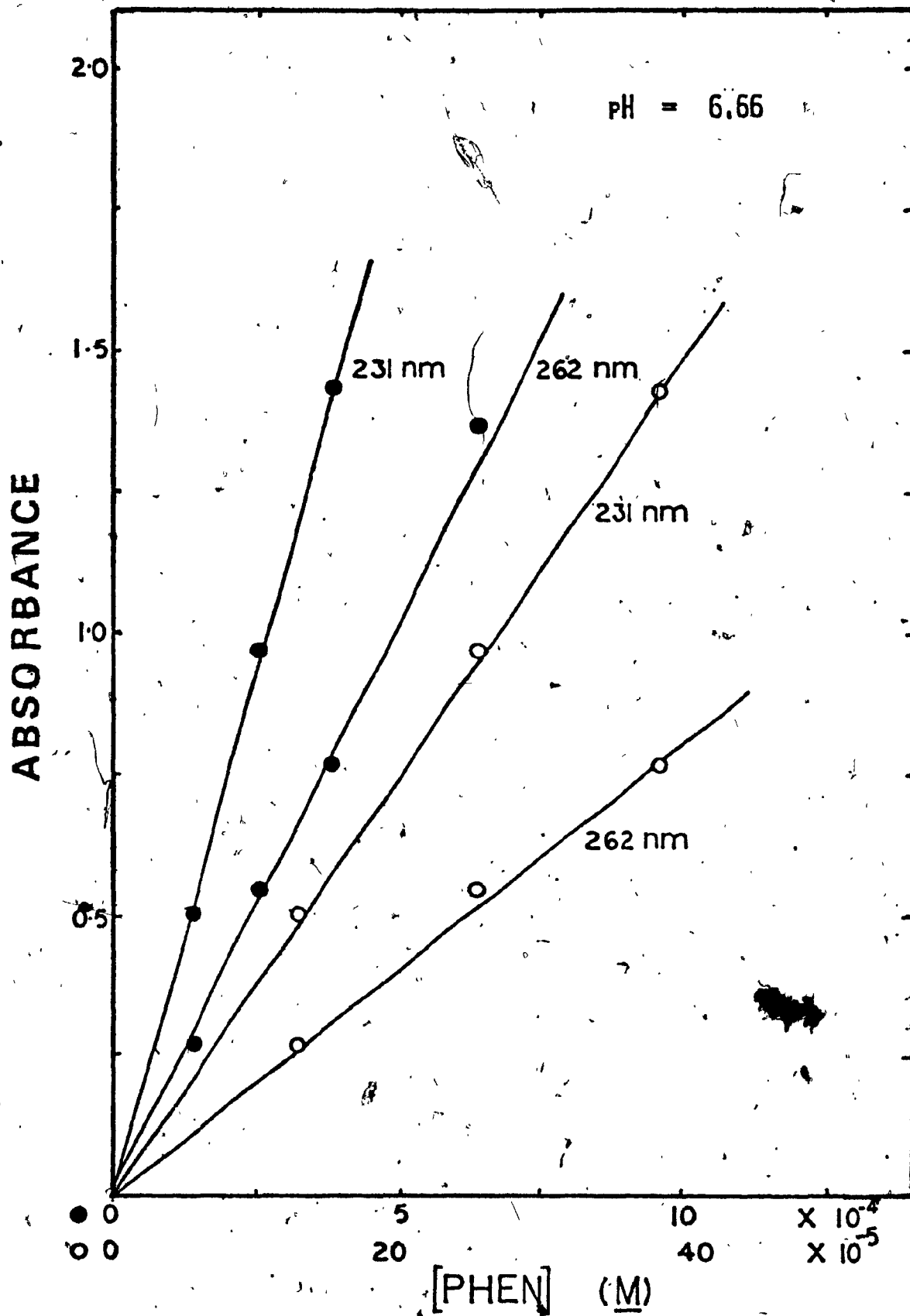
- (a)  $5.932 \times 10^{-4}$  M;
- (b)  $1.186 \times 10^{-4}$  M;
- (c)  $9.491 \times 10^{-6}$  M.



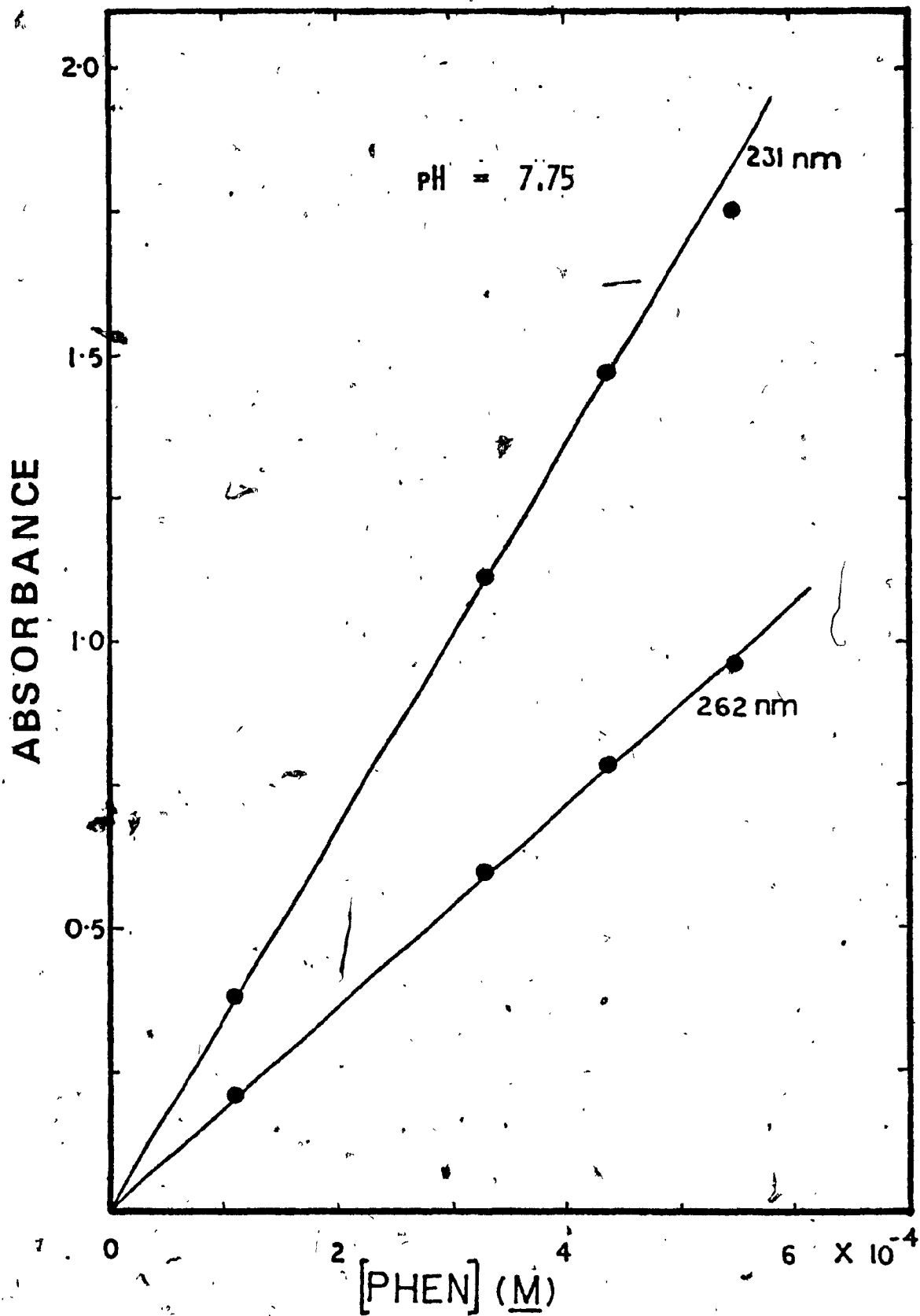
Appendix A. Calibration Curves (Absorbance versus [PHEN]) for 1,10-phenanthroline monohydrate at Various pH and  $[\text{OH}^-]$ :

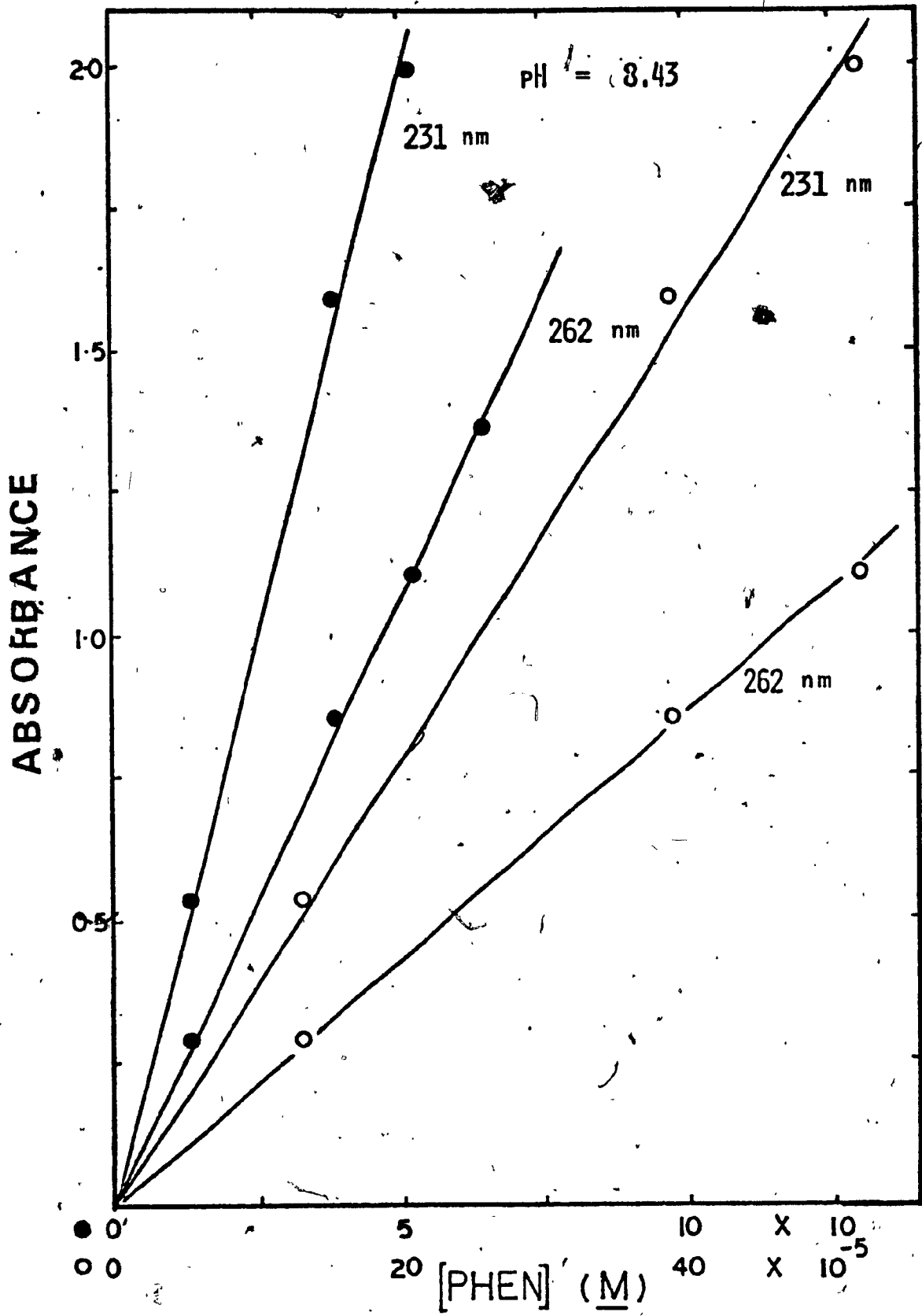
- a) pH = 5.53
- b) pH = 6.66
- c) pH = 7.75
- d) pH = 8.43
- e) pH = 8.88
- f) pH = 10.15
- g) pH = 11.14
- h) 0.80  $[\text{OH}^-]$

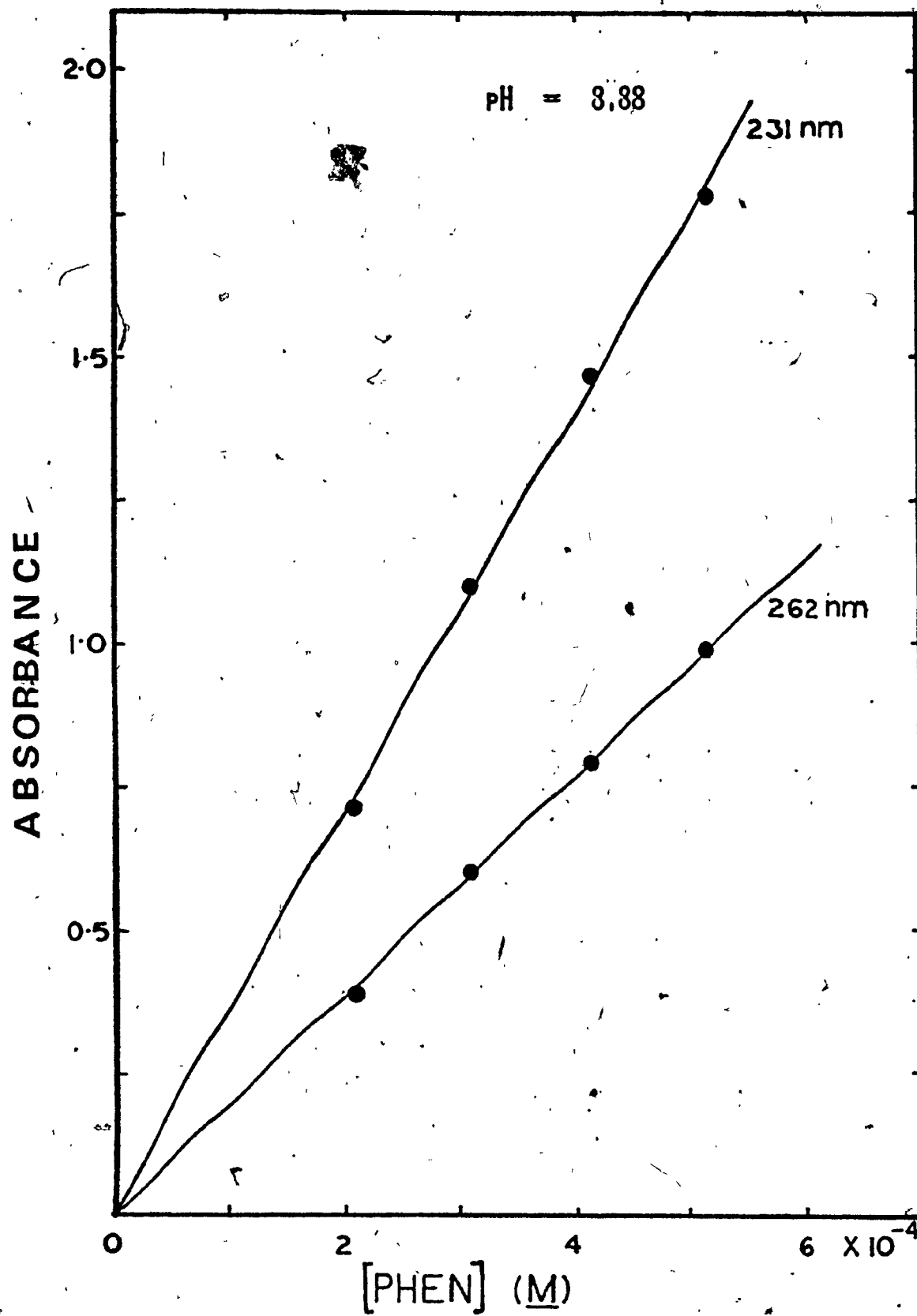


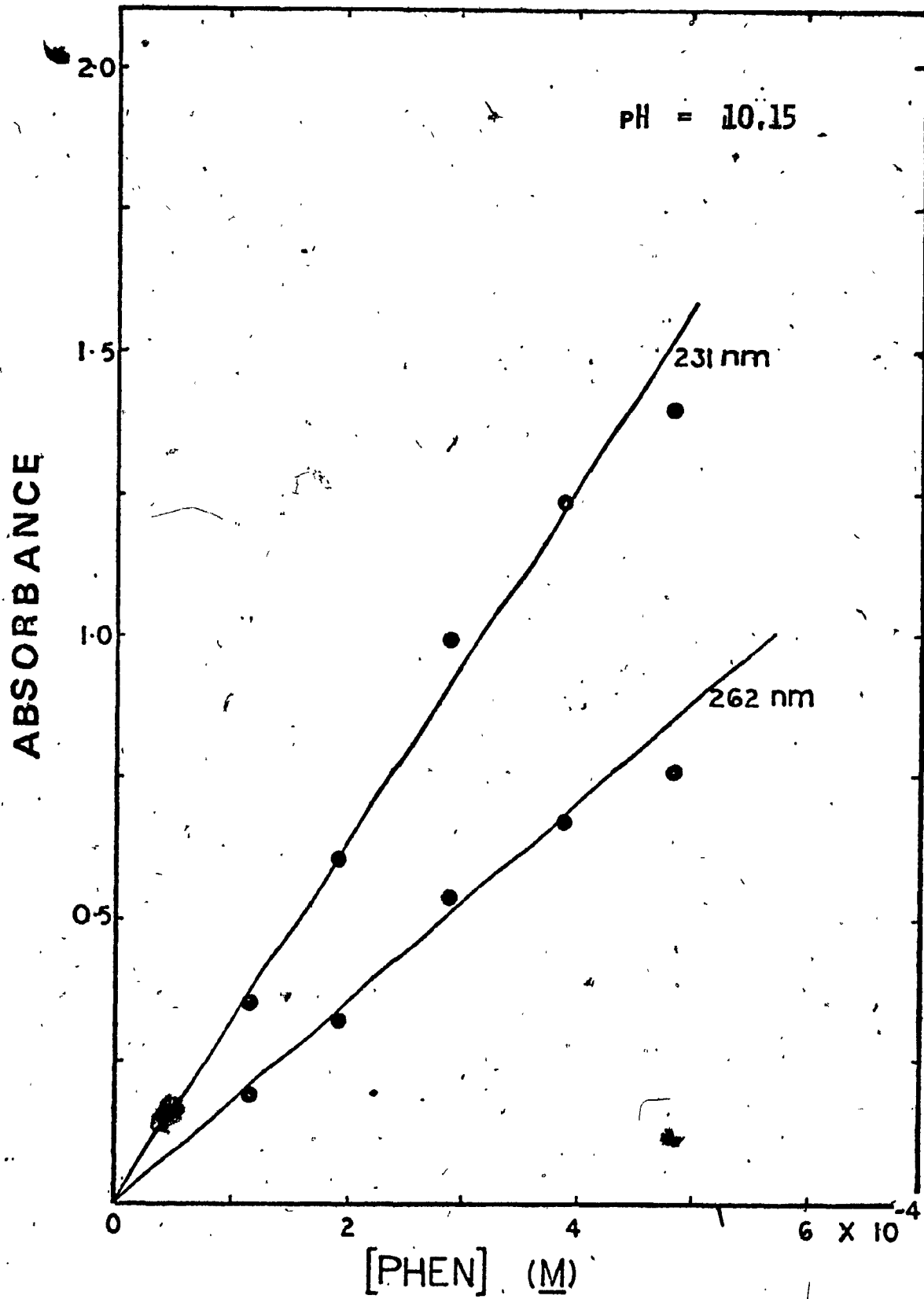


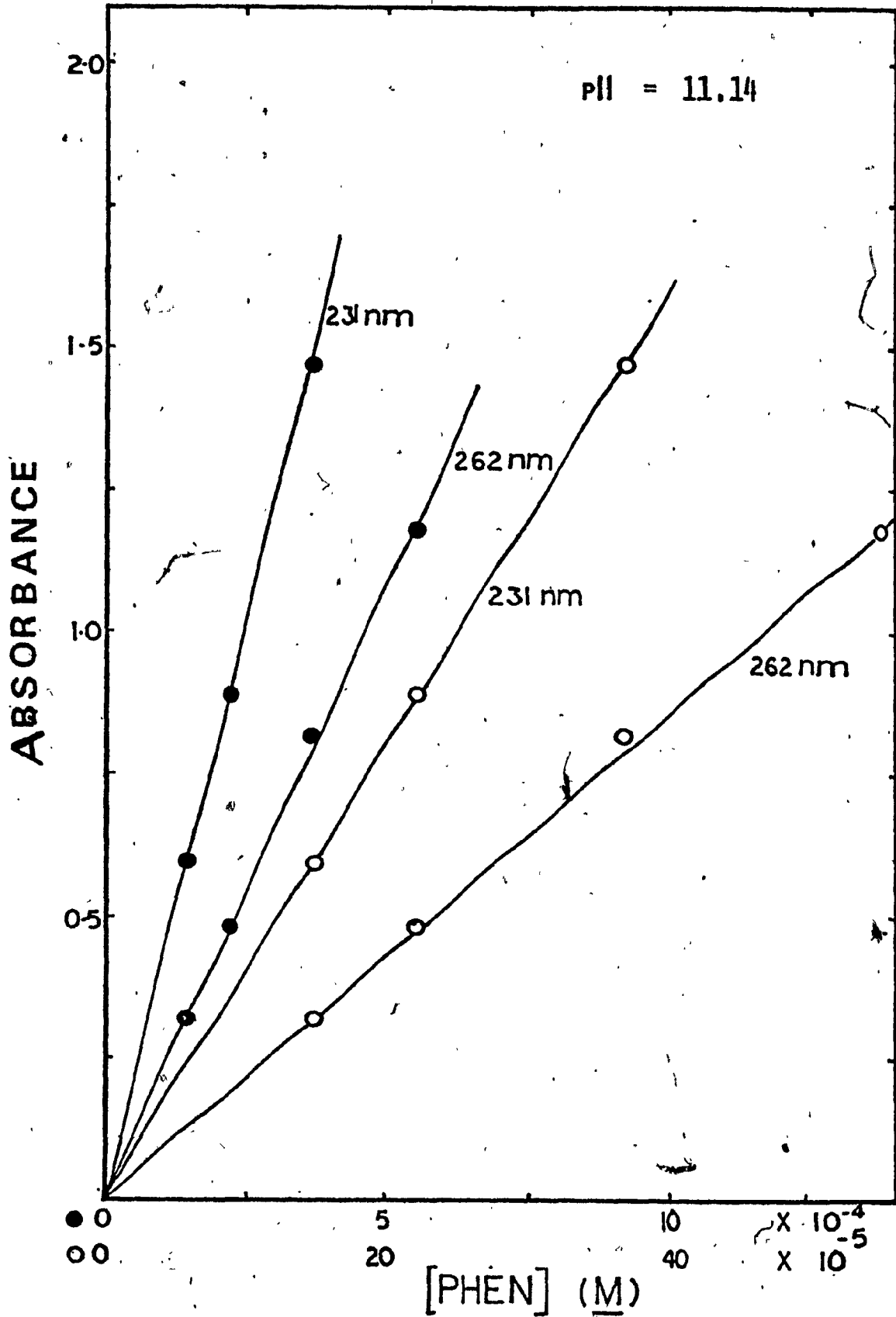


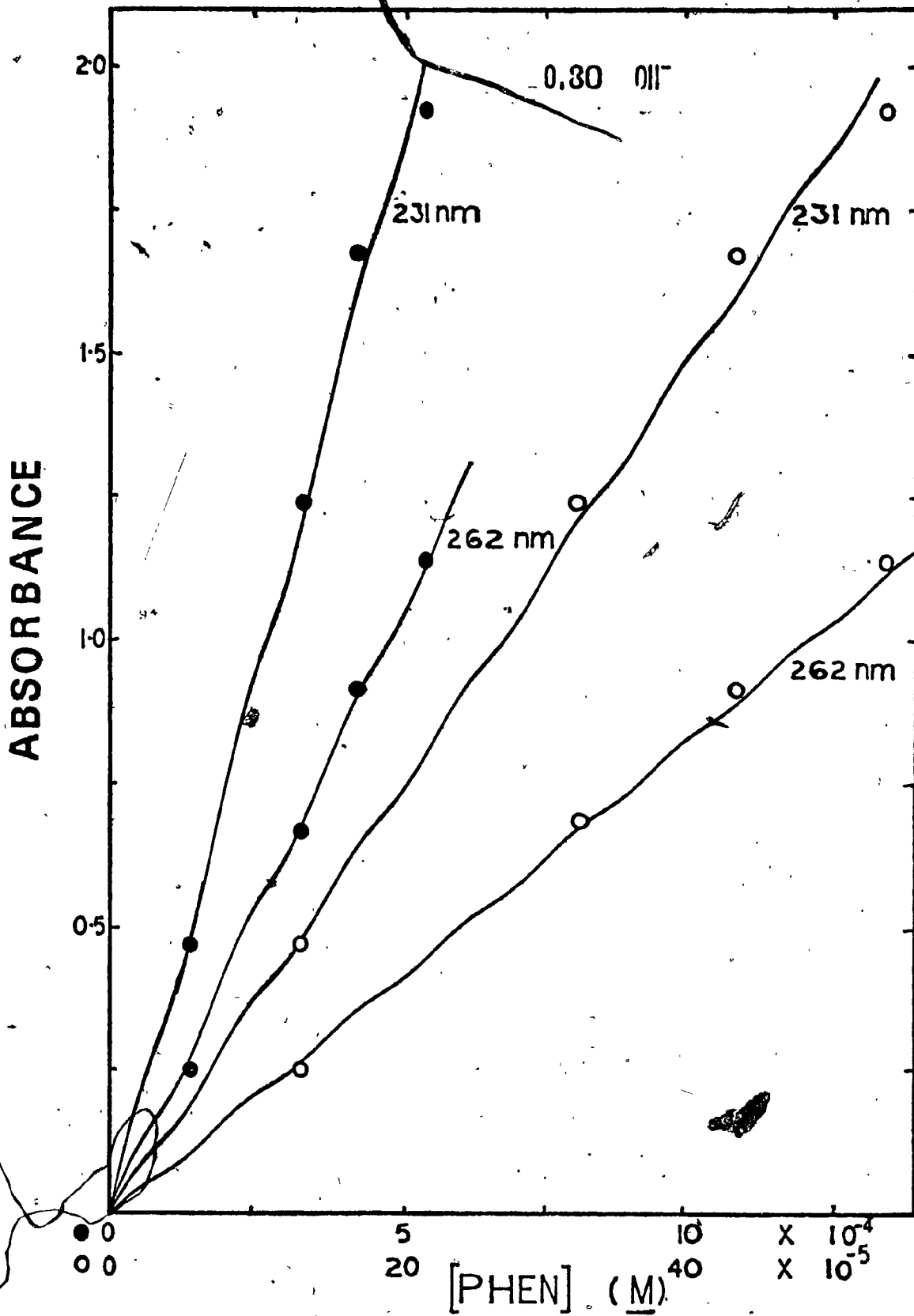












e)  $C_0 = 9.999 \times 10^{-4} \text{ M}$ ;  $\text{pH} = 7.59$ ;  $T = 31.1 \pm 0.1^\circ\text{C}$ .

Sample	Time (hr)	$A_{231}$	$A_{262}$	$10^{+5} [\text{PHEN}]$ ( $\bar{M}$ )	$\log \{ C_0 - [\text{PHEN}] \}$
$t_0$	0.0	0.217	0.130	6.400	-3.029
$t_1$	2.20	0.234	0.138	6.844	-3.031
$t_2$	4.12	0.260	0.162	7.829	-3.035
$t_3$	6.12	0.265	0.158	7.795	-3.035
$t_4$	8.23	0.296	0.172	8.591	-3.039
$t_5$	10.28	0.316	0.184	9.182	-3.042

f)  $C_0 = 1.009 \times 10^{-3}$  M; pH = 7.75; T =  $31.1 \pm 0.1^\circ\text{C}$ .

Sample	Time (hr)	A <sub>231</sub>	A <sub>262</sub>	$10^5 [\text{PHEN}]$ (M)	$\log (C_0 - [\text{PHEN}])$
$t_0$	0.0	0.135	0.071	3.726	-3.012
$t_1$	4.70	0.218	0.113	5.975	-3.023
$t_2$	8.05	0.221	0.122	6.249	-3.024
$t_3$	10.63	0.280	0.135	7.412	-3.029
$t_4$	25.63	0.430	0.233	12.045	-3.051
$t_5$	28.65	0.474	0.237	12.765	-3.055



g)  $C_0 = 1.014 \times 10^{-3} M$ ; pH = 8.43;  $T = 31.1 \pm 0.1^\circ C$ .

Sample	Time (hr)	A <sub>231</sub>	A <sub>262</sub>	$10^{+5} [PHEN] (M)$	$\log \{C_0 - [PHEN]\}$
t <sub>0</sub>	0.0	0.177	0.094	4.909	-3.016
t <sub>1</sub>	4.65	0.308	0.169	8.682	-3.033
t <sub>2</sub>	8.02	0.339	0.188	9.608	-3.037
t <sub>3</sub>	10.62	0.365	0.197	10.205	-3.040
t <sub>4</sub>	25.82	0.693	0.387	19.709	-3.088
t <sub>5</sub>	28.85	0.720	0.397	20.346	-3.091
t <sub>6</sub>	32.02	0.810	0.439	22.692	-3.104

h)  $C_0 = 1.004 \times 10^{-3}$  M; pH = 8.88; T =  $31.1 \pm 0.1^\circ\text{C}$ .

Sample	Time (hr)	A <sub>231</sub>	A <sub>262</sub>	$10^{+5}[\text{PHEN}]$ (M)	$\log \{C_0 - [\text{PHEN}]\}$
t <sub>0</sub>	0.0	0.219	0.120	6.169	-3.026
t <sub>1</sub>	4.62	0.325	0.181	9.230	-3.040
t <sub>2</sub>	7.98	0.385	0.213	10.898	-3.048
t <sub>3</sub>	10.58	0.442	0.248	12.601	-3.057
t <sub>4</sub>	25.78	0.717	0.397	20.304	-3.096
t <sub>5</sub>	28.82	0.795	0.439	22.482	-3.108
t <sub>6</sub>	31.93	0.859	0.473	24.257	-3.118

1)  $C_0 = 1.006 \times 10^{-3}$  M; pH = 8.45; T = 31.1  $\pm$  0.1°C.

Sample	Time (hr)	A <sub>231</sub>	A <sub>262</sub>	$10^{+5}$ [PHEN] (M)	$\log \{ C_0 - [PHEN] \}$
t <sub>0</sub>	0.0	0.188	0.108	5.425	-3.021
t <sub>1</sub>	2.22	0.248	0.146	7.247	-3.030
t <sub>2</sub>	4.10	0.274	0.159	7.948	-3.033
t <sub>3</sub>	6.12	0.302	0.180	8.882	-3.038
t <sub>4</sub>	8.22	0.356	0.210	10.414	-3.045

94)  $C_0 = 9.968 \times 10^{-4}$  M; pH = 10.10; T = 30.9 ± 0.1°C.

Sample	Time (hr)	A <sub>231</sub>	A <sub>262</sub>	10 <sup>+5</sup> [PHEN] (M)	log {C <sub>0</sub> - [PHEN]}
t <sub>1</sub>	0.32	0.010	0.005	0.269	-3.003
t <sub>2</sub>	1.23	0.030	0.016	0.834	-3.005
t <sub>3</sub>	3.26	0.070	0.036	1.911	-3.010
t <sub>4</sub>	5.38	0.121	0.068	3.452	-3.017
t <sub>5</sub>	7.74	0.165	0.093	4.715	-3.022
t <sub>6</sub>	9.87	0.179	0.098	5.040	-3.024
t <sub>7</sub>	11.60	0.237	0.130	6.680	-3.032

k)  $C_0 = 1.018 \times 10^{-3} \text{ M}$ ; pH = 10.15; T =  $31.1 \pm 0.1^\circ\text{C}$

Sample	Time (hr)	$A_{231}$	$A_{262}$	$10^{+5}[\text{PHEN}]$ (M)	$\log (C_0 - [\text{PHEN}])$
$t_0$	0.0	0.220	0.120	6.183	-3.019
$t_1$	3.78	0.331	0.174	9.134	-3.033
$t_2$	5.88	0.404	0.216	11.242	-3.043
$t_3$	7.88	0.428	0.230	11.940	-3.046
$t_4$	9.52	0.443	0.238	12.356	-3.048
$t_5$	11.55	0.500	0.271	14.008	-3.057

1)  $C_0 = 9.995 \times 10^{-4}$  M; pH = 10.50; T =  $31.2 \pm 0.1^\circ\text{C}$ .

Sample	Time (hr)	A <sub>231</sub>	A <sub>262</sub>	$10^{+5}$ [PHEN] (M)	$\log \{C_0 - [\text{PHEN}]\}$
t <sub>1</sub>	2.17	0.322	0.190	9.421	-3.043
t <sub>2</sub>	8.30	0.460	0.260	13.163	-3.062
t <sub>3</sub>	14.50	0.566	0.337	16.638	-3.079
t <sub>4</sub>	21.67	0.680	0.420	20.379	-3.099

m)  $C_0 = 1.004 \times 10^{-3} \text{ M}$ ;  $\text{pH} = 11.14$ ;  $T = 31.1 \pm 0.1^\circ\text{C}$ .

Sample	Time (hr)	$A_{231}$	$A_{262}$	$10^{+5} [\text{PHEN}]$ (M)	$\log\{C_0 - [\text{PHEN}]\}$
$t_1$	0.07	0.204	0.104	5.546	-3.023
$t_2$	1.77	0.299	0.158	8.272	-3.036
$t_3$	3.27	0.359	0.186	9.836	-3.043
$t_4$	4.83	0.417	0.225	11.656	-3.052
$t_5$	6.38	0.478	0.258	13.364	-3.060
$t_6$	7.93	0.497	0.268	13.888	-3.063

n)  $C_0 = 1.013 \times 10^{-3} \text{ M}$ ; pH = 11.67; T =  $31.1 \pm 0.1^\circ\text{C}$ .

Sample	Time (hr)	$A_{231}$	$A_{262}$	$10^{+5}[\text{PHEN}]$ ( $\bar{M}$ )	$\log \{C_0 - [\text{PHEN}]\}$
$t_0$	0.0	0.214	0.129	6.331	-3.022
$t_1$	1.22	0.323	0.173	8.996	-3.035
$t_2$	2.13	0.341	0.187	9.609	-3.038
$t_3$	5.48	0.572	0.318	16.231	-3.070
$t_4$	6.48	0.618	0.332	17.372	-3.076



o)  $C_0 = 9.991 \times 10^{-4}$  M; PH = 12.17; T = 31.1  $\pm$  0.1°C.

Sample	Time (hr)	A <sub>231</sub>	A <sub>262</sub>	$10^{+5}$ [PHEN] (M)	$\log \{C_0 - [PHEN]\}$
t <sub>1</sub>	0.50	0.274	0.149	7.689	-3.035
t <sub>2</sub>	1.05	0.328	0.174	9.092	-3.042
t <sub>3</sub>	1.55	0.368	0.198	10.272	-3.048
t <sub>4</sub>	2.03	0.414	0.223	11.563	-3.054
t <sub>5</sub>	2.52	0.474	0.240	12.843	-3.060

p)  $C_0 = 1.002 \times 10^{-3} \text{ M}$ ;  $0.10 [\text{OH}^-]$ ;  $T = 31.1 \pm 0.1^\circ\text{C}$ .

Sample	Time (min)	A <sub>231</sub>	A <sub>262</sub>	$10^{+5} [\text{PHEN}]$ (M)	$\log \{C_0 - [\text{PHEN}]\}$
t <sub>1</sub>	40.50	0.436	0.289	13.576	-3.062
t <sub>2</sub>	72.50	0.621	0.344	17.512	-3.083
t <sub>3</sub>	95.50	0.712	0.387	19.976	-3.096
t <sub>4</sub>	115.5	0.789	0.431	22.191	-3.108

q)  $C_0 = 1.001 \times 10^{-3} \text{ M}$ ;  $0.30 [\text{OH}^-]$ ;  $T = 31.1 \pm 0.1^\circ\text{C}$ .

Sample	Time (min)	A <sub>231</sub>	A <sub>262</sub>	$10^{+5} [\text{PHEN}]$ (M)	$\log \{C_0 - [\text{PHEN}]\}$
t <sub>1</sub>	5.75	0.059	0.033	1.680	-3.0074
t <sub>2</sub>	21.12	0.364	0.198	10.216	-3.046
t <sub>3</sub>	37.10	0.623	0.338	17.463	-3.083
t <sub>4</sub>	49.79	0.824	0.449	23.147	-3.114
t <sub>5</sub>	60.66	0.991	0.540	27.838	-3.141
t <sub>6</sub>	73.67	1.155	0.617	32.125	-3.168

r)  $C_0 = 1.001 \times 10^{-3}$  M;  $0.50$  [OH<sup>-</sup>];  $T = 31.1 \pm 0.1^\circ\text{C}$ .

Sample	Time (min)	A <sub>231</sub>	A <sub>262</sub>	$10^{+5}$ [PHEN] (M)	$\log \{C_0 - [\text{PHEN}]\}$
t <sub>1</sub>	12.50	0.452	0.232	12.328	-3.057
t <sub>2</sub>	19.25	0.583	0.306	16.075	-3.076
t <sub>3</sub>	26.17	0.824	0.449	23.147	-3.114
t <sub>4</sub>	32.00	0.874	0.477	25.070	-3.125
t <sub>5</sub>	32.00	0.920	0.510	26.068	-3.131
t <sub>6</sub>	42.25	---	0.602	31.095	-3.161
t <sub>7</sub>	42.25	1.078	0.592	30.400	-3.157
t <sub>8</sub>	50.50	---	0.692	35.744	-3.191
t <sub>9</sub>	50.50	1.240	0.684	35.047	-3.187

s)  $C_0 = 1.007 \times 10^{-3} \text{ M}$ ;  $0.80 [\text{OH}^-]$ ;  $T = 31.1 \pm 0.1^\circ\text{C}$ .

Sample	Time (min)	$A_{231}$	$A_{262}$	$10^{+5} [\text{PHEN}]$ (M)	$\log \{ C_0 - [\text{PHEN}] \}$
$t_1$	4.00	0.387	0.208	10.797	-3.046
$t_2$	17.00	1.100	0.592	30.709	-3.155
$t_3$	30.00	1.782	1.000	50.806	-3.302
$t_4$	41.00	---	1.236	63.843	-3.433
$t_5$	53.00	---	1.454	75.103	-3.592

t)  $C_0 = 1.001 \times 10^{-3}$  M;  $1.00$  [OH<sup>-</sup>];  $T = 31.1 \pm 0.1^\circ\text{C}$ .

Sample	Time (min)	A <sub>231</sub>	A <sub>262</sub>	$10^{+5}$ [PHEN] (M)	$\log \{C_0 - [\text{PHEN}]\}$
t <sub>1</sub>	9.50	0.876	0.466	24.314	-3.120
t <sub>2</sub>	15.00	1.402	0.752	39.074	-3.214
t <sub>3</sub>	21.00	1.812	0.970	50.451	-3.304
t <sub>4</sub>	26.92	---	1.232	63.636	-3.438
t <sub>5</sub>	34.00	---	1.382	71.384	-3.542
t <sub>6</sub>	38.50	---	1.520	78.512	-3.666

R

Appendix.D. Data for the Determination of the Observed  
Rate Constant  $k_{obs}$  for the  $[\text{Cr}(\text{bipy})_3]^{3+}$   
System at Various pH and  $[\text{OH}^-]$ .

a)  $C_0 = 1.015 \times 10^{-3} \text{ M}$ ; pH = 10.83; T = 11.1 ± 0.1°C.

Sample	Time (hr)	$A_{237}$	$A_{282}$	$10^5 [\text{BIPY}]$ (M)	$\log \{C_0 - [\text{BIPY}]\}$
$t_1$	0.41	0.010	0.010	0.22	-2.994
$t_2$	1.66	0.019	0.017	0.40	-2.995
$t_3$	3.91	0.040	0.042	0.84	-2.997
$t_4$	6.24	0.069	0.075	1.48	-3.00
$t_5$	8.32	0.082	0.095	1.79	-3.001
$t_6$	10.89	0.101	0.116	2.19	-3.003



b)  $C_0 = 1.02 \times 10^{-3}$  M; pH = 11.31; T = 11.1 ± 0.1°C.

Sample	Time (hr)	$A_{237}$	$A_{282}$	$10^{+5}[\text{BIPY}]$ (M)	$\log \{C_0 - [\text{BIPY}]\}$
$t_1$	0.55	0.019	0.018	0.40	-2.993
$t_2$	1.78	0.031	0.029	0.62	-2.994
$t_3$	3.79	0.048	0.055	1.05	-2.996
$t_4$	6.11	0.085	0.095	1.82	-2.999
$t_5$	8.20	0.104	0.121	2.26	-3.001
$t_6$	10.77	0.131	0.154	2.88	-3.004

c)  $C_0 = 1.008 \times 10^{-3} M$ ;  $pH = 11.82$ ;  $T = 11.1 \pm 0.1^\circ C$ .

Sample Time (hr)  $A_{237}$   $A_{282}$   $10^4 [BIPY] (M)$   $\log \{C_0 - [BIPY]\}$

$t_1$	0.15	0.009	0.010	0.212	-2.998
$t_2$	1.15	0.029	0.032	0.65	-2.999
$t_3$	2.28	0.051	0.057	1.10	-3.001
$t_4$	5.26	0.108	0.125	2.36	-3.007
$t_5$	7.53	0.144	0.175	3.20	-3.010
$t_6$	10.07	0.194	0.233	4.29	-3.015

d)  $C_0 = 9.805 \times 10^{-4} \text{ M}$ ;  $\text{pH} = 12.16$ ;  $T = 11.1 \pm 0.1^\circ\text{C}$ .

Sample	Time (hr)	$A_{237}$	$A_{282}$	$10^{+5}[\text{BIPY}]$ (M)	$\log \{C_0 - [\text{BIPY}]\}$
$t_1$	0.15	0.009	0.011	0.21	-3.009
$t_2$	0.94	0.036	0.042	0.78	-3.012
$t_3$	2.21	0.073	0.088	1.61	-3.016
$t_4$	4.96	0.163	0.195	3.60	-3.025
$t_5$	9.61	0.299	0.363	6.65	-3.039

e)  $C_0 = 9.854 \times 10^{-4}$  M;  $0.10$  [OH<sup>-</sup>];  $T = 11.1 \pm 0.1^\circ\text{C}$ .

Sample	Time (min)	A <sub>237</sub>	A <sub>282</sub>	$10^{+5}$ [BIPY] (M)	$\log \{C_0 - [BIPY]\}$
t <sub>1</sub>	9.00	0.035	0.046	0.80	-3.01
t <sub>2</sub>	28.20	0.079	0.094	1.75	-3.014
t <sub>3</sub>	46.15	0.121	0.143	2.65	-3.018
t <sub>4</sub>	68.85	0.170	0.204	3.75	-3.023
t <sub>5</sub>	95.90	0.222	0.268	4.92	-3.029
t <sub>6</sub>	123.55	0.283	0.339	6.28	-3.035

f)  $C_0 = 1.027 \times 10^{-3} \text{ M}$ ;  $0.50 \text{ M}$ ;  $T = 11.1 \pm 0.1^\circ\text{C}$ .

Sample	Time (min)	$A_{237}$	$A_{282}$	$10^5 [\text{BIPY}]$ (M)	$\log \{C_0 - [\text{BIPY}]\}$
$t_1$	6.15	0.191	0.229	4.21	-3.007
$t_2$	16.05	0.335	0.406	7.44	-3.021
$t_3$	27.15	0.480	0.585	10.68	-3.036
$t_4$	39.50	0.651	0.796	14.50	-3.054
$t_5$	51.55	0.770	0.928	17.06	-3.067

g)  $C_0 = 9.653 \times 10^{-4} M$ ;  $0.80 [OH^-]$ ;  $T = 11.1 \pm 0.1^\circ C$ .

Sample	Time (min)	A <sub>237</sub>	A <sub>282</sub>	$10^{+5} [BIPY]$ (M)	$\log \{C_0 - [BIPY]\}$
t <sub>1</sub>	6.00	0.379	0.453	8.35	-3.055
t <sub>2</sub>	15.70	0.622	0.753	13.78	-3.082
t <sub>3</sub>	24.60	0.838	1.002	18.45	-3.108
t <sub>4</sub>	34.20	1.052	1.268	23.80	-3.138
t <sub>5</sub>	42.95	1.252	1.520	27.80	-3.163
t <sub>6</sub>	52.2	1.418	1.700	31.30	-3.186

h)  $C_0 = 1.030 \times 10^{-3} \text{ M}$ ;  $1.00 \text{ [OH}^-]$ ;  $T = 11.1 \pm 0.1^\circ\text{C}$ .

Sample	Time (min)	$A_{237}$	$A_{282}$	$10^{+5} [\text{BIPY}]$ (M)	$\log \{C_0 - [\text{BIPY}]\}$
$t_1$	7.00	0.727	0.874	16.08	-3.061
$t_2$	16.60	1.180	1.444	26.35	-3.115
$t_3$	24.40	1.456	1.802	32.65	-3.153
$t_4$	30.50	1.642	---	37.20	-3.182

44

Appendix E. Data for the Determination of the Observed Rate Constant at pH 11.82 at 29.5°C, and 0.50 [OH<sup>-</sup>] at 7.5°C, for the [Cr(bipy)<sub>3</sub>]<sup>3+</sup> System in Oxygenated and Deoxygenated Solvents.

- 1a) pH 11.82 in Oxygenated Solvent;
- 1b) pH 11.82 in Deoxygenated Solvent;
- 2a) 0.50 [OH<sup>-</sup>] in Oxygenated Solvent;
- 2b) 0.50 [OH<sup>-</sup>] in Deoxygenated Solvent;



1a) pH = 11.82; T = 29.5 ± 0.1°C. Oxygenated solvent.

Sample	Time (hr)	$A_{287} = A_t$	$ (A_f - A_t) $	$\log  (A_f - A_t) $
$t_0$	0.04	0.876	0.546	-0.262
$t_1$	0.34	0.878	0.544	-0.264
$t_2$	1.06	0.918	0.504	-0.297
$t_3$	2.19	0.928	0.494	-0.306
$t_4$	3.06	0.946	0.476	-0.322
$t_5$	3.83	0.958	0.464	-0.333
$t_6$	5.38	0.976	0.446	-0.350
$t_7$	6.65	1.002	0.420	-0.376
$t_8$	7.91	1.024	0.398	-0.40
$t_9$	8.99	1.044	0.378	-0.422
$t_{10}$	10.13	1.07	0.352	-0.453
$t_{11}$	11.24	1.084	0.338	-0.470
$t_{12}$	12.6	1.104	0.318	-0.497

1b) pH = 11.82; T = 29.5 ± 0.1°C; Deoxygenated solvent.

Sample	Time (hr)	$A_{287} = A_t$	$ A_f - A_t $	$\log  (A_f - A_t) $
$t_0$	0.18	0.844	0.554	-0.256
$t_1$	1.14	0.866	0.532	-0.274
$t_2$	2.29	0.892	0.506	-0.296
$t_3$	3.28	0.920	0.478	-0.320
$t_4$	4.66	0.952	0.446	-0.350
$t_5$	5.82	0.976	0.422	-0.374
$t_6$	6.95	0.994	0.404	-0.393
$t_7$	8.14	1.015	0.383	-0.416
$t_8$	9.05	1.028	0.370	-0.431
$t_9$	10.32	1.050	0.348	-0.458
$t_{10}$	11.16	1.062	0.336	-0.473

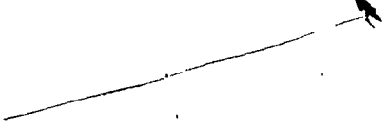
2a) 0.50 [OH<sup>-</sup>]; 7.5 ± 0.1°C; Oxygenated solvent.

Sample	Time <sup>o</sup> (hr)	A <sub>287</sub> = A <sub>t</sub>	(A <sub>f</sub> - A <sub>t</sub> )	log  (A <sub>f</sub> - A <sub>t</sub> )
t <sub>0</sub>	0.07	0.980	0.614	-0.212
t <sub>1</sub>	0.14	0.989	0.605	-0.218
t <sub>2</sub>	0.32	1.009	0.585	-0.233
t <sub>3</sub>	0.52	1.029	0.565	-0.248
t <sub>4</sub>	1.04	1.072	0.522	-0.282
t <sub>5</sub>	1.50	1.109	0.485	-0.314
t <sub>6</sub>	2.83	1.203	0.391	-0.408
t <sub>7</sub>	3.45	1.235	0.359	-0.445
t <sub>8</sub>	4.17	1.270	0.324	-0.489
t <sub>9</sub>	5.23	1.315	0.279	-0.554
t <sub>10</sub>	6.47	1.360	0.234	-0.631
t <sub>11</sub>	7.26	1.382	0.212	-0.674
t <sub>12</sub>	8.25	1.407	0.187	-0.728



2b) 0.50 [OH<sup>-</sup>]; T = 7.5 ± 0.1°C: Deoxygenated solvent.

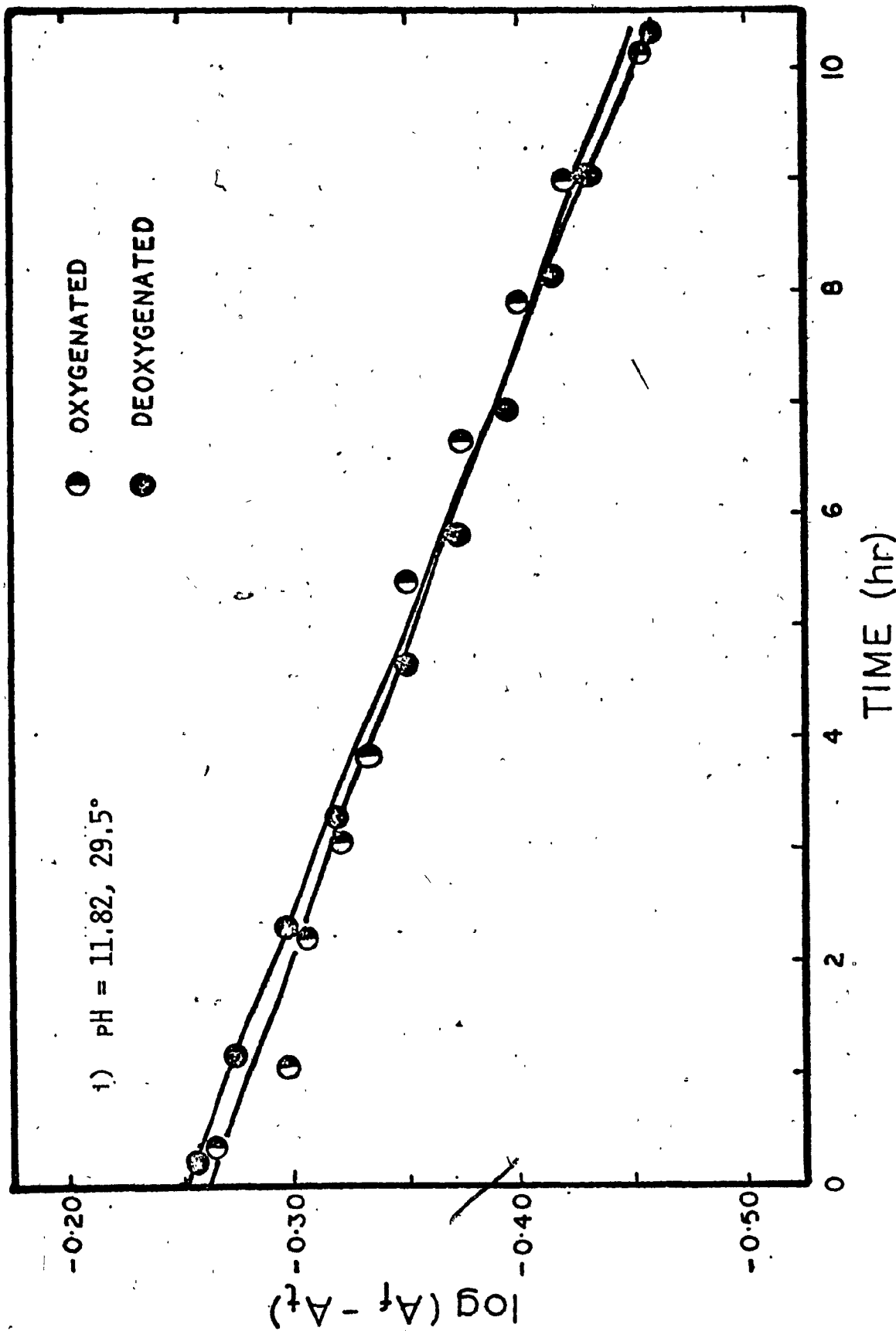
Sample	Time (hr)	A <sub>287</sub> = A <sub>t</sub>	A <sub>f</sub> - A <sub>t</sub>	log  (A <sub>f</sub> - A <sub>t</sub> )
t <sub>0</sub>	0.14	0.655	0.397	-0.402
t <sub>1</sub>	0.3	0.665	0.387	-0.413
t <sub>2</sub>	0.54	0.677	0.375	-0.426
t <sub>3</sub>	0.93	0.695	0.357	-0.448
t <sub>4</sub>	1.36	0.720	0.332	-0.479
t <sub>5</sub>	2.03	0.752	0.299	-0.523
t <sub>6</sub>	3.35	0.804	0.248	-0.606
t <sub>7</sub>	4.29	0.832	0.219	-0.658
t <sub>8</sub>	5.40	0.863	0.189	-0.724
t <sub>9</sub>	6.42	0.887	0.165	-0.784
t <sub>10</sub>	7.7	0.908	0.144	-0.843
t <sub>11</sub>	8.79	0.925	0.127	-0.898

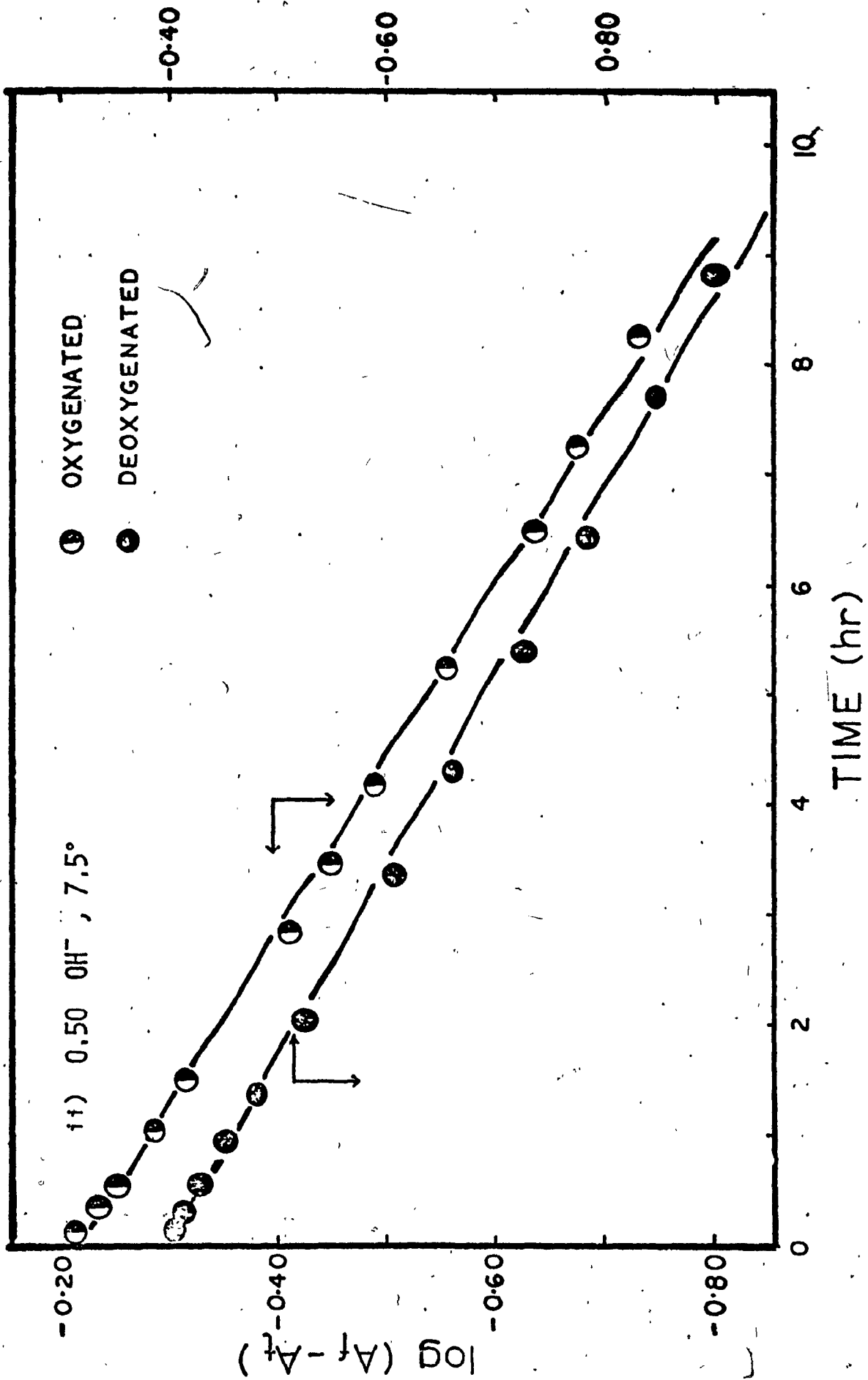


Appendix F. Plots of  $\log |(A_f - A_t)|$  versus Time for  
the Reaction Between  $[\text{Cr}(\text{bipy})_3]^{3+}$  and  
Hydroxide Ion in Oxygenated and Deoxy-  
genated Solvents:

i) pH = 11.82, 29.5°C;

ii) 0.50  $[\text{OH}^-]$ , 7.5°C.





Appendix G. Data for the Determination of the Observed Rate Constant as a Function of Temperature at Various pH and  $[OH^-]$  for  $[Cr(NN)_3]^{3+}$ :

a<sub>i</sub>)  $[Cr(phen)_3]^{3+}$  at pH 10.10;

a<sub>ii</sub>)  $[Cr(phen)_3]^{3+}$  at pH 12.17;

a<sub>iii</sub>)  $[Cr(phen)_3]^{3+}$  at 0.80  $[OH^-]$ ;

b<sub>i</sub>)  $[Cr(bipy)_3]^{3+}$  at pH 11.82;

b<sub>ii</sub>)  $[Cr(bipy)_3]^{3+}$  at 0.50  $[OH^-]$ .



a<sub>1</sub>) C<sub>0</sub> = 1.037 x 10<sup>-3</sup> M; pH = 10.10; T = 40.8 ± 0.1°C.

Sample	Time (min)	A <sub>231</sub>	A <sub>262</sub>	10 <sup>+5</sup> [PHEN] (M)	log {C <sub>0</sub> - [PHEN]}
t <sub>1</sub>	63.00	0.256	0.129	6.920	-3.014
t <sub>2</sub>	124.0	0.350	0.181	9.581	-3.026
t <sub>3</sub>	184.0	0.399	0.210	11.018	-3.033
t <sub>4</sub>	243.0	0.494	0.260	13.640	-3.060
t <sub>5</sub>	352.0	0.621	0.326	17.125	-3.063
t <sub>6</sub>	401.0	0.692	0.376	19.411	-3.074

$C_0 = 1.006 \times 10^{-3} M$ ; pH = 10.10; T = 50.8 ± 0.1°C.

Sample	Time (min)	A <sub>231</sub>	A <sub>262</sub>	$10^{+5} [PHEN] (M)$	$\log \{C_0 - [PHEN]\}$
t <sub>1</sub>	30.0	0.233	0.114	6.210	-3.025
t <sub>2</sub>	53.0	0.348	0.170	9.269	-3.039
t <sub>3</sub>	74.0	0.424	0.224	11.729	-3.051
t <sub>4</sub>	94.0	0.510	0.260	13.864	-3.062
t <sub>5</sub>	113.0	0.542	0.295	15.217	-3.069

$C_0 = 1.002 \times 10^{-3} \text{ M}$ ;  $\text{pH} = 10.10$ ;  $T = 60.8 \pm 0.1^\circ\text{C}$ .

Sample	Time (min)	$A_{231}$	$A_{262}$	$10^{+5}[\text{PHEN}]$ (M)	$\log \{C_0 - [\text{PHEN}]\}$
$t_1$	19.0	0.316	0.169	8.794	-3.039
$t_2$	33.0	0.465	0.251	13.001	-3.059
$t_3$	46.0	0.634	0.343	17.746	-3.084
$t_4$	57.0	0.720	0.389	20.139	-3.097
$t_5$	66.0	0.812	0.446	22.901	-3.112

$C_0 = 1.003 \times 10^{-3} \text{ M}$ ;  $\text{pH} = 10.10$ ;  $T = 71.0 \pm 0.1^\circ\text{C}$ .

Sample	Time (min)	A <sub>231</sub>	A <sub>262</sub>	$10^{+5}[\text{PHEN}]$ (M)	$\log \{C_0 - [\text{PHEN}]\}$
t <sub>1</sub>	9.25	0.222	0.126	6.366	-3.027
t <sub>2</sub>	15.83	0.400	0.220	11.289	-3.051
t <sub>3</sub>	22.92	0.568	0.309	15.943	-3.074
t <sub>4</sub>	27.58	0.789	0.428	22.113	-3.107
t <sub>5</sub>	33.58	0.920	0.502	25.861	-3.128

a<sub>11</sub>) C<sub>0</sub> = 1.006 x 10<sup>-3</sup> M; pH = 12.17; T = 21.2 ± 0.1°C.

Sample	Time (min)	A <sub>231</sub>	A <sub>262</sub>	10 <sup>+5</sup> [PHEN] (M)	log {C <sub>0</sub> - [PHEN]}
t <sub>1</sub>	5.00	0.214	0.118	6.047	-3.024
t <sub>2</sub>	44.50	0.228	0.118	6.244	-3.025
t <sub>3</sub>	79.00	0.253	0.132	6.956	-3.029
t <sub>4</sub>	131.85	0.272	0.136	7.325	-3.030
t <sub>5</sub>	195.70	0.325	0.172	8.998	-3.038
t <sub>6</sub>	237.75	0.349	0.187	9.722	-3.042

$C_0 = 9.991 \times 10^{-4} \text{ M}$ ; pH = 12.17; T =  $31.1 \pm 0.1^\circ\text{C}$ .

Sample	Time (min)	$A_{231}$	$A_{262}$	$10^{+5}[\text{PHEN}]$ (M)	$\log \{C_0 - [\text{PHEN}]\}$
$t_1$	30.00	0.274	0.149	7.689	-3.035
$t_2$	63.00	0.328	0.174	9.092	-3.042
$t_3$	93.00	0.368	0.198	10.272	-3.048
$t_4$	122.00	0.414	0.223	11.563	-3.054
$t_5$	151.00	0.474	0.240	12.843	-3.060

$C_0 = 1.004 \times 10^{-3} \text{ M}$ ; pH = 12.17; T =  $38.3 \pm 0.1^\circ\text{C}$ .

Sample	Time (min)	A <sub>231</sub>	A <sub>262</sub>	$10^{+5}[\text{PHEN}]$ (M)	$\log \{C_0 - [\text{PHEN}]\}$
t <sub>1</sub>	9.67	0.264	0.140	7.316	-3.032
t <sub>2</sub>	24.17	0.316	0.166	8.717	-3.038
t <sub>3</sub>	40.67	0.387	0.208	10.797	-3.048
t <sub>4</sub>	67.92	0.480	0.254	13.289	-3.060
t <sub>5</sub>	92.17	0.590	0.314	16.380	-3.076
t <sub>6</sub>	113.84	0.675	0.359	18.733	-3.088

$C_0 = 1.012 \times 10^{-3} M$ ;  $pH = 12.17$ ;  $T = 48.1 \pm 0.1^\circ C$ .

Sample	Time (min)	$A_{231}$	$A_{262}$	$10^{+5} [PHEN] (M)$	$\log \{C_0 - [PHEN]\}$
$t_1$	9.25	0.264	0.137	7.239	-3.027
$t_2$	18.10	0.389	0.204	10.722	-3.043
$t_3$	29.32	0.569	0.306	15.879	-3.069
$t_4$	40.63	0.700	0.362	19.161	-3.086
$t_5$	49.43	0.793	0.426	22.118	-3.102
$t_6$	59.08	0.909	0.487	25.320	-3.120
$t_7$	67.55	0.997	0.531	27.690	-3.134



a<sub>111</sub>) C<sub>0</sub> = 1.009 x 10<sup>-3</sup> M; 0.80 [OH<sup>-</sup>]; T = 15.5 ± 0.1°C.

Sample	Time (min)	A <sub>231</sub>	A <sub>262</sub>	10 <sup>+5</sup> [PHEN] (M)	log {C <sub>0</sub> - [PHEN]}
t <sub>1</sub>	5.40	0.119	0.060	3.218	-3.010
t <sub>2</sub>	14.50	0.243	0.130	6.764	-3.026
t <sub>3</sub>	27.45	0.391	0.211	10.931	-3.046
t <sub>4</sub>	52.70	0.678	0.368	19.008	-3.087
t <sub>5</sub>	85.05	0.947	0.518	26.653	-3.129
t <sub>6</sub>	120.9	1.302	0.690	36.071	-3.188



$C_0 = 1.008 \times 10^{-3} \text{ M}$ ;  $0.80 \text{ [OH}^-]$ ;  $T = 20.8 \pm 0.1^\circ\text{C}$ .

Sample	Time (min)	$A_{231}$	$A_{262}$	$10^{+5} \text{ [PHEN]} \text{ (M)}$	$\log \{C_0 - \text{[PHEN]}\}$
$t_1$	5.50	0.148	0.072	3.934	-3.014
$t_2$	14.60	0.414	0.222	11.537	-3.049
$t_3$	22.90	0.592	0.311	16.331	-3.073
$t_4$	31.15	0.764	0.415	21.428	-3.100
$t_5$	39.80	---	0.478	24.690	-3.119

$C_0 = 1.009 \times 10^{-3} \text{ M}$ ;  $0.80 [\text{OH}^-]$ ;  $T = 25.5 \pm 0.1^\circ\text{C}$ .

Sample	Time (min)	$A_{231}$	$A_{262}$	$10^{+5}[\text{PHEN}]$ (M)	$\log \{C_0 - [\text{PHEN}]\}$
$t_1$	5.50	0.178	0.093	4.897	-3.018
$t_2$	22.95	0.866	0.470	24.278	-3.116
$t_3$	35.95	1.244	0.658	34.432	-3.177
$t_4$	48.30	1.726	0.872	46.715	-3.266
$t_5$	57.05	1.764	0.982	50.088	-3.294

$C_0 = 1.025 \times 10^{-3} \text{ M}$ ;  $0.80 \cdot [\text{OH}^-]$ ;  $T = 30.6 \pm 0.1^\circ\text{C}$ .

Sample	Time (min)	$A_{231}$	$A_{262}$	$10^{+5}[\text{PHEN}]$ (M)	$\log \{C_0 - [\text{PHEN}]\}$
$t_1$	5.30	0.212	0.106	5.709	-3.014
$t_2$	16.70	0.956	0.514	26.678	-3.120
$t_3$	25.55	1.516	0.798	41.860	-3.217
$t_4$	32.30	1.746	0.964	49.371	-3.275

b<sub>f</sub>) C<sub>0</sub> = 1.008 x 10<sup>-3</sup> M; pH = 11.82; T = 11.1 ± 0.1°C.

Sample	Time (hr)	A <sub>237</sub>	A <sub>282</sub>	10 <sup>+5</sup> [BIPY] (M)	log{C <sub>0</sub> - [BIPY]}
t <sub>1</sub>	0.15	0.009	0.010	0.212	-2.998
t <sub>2</sub>	1.15	0.029	0.032	0.65	-2.999
t <sub>3</sub>	2.28	0.051	0.057	1.10	-3.001
t <sub>4</sub>	5.26	0.108	0.125	2.36	-3.007
t <sub>5</sub>	7.53	0.144	0.175	3.20	-3.010
t <sub>6</sub>	10.07	0.194	0.233	4.29	-3.015

$C_0 = 1.002 \times 10^{-3} \text{ M}$ ;  $\text{pH} = 11.82$ ;  $T = 16.8 \pm 0.1^\circ\text{C}$ .

Sample	Time (hr)	$A_{237}$	$A_{282}$	$10^{+5}[\text{BIPY}]$ (M)	$\log \{C_0 - [\text{BIPY}]\}$
$t_1$	0.48	0.022	0.025	0.50	-3.002
$t_2$	1.58	0.072	0.083	1.58	-3.006
$t_3$	2.77	0.116	0.136	2.55	-3.010
$t_4$	4.72	0.197	0.234	4.34	-3.018
$t_5$	6.61	0.262	0.314	5.79	-3.025

$C_0 = 1.026 \times 10^{-3} \text{ M}$ ;  $\text{pH} = 11.82$ ;  $T = 23.1 \pm 0.1^\circ\text{C}$ .

Sample	Time (hr)	A <sub>237</sub>	A <sub>282</sub>	$10^{+5}[\text{BIPY}]$ (M)	$\log \{C_0 - [\text{BIPY}]\}$
t <sub>1</sub>	0.76	0.075	0.086	1.62	-2.996
t <sub>2</sub>	1.63	0.150	0.176	3.29	-3.003
t <sub>3</sub>	2.55	0.231	0.273	5.05	-3.011
t <sub>4</sub>	3.87	0.335	0.404	7.42	-3.021
t <sub>5</sub>	4.80	0.408	0.493	9.05	-3.029

$C_0 = 1.017 \times 10^{-3} \text{ M}$ ; pH = 11.82; T = 29.8 ± 0.1°C.

Sample	Time (hr)	A <sub>237</sub>	A <sub>282</sub>	10 <sup>5</sup> [BIPY] (M)	log {C <sub>0</sub> - [BIPY]}
t <sub>1</sub>	0.17	0.032	0.035	0.70	-2.996
t <sub>2</sub>	1.29	0.245	0.297	5.45	-3.016
t <sub>3</sub>	1.91	0.355	0.434	7.91	-3.028
t <sub>4</sub>	2.51	0.472	0.575	10.50 <sub>A</sub>	-3.04
t <sub>5</sub>	3.16	0.580	0.709	12.92	-3.052
t <sub>6</sub>	3.73	0.671	0.824	14.98	-3.062



b<sub>11</sub>) C<sub>0</sub> = 1.007 x 10<sup>-3</sup> M; 0.50 [OH<sup>-</sup>]; T = 5.5 ± 0.1°C.

Sample	Time (min)	A <sub>237</sub>	A <sub>282</sub>	10 <sup>+5</sup> [BIPY] (M)	log {C <sub>0</sub> - [BIPY]}
t <sub>1</sub>	28.10	0.291	0.351	6.44	-3.026
t <sub>2</sub>	44.60	0.413	0.502	9.18	-3.039
t <sub>3</sub>	62.40	0.528	0.649	11.79	-3.051
t <sub>4</sub>	78.30	0.633	0.782	14.18	-3.063
t <sub>5</sub>	91.60	0.724	0.895	16.22	-3.073

$C_0 = 1.027 \times 10^{-3} \text{ M}$ ;  $0.50 \text{ [OH}^-]$ ;  $T = 11.1 \pm 0.1^\circ\text{C}$ .

Sample	Time (min)	$A_{237}$	$A_{282}$	$10^{+5} [\text{BIPY}]$ (M)	$\log \{C_0 - [\text{BIPY}]\}$
$t_1$	6.15	0.191	0.229	4.21	-3.007
$t_2$	16.05	0.335	0.406	7.44	-3.021
$t_3$	27.15	0.480	0.585	10.68	-3.036
$t_4$	39.50	0.651	0.796	14.50	-3.054
$t_5$	51.55	0.770	0.928	17.06	-3.067

$C_0 = 1.032 \times 10^{-3} \text{ M}$ ;  $0.50 \text{ [OH}^-]$ ;  $T = 17.5 \pm 0.1^\circ\text{C}$ .

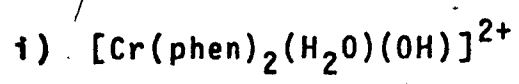
Sample	Time (min)	$A_{237}$	$A_{282}$	$10^{+5}[\text{BIPY}]$ (M)	$\log \{C_0 - [\text{BIPY}]\}$
$t_1$	16.65	0.509	0.621	11.34	-3.037
$t_2$	23.45	0.694	0.860	15.59	-3.058
$t_3$	30.30	0.894	1.084	19.88	-3.079
$t_4$	36.95	1.062	1.298	23.70	-3.01
$t_5$	44.05	1.242	1.520	27.70	-3.122

$C_0 = 1.031 \times 10^{-3} \text{ M}$ ;  $0.50 \text{ [OH}^-]$ ;  $T = 23.4 \pm 0.1^\circ\text{C}$ .

Sample	Time (min)	$A_{237}$	$A_{282}$	$10^{+5}[\text{BIPY}]$ (M)	$\log \{C_0 - [\text{BIPY}]\}$
$t_1$	6.00	0.232	0.282	5.15	-3.009
$t_2$	13.70	0.670	0.824	14.98	-3.055
$t_3$	20.45	1.027	1.297	23.28	-3.098
$t_4$	26.00	1.292	1.624	29.18	-3.131

Appendix H. Absorption Data (Absorbance values and Extinction Coefficients) for:

- i)  $[\text{Cr}(\text{phen})_2(\text{H}_2\text{O})(\text{OH})]^{2+}$ ;
- ii)  $[\text{Cr}(\text{phen})_2(\text{H}_2\text{O})_2]^{3+}$ ;
- iii)  $[\text{Cr}(\text{phen})_2(\text{OH})_2]^+$ .



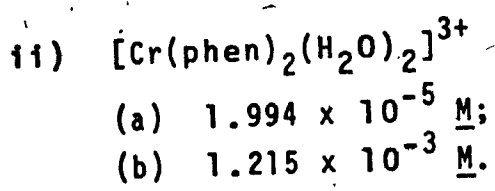
(a)  $1.994 \times 10^{-5} \text{ M}$ ;

(b)  $1.215 \times 10^{-3} \text{ M}$ .

$\lambda$ nm	Abs.	log $\epsilon$	$\lambda$ nm	Abs.	log $\epsilon$
210	1.625	4.911 (a)	300	0.322	4.208 (a)
215	1.412	4.85	305	0.269	4.13
220	1.276	4.806	310	0.207	4.016
225	1.218	4.785	315	0.154	3.888
230	1.105	4.743	320	0.121	3.783
235	0.836	4.622	325	0.091	3.659
240	0.538	4.431	330	0.068	3.533
245	0.370	4.268	335	0.059	3.471
247 <sub>min</sub>	0.361	4.258	340	0.048	3.381
250	0.374	4.273	345	0.038	3.28
255	0.447	4.350	350	1.750	3.158 (b)
260	0.568	4.454	360	0.970	2.902
265 <sub>max</sub>	0.706	4.549	370	0.452	2.570
270	0.822	4.615	380	0.322	2.423
275 <sub>max</sub>	0.877	4.643	390	0.270	2.347
280	0.787	4.596	400	0.233	2.283
285	0.596	4.475	410	0.191	2.196
290	0.440	4.343	420	0.161	2.122
295	0.355	4.250	430	0.121	1.998

$\lambda$ nm	Abs.	$\log \epsilon$	$\lambda$ nm	Abs.	$\log \epsilon$
440	0.079	1.813 (b)	610	0.133	0.942 (a)
<del>450</del>	<del>0.603</del>	1.599 (a)	620	0.102	0.827
460	0.458	1.479	630	0.079	0.716
470	0.482	1.502	640	0.062	0.611
480	0.495	1.513	650	0.048	0.50
490	0.606	1.601			
500	0.643	1.627			
508 <sub>max</sub>	0.650	1.631			
510	0.647	1.629			
520	0.618	1.609			
530	0.566	1.571			
540	0.500	1.517			
550	0.431	1.453			
560	0.365	1.381			
570	0.307	1.306			
580	0.254	1.223			
590	0.208	1.136			
600	0.169	1.046			





(a)  $1.994 \times 10^{-5} \text{ M}$ ;

(b)  $1.215 \times 10^{-3} \text{ M}$ .

$\lambda$ nm	Abs.	log $\epsilon$	$\lambda$ nm	Abs.	log $\epsilon$
215	1.570	5.305 (a)	295	0.339	4.241 (b)
220	0.683	4.944	300	0.318	4.214
225	0.504	4.812	305	0.242	4.095
230	0.436	4.748	310	0.175	3.954
235	0.805	4.617 (b)	315	0.120	3.790
240	0.525	4.431	320	0.089	3.661
245	0.352	4.258	325	0.068	3.544
247 <sub>min</sub>	0.344	4.248	330	0.055	3.452
250	0.361	4.269	335	0.050	3.410
255	0.442	4.356	340	0.042	3.334
260	0.566	4.464	345	0.036	3.268
265	0.703	4.558	350	0.036	3.269
270	0.837	4.634	360	0.024	3.092
274 <sub>max</sub>	0.891	4.661	370	---	---
275	0.889	4.66	380	---	---
280	0.750	4.586	390	---	---
285	0.523	4.429	400	---	---
290	0.390	4.302	410	---	---

$\lambda$ nm	Abs.	$\log \xi$ (c)	$\lambda$ nm	Abs.	$\log \xi$
420	1.762	2.064	590	0.426	1.448 (c)
430	1.385	1.96	600	0.360	1.375
440	0.970	1.805	610	0.297	1.291
450	0.730	1.682	620	0.240	1.199
460	0.557	1.564	630	0.187	1.090
470	0.520	1.534	640	0.148	0.989
480	0.536	1.548	650	0.114	0.875
490	0.572	1.576			
500	0.618	1.609			
510	0.655	1.635			
520	0.675	1.648			
528	0.682	1.652			
530	0.680	1.651			
540	0.667	1.643			
550	0.640	1.625			
560	0.601	1.597			
570	0.551	1.56			
580	0.491	1.51			

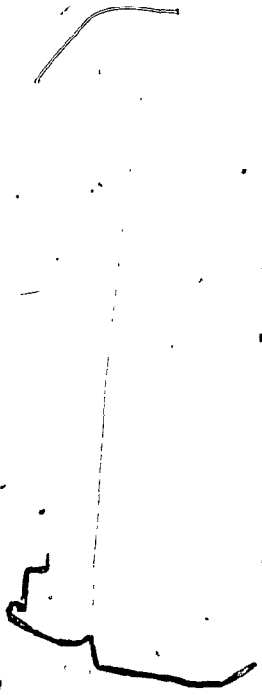
111)  $[\text{Cr}(\text{phen})_2(\text{OH})_2]^+$

(a)  $7.776 \times 10^{-6} \text{ M}$ ;

(b)  $1.994 \times 10^{-5} \text{ M}$ ;

(c)  $1.519 \times 10^{-2} \text{ M}$ .

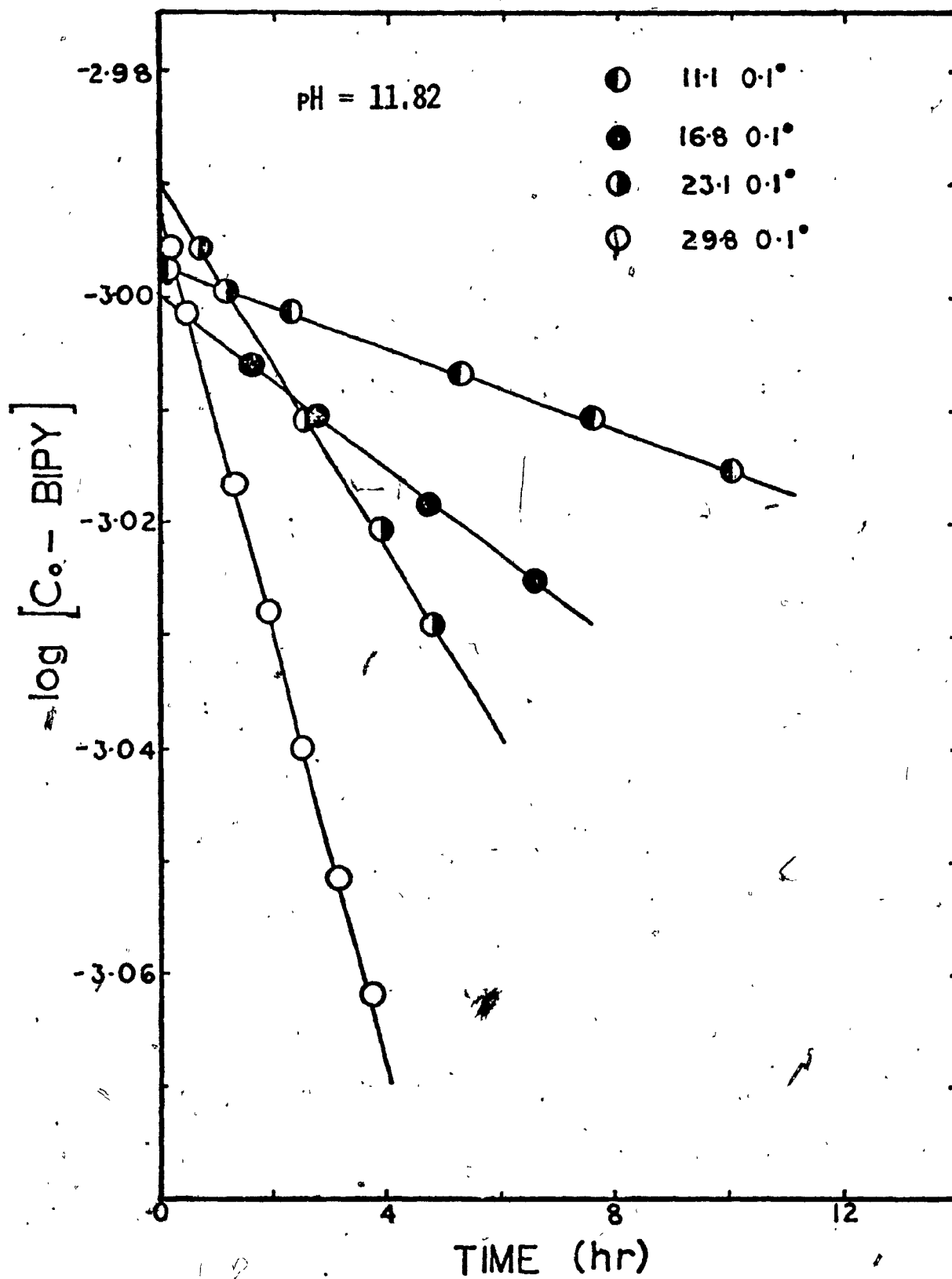
$\lambda$ nm	Abs.	$\log \epsilon$	$\lambda$ nm	Abs.	$\log \epsilon$
250	0.672	4.528 (a)	335	0.090	3.654 (a)
255 <sub>min</sub>	0.548	4.439	340	0.066	3.52
260	0.607	4.483	345	0.046	3.363
265	0.722	4.559	350	1.768	3.163 (b)
270	0.794	4.600	360	1.188	2.990
274 <sub>max</sub>	0.805	4.606	370	0.618	2.706
275	0.803	4.605	380	0.447	2.566
280	0.770	4.587	390	0.362	2.474
285	0.686	4.536	400	0.299	2.391
290	0.605	4.482	410	0.231	2.279
295	0.534	4.428	420	0.182	2.175
300	0.482	4.383	430	0.139	2.058
305	0.453	4.356	440	0.079	1.813
310	0.413	4.316	450	0.583	1.584 (a)
315	0.345	4.238	460 <sub>min</sub>	0.442	1.464
320	0.275	4.14	470	0.484	1.503
325	0.208	4.018	480	0.557	1.564
330	0.133	3.824	490	0.616	1.608



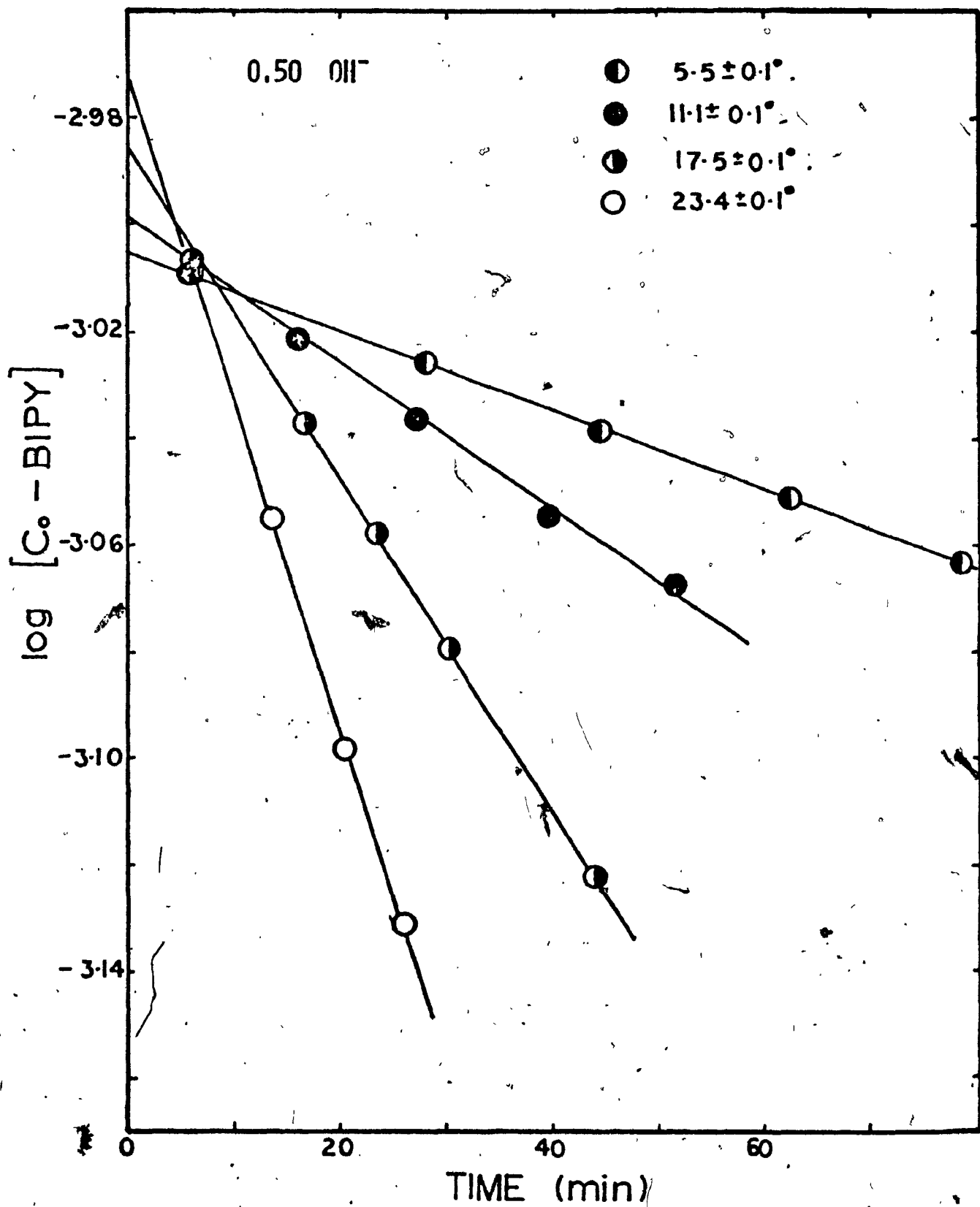
$\lambda$ nm	Abs.	$\log \epsilon$
500 <sub>max</sub>	0.640	1.625(a)
510	0.623	1.613
520	0.571	1.575
530	0.497	1.515
540	0.410	1.431
550	0.329	1.336
560	0.258	1.230
570	0.201	1.122
580	0.156	1.012
590	0.122	0.915
600	0.096	0.801
610	0.073	0.682
620	0.056	0.567
630	0.043	0.452
640	0.031	0.31
650	0.028	0.266

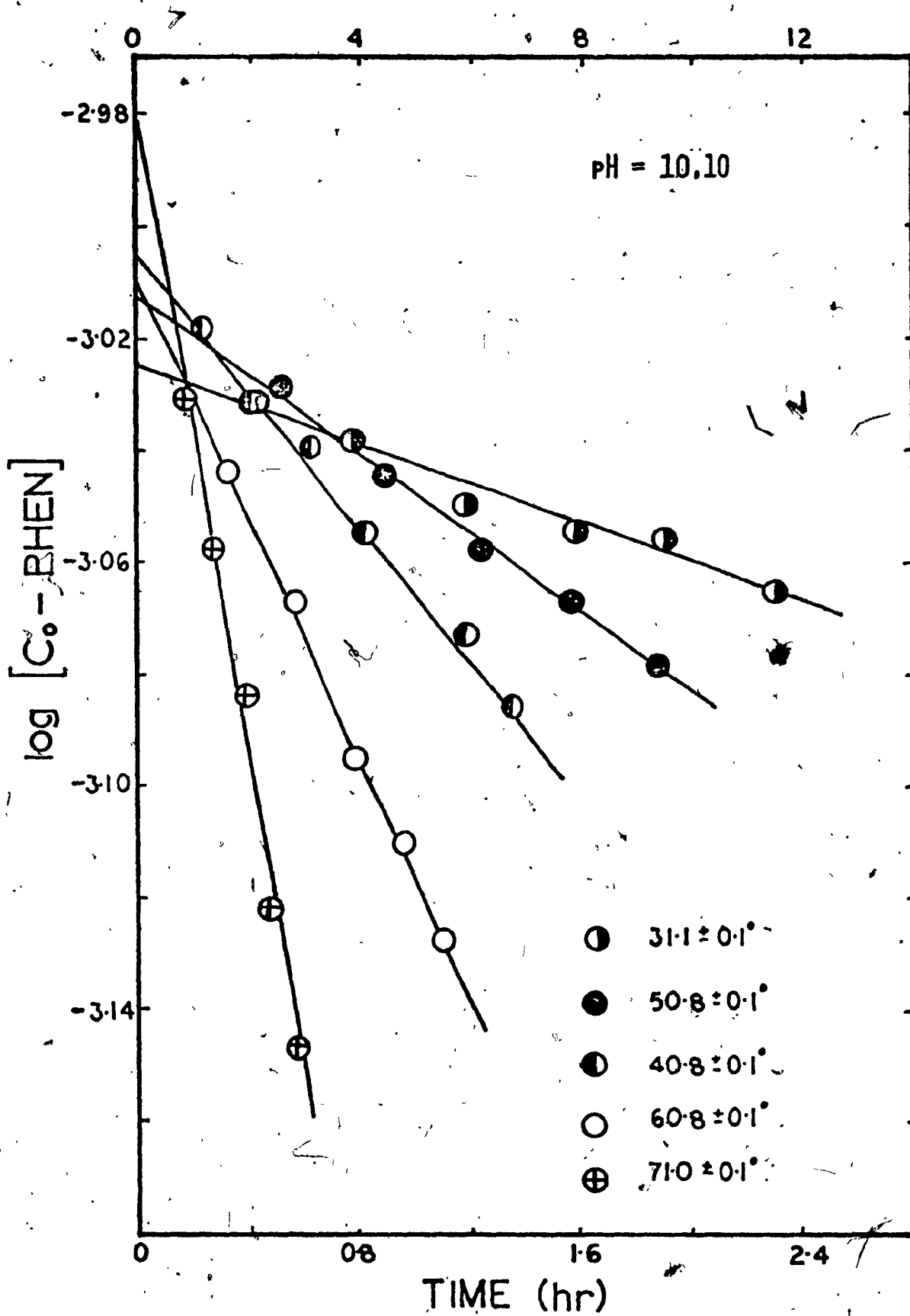
Appendix I. Determination of the Observed Rate Constants for the  $[\text{Cr}(\text{NN})_3]^{3+}$  Systems at Various Temperatures:

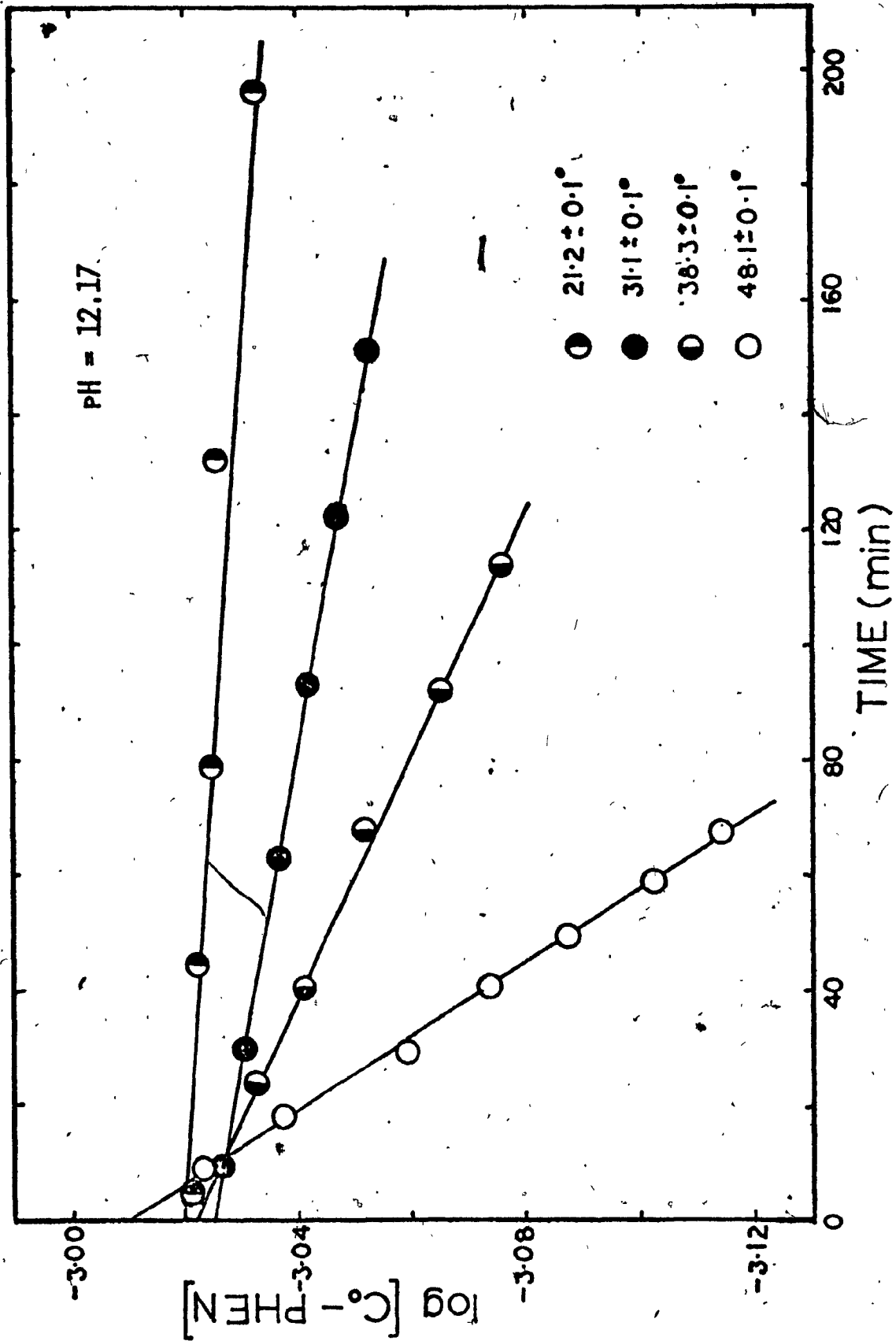
- i)  $[\text{Cr}(\text{bipy})_3]^{3+}$  System at pH 11.82 and  $0.50 [\text{OH}^-]$ .
- ii)  $[\text{Cr}(\text{phen})_3]^{3+}$  System at pH 10.10, pH 12.17, and  $0.80 [\text{OH}^-]$ .

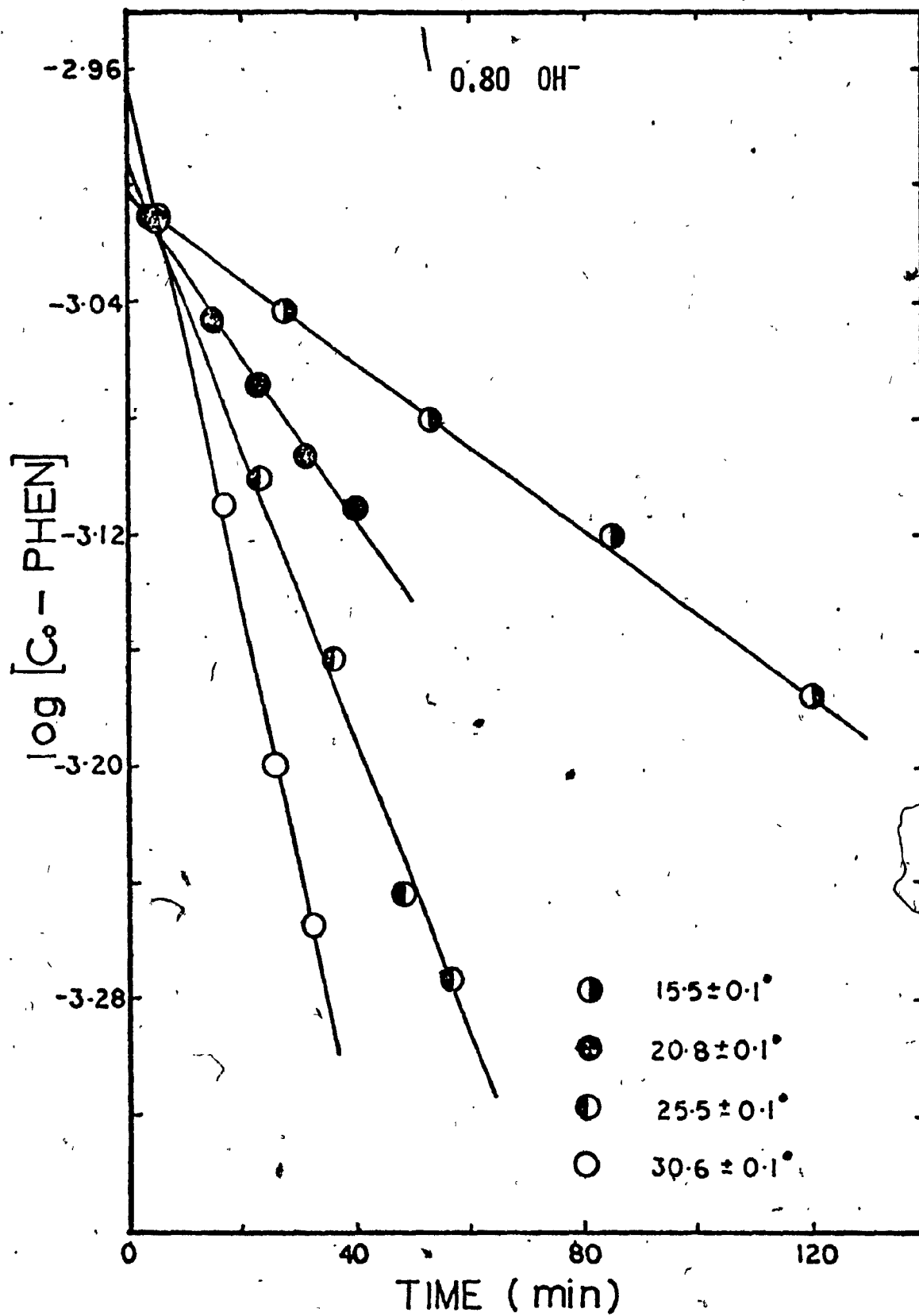












Appendix J. Data for the Absorption Spectrum of:

- i)  $[\text{Cr}(\text{bipy})_3](\text{ClO}_4)_3 \cdot 1/2\text{H}_2\text{O}$  in  
 $10^{-1}$  M Hydrochloric Acid;
- ii)  $[\text{Cr}(\text{phen})_3](\text{ClO}_4)_3 \cdot 2\text{H}_2\text{O}$  in  
 $10^{-1}$  M Hydrochloric Acid.

1)  $[\text{Cr}(\text{bipy})_3](\text{ClO}_4)_3 \cdot 1/2\text{H}_2\text{O}$  in  $10^{-1}$  M Hydrochloric Acid:

(a)  $3.370 \times 10^{-5}$  M;

(b)  $2.106 \times 10^{-4}$  M;

(c)  $1.053 \times 10^{-3}$  M.

where Abs. = absorbance,

$\xi$  = extinction coefficient in liter/mole/cm.

$\lambda$ nm	Abs.	$\xi$	$\lambda$ nm	Abs.	$\xi$
210	1.925	57118 (a)	295	0.550	16319 (a)
215	1.825	54151	300	0.666	19761
220	1.690	50145	305	0.775	22996
225	1.568	46525	310	0.823	24420
230	1.450	43024	313 <sub>max</sub>	0.848	25162
235	1.393	41333	315	0.827	24539
240	1.297	38484	320	0.575	17061
245	1.144	33945	325	0.372	11037
250	0.905	26853	330	0.308	9139
255	0.708	21008	335	0.299	8872
260	0.593	17595	340	0.298	8842
265	0.574	17032	345	0.302	8961
270	0.555	16468	350	0.281	8338
275	0.560	16616	350	1.593	7563 (b)
280	0.540	16023 (a)	360	1.223	5806
283 <sub>min</sub>	0.477	14154	370	0.438	2079
285	0.491	14569	380	0.242	1149
290	0.483	14331	390	0.215	1021

$\lambda$ nm	Abs.	$\xi$	$\lambda$ nm	Abs.	$\xi$
400	0.976	927 (c)	580	0.002	1.9 (c)
410	0.888	843	590	0.002	1.9
420	0.734	697	600	0.002	1.9
430	0.677	643	610	0.002	1.9
440	0.446	423	620	0.002	1.9
450	0.310	294	630	0.002	1.9
460	0.268	254	640	0.002	1.9
470	0.123	117	650	0.002	1.9
480	0.049	47			
490	0.029	28			
500	0.021	20			
510	0.014	13			
520	0.008	7.6			
530	0.005	4.7			
540	0.004	3.8			
550	0.002	1.9			
560	0.002	1.9			
570	0.002	1.9			



11)  $[\text{Cr}(\text{phen})_3](\text{ClO}_4)_3 \cdot 2\text{H}_2\text{O}$  in  $10^{-1}$  M Hydrochloric Acid:

(a)  $1.704 \times 10^{-5}$  M;

(b)  $2.129 \times 10^{-4}$  M;

(c)  $1.065 \times 10^{-3}$  M.

where Abs. = absorbance,

$\xi$  = extinction coefficient in liter/mole/cm

$\lambda$ nm	Abs.	$\xi$	$\lambda$ nm	Abs.	$\xi$
210	1.600	93924 (a)	290	0.481	28236 (a)
215	1.585	93044	295	0.372	21837
220	1.515	88934	300	0.321	18844
225	1.460	85706	305	0.277	16261
230	1.350	79249	310	0.243	14265
235	1.125	66628	315	0.227	13326
240	0.740	43440	320	0.220	12915
245	0.735	43146	325	0.212	12445
246 <sub>min</sub>	0.550	32286	330	0.191	11212
250	0.560	32874	335	0.170	9979
255	0.594	34869	340	0.149	8747
260	0.715	41972	345	0.120	7044
265	0.878	51541	350	0.091	5342
269 <sub>max</sub>	1.087	63810	350	1.010	4743 (b)
270	1.076	63164	360	0.820	3851
275	0.885	51952	370	0.407	1911
280	0.748	43910	380	0.284	1334
285	0.635	37276	390	1.085	1019

$\lambda$ nm	Abs.	$\epsilon$	$\lambda$ nm	Abs.	$\epsilon$
400	0.970	911 (c)	580	0.006	5.6
410	0.892	838	590	0.006	5.6
420	0.795	747	600	0.006	5.6
430	0.708	665	610	0.006	5.6
440	0.561	527	620	0.006	5.6
450	0.404	379	630	0.006	5.6
460	0.243	228	640	0.006	5.6
470	0.104	98	650	0.006	5.6
480	0.048	45			
490	0.029	29			
500	0.020	19			
510	0.012	11			
520	0.006	5.6			
530	0.006	5.6			
540	0.006	5.6			
550	0.006	5.6			
560	0.006	5.6			
570	0.006	5.6			

Appendix K. Data for the Absorption Spectrum of  
 $[\text{Rh}(\text{bipy})_3]\text{Cl}_3 \cdot 4.5\text{H}_2\text{O}$  in Methanol:

$$c = 1.899 \times 10^{-5} \text{ M}$$

where Abs. = absorbance  
 $\xi$  = extinction coefficient in  
liter/mole/cm.

$\lambda$ nm	Abs.	$\epsilon$	$\lambda$ nm	Abs.	$\epsilon$
210	1.345	70827	290	0.276	14534
213 <sub>max</sub>	1.405	73986	295	0.388	20116
215	1.375	72406	300	0.477	25119
220	1.133	59663	305	0.618	32543
225	0.850	44760	308 <sub>max</sub>	0.714	37599
230	0.685	36072	310	0.706	37178
235	0.696	36651	315	0.617	32491
240	0.771	40600	320	0.721	37967
242 <sub>max</sub>	0.781	41127	322 <sub>max</sub>	0.748	39389
245	0.763	40179	325	0.572	30121
250	0.603	31754	330	0.169	8899
255	0.324	17062	335	0.030	1580
260	0.265	13955	340	0.005	263
265	0.216	11374	345	0.002	105
270	0.186	9795	350	0.002	105
275	0.172	9057			
280	0.182	9584			
285	0.224	11796			

Appendix L. Data for the Absorption Spectrum of:

- i)  $[\text{Cr}(5\text{-Clphen})_3](\text{ClO}_4)_3 \cdot 2\text{H}_2\text{O}$  in  $10^{-1}$  M Hydrochloric Acid;
- ii)  $[\text{Cr}(4,7\text{-Me}_2\text{phen})_3](\text{ClO}_4)_3 \cdot 2\text{H}_2\text{O}$  in Methanol;
- iii)  $[\text{Cr}(4,7\text{-Ph}_2\text{phen})_3](\text{ClO}_4)_3 \cdot 4\text{H}_2\text{O}$  in Methanol;
- iv)  $[\text{Cr}(4,4'\text{-Ph}_2\text{bipy})_3](\text{ClO}_4)_3 \cdot 2\text{H}_2\text{O}$  in Methanol.

where

Abs. = Absorbance

$\epsilon$  = extinction coefficient in liter/mole/cm

1)  $[\text{Cr}(\text{5-C1phen})_3](\text{ClO}_4)_3 \cdot 2\text{H}_2\text{O}$  in  $10^{-1}$  M Hydrochloric Acid:

(a)  $6.871 \times 10^{-4}$  M;

(b)  $1.374 \times 10^{-4}$  M;

(c)  $1.649 \times 10^{-5}$  M.

$\lambda$ nm	Abs.	$\epsilon$	$\lambda$ nm	Abs.	$\epsilon$
210	1.600	97028 (c)	290	0.686	41601 (c)
215	1.580	95836	295	0.587	35597
220	1.465	88842	300	0.500	30321
225	1.340	81261	305	0.424	25713
230	1.290	78229	310	0.365	22135
235	1.255	76107	315	0.315	19102
240	1.178	71437	320	0.262	15888
245	0.895	54275	325	0.216	13099
250	0.600	36386	330	0.182	11037
253 min	0.564	34202	335	0.148	8975
255	0.572	34688	340	0.123	7459
260	0.658	39903	345	0.105	6367
265	0.808	48999	350	0.090	5458
270	0.965	58520	355	0.080	4851
274 max	1.023	62038	360	0.070	4245
275	1.023	62038	370	0.472	3435 (b)
280	0.909	55124	380	0.288	2096
285	0.777	47120	390	0.180	1310



$\lambda$ nm	Abs.	$\xi$	$\lambda$ nm	Abs.	$\xi$
400	0.144	1048 (b)	580	0.033	48 (a)
410	0.125	910	590	0.030	44
420	0.555	808	600	0.030	44
430	0.510	742	610	0.030	44
440	0.458	666	620	0.030	44
450	0.370	538	630	0.030	44
460	0.303	441	640	0.030	44
470	0.236	343	650	0.030	44
480	0.160	233			
490	0.108	157			
500	0.086	125			
510	0.076	111			
520	0.067	98			
530	0.059	86			
540	0.051	74			
550	0.045	66			
560	0.040	58			
570	0.036	52			

11)  $[\text{Cr}(4,7\text{-Me}_2\text{phen})_3](\text{ClO}_4)_3 \cdot 2\text{H}_2\text{O}$  in Methanol:

(a)  $1.038 \times 10^{-3} \text{ M}$

(b)  $2.077 \times 10^{-4} \text{ M}$

(c)  $1.661 \times 10^{-5} \text{ M}$

$\lambda$ nm	Abs.	$\epsilon$	$\lambda$ nm	Abs.	$\epsilon$
210	1.330	78628 (c)	290	0.605	35353 (c)
215	1.370	80993	295	0.515	30151
220	1.285	75968	300	0.460	26722
225	1.240	73308	305	0.430	25126
230	1.210	71543	310	0.395	23056
235	1.110	65622	315	0.320	18622
240	0.980	57937	320	0.260	15075
245	0.820	48478	325	0.215	12415
249 <sub>min</sub>	0.784	47189	330	0.185	10641
250	0.785	46408	335	0.160	9164
255	0.865	51138	340	0.145	8277
260	1.000	59119	345	0.125	7390
265	1.140	67396	350	0.100	5616
269 <sub>max</sub>	1.205	72529	355	0.105	6208 (b)
270	1.205	71238	357 <sub>max</sub>	1.225	5794 (b)
275	1.070	63258	360	0.105	6208
280	0.865	50547	370	0.530	2507 (b)
285	0.720	42270	380	1.330	1258 (a)

$\lambda$ nm	Abs.	$\xi$	$\lambda$ nm	Abs.	$\xi$
390	1.155	1092(a)	570	0.022	21(a)
400	1.090	1031	580	0.021	20
410	1.020	965	590	0.020	19
420	0.960	908	600	0.018	17
430	0.827	782	610	0.018	17
440	0.634	600	620	0.016	15
450	0.525	497	630	0.015	14
460	0.333	315	640	0.011	10
470	0.169	160	650	0.011	10
480	0.090	85			
490	0.062	59			
500	0.052	49			
510	0.042	40			
520	0.038	36			
530	0.035	33			
540	0.028	26			
550	0.025	24			
560	0.025	24			

111)  $[\text{Cr}(\text{4,7-Ph}_2\text{phen})_3](\text{ClO}_4)_3 \cdot 4\text{H}_2\text{O}$  in Methanol:

(a)  $7.537 \times 10^{-4}$  M:

(b)  $1.206 \times 10^{-4}$  M:

(c)  $2.412 \times 10^{-5}$  M:

(d)  $9.648 \times 10^{-6}$  M.

$\lambda$ nm	Abs.	$\epsilon$	$\lambda$ nm	Abs.	$\epsilon$
210	1.210	125421 (d)	295	0.725	75149 (d)
215	1.163	120549	300	0.743	77015
220	1.082	112153	305	0.770	79813
225	0.976	101166	307 <sub>max</sub>	0.773	80124
230	0.855	88642	310	0.767	79502
235	0.728	75460	315	0.723	74942
240	0.611	63332	320	0.650	67375
245	0.510	52863	325	0.577	59808
250	0.402	41669	330	0.502	52034
255	0.348	36072	335	0.418	43327
256 <sub>min</sub>	0.347	35968	340	0.343	35553
260	0.324	33584	345	0.297	30785
265	0.419	43431	350	0.276	28608
270	0.516	53485	355	0.268	27779
275	0.635	65820	360	0.258	26743
280	0.738	76496	370	0.568	23551 (c)
285 <sub>max</sub>	0.764	79192	380	0.474	19653
290	0.739	76600	390	0.303	12563

$\lambda$ nm	Abs.	$\epsilon$	$\lambda$ nm	Abs.	$\epsilon$
400	0.640	5307 (b)	580	0.010	83 (b)
410	0.355	2944	590	0.010	83
420	0.288	2388	600	0.010	83
430	0.263	2181	610	0.010	83
440	0.251	2081	620	0.010	83
450	0.239	1982	680	0.010	83
460	0.215	1783	640	0.010	83
470	0.188	1559	650	0.010	83
480	0.160	1327			
490	0.121	1003			
500	0.074	614			
510	0.036	299			
520	0.018	149			
530	0.012	96			
540	0.010	83			
550	0.010	83			
560	0.010	83			
570	0.010	83			

1v)  $[\text{Cr}(4,4'\text{-Ph}_2\text{bipy})_3](\text{ClO}_4)_3 \cdot 2\text{H}_2\text{O}$  in Methanol:

(a)  $5.932 \times 10^{-4}$  M;

(b)  $1.186 \times 10^{-4}$  M;

(c)  $9.491 \times 10^{-6}$  M.